NASA CONTRACTOR REPORT 166309

UH-60A Black Hawk Engineering Simulation Program: Volume I - Mathematical Model

(NASA-CR-166309) UH-60A BLACK HAWK ENGINEERING SIMULATION PROGRAM. VOLUME 1: MATHEMATICAL MODEL Final Report (Sikorsky Aircraft, Stratford, Conn.) 359 p HC A16/MF A01 CSCL 01C G3/08

N84-28806

Unclas 19790

J.J. Howlett

CONTRACT NAS2-10626
December 1981

NASA

NASA CONTRACTOR REPORT 166309

UH-60A Black Hawk Engineering Simulation Program: Volume I - Mathematical Model

J.J. Howlett
United Technologies
Sikorsky Aircraft
Stratford, Connecticut 06602

Prepared for
Ames Research Center
under Contract NAS2-10626

National Aeronautics and
Space Administration

Ames Research Center
Moffett Field, California 94035

SIKORSKY AIRCRAFT UNITED TECHNOLOGIES

DOCUMENT NO. SER 70452

TABLE OF CONTENTS

PRECEDING PAGE BLANK NOT FILMED

ii, iii

SA 29 REV. 6

SUMMARY

A non-linear mathematical model of the UH-60A BLACK HAWK helicopter has been developed under Contract NAS2-10626. This mathematical model, which is based on the Sikorsky General Helicopter (Gen Hel) Flight Dynamics Simulation, provides the Army with an engineering simulation for Performance and Handling Qualities evaluations. Initially it will be applied in an analysis mode with eventual application to real time pilot-in-the-loop simulation.

This mathematical model is a total systems definition of the BLACK HAWK helicopter represented at a uniform level of sophistication considered necessary for Handling Qualities evaluations. The model is a total force, large angle representation in six rigid body degrees of freedom. Rotor blade flapping, lagging and hub rotational degrees of freedom are also represented. In addition to the basic helicopter modules, supportive modules have been defined for the landing interface, power unit, ground effects and gust penetration. Information defining the cockpit environment relevant to pilot-in-the-loop simulation is presented. This same model was activated on Sikorsky's DEC PDP KL10 computer to generate check cases for use during the validation of the simulation at NASA.

Volume I of this report defines the mathematical model using a modular format. The documentation of each module is self-contained and includes a description, mathematical definition and input for the BLACK HAWK. Volume II provides background and descriptive information supportive to an understanding of the mathematical model.

2.0 INTRODUCTION

This report is Volume I of two volumes, which document the mathematical model of the UH-60A BLACK HAWK helicopter. This work was funded under Contract NAS2-10626 by the U.S. Army Research and Technology Laboratories (AVRADCOM) Ames Research Center.

The objective of this contract was to provide the Army and NASA with a well documented, operational and verified engineering simulation of the BLACK HAWK helicopter. This work, undertaken by Sikorsky, provides the Army with a flying qualities analysis methodology for the BLACK HAWK helicopter which could eventually be extended to a real time pilot-in-loop simulation. The mathematical model provided under this contract is a total system, free flight representation based on the Sikorsky General Helicopter (Gen Hel) Flight Dynamics simulation. It is defined at a uniform level of sophistication currently considered appropriate for handling qualities evaluations. This model is also considered to give representative performance trends, but should not be used to define critical performance characteristics. The modular format presented facilitates the introduction of additional or more sophisticated modules.

Volume I of this report documents the basic BLACK HAWK mathematical model, and in addition, defines supportive routines developed by Sikorsky under this contract. These routines include a landing interface, power unit, ground effects and rotor gust penetration models. Presented in this volume is an Overview of the Simulation Model, Section 3, followed by a Description of the BLACK HAWK helicopter in Section 4. Section 5 contains the documentation of the Simulation modules. Each of the module definitions is segregated with its own Table of Contents. Section 6 contains information defining the BLACK HAWK cockpit relevant to pilot-in-the-loop simulation. A single copy Appendix to Volume I, containing extensive program verification data generated from a similar model on the Sikorsky Simulation Facility, provides NASA and Sikorsky with the necessary information for validating the BLACK HAWK helicopter simulation on the Ames Simulation facility.

Volume II of this report documents,the derivation of the equations, the assumptions inherent in the model and provides supportive discussion to aid in the understanding of the mathematical model.

3.0 OVERVIEW OF THE SIMULATION MODEL

The mathematical model of BLACK HAWK provided under this contract is based on the Sikorsky General Helicopter (Gen Hel) Flight Dynamics Simulation. This model is a generalized, modularized analytical representation of a total helicopter system. It normally operates in the time domain and allows the simulation of any steady or maneuvering flight condition which can be experienced by a pilot.

The overall structure of the model is presented on figures 3.1 and 3.2 in functional and block diagram format respectively. The solution in terms of aircraft motion is obtained iteratively by summing the component forces and moments acting at the aircraft's center of gravity and subsequently obtaining the body axes accelerations. Resulting velocities and displacements then condition the environment for the components on the next pass through the program. The datum axes system used are a set of right coordinate body axes with the origin at the fuselage center of gravity. The X axis points towards the nose of the aircraft and is parallel to the center line of the aircraft. All calculations are related to this axis system. The final aircraft motion is transferred into earth axes for simulator, VFR display and instrumentation drives. The mathematical module defining the equations of motion are presented in Section 5.10.

The basic model is a total force, non-linear, large angle representation in six rigid body degrees of freedom. In addition, rotor rigid blade flapping, lagging and hub rotational degrees of freedom are represented. The latter degree of freedom is coupled to the engine and fuel control. Motion in the lag degree of freedom is resisted by a non-linear lag damper model.

The total rotor forces and moments are developed from a combination of the aerodynamic, mass and inertia loads acting on each simulated blade. The rotor aerodynamics are developed using a blade element approach. The angle of attack and dynamic pressure on individual blade segments are determined from the three orthogonal velocity components. These arise as a result of airframe motion, rotor speed, blade motion and downwash resulting from the generation of thrust. In the latter case, which represents the air mass degree of freedom, a uniform downwash is derived from momentum considerations, passed through a first order lag, and then distributed first harmonically as a function of rotor wake skew angle and the aerodynamic hub moment. Finally, blade geometric pitch is summed with the inflow angle of attack to obtain the total angle of attack at the blade segment. The full angle of attack range for blade aerodynamics is represented as a function of Mach number.

Blade inertia, mass and weight effects are fully accounted for and their resulting loads, dependent on blade and aircraft motion, are added to the aerodynamic loads for each blade. This summation gives the shear loads on the blade root hinge pins. Total rotor forces are obtained by summing all the blade hinge pin shears with regard to azimuth. Rotor moments result from the offset of the hinge shears from the center of the shaft. Blade flapping and lagging motion is determined from aerodynamic and inertia moments about the hinge pins. During one pass through the program all segments and all simulated blades are computed. If because of execution time considerations the simulated number of blades are not made equal to the actual number, then they are redistributed in azimuth accordingly. The mathematical module defining the rotor is presented in Section 5.1.

The fuselage is defined by six component aerodynamic characteristics which are loaded from wind tunnel data which have been extend analytically to large angles. The angle of attack at the fuselage is developed from the free stream plus interference effects from the rotor. These interference effects are based on rotor loading and rotor wake skew angle. Local velocity effects are not accounted for. The mathematical module defining the fuselage is presented in Section 5.2.

The aerodynamics of the empennage are treated separately from the forward airframe. This separate formulation allows good definition of non-linear tail characteristics that would otherwise be lost in the simplifications of multivariate total aircraft maps. With this approach, changes to the empennage can be made without reloading basic airframe maps. The angles of attack at the empennage are developed from the free stream velocity, plus rotor wash and airframe wash. Dynamic pressure effects from the airframe are accounted for by factoring the free stream velocity component. By necessity the wash and dynamic pressure effects are averaged over the stabilizing surfaces. The tail rotor is represented by the linearised closed form Bailey theory solution. Terms in tip speed ratio greater than μ squared have been eliminated. The airflow encounted by the tail rotor is developed in the same manner as the empennage. An empirical blockage factor, due to the proximity of the vertical tail, is applied to the thrust output. The mathematical modules defining the Empennage and tail rotor are presented in Sections 5.3 and 5.4 respectively.

The flight control system for BLACK HAWK presented in this model covers the primary mechanical flight control sytem and the Automatic Flight Control System (AFCS). The latter incorporates the Stability Augmentation System (SAS), the Pitch Bias Actuator (PBA), the Flight Path Stabilization (FPS) and the Stabilator mechanization. These automatic control functions collectively enhance the stability and control characteristics of the BLACK HAWK. The analytical definition of the control system given in Section 5.5 incorporates the Sensors, shaping networks, logic switching, authority limits and actuators. Some of these components have wide band-widths which are beyond the frequencies normally associated with piloted simulation. They have been included for completeness and accuracy in analytical evaluations. The model provided represents the control system in a complete manner except for the FPS. In this case only the attitude hold and turn features have been defined.

The engine/fuel control model provided with this simualtion is a linearized representation with coefficients which vary as a function of engine operating condition. The model adequately provides for closing the rotor shaft speed loop throughout the normal operating envelope of the helicopter. However, maneuvers which result in significant rotor speed excursions may result in discrepancies in the simulation. This engine module should not be used for engine performance evaluation. The modular formulation does however, facilitates the introduction of a sophisticated model if necessary at a later time. The interface of the engine with the rotor module, shown on Figure 3.3, is via the rotor clutch. This is programmed to disengage the rotor shaft from the engine if rotor required torque drops below zero. Under these circumstances, the engine speed feedback to the fuel control will cause the engine to seek an operating condition dictated by the control. The clutch will reengage when the rotor speed drops below power turbine speed. The engine fuel control equations are presented in Section 5.6.

The landing interface module, Section 5.7, allows for ground contact. It is a generalized representation consisting of a landing gear force reaction model complete with all necessary space/body geometry calculations to track a free helicopter during a landing onto level ground. The landing gear is represented by separate non-linear tire and strut dynamic characteristics. Tire in-ground-plane loads are developed as a non-linear function of the tire deflection and normal load. These forces are adjusted depending on the friction criteria which determines tire skid properties at the ground plane. The strut is simulated by an isentropic air spring and velocity squared damper in parallel. The output loads from the three landing gears are finally transferred to the center of gravity where they are summed with other external forces and moments.

Section 5.8 defines a simplified ground effects model. During the development of this module it was evident that anything more than a simple model based empirically on distance above the ground plane, was beyond the scope of this contract. The model provided, adjusts the downwash at the rotor (and therefore rotor loads) as a function of height above the ground plane and forward speed (in terms of rotor wake skew angle).

The gust penetration routine documented in Section 5.9 provides for a gust front passing across the rotor disc from any direction. Behind the front, gust velocities are varied with distance from the front. The variation can be prescribed by a choice of several discrete velocity profiles or a continuous turbulence form due to Dryden. Each rotor blade element and the aerodynamic centers of fuselage and tail components may be subjected to horizontal and vertical gust velocities whose magnitude is a function of the geometric distance from the traversing gust front. Thus penetration or velocity distributional effects are almost fully accounted for in the rotor simulation and are adequately dealt with in the fuselage/tail model.

GENHEL FLIGHT DYNAMICS SIMULATION

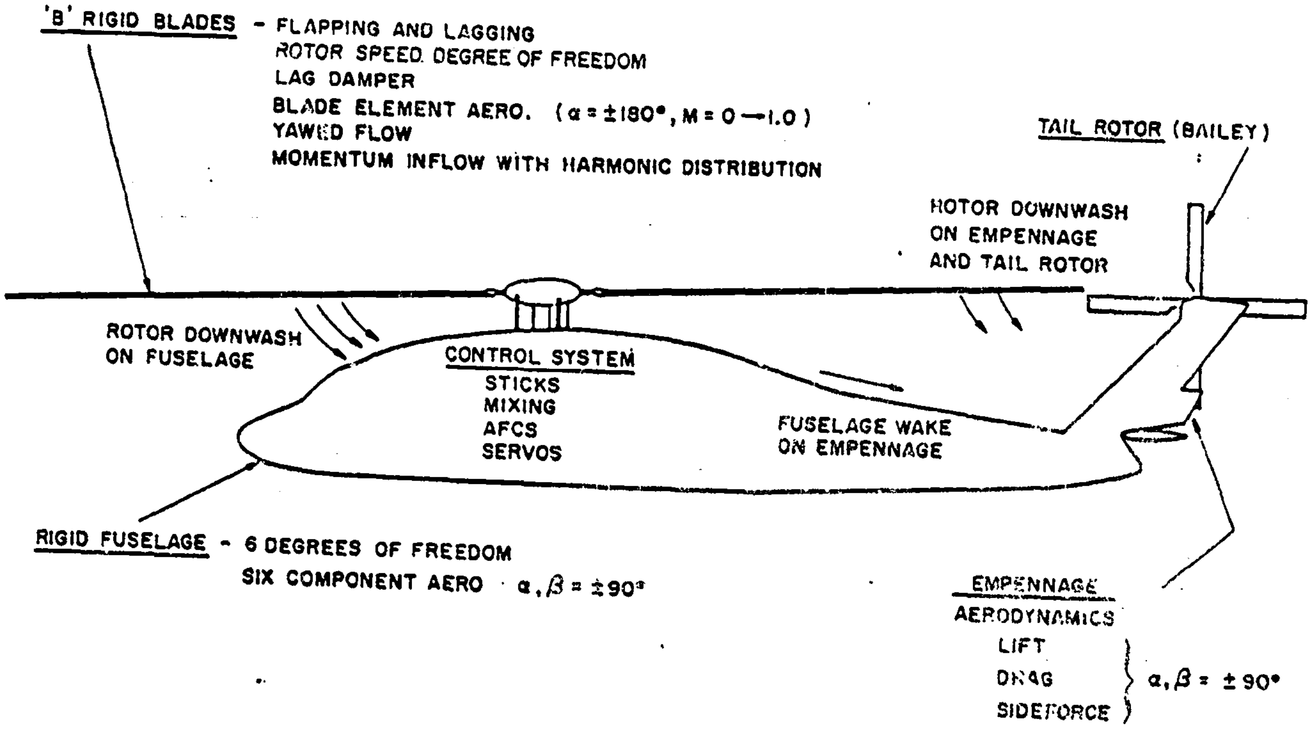

FIGURE 3.1

DOCUMENT NO. SER 70452

GEN. HEL. FLIGHT DYNAMICS SIMULATION MODEL

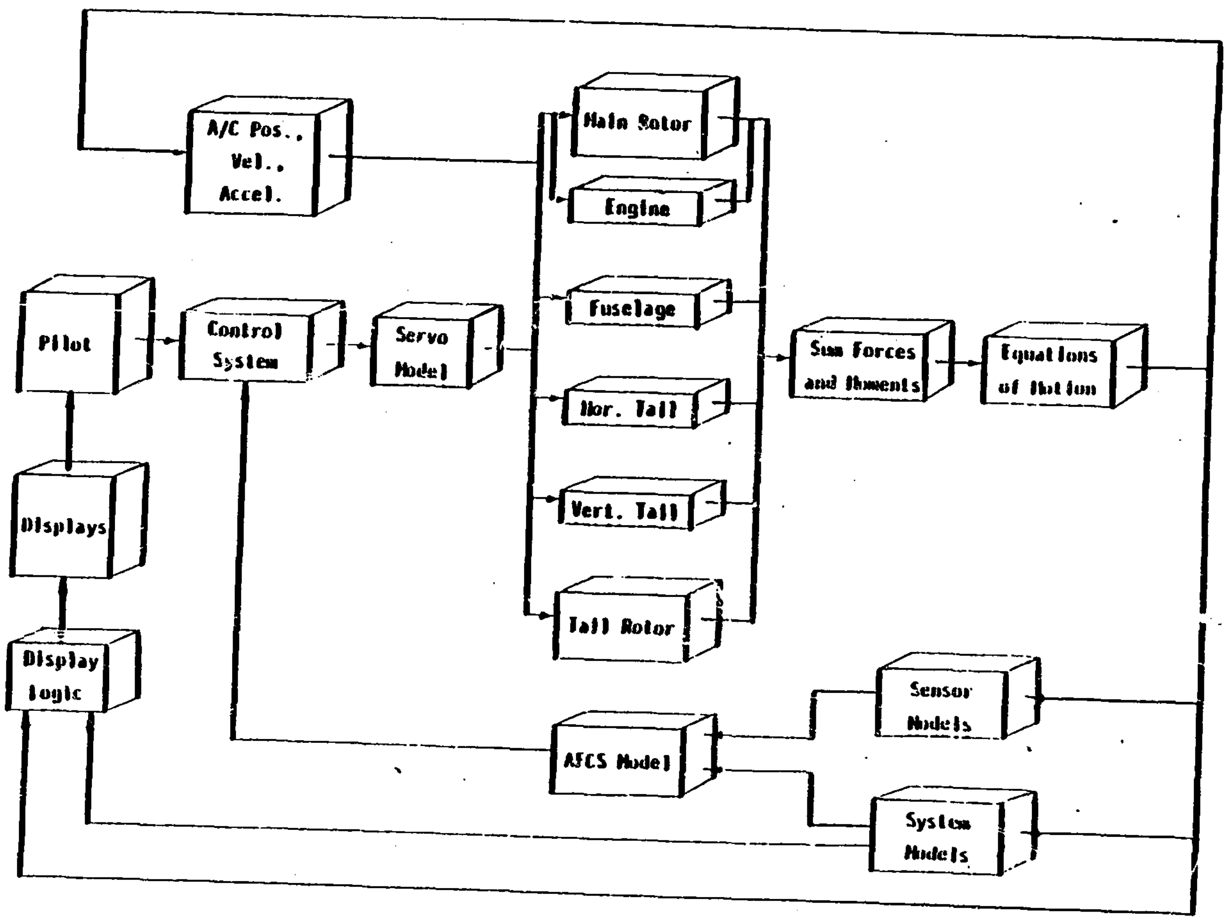

Figure 3.2

ENGINE INTEGRATION INTO GEN HEL

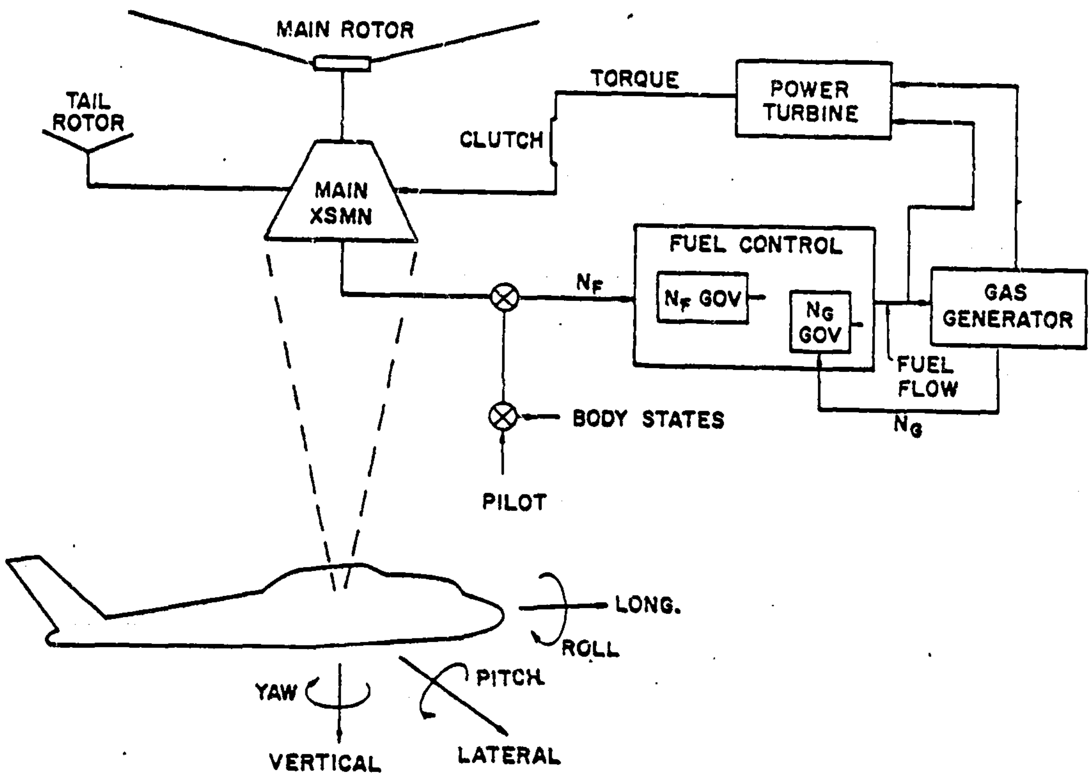

FIGURE 3.3

4.0 Description of the BLACK HAWK Helicopter

The UH-60A BLACK HAWK, shown in the figures 4.1 and 4.2, is a utility transport helicopter developed by Sikorsky for the Army under the UTTAS program. This medium-sized helicopter is designed to carry eleven combat-equipped troops and a crew of three. The Basic Structural Design Gross Weight is 16,825 lbs. with a maximum Alternate Gross Weight of 20,250 pounds. Missions include: Troop Assault, Aeromedical Evacuation, Aerial Recovery and Extended Range Missions. The BLACK HAWK has a maximum level flight speed in excess of 160 knots and a diving speed in excess of 170 knots.

The BLACK HAWK has a single main rotor and a canted tail rotor as shown on the general arrangement drawing, figure 4.3. A list of physical characteristics is given on Table 4.1. The main rotor consists of four fully articulated titanium/fiberglass blades which are retained by a flexible elastomeric bearing in a forged titanium single piece hub and restrained in plane by a conventional hydraulic lag damper. The 11.0 feet diameter four bladed tail rotor is a bearing-less cross-beam arrangement with the shaft tilted 20 degrees upwards. Both rotors have an SC 1095 aerofoil section. The aircraft is powered by two General Electric Company, T 700-GE-700 engines mounted on top of the cabin which together provide approximately 2,800 h.p. at normal continuous rating. These engines have Hamilton Standard hydraulic, and General Electric Company electronic fuel control components. The drive system consists of main, intermediate, and tail gear boxes with interconnecting shafts.

The flight control system on the BLACK HAWK is a redundant hydro-electrical-mechanical system. It includes three two stage main rotor servos, a Stability Augmentation System (SAS), a Flight Path Stability System (FPS), and a triple redundant hydraulic supply. The horizontal tail rotates from a positive angle of about 40° in hover up to zero with increasing forward speed.

A summary of the mass properties characteristics is given on Table 4.2. Recommended overall longitudinal center of gravity limits are given on figure 4.4.

A more comprehensive description of the BLACK HAWK helicopter is given in References 4.1.1, 4.1.2, and 4.1.3.

4.1 References

4.1.1 Flight International, Week Ending 25 February 1978, Article by Mark Lambert.

4.1.2 U.S. Army UH-60A Helicopter Development Production Program. Prime Item Development Specification (PIDS) DARCOM-CP-2222-S1000D Part I October 15, 1979.

4.1.3 UH-60A Familiarization Training Course Manual - Sikorsky Training Document.

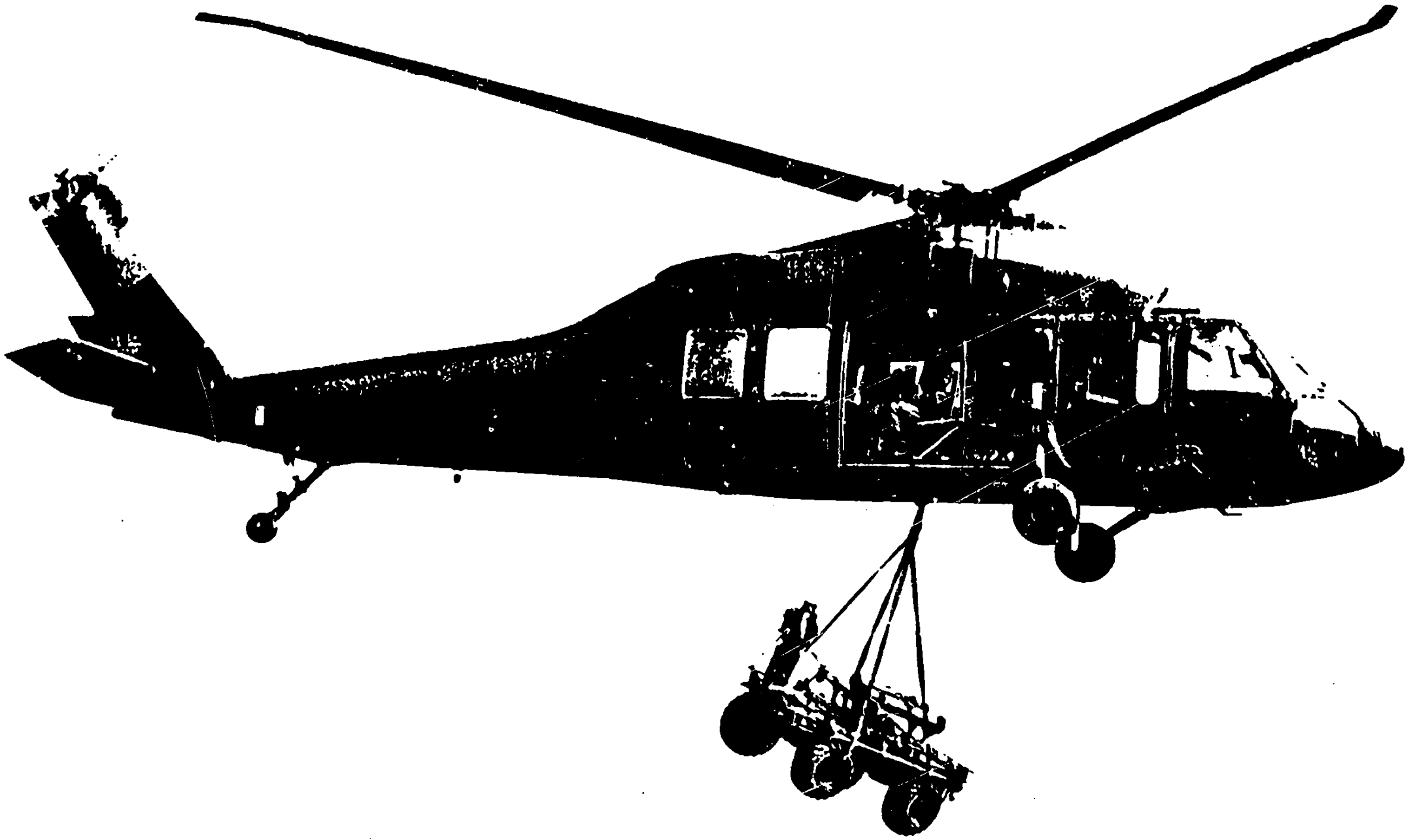

UH-60A BLACK HAWK HELICOPTER

FIGURE 4.1

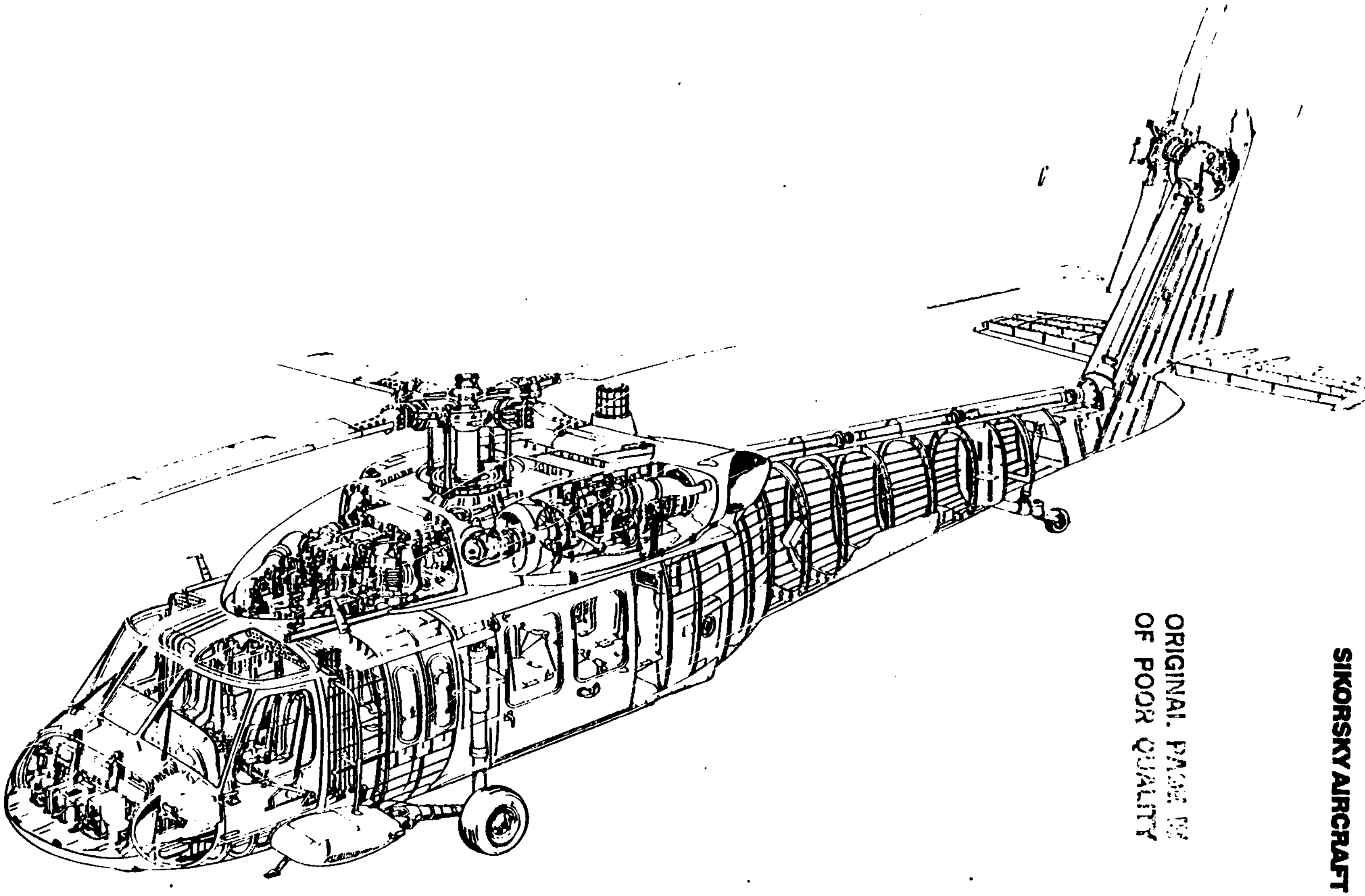

UH-60A BLACK HAWK

FIGURE 4.2

ORIGINAL PAGE IS
OF POOR QUALITY

SIKORSKY AIRCRAFT
Division of UNITED TECHNOLOGIES

ORIGINAL PAGE IS OF POOR QUALITY

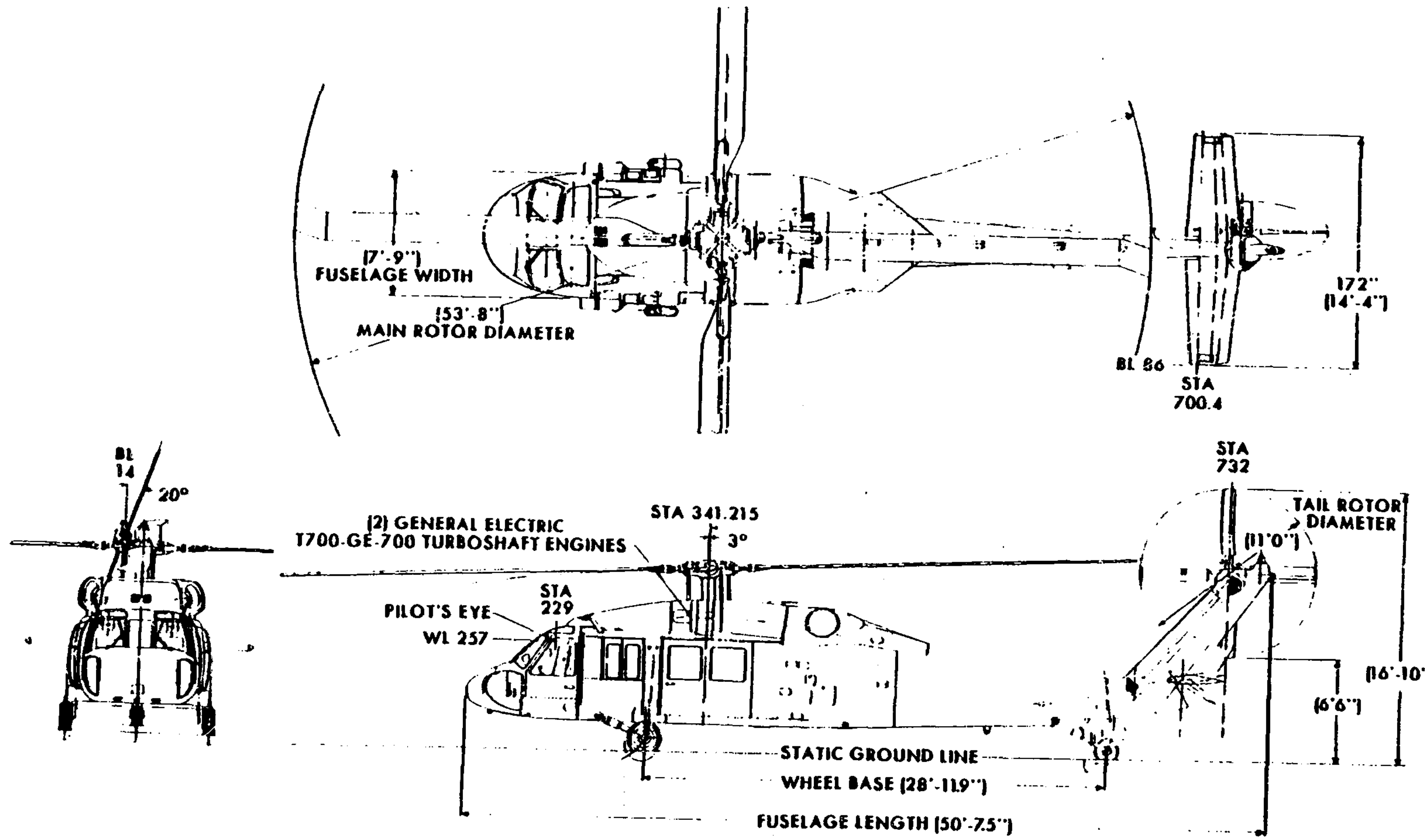

UH-60A BLACK HAWK GENERAL ARRANGEMENT

FIGURE 4.3

UH-60A BLACK HAWK RECOMMENDED LONGITUDINAL CENTER OF GRAVITY LIMITS

(DATA FROM SER-70288 PREPARED UNDER CONTRACT DAAJ01-77-C-0001(P6A)

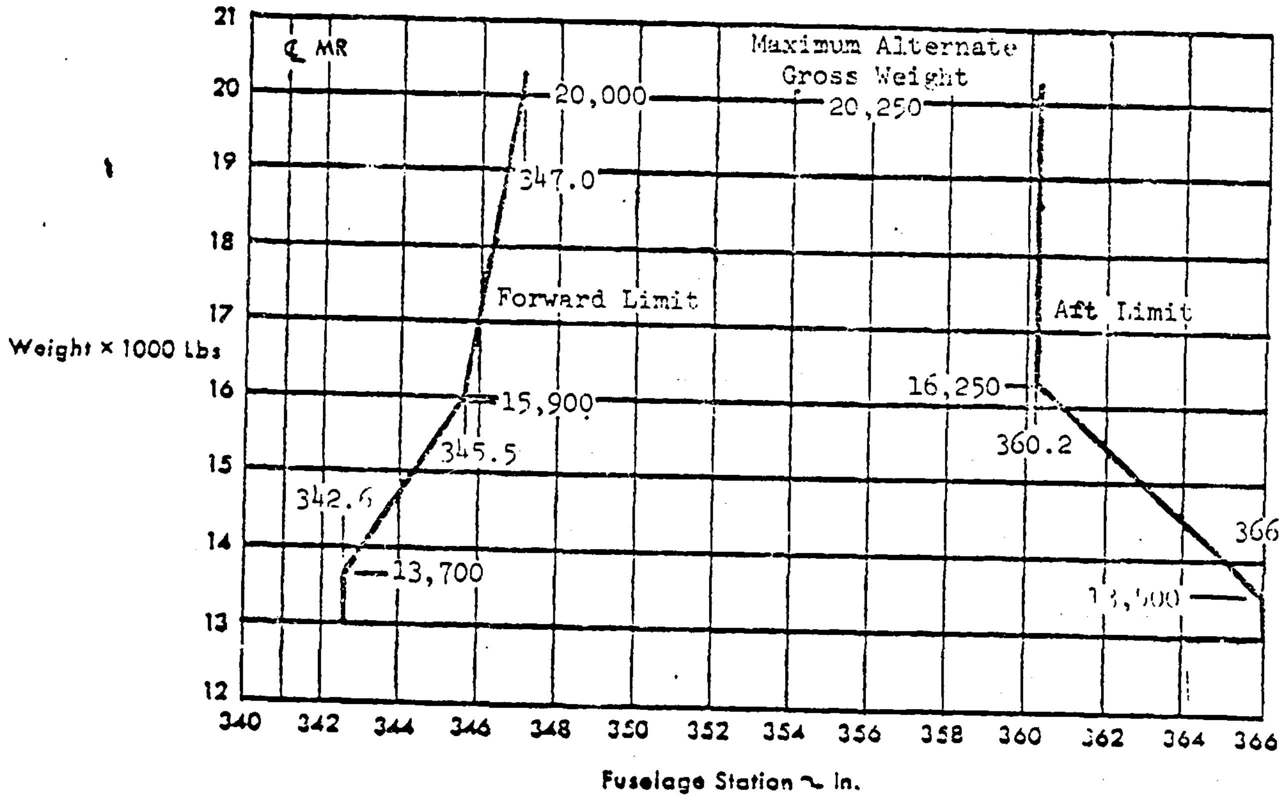

FIGURE 4.4

BLACK HAWK

TABLE 4.1. LIST OF PHYSICAL CHARACTERISTICS

MAIN ROTOR

Diameter	53.67
Blades	4
Chord	1.75 ft.
Airfoil	SC 1095
Blade Area	186.8 ft^2
Solidity	.0826
Tip Sweep	20 Deg.
Twist	-18 Deg.
Shaft Angle	3 Deg.

TAIL ROTOR

Diameter	11 ft.
Blades	4
Chord	.81 ft.
Airfoil	SC 1095
Blade Area	17.82 ft^2
Solidity	.1875
Twist	-18 Deg.
Cant Angle	20 Deg.

HORIZONTAL STABILATOR

Span	14.38 ft.
Area	45 ft^2
Root Chord	3.67 ft.
Tip Chord	2.54 ft.
Sweep ($\frac{1}{4}$C)	0 Deg.
Aspect Ratio	4.6
Airfoil	NACA 0014
Incidence/Dihedral	0 Deg.

VERTICAL STABILIZER

Span	8.167 ft.
Area	32.3 ft^2
Root Chord	6 ft.
Tip Chord	2.83 ft.
Sweep ($\frac{1}{4}$C)	41 Deg.
Aspect Ratio	1.92
Airfoil	NACA 0021 (Mod)

GENERAL

Overall Length	64.83 ft.
Fuselage Length	50.06 ft.
Wheel Tread	8.88 ft.
Wheel Base	28.93 ft.

ORIGINAL PAGE IS
OF POOR QUALITY

SIKORSKY AIRCRAFT UNITED TECHNOLOGIES

DOCUMENT NO. SER 70452

BLACK HAWK

TABLE 4.2. SUMMARY OF MASS PROPERTIES CHARACTERISTICS

		CENTER OF GRAVITY POSITION		MOMENT OF INERTIA Lb-In-Sec^2			
CONDITION	WEIGHT	STA	WL	I_{xx}	I_{yy}	I_{zz}	I_{xz}
Design Mission - Troops	16000.9	358.0	251.0	65550	473626	442646	18886
Aeromedical Mission	15479.3	359.0	251.1	64058	475389	441954	19510
Aerial Recovery Mission	20250.0	359.6	234.7	100200	502116	430804	22130
Extended Range Mission	19193.7	352.5	245.1	74633	502044	461813	28076
Basic Structural Design-Fwd.	16330.9	345.7	248.3	71141	500923	465328	34144
Basic Structural Design-Aft	16330.9	360.2	249.5	68263	465774	432719	18268
Maximum Alternate GW-Fwd	20250.0	347.1	244.4	79532	514803	479012	33850
Maximum Alternate GW-Aft	20250.0	360.2	245.1	77898	482141	447627	18408

(Data from SER-70288 Prepared Under Contract DAAJ01-77-C-0001(P6A)

SA 29 REV. G

SIKORSKY AIRCRAFT UNITED TECHNOLOGIES

DOCUMENT NO. SER 70452

5.1 MAIN ROTOR MODULE

CONTENTS

5.1 Main Rotor Module

5.1.1 Module Description

The main rotor model is based on a blade element analysis in which total rotor forces and moments are developed from a combination of aerodynamic, mass and inertia loads acting on each simulated blade. The blade segment set up option defined for this Black Hawk model is that of equal annuli area swept by the segment. This technique allows the number of segments to be minimized and distributes the segments towards the higher dynamic pressure areas.

The total forces acting on the blade are derived from the total acceleration and velocity components at the blade together with control inputs. Accelerations develop from body motion and blade motion. Velocity components are made up of body velocities, gust velocities, the rotor's own downwash and blade motion.

Before calculations at the blade segment can be executed several axes transformations must be implemented. Initially body axes angular and translational accelerations and velocities are transferred to the rotor hub and rotated through the shaft inclination angles i_θ and i_ϕ into rotor shaft axes. These angles with positive rotation of i_θ about the Y_H axis followed by i_ϕ about the resulting X_s axis are shown in Figure 1.1.1. The body velocities are non-dimensionalized by rotor tip speed ($\Omega_T R_T$) to conform with usual helicopter analysis practice. Motion accruing from the rotor shaft degree of freedom is derived from the engine module.

The rotor airmass degree of freedom is primarily based on a uniform downwash distribution developed from rotor thrust by application of momentum theory. This uniform downwash, which is passed through a first order lag, is modified to account for the changing distribution with forward speed and aerodynamic pitching and rolling moment loading on the rotor. In the first case the resulting uniform downwash is distributed 1st harmonically around the azimuth as a cosine function depending on the inclination of the rotor wake. The desirability of including this first harmonic distribution, which results in a uniform downwash at hover and a weighted distribution towards the aft of the rotor disc at high speed, is discussed in Reference 1.6.1. Since this effect is really dependent on the resultant velocity vector a lateral velocity term is also added. The desirability of adding a harmonic distribution of downwash depending on aerodynamic rotor moments has not been established for Black Hawk but the necessary equations are incorporated for completeness.

The remaining contribution to the velocities at the blade segment is that due to blade motion. Blade flapping and lagging velocities and angles are obtained by application of a Fourier prediction technique, rather than direct integration of acceleration. This approach is derived in Reference 1.6.2. This method although simple has been shown to be stable and accurate for the frequencies of concern in helicopter stability and control evaluations.

The blade segment total velocity components are developed in three parts. Those independent of segment position, those dependent on segment position and interference effects made up of downwash and gust effects. The velocities at the blade segments are obtained by transforming the fixed shaft vectors into the rotating hub axes system, then transferring to the blade hinge position, transforming into blade span axes through the Euler angles β (flapping) and δ (lagging) and finally transferring to the segment position on the blade. These transformations are illustrated on figure 1.1.2. These total velocity components are subsequently used to calculate the resultant velocity, local Mach number, yawed angle of attack and flow yaw angle. It should be noted that the radial component of velocity is ommitted in calculating the Mach Number which is used in the aerodynamic map look-up. Reference 1.6.3, which describes the use of simple sweep theory, indicates that Mach Number should be based on the unyawed component of flow.

The total local segment angle of attack on the blade is made up of the blade local pitch angle and the yawed angle of attack at the segment. The former is made up of the control impressed pitch (collective θ_{CUFF}, cyclic A_{1S}, B_{1S}), pitch/flap coupling (δ_3), pitch/lag coupling (α_1), preformed blade twist and a dynamic component of blade twist due to torsional elastic deformation. This emperical dynamic component is prescribed harmonically based on blade loading. The yawed angle of attack is complicated by the requirement to resolve blade pitch into the local stream direction as shown in Figure 1.1.3. The resulting equation assumes the series approximation for the tangent of blade pitch.

The treatment of the blade segment aerodynamic force calculation is completely non-linear. Lift and drag characteristics are provided for the range $-180 \leq \alpha \leq 180$. Bivariate maps as a function of angle of attack and Mach Number are used in the range $-30 \leq \alpha \leq +30$ allowing good definition of blade stall. The complete coverage of angle of attack allows good definition of aerodynamic characteristics on the retreating blade side of the disc. This is important at high advance ratios. The blade segment lift coefficient is determined by applying simple sweep theory to the unyawed blade aerodynamic data. This is rigorously applied in the linear lift range where the entry to the unyawed lift coefficient is transformed by the cosine of the yaw angle (i.e. $\alpha_{TRANS} = \alpha_Y \cos\gamma$) and the entry Mach Number is a function of the unyawed component of flow. At higher angles of attack some liberties are taken where sweep theory is not valid. These steps are taken to aviod discontinuities in blade lift data as the blade proceeds around the azimuth. Discontinuities can result in an unstable flapping and lagging solution. The application of sweep theory to the determination of drag is not well established. For this model, drag is determined by entering the drag map data with the actual yawed angle of attack. ($\alpha_{TRANS} = \alpha_Y$). A development of sweep theory can be found in Reference 1.6.3. Sikorsky evaluations of this theory, as applied to rotors, are documented in Reference 1.6.4. The map entry logic is developed in the equations. It should be noted that a tip loss factor is applied to the tip segment. Univariate and bivariate maps of blade lift and drag coefficients as a function of α_{TRANS} and Mach Number are given in Section 5.1.5. The aerodynamic segmental loads are resolved from local wind axes into blade span axes and summed along each blade to obtain root shears at the hinge. These forces are subsequently transformed into rotating shaft axes. It should be noted that β and δ are Euler angles and order of treatment must be observed. The aerodynamic moments used in the flapping and lagging motion equations are calculated at this point in the flow. Also, it is convenient to develop the aerodynamic feedbacks for the rotor downwash calculation at this time.

The blade inplane or lagging motion is restrained by a damper system. In the case of Black Hawk the damper is non-linear and the kinematics of this system are complicated by geometry. A generalized representation is utilized as presented on Figure 1.1.4. Essentially the relative positions of the pick-ups of the damper on the hub and blade are tracked. From these values an axial velocity is determined. This velocity is used to enter the map data presented in Section 5.1.5. The output of this map, which is an axial force, is multiplied by the instantaneous moment arm to obtain the damper moment about the hinge. Although flapping restraint equations are included they will not be activated for Black Hawk.

The contributions to the lagging and flapping motion about the hinge are the aerodynamic moments, the hinge restraint moments and the inertia moments. The aerodynamic and hinge restraint components have been previously discussed. The inertia components have been explicitly introduced into the flapping and lagging equations of motion. It should be noted that lagging motion takes place in an intermediate set of blade span axes because of the definition of the Euler angles. Also small terms have been eliminated from these equations. A software provision to inhibit the lagging degree of freedom has been incorporated.

Before the final shear forces and hub moments can be developed it is necessary to calculate the inertia shear loading on the hinge pins. Again small terms have been eliminated. Subsequent to these calculations the three component total shears at the hinge are determined and the total rotor forces in fixed shaft axes at the hub center developed. The rotor hub moments result from a combination of the shear forces at the hinge pins and moments from the blade hinge restraint. An arithmetic manipulation of the equations is introduced on these final equations which allow the simulated blades to be different from the actual number. This artifice is intended for use in piloted simulation where computer execution time is critical. With the lagging degree of freedom operating, the major portion of rotor torque is developed through the lag damper. Therefore, if lagging degree of freedom is selected out, an alternative equation containing the aerodynamic moment must be introduced as specified.

The oscillating nature of the rotor forces and moments make it expedient to filter the outputs under some circumstances. A simple first order filter is used. The final rotor forces and moments are obtained by transforming the filtered shaft axes forces and moments into body axes with the origin at the center of gravity. These are eventually summed with other component outputs to give the total external forces and moments at the center of gravity.

It is necessary to make provision in these final rotor outputs for the option of selecting to run with the engine module in or out. If the engine is selected out, perfect rotor speed governing is assummed and the shaft torque reaction on the airframe is assummed equal to rotor required torque. If the engine module is activated then its output torque is introduced into the airframe.

Finally, the rotor wake skew angle is determined. This is the angle that the center line of the rotor wake makes with the rotor shaft. It is the dependent parameter used to establish the variation of rotor wash on the fuselage, wing and tail.

The sequencing of the program flow in the main rotor is critical and should follow the equation flow in Section 5.1.2.

A block diagram of the Main Rotor Module is given on figure 1.1.5. All input data for the Black Hawk Main Rotor is specified in Section 5.1.5.

BODY AXES TO SHAFT AXES TRANSFORMATION

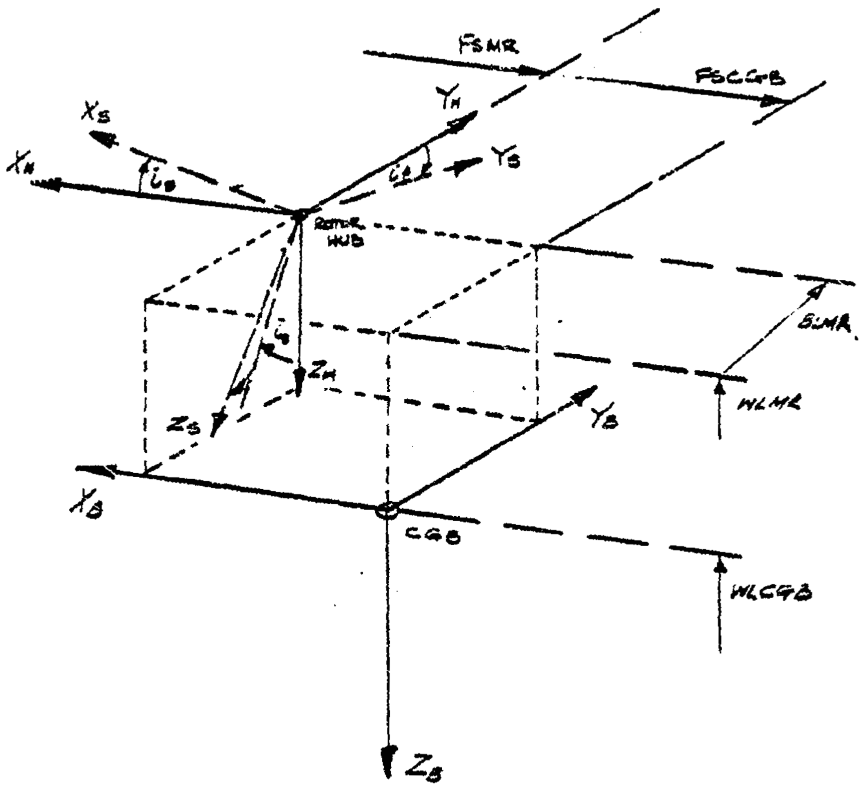

X_B, Y_B, Z_B Body Axes System
X_H, Y_H, Z_H Hub Axes System
X_S, Y_S, Z_S Shaft Axes System

FIGURE 1.1.1

SHAFT AXES TO ROTATING BLADE SPAN AXES TRANSFORMATION

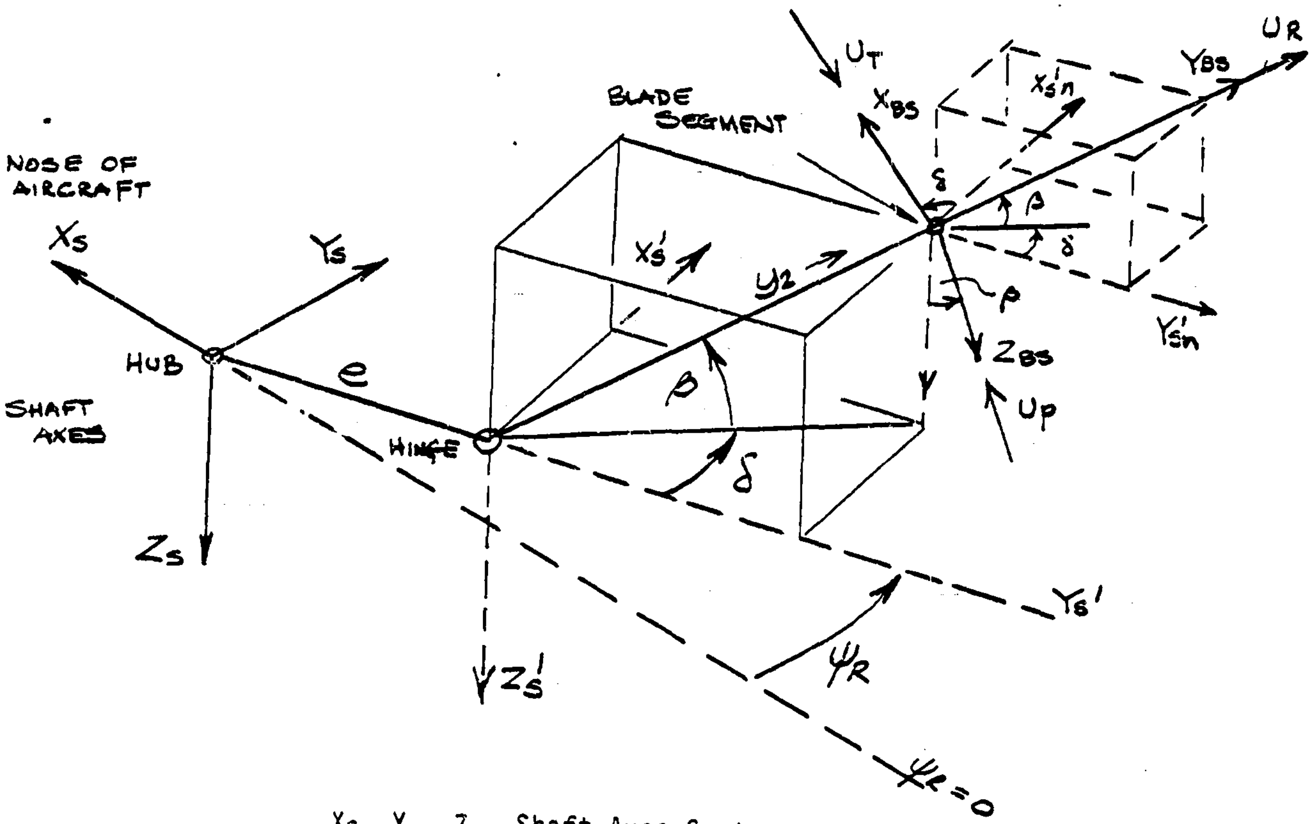

X_S, Y_S, Z_S Shaft Axes System
X_S', Y_S', Z_S' Rotating Shaft Axes System
X_{BS}, Y_{BS}, Z_{BS} Blade Span Axes System

U_T, U_R, U_P Blade Element Velocities Along X_{BS}, Y_{BS}, Z_{BS} Respectively

δ and β are Euler Angles with δ Rotation about Z_S' then β Rotation About X_{BS}.

FIGURE 1.1.2

DEFINITION OF YAWED ANGLE OF ATTACK

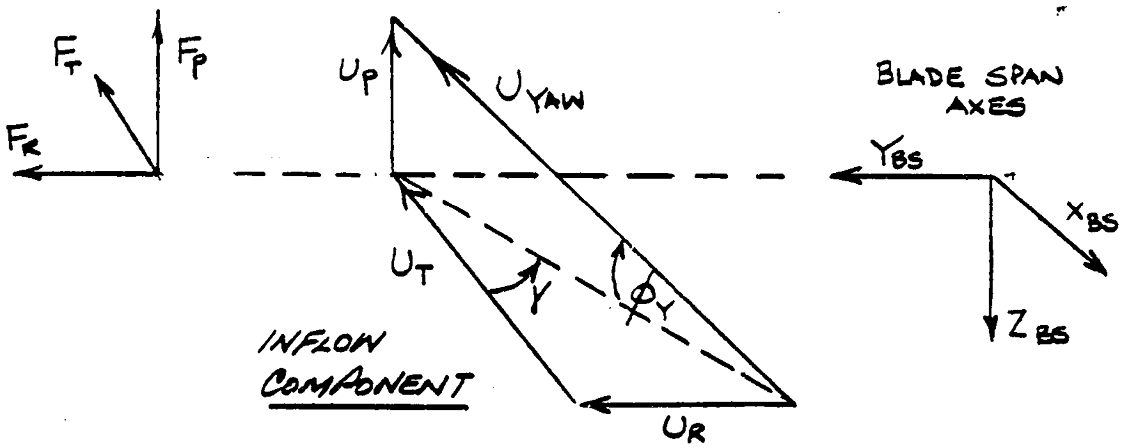

TOTAL YAWED ANGLE OF ATTACK = $\phi_Y + \theta_Y$

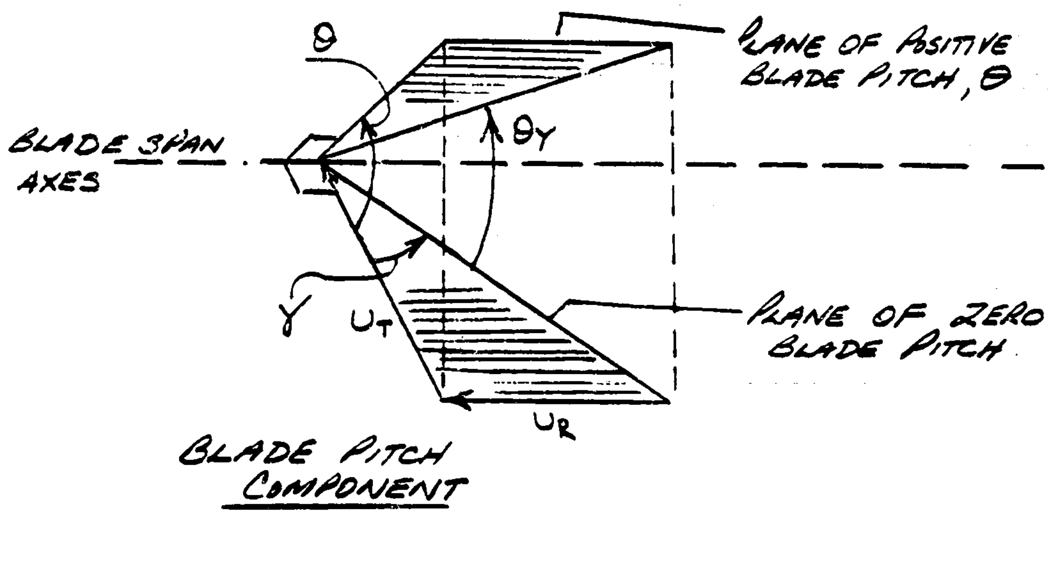

FIGURE 1.1.3

LAG DAMPER KINEMATIC GEOMETRY

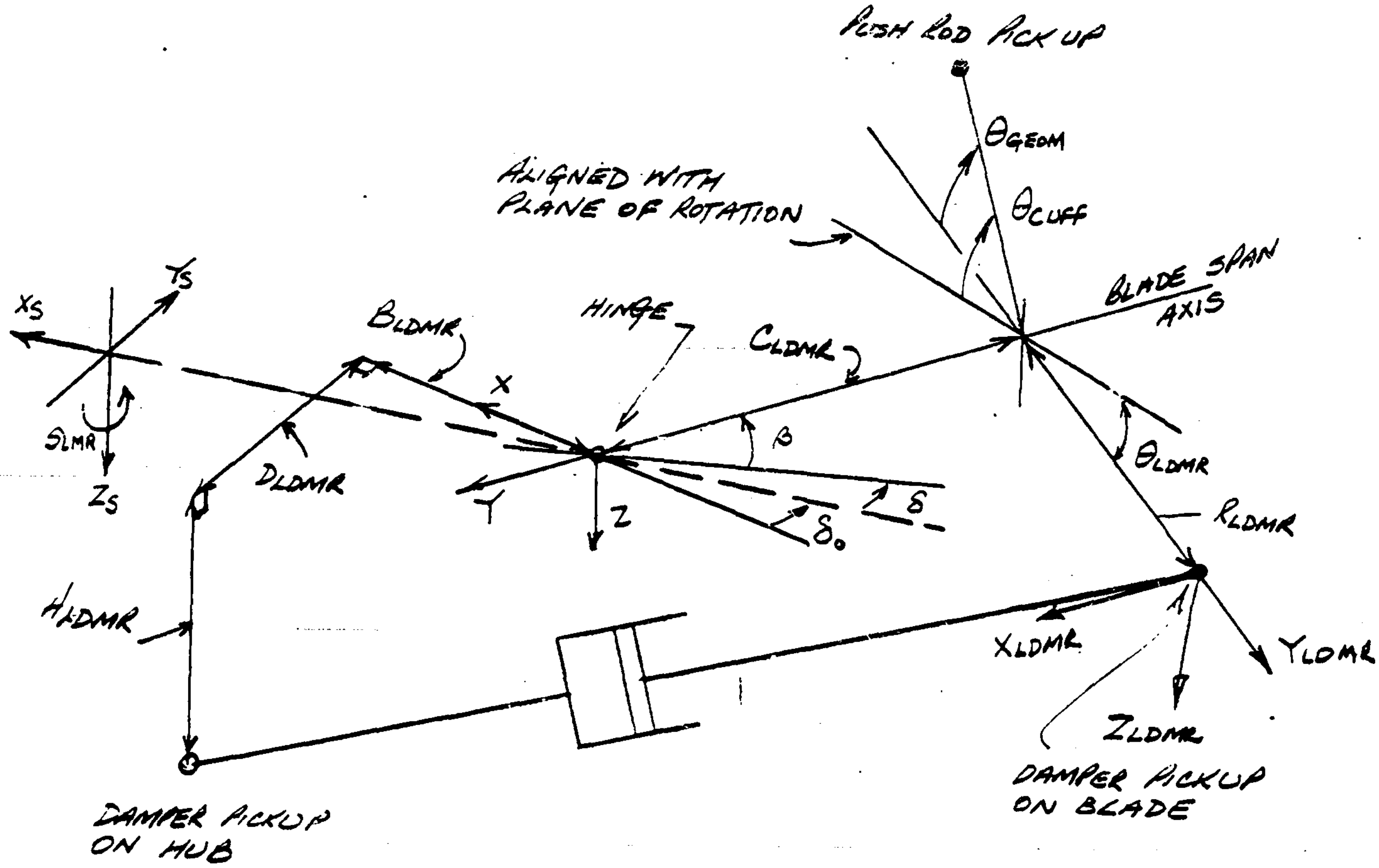

$(XYZ)_{LDMR}$ Lag Damper Axes

X_{LDMR} Aligned with the blade span

and $(Y,Z)_{LDMR}$ rotated through Θ_{LDMR}

FIGURE 1.1.4

MAIN ROTOR FLOW DIAGRAM

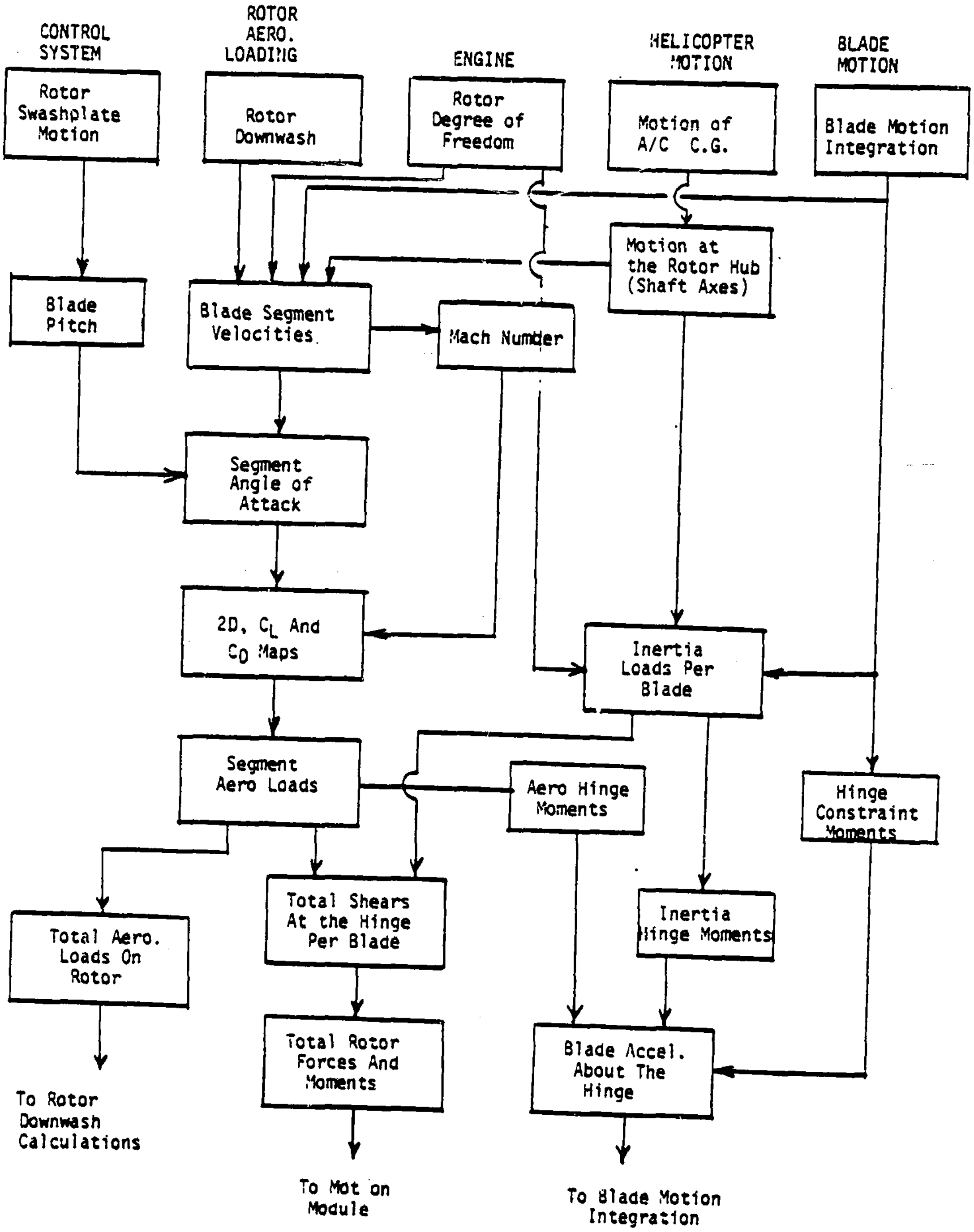

FIGURE 1.1.5

5.1.2 MAIN ROTOR MODULE EQUATIONS

BLADE GEOMETRY

BLADE SEGMENTS BASED ON EQUAL ANNULII AREA

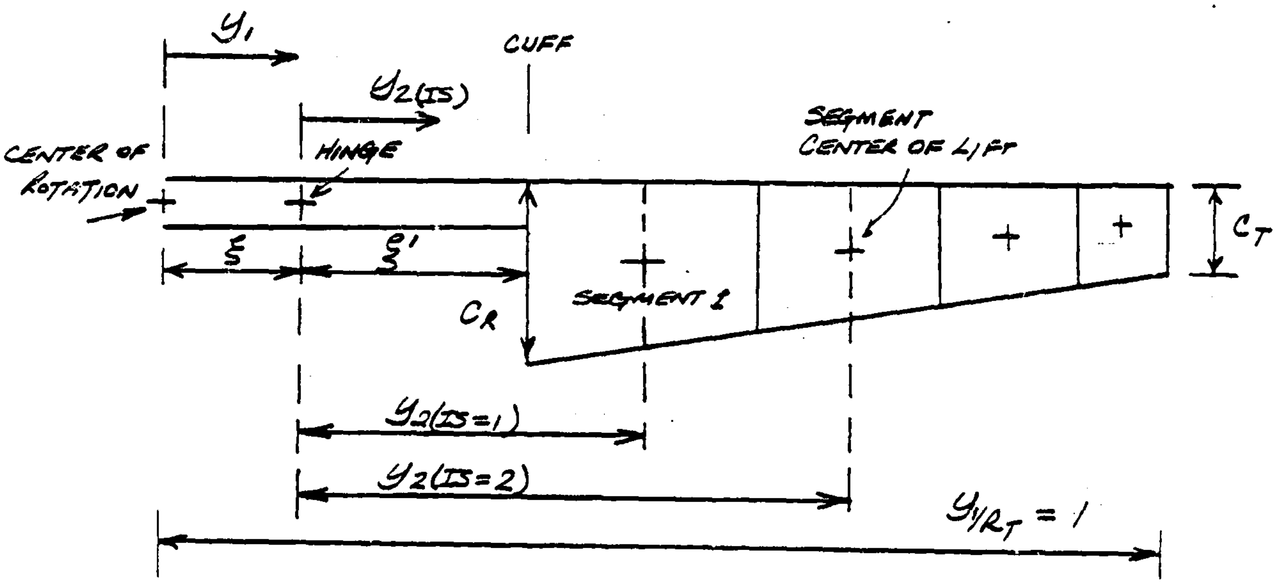

HINGE OFFSET (KSGMR) $\xi = e/R_T$ NORMALIZED BY R_T

SPAR LENGTH $\xi' = e'/R_T$ NORMALIZED BY R_T

ACTUAL BLADE LENGTH $= 1-\xi-\xi'$ NORMALIZED BY R_T

SEGMENT MIDPOINT FOR FIRST SEGMENT (NORMALIZED) (KMRBK)

$$y_{2_{IS=1}} = \left\{\left[\frac{1-(\xi+\xi')^2}{2N_{SS}}\right] + (\xi+\xi')^2\right\}^{1/2} - \xi$$

NOTE. THE COMPUTER PROGRAM MNEMONICS FOR THE RHS OF THE EQUATIONS ARE INDICATED THUS (- - -).

SUBSEQUENT MIDPOINTS
$$y2_{(IS=2 \cdots NSS)} = \left\{ \left[\frac{1-(\xi+\xi')^2}{N_{SS}} \right] + \left(\xi + y2_{(IS-1)}\right)^2 \right\}^{1/2} - \xi$$

SEGMENT WIDTH
$$\Delta y_{IS} = \left[y_{OUTB_{IS}} - y_{INB_{IS}} \right]$$

WHERE
$$y_{OUTB_{IS}} = \left\{ (y2_{IS} + \xi)^2 + \left(\frac{1-(\xi+\xi')^2}{2 \cdot N_{SS}} \right) \right\}^{1/2}$$

$$y_{INB_{IS}} = \left\{ (y2_{IS} + \xi)^2 - \left(\frac{1-(\xi+\xi')^2}{2 \cdot N_{SS}} \right) \right\}^{1/2}$$

SEGMENT MEAN CHORD (FT)
$$C_{y_{IS}} = \left[\frac{(C_T - C_R)}{(1-\xi-\xi')} \cdot \left(\frac{y_{OUTB_{IS}} + y_{INB_{IS}} - 2(\xi+\xi')}{2} \right) \right] + C_R$$

SEGMENT AREA $(FT)^2$
$$S_{y_{IS}} = R_T \left(C_{y_{IS}} \right) \left(y_{OUTB_{IS}} - y_{INB_{IS}} \right)$$

EFFECT OF ROTOR BLADE WEIGHT ON CG POSITION

$$W_{BD} = WEIGHT - b\,W_b$$

$$FSCGB = \frac{(WEIGHT \cdot FSCG - b \cdot W_b\, FSMR)}{W_{BD}}$$

$$WLCGB = \frac{(WEIGHT \cdot WLCG - b \cdot W_b\, WLMR)}{W_{BD}}$$

$$BLCGB = \frac{(WEIGHT \cdot BLCG - b \cdot W_b\, BLMR)}{W_{BD}}$$

TRANSLATIONAL ACCELERATIONS AT THE ROTOR HUB (BODY AXES)

$$\dot V_{XH} = \dot V_{Xb} - r V_{Yb} + q V_{Zb} - X_H(q^2+r^2) + Y_H(pq - \dot r) + Z_H(pr + \dot q) + g_x$$
(VXH.MK)

$$\dot V_{YH} = \dot V_{Yb} - p V_{Zb} + r V_{Xb} + X_H(pq + \dot r) - Y_H(p^2+r^2) + Z_H(qr - \dot p) + g_y$$
(VYH.MK)

$$\dot V_{ZH} = \dot V_{Zb} + p V_{Yb} - q V_{Xb} + X_H(pr - \dot q) + Y_H(qr + \dot p) - Z_H(p^2+q^2) + g_z$$
(VZH.MK)

WHERE

$$g_x = g \sin\Theta_b$$

$$g_y = -g \sin\phi_b \cos\Theta_b$$

$$g_z = -g \cos\phi_b \cos\Theta_b$$

THESE ARE WEIGHT VECTORS ADDED FOR CONVENIENCE AT THIS POINT

$$X_H = (FSCGb - FSMR)/12$$

$$Y_H = (BLCGb - BLMR)/12$$

$$Z_H = (WLCGb - WLMR)/12$$

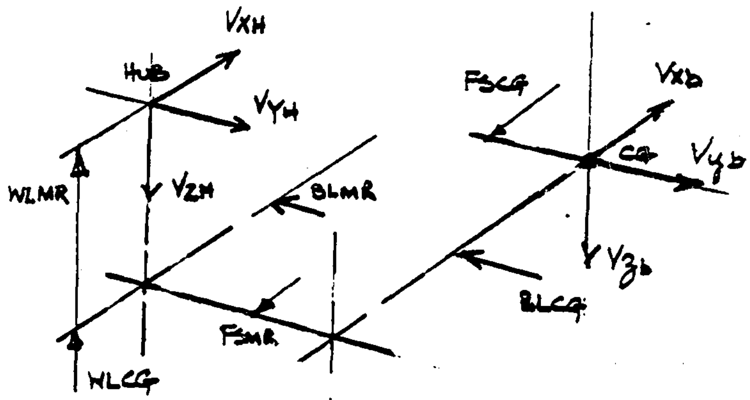

TRANSLATIONAL VELOCITIES AT THE ROTOR HUB (BODY AXES)

$$\mu_{XH} = \frac{1}{\Omega_T R_T}\left\{V_{Xb} + V_{Xg} + q.Z_H - r.Y_H\right\}$$
(MUXHMK)

$$\mu_{YH} = \frac{1}{\Omega_T R_T}\left\{V_{Yb} + V_{Yg} + r.X_H - p.Z_H\right\}$$
(MUYHMK)

$$\mu_{ZH} = \frac{1}{\Omega_T R_T}\left\{V_{Zb} + V_{Zg} - q.X_H + p.Y_H\right\}$$
(MUZHMK)

BODY TO SHAFT AXES TRANSFORMATION MATRIX

$$[A_{BDSH}] = \begin{bmatrix} \cos i_\theta, & 0, & -\sin i_\theta \\ \sin i_\theta \sin i_\phi, & \cos i_\phi, & \cos i_\theta \sin i_\phi \\ \sin i_\theta \cos i_\phi, & -\sin i_\phi, & \cos i_\theta \cos i_\phi \end{bmatrix}$$

NOTE i_θ AND i_ϕ ARE EULER ANGLES WITH POSITIVE ROTATION OF i_θ ABOUT Y_H THE i_ϕ ABOUT A RESULTING X_S

BODY TRANSLATIONAL ACCELERATIONS AT THE HUB (SHAFT AXES)

$$\begin{bmatrix} \dot{V}_{XS} \\ \dot{V}_{YS} \\ \dot{V}_{ZS} \end{bmatrix} = [A_{BDSH}] \begin{bmatrix} \dot{V}_{XH} \\ \dot{V}_{YH} \\ \dot{V}_{ZH} \end{bmatrix} \quad \begin{matrix} ,(VXS.MR) \\ ,(VYS.MR) \\ ,(VZS.MR) \end{matrix}$$

BODY ANGULAR ACCELERATIONS AT THE HUB (SHAFT AXES)

$$\begin{bmatrix} \dot{p}_S \\ \dot{q}_S \\ \dot{r}_S \end{bmatrix} = [A_{BDSH}] \begin{bmatrix} \dot{p} \\ \dot{q} \\ \dot{r} \end{bmatrix} \quad \begin{matrix} ,(PS.MR) \\ ,(QS.MR) \\ ,(RS.MR) \end{matrix}$$

BODY TRANSLATIONAL VELOCITIES AT THE HUB (SHAFT AXES)

$$\begin{bmatrix} u_{xs} \\ u_{ys} \\ u_{zs} \end{bmatrix} = \begin{bmatrix} A_{BDSH} \end{bmatrix} \begin{bmatrix} u_{xH} \\ u_{yH} \\ u_{zH} \end{bmatrix}$$

, (MUXSMR)
, (MUYSMR)
, (MUZSMR)

BODY ANGULAR VELOCITIES AT THE HUB (SHAFT AXES)

$$\begin{bmatrix} p_s \\ q_s \\ r_s \end{bmatrix} = \begin{bmatrix} A_{BDSH} \end{bmatrix} \begin{bmatrix} p \\ q \\ r \end{bmatrix}$$

, (PSMR)
, (QSMR)
, (RSMR)

ROTOR SHAFT SPEED DEGREE OF FREEDOM

$$OMG.MR = \Omega_T \left(\frac{\dot{\Omega}}{\Omega_T}\right), \quad \left(\frac{\dot{\Omega}}{\Omega_T}\right) \equiv OMR.MR$$

$$OMGMR = \Omega_T \left(\frac{\Omega}{\Omega_T}\right), \quad \left(\frac{\Omega}{\Omega_T}\right) \equiv OMRMR$$

OMR.MR, OMRMR ARE DERIVED FROM THE ENGINE MODULE IF SELECTED. IF NOT SELECTED $\Omega = \Omega_T$

ROTOR AZIMUTH UPDATE CALCULATION

IF DELPSR = 0, $\Delta\psi_R = 57.3 * \Omega * TIME$

IF DELPSR $\neq$ 0, $\Delta\psi_R = DELPSR$ TYPICALLY USED IN THE REAL TIME APPLICATION

$\psi_R = \psi_R + \Delta\psi_R$, IF $\psi_R \leq 180°$,(PSIMR)

$\psi_R = \psi_R + \Delta\psi_R - 360°$, IF $\psi_R > 180°$

SNPSMR$_1$, CSPSMR$_1$ DERIVED FROM SINCOS(ψ_R) ROUTINE FOR BLADE #1

$$SNPSMR_{IB} = \sin\left(\psi_{R\,IB-1} + \frac{360}{NBS}\right), \quad IB = 2, \text{---} NBS$$

$$CSPSMR_{IB} = \cos\left(\psi_{R\,IB-1} + \frac{360}{NBS}\right), \quad IB = 2, \text{---} NBS.$$

FLAPPING RATE AND DISPLACEMENT

$$\underset{(BRMR)}{\dot{\beta}_{IB\,(t)}} = \ddot{\beta}_{IB\,(t-1)}\left(\frac{\sin\Delta\psi_R}{\Omega}\right) + \dot{\beta}_{IB\,(t-1)}\cos\Delta\psi_R \qquad IB = 1, NBS$$

$$\underset{(BRMR)}{\beta_{IB\,(t)}} = \beta_{IB\,(t-1)} + \dot{\beta}_{IB\,(t-1)}\frac{\sin\Delta\psi_R}{\Omega} + \left(\frac{1-\cos\Delta\psi_R}{\Omega^2}\right)\ddot{\beta}_{IB\,(t-1)} \qquad IB = 1, NBS$$

$$A0FMR = \frac{57.3}{bs}\cdot\sum_{IB=1}^{NBS}\beta_{IB}$$

$$A1FMR = -2*\frac{57.3}{bs}\sum_{IB=1}^{NBS}\beta_{IB}\cos\psi_{IB}$$

$$B1FMR = -2*\frac{57.3}{bs}\sum_{IB=1}^{NBS}\beta_{IB}\sin\psi_{IB}$$

LAGGING RATE AND DISPLACEMENT

$$\underset{(LG.MR)}{\dot{\delta}_{IB\,t}} = \ddot{\delta}_{IB\,(t-1)}\left(\frac{\sin\Delta\psi_R}{\Omega}\right) + \dot{\delta}_{IB\,(t-1)}\cos\Delta\psi_R \qquad IB = 1, \cdot\cdot NBS$$

$$\underset{(LGMR)}{\delta_{IB\,t}} = \delta_{IB\,(t-1)} + \dot{\delta}_{IB\,(t-1)}\frac{\sin\Delta\psi_R}{\Omega} + \left(\frac{1-\cos\Delta\psi_R}{\Omega^2}\right)\ddot{\delta}_{IB\,(t-1)}$$

$$IB = 1, \cdot\cdot NBS$$

$$ADLMR = \frac{57.3}{b_s} \sum_{IB=1}^{NBS} \delta_{IB}$$

$$A1LMR = \frac{2*57.3}{b_s} \sum_{IB=1}^{NBS} \delta_{IB} \cos \psi_{IB}$$

$$B1LMR = \frac{2*57.3}{b_s} \sum_{IB=1}^{NBS} \delta_{IB} \sin \psi_{IB}$$

BLADE FLAPPING AND LAGGING ANGLE COEFFICIENTS

$$\left.\begin{matrix} SNBRMR_{IB} \\ CSBRMR_{IB} \end{matrix}\right\} \text{ DERIVED FROM SINCOS } (57.3\beta_{IB}) \text{ ROUTINE}$$

$$\left.\begin{matrix} SNLGMR_{IB} \\ CSBRMR_{IB} \end{matrix}\right\} \text{ DERIVED FROM SINCOS } (57.3\beta_{IB}) \text{ ROUTINE}$$

$$SNPLMR_{IB} = \sin(\psi_{IB} + \delta_{IB}) \quad , \quad IB = 1, \cdots NBS$$

$$CSPLMR_{IB} = \cos(\psi_{IB} + \delta_{IB}) \quad , \quad IB = 1, \cdots NBS$$

ORIGINAL PAGE IS
OF POOR QUALITY

SIKORSKY AIRCRAFT UNITED TECHNOLOGIES

DOCUMENT NO. SER 70452

MAIN ROTOR AIRMASS DEGREE OF FREEDOM

GLAUERT DOWNWASH FACTORS

$$\mu_{TOT} = \left(\mu_{XS}^2 + \mu_{YS}^2 + \lambda_{0_{(E-1)}}^2 \right)^{1/2}$$
(UTOTMR)

$$K1X = \frac{\left(\mu_{XS}^2 + \mu_{YS}^2 \right)^{1/2} \mu_{XS}}{\mu_{TOT}^2}$$
(K1XMR)

$$K1Y = \frac{\left(\mu_{XS}^2 + \mu_{YS}^2 \right)^{1/2} \mu_{YS}}{\mu_{TOT}^2}$$
(K1YMR)

UNIFORM PLUS HARMONIC INFLOW

$$C_{TA} = \frac{T_{HA}}{\left(\rho \pi \Omega_T^2 R_T^4 \right)}$$
(CTHAMR)

$$C_{MHA} = \frac{M_{HA}}{\left(\rho \pi \Omega_T^2 R_T^5 \right)}$$
(CMHAMR)

$$C_{LHA} = \frac{L_{HA}}{\left(\rho \pi \Omega_T^2 R_T^5 \right)}$$
(CLHAMR)

SA 29 REV. 6

$$D_{WO}(S) = \frac{K_{CT}\ C_{TA}}{2\mu_{TOT}} \left\{ \frac{1}{1+\left(\frac{T_{DWO}}{\mu_{TOT}}\right)S} \right\}$$
(DWSHMR)

$$D_{WC}(S) = \frac{K_{CM}\ C_{MHA}}{\mu_{TOT}} \left\{ \frac{1}{1+\left(\frac{T_{DWC}}{\mu_{TOT}}\right)S} \right\}$$
(DWCMR)

$$D_{WS}(S) = \frac{K_{SM}\ C_{LHA}}{\mu_{TOT}} \left\{ \frac{1}{1+\left(\frac{T_{DWS}}{\mu_{TOT}}\right)S} \right\}$$
(DWSMR)

NOTE LAG OPERATES ON $\left(\frac{C_{TA}}{\mu_{TO}}\right)$ TERM ETC.

TOTAL DOWNWASH CONTRIBUTION AT THE ROTOR DISK

$$UPDMR_I = -D_{WO}\cos\beta_{IB} + (D_{WC} - K1X\,D_{WO})\cos\beta_{IB}\left(\xi\cos\psi_{IB} + y_{2n_{IS}}\cos(\psi+\delta)_{IB}\right) + (D_{WS} + K1Y.D_{WO})\cos\beta_{IB}\left\{\xi\sin\psi_{IB} + y_{2n_{IS}}\sin(\psi+\delta)_{IB}\right\}$$

$$UTDMR_I = 0$$

$$URDMR_I = -D_{WO}\sin\beta_{IB} + (D_{WC} - K1X.D_{WO})\sin\beta_{IB}\left(\xi\cos\psi_{IB} + y_{2n_{IS}}\cos(\psi+\delta)_{IB}\right) + (D_{WS} + K1Y.D_{WO})\sin\beta_{IB}\left\{\xi\sin\psi_{IB} + y_{2n_{IS}}\sin(\psi+\delta)_{IB}\right\}$$

$$\lambda = \mu_{zs} - D_{WO} + \mu_{GAVMR}$$

$I_B = 1 \cdots NBS$
$I_S = 1 \cdots NSS$
$I = 1 \cdots (NBS-1)\,NSS$

TOTAL BLADE SEGMENT INTERFERENCE VELOCITIES

$$UPIMRI_I = UPDMR_I + UPWMR_I + UPGMR_I$$

$$UTIMRI_I = UTDMR_I + UTWMR_I + UTGMR_I$$

$$URIMRI_I = URDMR_I + URWMR_I + URGMR_I$$

AIRFRAME UPWASH TERMS NOT CURRENTLY DEFINED FOR BLACK HAWK.

BLADE SEGMENT VELOCITIES

$$UPAMR_{IB} = -\mu_{XS} \sin\beta_{IB} \cos(\psi+\delta)_{IB} + \mu_{YS} \sin\beta_{IB} \sin(\psi+\delta)_{IB} + \mu_{ZS} \cos\beta_{IB} + \frac{\xi}{\Omega_T}\left\{\cos\beta_{IB}\left(q_S \cos\psi_{IB} + p_S \sin\psi_{IB}\right) - \sin\beta_{IB} \sin\delta_{IB} \left(r_S - \Omega\right)\right\}$$

$$UPBMR_{IB} = \left\{-\dot{\beta}_{IB} + q_S \cos(\psi+\delta)_{IB} + p_S \sin(\psi+\delta)_{IB}\right\}$$

$$\underset{(UPMR_I)}{UP_I} = UPAMR_{IB} + \frac{Y_{2N_{IS}}}{\Omega_T} * UPBMR_{IB} + UPIMR_I$$

$$UTAMR_{IB} = \mu_{XS} \sin(\psi+\delta)_{IB} + \mu_{YS} \cos(\psi+\delta)_{IB} - \frac{\xi}{\Omega_T} \cos\delta_{IB} \left(r_S - \Omega\right)$$

$$UTBMR_{IB} = \dot{\delta}_{IB} \cos\beta_{IB} + \sin\beta_{IB}\left(p_S \cos(\psi+\delta)_{IB} - q_S \sin(\psi+\delta)_{IB}\right) - \cos\beta_{IB}\left(r_S - \Omega\right)$$

$$\underset{(UTMR_I)}{UT_I} = UTAMR_{IB} + \frac{Y_{2N_{IS}}}{\Omega_T} * UTBMR_{IB} + UTIMR_I$$

ORIGINAL PAGE IS
OF POOR QUALITY

$$URAMR_{IB} = \mu_{XS} \cos\beta_{IB} \cos(\psi+\delta)_{IB} - \mu_{YS} \cos\beta_{IB} \sin(\psi+\delta)_{IB} + \mu_{ZS} \sin\beta_{IB}$$
$$+ \frac{\xi}{\Omega_T} \left\{ \sin\beta_{IB} \left(q_S \cos\psi_{IB} + p_S \sin\psi_{IB} \right) + \cos\beta_{IB} \sin\delta_{IB} \left(r_S - \Omega \right) \right\}$$

$$U_{R_I} = URAMR_{IB} + URIMR_I$$
$(URMR_I)$

WHERE $IS = 1 \ldots\ldots NSS$
$I = 1 \ldots\ldots NSS * NBS$

RESULTANT VELOCITY AT THE BLADE SEGMENT

$$U_{Y_I} = \left(U_{T_I}^2 + U_{P_I}^2 + U_{R_I}^2 \right)^{1/2}$$
$(UYAWMR)$

MACH NUMBER FOR BLADE MAP LOOK-UP

$$MACHMR_I = \left(U_{T_I}^2 + U_{P_I}^2 \right)^{1/2} \frac{\Omega_T R_T}{a}$$

YAW ANGLE OF FLOW ON SEGMENT

$$\cos\gamma_I = \frac{|U_{T_I}|}{\left(U_{T_I}^2 + U_{R_I}^2 \right)^{1/2}}$$
$(CSGMMR_I)$

SA 29 REV. 6

BLADE SEGMENT GEOMETRIC PITCH ANGLE (BLADE SPAN AXES)

$$THOAMR_{IB} = \theta_{CUFF} - A_{1S}\cos(\psi_R + \Delta SP)_{IB} - B_{1S}\sin(\psi_R + \Delta SP)_{IB}$$
$$- 57.3\,\beta_{IB}\tan\delta_3$$
$$+ 57.3\,\delta_{IB}\,K\alpha 1 + (57.3\,\delta_{IB})^2 K\alpha 2$$

BLADE SEGMENT DYNAMIC TWIST

$$FPDYMR_{IB} = \left[FPD_{IB}^{2} + FTD_{IB}^{2} \right]^{1/2}$$

$$(FPOMR)\quad FPO_{IB} = \frac{1}{b_s}\cdot\left(\frac{b}{b_s}\right)\sum_{IB=1}^{NBS}\left(FPDYMR_{IB}\right)$$

$$(FPCMR)\quad FPC_{IB} = \frac{2}{b_s}\left(\frac{b}{b_s}\right)\sum\left(FPDYMR_{IB}\cos(\psi_R + \delta)\right)$$

$$(FPSMR)\quad FPS_{IB} = \frac{2}{b_s}\left(\frac{b}{b_s}\right)\sum_{1}\left(FPDYMR_{IB}\sin(\psi_R + \delta)\right)$$

$$MODESP_{IS} = .28 + .72\sin\left[90\{y_{2_{IS}} + \xi\}\right]$$

$$\theta_{DYTIP_{IB}} = K_{FPO}\,FPO_{IB} + K_{FPC}\cdot FPC_{IB}\cos(\psi+\delta) + K_{FPS}\cdot FPS_{IB}\sin(\psi+\delta)$$

$$THDYMR_{I} = \theta_{DYTIP_{IB}}\cdot MODESP_{IS}$$

ACTUAL SEGMENT GEOMETRIC BLADE PITCH

$$\theta_I = THOAMR_{I6} + THDYMR_I + f(XSEGMR)$$

$f(XSEGMR)$ DEFINES THE PREFORMED BLADE TWIST - TABLE 1.5.1
FIGURE 1.5.1

$$XSEGMR = y_{2(I3)} + \xi$$

BLADE SEGMENT ANGLE OF ATTACK

THIS ANGLE OF ATTACK IS RESOLVED IN THE DIRECTION OF THE LOCAL SEGMENT AIRFLOW

$$\underset{(AFYNMR)}{\alpha_Y} = \tan^{-1}\left\{\frac{\left[U_{T_I}\left(\theta_{A_I} + \frac{\theta_{A_I}^3}{3} + \frac{2}{15}\theta_{A_I}^5\right) + U_{P_I}\right]/|\cos\gamma_I|}{\left[U_{T_I} - U_{P_I}\left(\theta_{A_I} + \frac{\theta_{A_I}^3}{3} + \frac{2}{15}\theta_{A_I}^5\right)\cos^2\gamma_I\right]}\right\}$$

WHERE $\theta_{A_I} = \frac{\theta_I}{57.3}$ RADS

NOTE: $\tan\theta_{A_I} \doteq \theta_{A_I} + \frac{\theta_{A_I}^3}{3} + \frac{2}{15}\theta_{A_I}^5$

TABLE LOOK-UP ALGORITHM FOR SEGMENT AERODYNAMICS

If $\alpha_{y_I} \geq 0$

$IB = 1 \cdots NBS$
$IS = 1 \cdots NSS$
$I = 1 \cdots (NBS-1)NSS$

if $0 < \alpha_{y_I}/|\cos\delta_I| < ACL1MR$

$$\alpha_{TRANS_I} = \alpha_{y_I}/|\cos\delta_I|$$

if $ACL1MR < \alpha_{y_I}/|\cos\delta_I| \leq (180/|\cos\delta_I|) - (180 - ACL2MR)$

$$\alpha_{TRANS_I} = \frac{(\alpha_{y_I}/|\cos\delta_I| - ACL1MR)(ACL2MR - ACL1MR)}{180/|\cos\delta_I| - 180 + (ACL2MR - ACL1MR)} + ACL1MR$$

if $180/|\cos\delta_I| - (180 - ACL2MR) < \alpha_{y}/|\cos\delta_I| < 180/|\cos\delta_I|$

$$\alpha_{TRANS_I} = 180 - (180 - \alpha_{y_I}) * /|\cos\delta_I|$$

If $\alpha_{y_I} < 0$

if $ACL3MR < \alpha_{y_I}/|\cos\delta_I| < 0$

$$\alpha_{TRANS_I} = \alpha_{y_I}/|\cos\delta_I|$$

if $-180/|\cos\delta_I| + (ACL4MR + 180) \leq \alpha_{y_I}/|\cos\delta_I| < ACL3MR$

$$\alpha_{TRANS_I} = \frac{(\alpha_{y_I}/|\cos\delta_I| - ACL3MR)(ACL4MR - ACL3MR)}{180 - 180/|\cos\delta_I| + (ACL4MR - ACL3MR)} + ACL3MR$$

if $-180 < \alpha_{y} < -180/|\cos\delta_I| + (ACL4MR + 180)$

$$\alpha_{TRANS_I} = -180 + (\alpha_{y_I} + 180)/|\cos\delta_I|$$

SEGMENT AERODYNAMIC COEFFICIENTS

$$C_{LY_I} = f(\alpha_{TRANS_I}, MACHMR_I)$$
$$\underset{(CLMR_I)}{C_{LY_I}} = f(\alpha_{TRANS_I})$$

MAP – CLMRMP
FIGURE 1.5.2(a), (b)
TABLE 1.5.2

$$C_{DY_I} = f(\alpha_{Y_I}, MACHMR_I)$$
$$\underset{(CDMR_I)}{C_{DY_I}} \quad f(\alpha_{Y_I})$$

MAP – CDMRMP
FIGURE 1.5.3(a), (b)
TABLE 1.5.3

LIFT COEFFICIENT TIP LOSS CORRECTION

$$\underset{(CLMR_I)}{C_{LY_I}} = C_{LY_I} * (\text{SEGMENT LOSS FACTOR})_I$$

IF THE OUTER END OF THE SEGMENT, $y_{OUTB_{IS}} \leq BTLMR$

$$(\text{SEGMENT LOSS FACTOR})_I = 1.0$$

IF THE INNER END OF THE SEGMENT, $y_{INB_{IS}} > BTLMR$

$$(\text{SEGMENT LOSS FACTOR})_I = 0.0$$

IF THE INNER END OF THE SEGMENT, $y_{INB_{IS}} \leq BTLMR$

$$(\text{SEGMENT LOSS FACTOR})_I = \left(\frac{BTLMR - y_{INB_{IS}}}{\Delta y_{IS}}\right)$$

TOTAL DRAG COEFFICIENT

$$\underset{(CDMR_I)}{C_{DY_I}} = C_{DY_I} - \Delta C_{DMR}$$

BLADE SEGMENT FORCES (BLADE SPAN AXES)

$$F_{P_I} = \frac{1}{2}\rho \Omega_T^2 R_T^3 (C_y \cdot \Delta y)_{IS}\, u_{y_I} \left\{ C_{LY_I} \frac{U_{T_I}}{|\cos\gamma_I|} + C_{DY_I} U_{P_I} \right\}$$
$(FPMR_I)$

$$F_{T_I} = \frac{1}{2}\rho \Omega_T^2 R_T^3 (C_y \Delta y)_{IS}\, u_{y_I} \left\{ C_{DY_I} U_{T_I} - C_{LY_I} U_{P_I} |\cos\gamma_I| \right\}$$
$(FTMR_I)$

$$F_{R_I} = \frac{1}{2}\rho \Omega_T^2 R_T^3 (C_y \Delta y)_{IS}\, u_{y_I} \left\{ C_{DY_I} - C_{LY_I} \frac{U_{P_I} |\cos\gamma_I|}{U_{T_I}} \right\} U_{R_I}$$
$(FRMR_I)$

AERODYNAMIC SHEARS PER BLADE (BLADE SPAN AXES)

$$F_{PB_{IB}} = \sum_{IS=1}^{NSS} F_{P_I}$$
$(FPBMR)$

$$F_{TB_{IB}} = \sum_{IS=1}^{NSS} F_{T_I}$$
$(FTBMR)$

$$F_{RB_{IB}} = \sum_{IS=1}^{NSS} F_{R_I}$$
$(FRBMR)$

AERODYNAMIC MOMENTS ABOUT THE HINGE
(BLADE SPAN AXES, FLAPPING MOTION IS IN $Y_{BS} \sim Z_{BS}$ PLANE)

FLAPPING $$M_{FAB_{IB}} = R_T \sum_{IS=1}^{NSS} y_{2_{IS}} \cdot F_{P_I}$$
$(MFABMR)$

LAGGING $$M_{LAB_{IB}} = R_T \sum_{IS=1}^{NSS} y_{2_{IS}} F_{T_I}$$
$(MLABMR)$

AERODYNAMIC MOMENTS ABOUT THE HINGE
FIXED SHAFT AXES, FLAPPING COMPONENT ONLY. THESE TERMS USED AS DRIVER FOR 1ST HARMONIC INFLOW.

$$\mathcal{L}_{HA} \ (LHAMR) = -\frac{b}{b_S} \sum_{IB=1}^{NBS} M_{FAB_{IB}} \sin(\psi+\delta)_{IB}$$

$$M_{HA} \ (MHAMR) = -\frac{b}{b_S} \sum_{IB=1}^{NBS} M_{FAB_{IB}} \cos(\psi+\delta)_{IB}$$

AERODYNAMIC SHEARS PER BLADE (ROTATING SHAFT AXES)

$$F_{XA_{IB}} \ (FXAMR) = F_{RB_{IB}} \cos\beta_{IB} \sin\delta_{IB} - F_{TB_{IB}} \cos\delta_{IB} - F_{PB_{IB}} \sin\beta_{IB} \sin\delta_{IB}$$

$$F_{YA_{IB}} \ (FYAMR) = F_{RB_{IB}} \cos\beta_{IB} \cos\delta_{IB} + F_{TB_{IB}} \sin\delta_{IB} - F_{PB_{IB}} \sin\beta_{IB} \cos\delta_{IB}$$

$$F_{ZA_{IB}} \ (FZAMR) = -\left[F_{RB_{IB}} \sin\beta_{IB} + F_{PB_{IB}} \cos\beta_{IB}\right]$$

AERODYNAMIC THRUST COMPONENT (SHAFT AXES)
USED IN UNIFORM DOWNWASH CALCULATION

$$T_{HA} \ (THAMR) = -\frac{b}{b_S} \sum_{IB=1}^{NBS} F_{ZA_{IB}}$$

BLADE LAG DAMPER KINEMATICS

COMPONENTS OF LAG DAMPER DISPLACEMENT

$$X_{LDMR_{IB}} = A_{LDMR}\sin\beta_{IB} + B_{LDMR}\cos(\delta+\delta_0)_{IB}\cos\beta_{IB} + C_{LDMR} + D_{LDMR}\sin(\delta+\delta_0)_{IB}\cos\beta_{IB}$$

$$Y_{LDMR_{IB}} = -R_{LDMR}\cos\theta_{LDMR_{IB}} - B_{LDMR}\sin(\delta+\delta_0)_{IB} + D_{LDMR}\cos(\delta+\delta_0)_{IB}$$

$$Z_{LDMR_{IB}} = A_{LDMR}\cos\beta_{IB} - R_{LDMR}\sin\theta_{LDMR_{IB}} - B_{LDMR}\sin\beta_{IB}\cos(\delta+\delta_0)_{IB} - D_{LDMR}\sin\beta_{IB}\sin(\delta+\delta_0)_{I}$$

WHERE

$$\theta_{LDMR_{IB}} = THOAMR_{IB} - \theta_{GEOMR}$$

(LDMR) $$LDT_{IB} = \left(X^2_{LDMR_{IB}} + Y^2_{LDMR_{IB}} + Z^2_{LDMR_{IB}}\right)^{1/2} \quad \text{INS}$$

(LD.MR) $$\dot{LDT}_{IB} = \left[LDT_{(t)} - LDT_{(t-1)}\right]\frac{1}{\Delta t}$$

(FLD.MR) $$F_{\dot{\delta}_{IB}} = \frac{\dot{LDT}_{IB}}{|\dot{LDT}_{IB}|}\, f\left(\dot{LDT}_{IB}\right)$$ MAP-LDMRMP FIGURE 1.5.4(a),(b) TABLE 1.5.4

(MLLDMR) $$M_{LLD_{IB}} = -F_{\dot{\delta}_{IB}}\Big[R_{LDMR}\cos\theta_{LDMR}\left\{\frac{X_{LDMR}}{L_{DT}}\cos\beta - \frac{Z_{LDMR}}{L_{DT}}\sin\beta\right\} + \frac{Y_{LDMR}}{L_{DT}}\left\{C_{LDMR}\cos\beta + R_{LDMR}\sin\theta_{LDMR}\sin\beta\right\}\Big]_{IB}$$

$$\underset{(MFLDMR)}{M_{FLD_{IB}}} = -F_{\dot{\delta}_{IB}} \left[\frac{Z_{LDMR}}{L_{DT}} C_{LDMR} + \frac{X_{LDMR}}{L_{DT}} \cdot R_{LDMR} \sin \theta_{LDMR} \right]_{IB}$$

$$\underset{(MFFDMR)}{M_{FFD_{IB}}} = -\left[K_\beta \beta + K_{\dot{\beta}} \dot{\beta} \right]_{IB}$$

$$\underset{(MLFDMR)}{M_{LFD_{IB}}} = 0$$

$$\underset{(DLHBMR)}{\Delta L_{HBC_{IB}}} = \left(M_{FLD} + M_{FFD}\right)_{IB} \sin\left(\psi + \delta\right)_{IB}$$

$$\underset{(DMHBMR)}{\Delta M_{HBC_{IB}}} = \left(M_{FLD} + M_{FFD}\right)_{IB} \cos\left(\psi + \delta\right)_{IB}$$

$$\underset{(DNHBMR)}{\Delta N_{HBC_{IB}}} = M_{LLD_{IB}}$$

BLADE LAGGING DEGREE OF FREEDOM (ROTATING SHAFT AXES)

$$\underset{(LG..MR)}{\ddot{\delta}_{IB}} = \frac{M_b}{I_b \cos\beta_{IB}} \Big[\sin\delta_{IB} \left\{ \dot{V}_{YS} \sin\psi_{IB} - \dot{V}_{XS} \cos\psi_{IB} - e\left(r_s - \Omega\right)^2 \right\}$$
$$- \cos\delta_{IB} \left\{ \dot{V}_{XS} \sin\psi_{IB} + \dot{V}_{YS} \cos\psi_{IB} + e\left(\dot{\Omega} - \dot{r}_s\right) \right\} \Big]$$
$$+ \frac{\sin\beta_{IB}}{\cos\beta_{IB}} \left[2\dot{\beta}_{IB}\left(\Omega + \dot{\delta}_{IB} - r_s\right) + \dot{q}_s \sin(\psi + \delta)_{IB} - \dot{p}_s \cos(\psi + \delta)_{IB} \right] + (\dot{r}_s - \dot{\Omega})$$
$$+ 2\dot{\beta}_{IB} \left[\cos\delta_{IB}\left(q_s \sin\psi_{IB} - p_s \cos\psi_{IB}\right) + \sin\delta_{IB}\left(p_s \sin\psi_{IB} + q_s \cos\psi_{IB}\right) \right]$$
$$+ \left[\frac{M_{LLD} + M_{LFD}}{I_b \cos^2\beta} \right]_{IB} - \left[\frac{M_{LAB}}{I_b \cos\beta} \right]_{IB}$$

SOFTWARE SWITCH - NO LAG DEGREE OF FREEDOM, $\ddot{\delta} = \dot{\delta} = \delta = 0$

BLADE FLAPPING DEGREE OF FREEDOM (ROTATING SHAFT AXES)

$$\ddot{\beta}_{IB} = \frac{M_b}{I_b}\Bigg[\cos\beta_{IB}\Big\{\dot{V}_{Zs} + e\Big[2\Omega\left(p_s\cos\psi_{IB} - q_s\sin\psi_{IB}\right) + \dot{p}_s\sin\psi_{IB} + \dot{q}_s\cos\psi_{IB}\Big]\Big\}$$

(BR..MR)

$$+\sin\beta_{IB}\cos\delta_{IB}\Big\{\dot{V}_{Ys}\sin\psi_{IB} - \dot{V}_{Xs}\cos\psi_{IB} - e\left(r_s - \Omega\right)^2\Big\}\Bigg]$$

$$+\cos^2\beta_{IB}\Bigg[\cos\delta_{IB}\Big\{\dot{p}_s\sin\psi_{IB} + \dot{q}_s\cos\psi_{IB} - 2\left(\dot{\delta}_{IB} + \Omega\right)\left(q_s\sin\psi_{IB} - p_s\cos\psi_{IB}\right)\Big\}$$

$$-2\Omega\sin\delta_{IB}\left(p_s\sin\psi_{IB} + q_s\cos\psi_{IB}\right)\Bigg]$$

$$+\cos\beta_{IB}\sin\beta_{IB}\Big[2\dot{\delta}_{IB}\left(r_s - \Omega\right) - \left(r_s - \Omega\right)^2\Big]$$

$$+\left(\frac{M_{FAB} + M_{FFD} + M_{FLD}}{I_b}\right)_{IB}$$

INERTIA SHEARS AT THE HINGE PER BLADE

$$FXI_{IB} = M_b\Big[\cos\beta_{IB}\cos\delta_{IB}(\dot{r}_s-\dot{\Omega}-\ddot{\delta}_{IB}) + 2\sin\beta_{IB}\cos\delta_{IB}\{\dot{\delta}_{IB}\dot{\beta}_{IB}-(r_s-\Omega)\dot{\beta}_{IB}\}$$

(FXIMR)

$$+\cos\beta_{IB}\sin\delta_{IB}\{\dot{\delta}_{IB}^2+\dot{\beta}_{IB}^2-2(r_s-\Omega)\dot{\delta}_{IB}+(r_s-\Omega)^2\}$$

$$+2\dot{\beta}_{IB}\cos\beta_{IB}(p_s\cos\psi_{IB}-q_s\sin\psi_{IB})+\sin\beta_{IB}\sin\delta_{IB}\ddot{\beta}_{IB}\Big]$$

$$-\frac{W_b}{g}\Big[\dot{V}_{XS}\sin\psi_{IB}+\dot{V}_{YS}\cos\psi_{IB}\Big]$$

$$FYI_{IB} = M_b\Big[\cos\beta_{IB}\cos\delta_{IB}\{\dot{\delta}_{IB}^2+\dot{\beta}_{IB}^2-2(r_s-\Omega)\dot{\delta}_{IB}+(r_s-\Omega)^2\}$$

(FYIMR)

$$+\sin\beta_{IB}\cos\delta_{IB}(\ddot{\beta}_{IB})+\cos\beta_{IB}\sin\delta_{IB}(\ddot{\delta}_{IB})$$

$$-2\dot{\beta}_{IB}\cos\beta_{IB}(p_s\sin\psi_{IB}+q_s\cos\psi_{IB})+\frac{W_b e}{g M_b}(r_s-\Omega)^2\Big]$$

$$+\frac{W_b}{g}\Big[\dot{V}_{XS}\cos\psi_{IB}-\dot{V}_{YS}\sin\psi_{IB}\Big]$$

$$FZI_{IB} = M_b\Big[\ddot{\beta}_{IB}\cos\beta_{IB}-\dot{\beta}_{IB}^2\sin\beta_{IB}+\sin\beta_{IB}\cos\delta_{IB}2\dot{\beta}_{IB}(p_s\sin\psi_{IB}+q_s\cos\psi_{IB})$$

(FZIMR)

$$+\cos\beta_{IB}\sin\delta_{IB}\{2(\Omega+\dot{\delta}_{IB})(p_s\sin\psi_{IB}+q_s\cos\psi_{IB})+\dot{q}_s\sin\psi_{IB}-\dot{p}_s\cos\psi_{IB}\}$$

$$-\cos\beta_{IB}\cos\delta_{IB}\{2(\Omega+\dot{\delta}_{IB})(p_s\cos\psi_{IB}-q_s\sin\psi_{IB})+\dot{p}_s\sin\psi_{IB}+\dot{q}_s\cos\psi_{IB}\}$$

$$-\frac{W_b e}{g M_b}\{2\Omega(p_s\cos\psi_{IB}-q_s\sin\psi_{IB})+\dot{p}_s\sin\psi_{IB}+\dot{q}_s\cos\psi_{IB}\}\Big]$$

$$-\frac{W_b}{g}\Big[\dot{V}_{Z_S}\Big]$$

TOTAL SHEAR FORCE AT THE HINGE (ROTATING AXES)

$$\underset{(FXTMR)}{F_{XT_{IB}}} = F_{XA_{IB}} + F_{XI_{IB}}$$

$$\underset{(FYTMR)}{F_{YT_{IB}}} = F_{YA_{IB}} + F_{YI_{IB}}$$

$$\underset{(FZTMR)}{F_{ZT_{IB}}} = F_{ZA_{IB}} + F_{ZI_{IB}}$$

TOTAL ROTOR FORCES (FIXED SHAFT AXES)

$$\underset{(THMR)}{T_H} = -\frac{b}{b_S}\sum_{IB=1}^{NBS} F_{ZT_{IB}}$$

$$\underset{(HHMR)}{H_H} = \frac{b}{b_S}\sum_{IB=1}^{NBS}\left(F_{YT}\cos\psi - F_{XT}\sin\psi\right)_{IB}$$

$$\underset{(JHMR)}{J_H} = -\frac{b}{b_S}\sum_{IB=1}^{NBS}\left(F_{XT}\cdot\cos\psi + F_{YT}\sin\psi\right)_{IB}$$

ROTOR HUB MOMENTS (FIXED SHAFT AXES)

$$\underset{(MHMR)}{M_H} = \frac{b}{b_S} \sum_{IB=1}^{NBS} \left(e\, F_{ZT_{IB}} \cos\psi_{IB} + \Delta M_{HB_{IB}} \right)$$

$$\underset{(LHMR)}{L_H} = \frac{b}{b_S} \sum_{IB=1}^{NBS} \left(e\, F_{ZT_{IB}} \sin\psi_{IB} + \Delta L_{HB_{IB}} \right)$$

$$\underset{(QHMR)}{Q_H} = -\frac{b}{b_S} \sum_{IB=1}^{NBS} \left(e\, F_{XT_{IB}} - \Delta N_{HB_{IB}} \right)$$

IF LAG DEGREE OF FREEDOM IS FIXED

SET - $\delta = \dot{\delta} = \ddot{\delta} = 0$, $M_{LLD_{IB}} = M_{FLD_{IB}} = 0$

SET $\underset{(QHMR)}{Q_H} = -\frac{b}{b_S} \sum_{IB=1}^{NBS} \left(e\, F_{XT_{IB}} - M_{LAB_{IB}} \cos\beta_{IB} \right)$

SA 29 REV. 6

MAIN ROTOR OUTPUT FILTER

$$\begin{bmatrix} H_{HB} \\ J_{HB} \\ T_{HB} \\ L_{HB} \\ M_{HB} \\ Q_{HB} \end{bmatrix} = \frac{1}{(T_{FILMR} S + 1)} \begin{bmatrix} H_H \\ J_H \\ T_H \\ L_H \\ M_H \\ Q_H \end{bmatrix}$$

H FILTER CONSTANT
$T_{FILMR} < \Delta t$ ELIMINATES THE FILTER

ROTOR DEGREE OF FREEDOM.

THESE EQUATIONS ARE DEFINED IN THE ENGINE MODULE

ROTOR FORCE AND MOMENT OUTPUT TRANSFORMATION

TRANSFORMATION OF ROTOR FORCES INTO BODY AXES

$$\begin{bmatrix} X_{MR} \\ Y_{MR} \\ Z_{MR} \end{bmatrix} = \begin{bmatrix} A_{SHBD} \end{bmatrix} \begin{bmatrix} -H_{HB} \\ -J_{HB} \\ -T_{HB} \end{bmatrix}$$

$$\begin{bmatrix} L_{MR} \\ M_{MR} \\ N_{MR} \end{bmatrix} = \begin{bmatrix} A_{SHBD} \end{bmatrix} \begin{bmatrix} L_{HB} \\ M_{HB} \\ Q_E \end{bmatrix} + \begin{bmatrix} Y_H Z_{MR} - Z_H Y_{MR} \\ Z_H X_{MR} - X_H Z_{MR} \\ X_H Y_{MR} - Y_H X_{MR} \end{bmatrix}$$

WHERE $\left[A_{SHBD}\right] = \left[A_{BDSH}\right]^T$

$Q_E = Q_{HB}$ IF ROTOR DEGREE OF FREEDOM IS NOT SELECTED

$Q_E = Q_E$ FROM THE ENGINE MODULE
(QHEG)

SA 29 REV. 6

ROTOR WAKE SKEW ANGLE

$$\underset{(CHIPMR)}{\chi_{PMR}} = \tan^{-1}\left\{\frac{\mu_{xs}}{|\lambda|}\right\} + AAIFMR$$

ROTOR HORSEPOWER REQUIRED

$$HPMR = \frac{Q_{HB} * \Omega_{MR}}{550}$$

ROTOR FORCE AND MOMENT COEFFICIENTS

$$\frac{C_T}{\sigma}, \frac{C_H}{\sigma}, \frac{C_J}{\sigma} = \frac{1}{\rho b C_{.75} \Omega_T^2 R_T^3}\left\{T_{HB}, H_{HB}, J_{HB}\right\}$$

$$\frac{C_M}{\sigma}, \frac{C_L}{\sigma}, \frac{C_Q}{\sigma} = \frac{1}{\rho b C_{.75} \Omega_T^2 R_T^4}\left\{M_{HB}, L_{HB}, Q_{HB}\right\}$$

5.1.3 MAIN ROTOR MODULE INPUT/OUTPUT DATA TRANSFER

INPUT TRANSFER

*PARAMETER	ORIGIN MODULE
THETAØ	FLIGHT CONTROL
A1S	
B1S	
OMR.MR	ENGINE
OMRMR	
QHBEG	
DWSHMR	GROUND EFFECTS
UPGMR$_I$	GUST
UTGMR$_I$	
URGMR$_I$	
UGAVMR	
VXBDOT	MOTION
VYBDOT	
VZBDOT	
PDOT	
QDOT	
RDOT	
VXB	
VYB	
VZB	
P	
Q	
R	
THETAB	
PHIB	
PSIB	

OUTPUT TRANSFER

*PARAMETER	DESTINATION MODULE
FSCGB	FUSELAGE EMPENNAGE
WLCGB	
DWSHMR	
CHIPMR	
AIFMR	
OMGMR	TAIL ROTOR
QHMR	ENGINE
UTOTMR	GROUND EFFECTS
DWSHMR	
LAMMR	
XMR	MOTION
YMR	
ZMR	
LMR	
MMR	
NMR	

* COMPUTER MNEMONICS

5.1.4 NOTATION FOR THE MAIN ROTOR MODULE

SYMBOL USED IN EQUATIONS	PROGRAM MNEMONIC	UNITS	DESCRIPTION
(IB)	-	INDEX	Indicating 1...NBS blades simulated
(IS)	-	INDEX	Indicating 1...NSS segments/blade simulated
(I)	-	INDEX	Indicating 1...(NBS-1)NSS blade segments
e	OFSTMR	FT	Blade hinge offset from center of rotation
e'	SPRLMR	FT	Spar length exposed
R_T	RMR	FT	Rotor radius
Ω_T	OMGTMR	RADS/SEC	Rotor nominal input rotational speed
ξ	KSGMR	ND	Normalized offset
ξ'	-	ND	Normalized spar length.
$Y_{2(IS)}$	KMRBK1	ND	Distance from hinge to segment midpoint
$C_{Y(IS)}$	-	FT	Segment chord
C_T	CHDTMR	FT	Blade top chord
C_R	CHDRMR	FT	Blade root chord
$S_{Y(IS)}$	-	FT^2	Blade segment area
WEIGHT	WEIGHT	LB	Total helicopter weight
b	BMR		Number of rotor blades
W_b	WTBDMR	LB	Weight of one blade
W_{bd}	WTBOD	LB	Weight of helicopter less blades
F_{SCG}	FSCG	INS	Total helicopter c.g. position
WL_{CG}	WLCG	INS	
F_{SCGB}	FSCGB	INS	C.G. position less rotor blades
WLCGB	WLCGB	INS	

5.1.4 (Cont.d) NOTATION FOR THE MAIN ROTOR MODULE

SYMBOL USED IN EQUATIONS	PROGRAM MNEMONIC	UNITS	DESCRIPTION
FSMR	FSMR	INS	Fuselage station for the main rotor
WLMR	WLMR	INS	Waterline station for the main rotor
$\dot{V}_{xb}$	VXBDOT	FT/SEC^2	Accel. along X-axis
$\dot{V}_{yb}$	VYBDOT	FT/SEC^2	Accel. along Y-axis
$\dot{V}_{zb}$	VZBDOT	FT/SEC^2	Accel. along Z-axis
$\dot{p}$	PDOT	RADS/SEC^2	Angular accel about X-axis
$\dot{q}$	QDOT	RADS/SEC^2	Angular accel about Y-axis
$\dot{r}$	RDOT	RADS/SEC^2	Angular accel about Z-axis
V_{xb}	VXB	FT/SEC	Vel. along X-axis
V_{yb}	VYB	FT/SEC	Vel. along Y-axis
V_{zb}	VZB	FT/SEC	Vel. along Z-axis
p	P	RADS/SEC	Angular rate about X-axis
q	Q	RADS/SEC	Angular rate about Y-axis
r	R	RADS/SEC	Angular rate about Z-axis
X_H	-	FT	Longitudinal rotor arm
Y_H	-	FT	Lateral rotor arm
Z_H	-	FT	Vertical rotor arm
θ_b	THETAB	DEG	Pitch attitude
ϕ_b	PHIB	DEG	Roll attitude
ψ_b	PSIB	DEG	Heading
g_x	-	FT/SEC^2	Gravity vectors
g_y	-	FT/SEC^2	
g_z	-	FT/SEC^2	
V_{XG}	V_{XG}	FT/SEC	Point gust velocities. For use when gust penetration is not required.
V_{YG}	V_{YG}	FT/SEC	
V_{ZG}	V_{ZG}	FT/SEC	

5.1.4 (Cont'd) NOTATION FOR THE MAIN ROTOR MODULE

SYMBOL USED IN EQUATIONS	PROGRAM MNEMONIC	UNITS	DESCRIPTION
μ_{XH}	MUXHMR	ND	Hub velocities - normalized
μ_{YH}	MUYHMR	ND	
μ_{ZH}	MUZHMR	ND	
μ_{XS}	MUXSMR	ND	Shaft velocities - normalized
μ_{YS}	MUYSMR	ND	
μ_{ZS}	MUZSMR	ND	
p_S	PSMR	RADS/SEC	Shaft angular rates
q_S	QSMR	RADS/SEC	
R_S	RSMR	RADS/SEC	
$\dot{p}_S$	PS.MR	RADS/SEC^2	Shaft angular acceleration
$\dot{q}_S$	QS.MR	RADS/SEC^2	
$\dot{r}_S$	RS.MR	RADS/SEC^2	
$\dot{V}_{XH}$	VXH.MR	FT/SEC^2	Hub accelerations
$\dot{V}_{YH}$	VYH.MR	FT/SEC^2	
$\dot{V}_{ZH}$	VZH.MR	FT/SEC^2	
$\dot{V}_{XS}$	VXS.MR	FT/SEC^2	Shaft accelerations
$\dot{V}_{YS}$	VYS.MR	FT/SEC^2	
$\dot{V}_{ZS}$	VZS.MR	FT/SEC^2	
$\dot{\Omega}$	OMG.MR	RADS/SEC^2	Rotor shaft acceleration
Ω	OMGMR	RADS/SEC	Rotor shaft speed
Ω_T	OMGTMR	RADS/SEC	Rotor shaft datum speed

5.1.4 (Cont'd) NOTATION FOR THE MAIN ROTOR MODULE

SYMBOL USED IN EQUATIONS	PROGRAM MNEMONIC	UNITS	DESCRIPTION
-	OMR.MR	ND	Rotor shaft acceleration ratio
-	OMRMR	ND	Rotor shaft speed ratio
ψ_R	PSIMR	DEG	Rotor azimuth position
β	BRMR	RADS	Flapping angle
$\dot{\beta}$	BR.MR	RADS/SEC	Flapping rate
$\ddot{\beta}$	BR..MR	$RADS/SEC^2$	Flapping acceleration
δ	LGMR	RADS	Lagging angle
$\dot{\delta}$	LG.MR	RADS/SEC	Lagging rate
$\ddot{\delta}$	LG..MR	$RADS/SEC^2$	Lagging acceleration
A_{AOF}	AOFMR	DEG	Steady flapping (coning)
A_{A1F}	A1FMR	DEG	Long. first harmonic flapping
B_{B1F}	B1FMR	DEG	Lateral first harmonic flapping
A_{AOL}	AOLMR	DEG	Steady lagging
A_{A1L}	A1LMR	DEG	Long. first harmonic lagging
B_{B1L}	B1LMR	DEG	Lateral first harmonic lagging
μ_{TOT}	UTOTMR	ND	Total velocity component at the rotor
K_{1X}	K1XMR	ND	Longitudinal Glauert inflow factor
K_{1Y}	K1YMR	ND	Lateral Glauert inflow factor
T_{HA}	THAMR	LB	Aerodynamic component of thrust
M_{HA}	MHAMR	FT LB	Aerodynamic component of pitching moment
L_{HA}	LHAMR	FT LB	Aerodynamic component of rolling moment
ρ	RHO	$SLUGS/FT^3$	Air density
C_{TA}	CTHAMR		Thrust coefficient
C_{MHA}	CMHAMR		Pitching moment coefficient
C_{LHA}	CLHAMR		Rolling moment coefficient

5.1.4 (Cont'd) NOTATION FOR THE MAIN ROTOR MODULE

SYMBOL USED IN EQUATIONS	PROGRAM MNEMONIC	UNITS	DESCRIPTION
K_{CT}	KCTMR	ND	Gain factors on harmonic inflow
K_{CM}	KCMMR	ND	
K_{SM}	KSLMR	ND	
T_{DWO}	TDWOMR		Time factors on harmonic inflow
T_{DWC}	TDWCMR		
T_{DWS}	TDWSMR		
D_{WO}	DWSHMR	1/RADS	Uniform component of downwash at the rotor disk
D_{WC}	DWCMR	1/RADS	Cosine component of downwash
D_{WS}	DWSMR	1/RADS	Sine component of downwash
U_{PDMR_I}	UPDMR	1/RADS	Total components of downwash in blade span axes
U_{TDMRI}	UTDMR	1/RADS	
U_{RDMRI}	URDMR	1/RADS	
λ	LAMBMR	1/RADS	Total normal rotor inflow velocity
μ_{gAVMR}	VGAVMR	1/RADS	Average gust velocity-used with gust penetration routine.
U_{PIMRI}	UPIMRI	1/RADS	Total segment interference velocities in blades span axes
U_{TIMRI}	UTIMRI	1/RADS	
U_{RIMRI}	URIMRI	1/RADS	
U_{PGMRI}	UPGMRI	1/RADS	Gust penetration components at the blade segment in blade span axes.
U_{TGMRI}	UTGMRI	1/RADS	
U_{RGMRI}	URGMRI	1/RADS	
UPWMRI	UPWMRI		
UTWMRI	UTWMRI	1/RADS	Airframe upwash components
URNMRI	URWMRI		

SA 29 REV. G

5.1.4 (Cont'd) NOTATION FOR THE MAIN ROTOR MODULE

SYMBOL USED IN EQUATIONS	PROGRAM MNEMONIC	UNITS	DESCRIPTION
U_{PAMR}	UPAMR	1/RADS	Blade segment total velocity components in blade span axes.
U_{PBMR}	UPBMR	1/RADS	
U_P	UPMR	1/RADS	
U_{TAMR}	UTAMR	1/RADS	
U_{TBMR}	UTBMR	1/RADS	
U_T	UTMR	1/RADS	
U_{RAMR}	URAMR	1/RADS	
U_{RBMR}	URBMR	1/RADS	
U_R	URMR	1/RADS	
U_Y	UYAWMR	1/RADS	Total flow component at the blade segment
M_{ACHMR}	MACHMR		Blade segment Mach Number.
a	VSOUND	FT/SEC	Speed of sound
$\cos\gamma$	CSGMMR		Cosine of segment flow skew angle
θ_{CUFF}	THETAØ	DEG	Collective blade pitch
A_{1S}	A1S	DEG	Lateral cyclic blade pitch
B_{1S}	B1S	DEG	Longitudinal cyclic blade pitch
Δ_{SP}	DELSMR	DEG	Swashplate phase angle
δ_3	DEL3MR	DEG	Hinge angle-Pitch/Flap coupling
K_1	KAF1MR		Hinge angle coefficients -
K_2	KAF2MR		Pitch/Lag coupling
T_{HOAMR}	THØAMR	DEG	Geometric blade pitch angle
F_{PDYMR}	FPDYMR	LB	Resultant force at blade root
b_s	NBSMR		Number of blades simulated
-	NSSMR		Number of segments simulated
F_{po}	FPOMR	LB	Harmonic components of the blade resultant force
F_{pc}	FPCMR	LB	
F_{ps}	FPSMR	LB	

5.1.4 (Cont'd) NOTATION FOR THE MAIN ROTOR MODULE

SYMBOL USED IN EQUATIONS	PROGRAM MNEMONIC	UNITS	DESCRIPTION
MODESP	-		Equivalent blade first torsional mode
K_{FPO}	KFPOMR		Harmonic weighting coefficients for blade torsional wind-up.
K_{FPC}	KFPCMR		
K_{FPS}	KFPSMR		
T_{HDYMR}	THDYMR	DEG	Blade segment torsional deflection
θ_I		DEG	Actual blade segment geometric pitch
α_Y	AFYWMR	DEG	Blade segment angle of attack
A_{CL1MR}	ACL1MR	DEG	Angle of attack break points for lift curve.
A_{CL2MR}	ACL2MR	DEG	
A_{CL3MR}	ACL3MR	DEG	
A_{CL4MR}	ACL4MR	DEG	
α_{TRANS}	AFTFMR	DEG	Transformed angle of attack for map entry
C_{LY}	CLMR	-	Blade segment lift coefficient
C_{DY}	CDMR	-	Blade segment drag coefficient
BTLMR	BTLMR	-	Blade tip lift loss factor
ΔC_{DMR}	DCDMR		Profile drag correction
F_P	FPMR	LB	Segment aero forces
F_T	FTMR	LB	
F_R	FRMR	LB	
F_{pb}	FPBMR	LB	Blade aero forces - blade span axis
F_{Tb}	FTBMR	LB	
F_{Rb}	FRBMR	LB	
F_{XA}	FXAMR	LB	Blade aero forces-shaft rotating axis
F_{YA}	FYAMR	LB	
F_{ZA}	FZAMR	LB	

SA 29 REV. G

5.1.4 (Cont'd) NOTATION FOR THE MAIN ROTOR MODULE

SYMBOL USED IN EQUATIONS	PROGRAM MNEMONIC	UNITS	DESCRIPTION
F_{XI}	FXIMR	LB	Blade inertial forces-shaft rotating axis
F_{YI}	FYIMR	LB	
F_{ZI}	FZIMR	LB	
F_{XT}	FXTMR	LB	Blade total forces-shaft rotating axis
F_{YT}	FYTMR	LB	
F_{ZT}	FZTMR	LB	
M_{FAB}	MFABMR	FT LB	Aero moments about hinge-blade span axis
M_{LAB}	MLABMR	FT LB	
T_{HA}	THAMR	LB	Aerodynamic component of thrust force
M_{HA}	MHAMR	FT LB	Aerodynamic component of pitching moment
L_{HA}	LHAMR	FT LB	Aerodynamic component of rolling moment
A_{LDMR}	ALDMR	INS	Input constants defining the geometry of the lag damper kinematics
B_{LDMR}	BLDMR	INS	
C_{LDMR}	CLDMR	INS	
D_{LDMR}	DLDMR	INS	
RLDMR	RLDMR	INS	
θ_{GEOMR}	THLDMR	DEG	
δ_o	LAGOMR	DEG	
X_{LDMR}	XLDMR	INS	Component displacemnet of lag damper (relative pick up points)
Y_{LDMR}	YLDMR	INS	
Z_{LDMR}	ZLDMR	INS	
L_{DT}	LDMR	INS	Axial displacement of lag damper
$\dot{L}_{DT}$	LD.MR	INS/SEC	Axial rate of lag damper
$F_{\dot{\delta}}$	FLD.MR	LB	Axial force output from lag damper.
M_{FFD}	MFFDMR	FT LB	Flapping moment due to flap damper
M_{FLD}	MFLDMR	FT LB	Flapping moment due to lag damper
M_{LLD}	MLLDMR	FT LB	Lagging moment due to lag damper
M_{LFD}	MLFDMR	FT LB	Lagging moment due to flap damper

5.1.4 (Cont'd) NOTATION FOR THE MAIN ROTOR MODULE

SYMBOL USED IN EQUATIONS	PROGRAM MNEMONIC	UNITS	DESCRIPTION
ΔL_{HBC}	DLHBMR	FT LB	Delta moments at hub due to blade constraints.
ΔM_{HBC}	DMHBMR	FT LB	
ΔN_{HBC}	DNHBMR	FT LB	
K_{β}	KBETA	FT LB/RADS	Flapping spring stiffness
$K_{\dot{\beta}}$	KBETA.	FT LB/RAD/SEC	Flapping damper rate
M_b	MBMR	SLUGS FT	1st mass moment of blade about the hinge
I_b	IBMR	SLUGS FT^2	Inertia of blade about the hinge
W_b	WTBDMR	LB	Weight of one blade
H_H	HHMR	LB	Total force component outputs from the rotor in shaft axes at the hub
J_H	JHMR	LB	
T_H	THMR	LB	
L_H	LHMR	FT LB	Total moment component outputs from the rotor in shaft axes at the hub
M_H	MHMR	FT LB	
Q_H	QHMR	FT LB	
H_{HB}	HHBMR	LB	Filtered rotor forces and moments in shaft axes at the hub.
J_{HB}	JHBMR	LB	
T_{HB}	THBMR	LB	
L_{HB}	LHBMR	FT LB	
M_{HB}	MHBMR	FT LB	
Q_{HB}	QHBMR	FT LB	
T_{FILMR}	TFILMR	SEC	Rotor force and moment filter time constant
Q_E	QHEG	FT LB	Engine torque - supplied by engine module if selected.

5.1.4 (Cont'd) NOTATION FOR THE MAIN ROTOR MODULE

SYMBOL USED IN EQUATIONS	PROGRAM MNEMONIC	UNITS	DESCRIPTION
X_{MR}	XMR	LB	Rotor forces and moments in body axes at the fuselage c.g.
Y_{MR}	YMR	LB	
Z_{MR}	ZMR	LB	
L_{MR}	LMR	FT LB	
M_{MR}	MMR	FT LB	
N_{MR}	NMR	FT LB	
χ_{PMR}	CHIPMR	DEG	Rotor wake skew angle
HPMR	HPMR	HP	Horsepower required by rotor.
$C_{T/\sigma}$	CTSGMR		Rotor shaft axes force and moment coefficients (output only).
$C_{H/\sigma}$	CHSGMR		
$C_{J/\sigma}$	CJSGMR		
$C_{M/\sigma}$	CMSGMR		
$C_{L/\sigma}$	CLSGMR		
$C_{Q/\sigma}$	CQSGMR		

5.1.5 BLACK HAWK MAIN ROTOR INPUT DATA

CONSTANTS

$R_T = 26.83$
$\Omega_T = 27.0$
$b = 4$
$i_\phi = 0$
$i_\theta = -3$
$\Delta_{SP} = -9.7$
$C_T = 1.73$
$C_R = 1.73$
$C_{.75} = 1.73$
$e = 1.25$
$e' = 3.83$
$W_b = 256.9$
$M_b = 86.7$
$I_b = 1512.6$
$B_{LTMR} = .97$
$\Delta C_{DMR} = .002$
$K_\beta = 0$
$K_{\dot\beta} = 0$
$K_{\alpha 1} = 0$
$K_{\alpha 2} = 0$
$K_{CT} = 1.0$
$K_{CM} = 0$
$K_{CL} = 0$
$TDWO = .01038$
$TDWC = 0$
$TDWS = 0$
$\rho = .002378$
$a = 1117.0$

$FSMR = 341.2$
$WLMR = 315.0$
$BLMR = 0$
$A_{LDMR} = .227$
$B_{LDMR} = 3.242$
$C_{LDMR} = 12.040$
$D_{LDMR} = 10.0102$
$R_{LDMR} = 6.898$
$\theta_{GEOMR} = +17.481$
$\delta_0 = 7$
$T_{FILMR} = .3$ SECS
$K_{FPC} = 0$
$K_{FPS} = 0$
$NBS = 4$
$NSS = 5$
$\delta_3 = 0$

$$K_{FP0} = -.0003 - (.0000044)(V_{KT} - 100)$$
$$-.00052 \le K_{FP0} \le -.0003$$

$WEIGHT = 16638.0$
$FSCG = 355.9$
$WLCG = 248.2$
$BLCG = 0$

BLACK HAWK BLADE TWIST INPUT

MAP NAME: TWMAMP
MAP TYPE: UVA
INPUT VARIABLE(S): XSEGMR
OUTPUT VARIABLE: TWSTMR

PRIMARY MAP:
0.00 (LOWER LIMIT)
1.00 (UPPER LIMIT)
0.05 (DELTA)

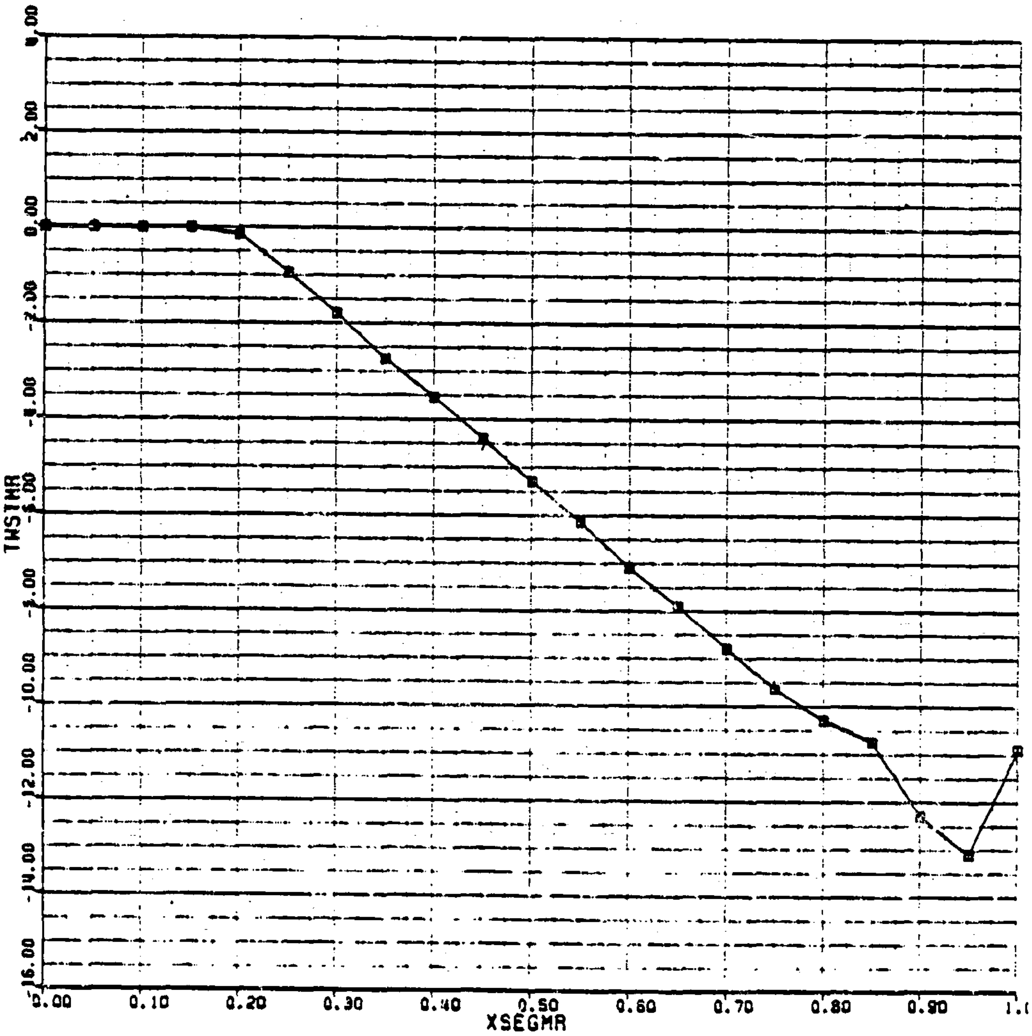

FIGURE 1.5.1

ORIGINAL PAGE IS
OF POOR QUALITY

SIKORSKY AIRCRAFT UNITED TECHNOLOGIES

DOCUMENT NO. SER 70452

BLACK HAWK MAIN ROTOR BLADE SECTION LIFT COEFFICIENT - AIRFOIL SC 1095

BLACKHAWK - NASA STUDY 26-SEP-80 CLMAMP (1/2)

MAP NAME:		CLMAMP	
MAP TYPE:		BIVUVA	
INPUT VARIABLE(S):	AFTFMA		MACHMA
OUTPUT VARIABLE:		CLMA	
PRIMARY MAP:	-32.00	(LOWER LIMIT)	0.00
	32.00	(UPPER LIMIT)	1.00
	2.00	(DELTA)	0.10
SECONDARY MAP:	-180.00	(LOWER LIMIT)	
	180.00	(UPPER LIMIT)	
	2.00	(DELTA)	

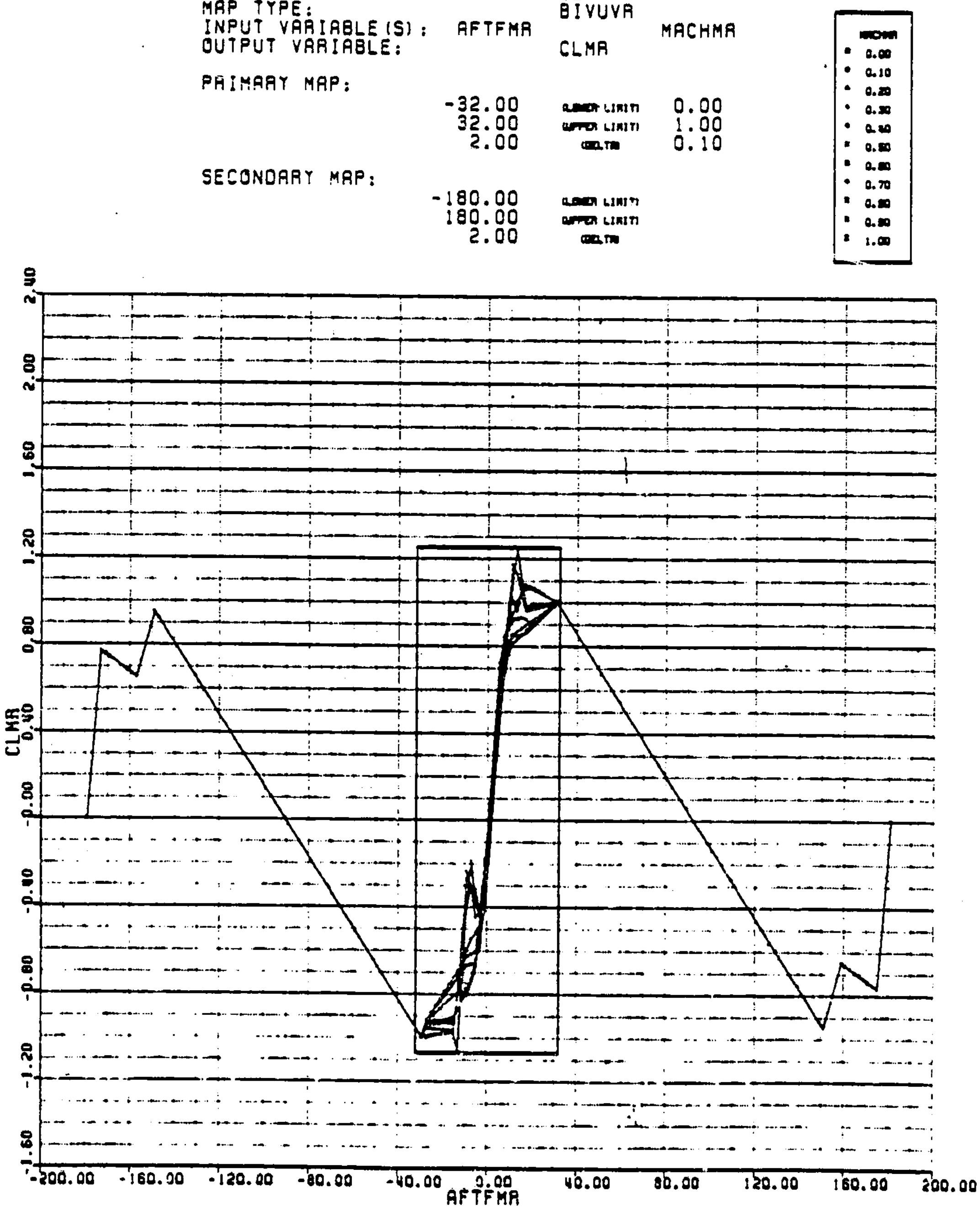

FIGURE 1.5.2(a)

SA 29 REV. G

BLACK HAWK MAIN ROTOR BLADE SECTION LIFT COEFFICIENT - AIRFOIL SC 1095 (Cont'd)

BLACKHAWK - NASA STUDY 26-SEP-80 CLMAMP (2/2)

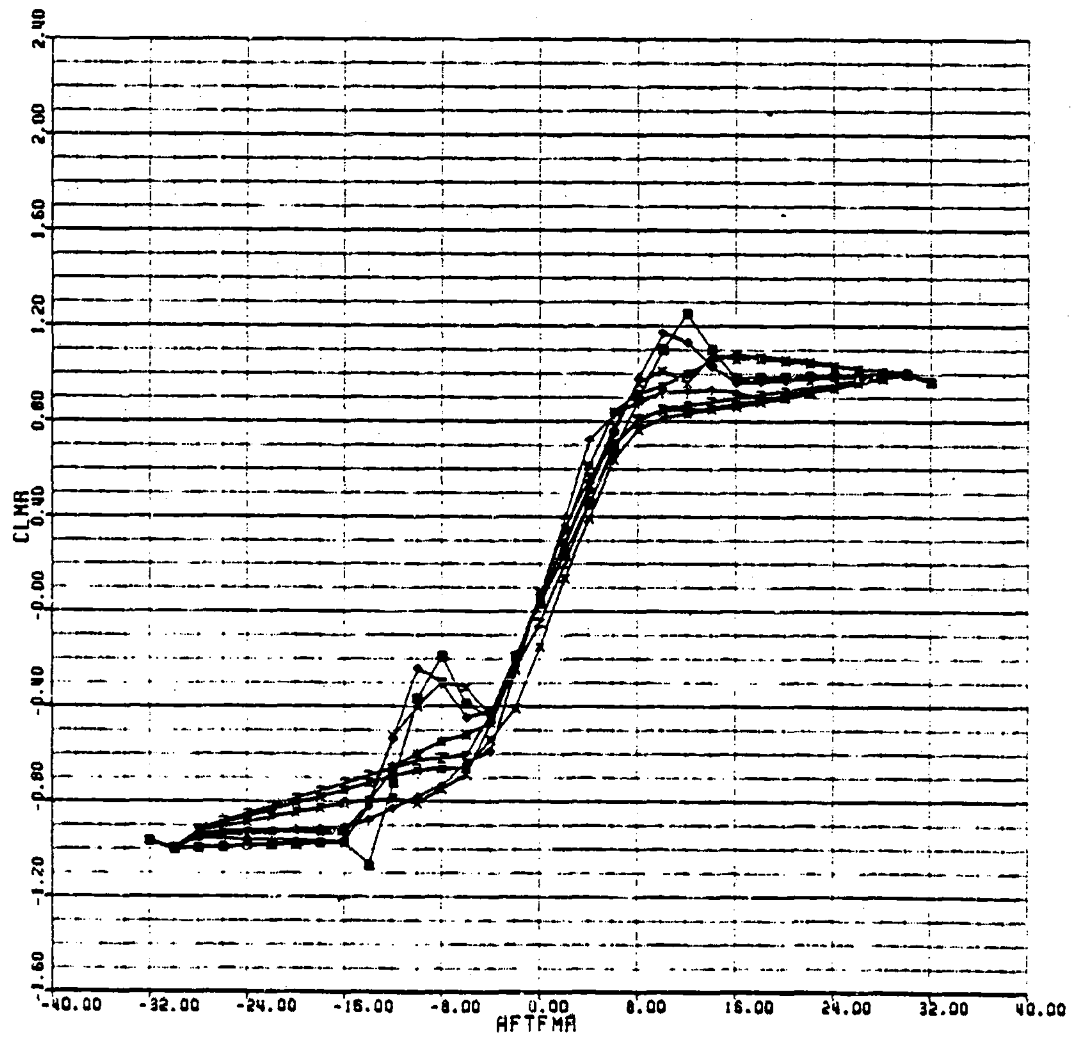

FIGURE 1.5.2(b)

BLACK HAWK MAIN ROTOR BLADE SECTION DRAG COEFFICIENT - AIRFOIL SC 1095

BLACKHAWK - NASA STUDY 26-SEP-80 CDMAMP (1/2)

```
MAP NAME:                       CDMAMP
MAP TYPE:                       BIVUVA
INPUT VARIABLE(S):   AFYWMA              MACHMA
OUTPUT VARIABLE:                CDMA
PRIMARY MAP:
                     -32.00   LOWER LIMIT   0.00
                      32.00   UPPER LIMIT   1.00
                       2.00   DELTA         0.10
SECONDARY MAP:
                    -180.00   LOWER LIMIT
                     180.00   UPPER LIMIT
                       2.00   DELTA
```

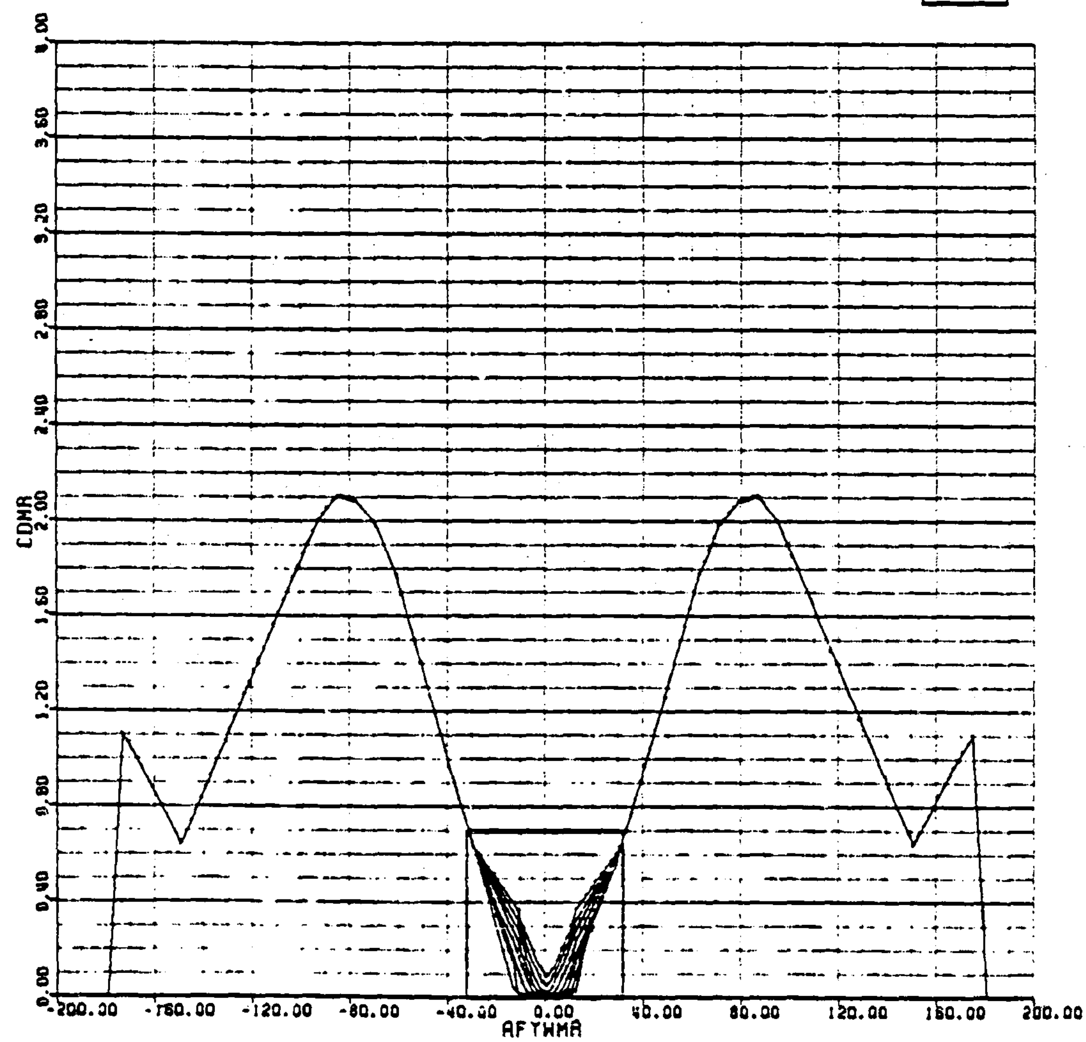

FIGURE 1.5.3(a)

BLACK HAWK MAIN ROTOR BLADE SECTION DRAG COEFFICIENT - AIRFOIL SC 1095 (Cont'd)

BLACKHAWK - NASA STUDY 26-SEP-80 CDNAMP (2/2)

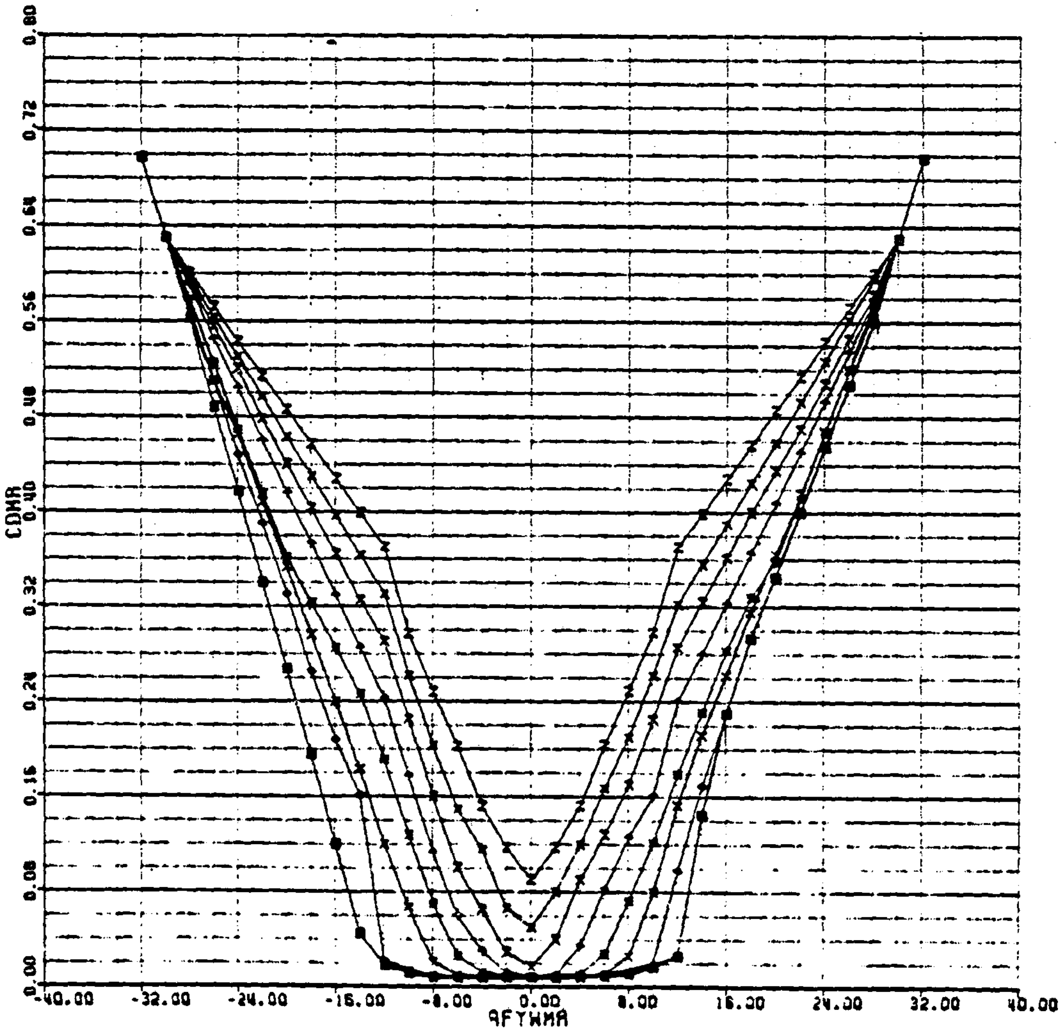

FIGURE 1.5.3(b)

BLACK HAWK MAIN ROTOR BLADE LAG DAMPER FORCE CHARACTERISTICS

BLACKHAWK - NASA STUDY 26-SEP-80 LDMAMP (1/2)

MAP NAME: LDMAMP
MAP TYPE: UVSUVS
INPUT VARIABLE(S): LD.MA
OUTPUT VARIABLE: FLD.MA

PRIMARY MAP:
-2.00 (LOWER LIMIT)
2.00 (UPPER LIMIT)
0.10 (DELTA)

SECONDARY MAP:
-7.00 (LOWER LIMIT)
7.00 (UPPER LIMIT)
1.00 (DELTA)

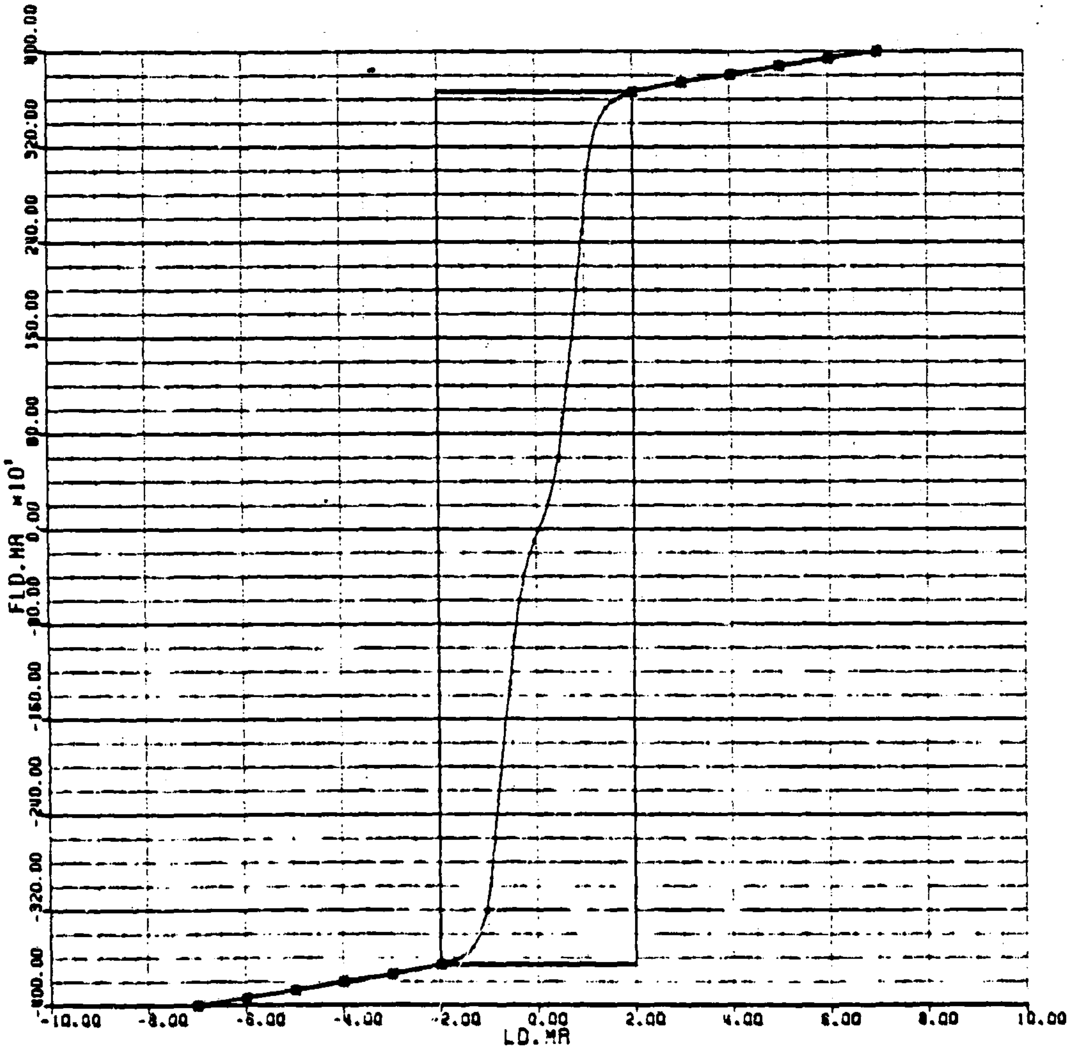

FIGURE 1.5.4(a)

ORIGINAL PAGE IS
OF POOR QUALITY

SIKORSKY AIRCRAFT UNITED TECHNOLOGIES

DOCUMENT NO. SER 70452

BLACK HAWK MAIN ROTOR BLADE LAG DAMPER FORCE CHARACTERISTICS (Cont'd)

BLACKHAWK - NASA STUDY 26-SEP-80 LDMAMP (2/2)

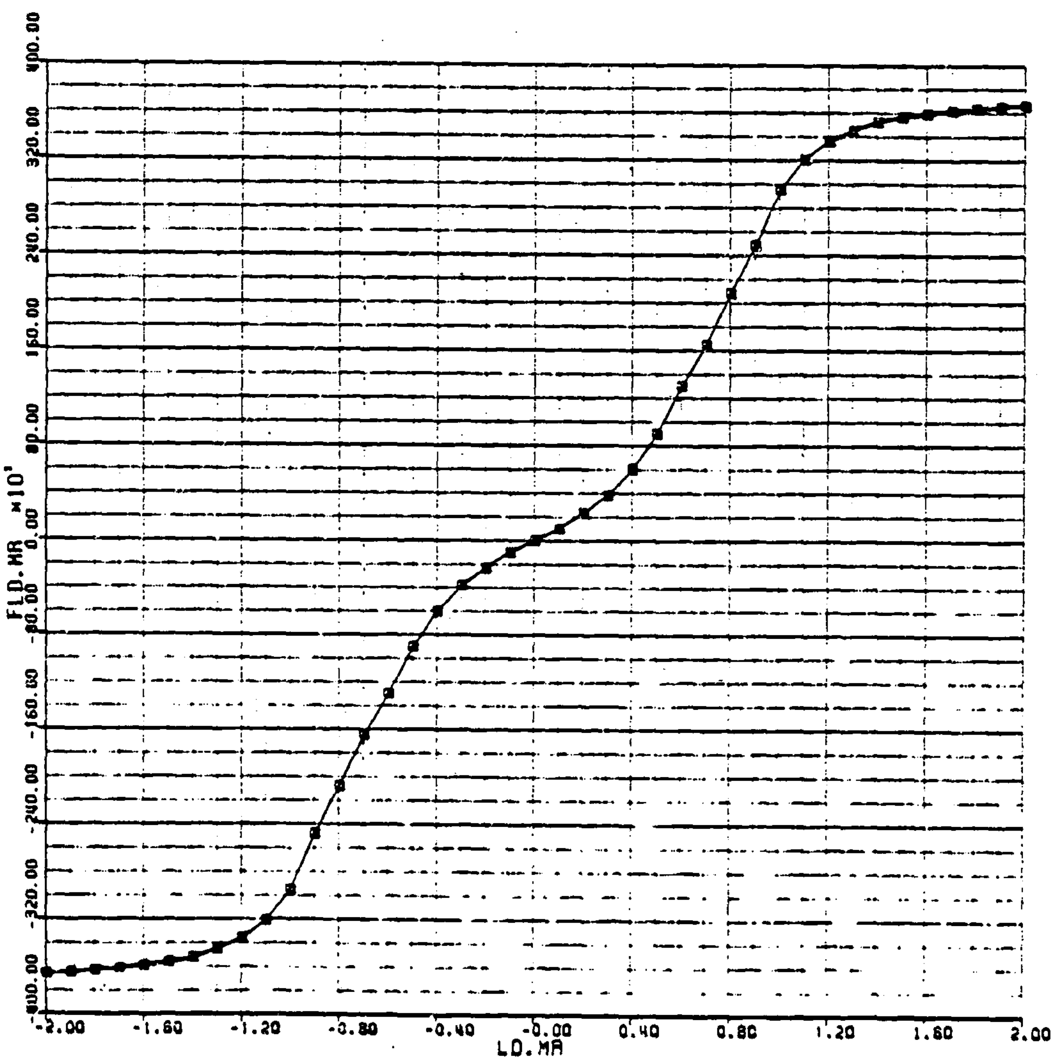

FIGURE 1.5.4(b)

SA 29 REV. G

TABLE 1.5.1

BLACK HAWK MAIN ROTOR PRESET BLADE TWIST

```
TWMRMP::UVR##                  ;MAP ARGUMENT:LOOK UP ROUTINE
        XSEGMR##               ;INPUT VARIABLE
        TWSTMR##               ;OUTPUT VARIABLE
        TWMRLO                 ;MAP NAME
   EXP  Ø.Ø,1.Ø,Ø.Ø5           ;LOWER LIMIT,UPPER LIMIT,DELTA
TWMRLO:  EXP    Ø.Ø,      Ø.Ø,      Ø.Ø,      Ø.Ø,      -Ø.15
         EXP   -Ø.95,    -1.8,     -2.75,    -3.55,     -4.4
         EXP   -5.3,     -6.15,    -7.1,     -7.9,      -8.8
         EXP   -9.65,    -1Ø.3,    -1Ø.75,   -12.3,     -13.1
               -1Ø.9
```

TABLE 1.5.2

BLACK HAWK MAIN ROTOR BLADE SECTION LIFT COEFFICIENT - AIRFOIL SC1095

```
ACL1MR: 11.Ø
ACL2MR: 172.Ø
ACL3MR: -5.Ø
ACL4MR: -172.Ø


                                ; ** ROTOR COEF. OF LIFT MAP **
CLMRMP: BIVUVR##                ;MAP ARGUMENT:LOOK UP ROUTINE
          AFTFMR##(17)          ;INPUT VARIABLE #1,
         MACHMR##(A17)          ;INPUT VARIABLE #2
         CLMR##(A17)            ;OUTPUT VARIABLE
         CLMRLO                 ;PRIMARY (BASIC) MAP NAME
EXP   -32.Ø,32.Ø,2.Ø,   33;LOW. LIM., UP. LIM., DELTA, # ITEMS
EXP   Ø.Ø,1.Ø,.1                ;LOW. LIM., UP. LIM., DELTA
         CLMRHI                 ;SECONDARY (HIGH ANGLE) MAP NAME
EXP -18Ø.Ø,18Ø.Ø,2.Ø            ;LOW. LIM., UP. LIM., DELTA

                  ; PRIMARY MAP: AFTFMR FROM -32 TO 32,DELTA=2,MACHMR FROM Ø TO 1.
                  ; MACH NO.=.Ø
CLMRLO: EXP       -Ø.9675,   -1.Ø,      -Ø.996,    -Ø.992,    -Ø.988
        EXP       -Ø.984,    -Ø.98Ø,    -Ø.976,    -Ø.972,    -1.Ø7
        EXP       -Ø.724,    -Ø.37,     -Ø.19,     -Ø.39,     -Ø.45
        EXP       -Ø.19,      Ø.Ø3,      Ø.243,     Ø.46,      Ø.67
        EXP        Ø.89,      1.1Ø,      1.25,      1.1Ø,      Ø.98
        EXP        Ø.9828,    Ø.9856,    Ø.9884,    Ø.9912,    Ø.994Ø
        EXP        .997,      1.Ø,       Ø.9675

                  ; MACH NO.=.1
        EXP       -Ø.9675,   -1.Ø,      -Ø.996,    -Ø.992,    -Ø.988
        EXP       -Ø.984,    -Ø.98Ø,    -Ø.976,    -Ø.972,    -1.Ø7
        EXP       -Ø.724,    -Ø.37,     -Ø.19,     -Ø.39,     -Ø.45
        EXP       -Ø.19,      Ø.Ø3,      Ø.243,     Ø.46,      Ø.67
        EXP        Ø.89,      1.1Ø,      1.25,      1.1Ø,      Ø.98
        EXP        Ø.9828,    Ø.9856,    Ø.9884,    Ø.9912,    Ø.994Ø
        EXP        .997,      1.Ø,       Ø.9675

                  ; MACH NO.=.2
        EXP       -Ø.9675,   -1.Ø,      -Ø.996,    -Ø.992,    -Ø.988
        EXP       -Ø.984,    -Ø.98Ø,    -Ø.976,    -Ø.972,    -1.Ø7
        EXP       -Ø.724,    -Ø.37,     -Ø.19,     -Ø.39,     -Ø.45
        EXP       -Ø.19,      Ø.Ø3,      Ø.243,     Ø.46,      Ø.67
        EXP        Ø.89,      1.1Ø,      1.25,      1.1Ø,      Ø.98
        EXP        Ø.9828,    Ø.9856,    Ø.9884,    Ø.9912,    Ø.994Ø
        EXP        Ø.997,     1.Ø,       Ø.9675

                  ; MACH NO.=.3
        EXP       -Ø.9675,   -1.Ø,      -Ø.996,    -Ø.992,    -Ø.988
        EXP       -Ø.984,    -Ø.98Ø,    -Ø.976,    -Ø.972,    -1.Ø7
        EXP       -Ø.724,    -Ø.37,     -Ø.19,     -Ø.39,     -Ø.45
        EXP       -Ø.19,      Ø.Ø3,      Ø.243,     Ø.46,      Ø.67
        EXP        Ø.89,      1.1Ø,      1.25,      1.1Ø,      Ø.98
        EXP        Ø.9828,    Ø.9856,    Ø.9884,    Ø.9912,    Ø.994
        EXP        Ø.997,     1.Ø,       Ø.9675
```

TABLE 1.5.2 (Cont'd)

```
      ; MACH NO.=.4
EXP   -Ø.9675,  -1.Ø,     -Ø.955,   -Ø.96,    -Ø.962
EXP   -Ø.964,   -Ø.966,   -Ø.968,   -Ø.97Ø,   -Ø.82
EXP   -Ø.535,   -Ø.24,    -Ø.3Ø,    -Ø.45,    -Ø.42
EXP   -Ø.185,    Ø.Ø5,     Ø.28Ø,    Ø.51Ø,    Ø.75
EXP    Ø.98,     1.17,     1.13,     1.Ø3,     Ø.96
EXP    Ø.9657,   Ø.9714,   Ø.9771,   Ø.9828,   Ø.9885
EXP    Ø.9942,   1.Ø,      Ø.9675

      ; MACH NO.=.5
EXP   -Ø.9675,  -1.Ø,     -Ø.94,    -Ø.93,    -Ø.92
EXP   -Ø.925,   -Ø.93,    -Ø.935,   -Ø.94,    -Ø.8Ø
EXP   -Ø.525,   -Ø.4,     -Ø.3,     -Ø.32,    -Ø.44
EXP   -Ø.195,    Ø.Ø5,     Ø.295,    Ø.53,     Ø.78
EXP    Ø.96,     1.Ø1,     Ø.96,     1.Ø8,     1.Ø6
EXP    1.Ø7,     1.Ø6,     1.Ø5,     1.Ø35,    1.Ø2
EXP    1.Ø1,     1.Ø,      Ø.9675

      ; MACH NO.=.6
EXP   -Ø.9675,  -1.Ø,     -Ø.946,   -Ø.942,   -Ø.938
EXP   -Ø.934,   -Ø.93,    -Ø.926,   -Ø.922,   -Ø.8Ø5
EXP   -Ø.66,    -Ø.6,     -Ø.55,    -Ø.52,    -Ø.47
EXP   -Ø.195,    Ø.Ø75,    Ø.34,     Ø.613,    Ø.84
EXP    Ø.915,    Ø.947,    1.Ø,      1.Ø54,    1.Ø8
EXP    1.Ø63,    1.Ø53,    1.Ø42,    1.Ø31,    1.Ø2
EXP    1.Ø1,     1.Ø,      Ø.9675

      ; MACH NO.=.7
EXP   -Ø.9675,  -1.Ø,     -Ø.944,   -Ø.938,   -Ø.932
EXP   -Ø.926,   -Ø.92Ø,   -Ø.914,   -Ø.9Ø8,   -Ø.88
EXP   -Ø.83,    -Ø.78,    -Ø.735,   -Ø.64,    -Ø.59
EXP   -Ø.255,    Ø.Ø7,     Ø.395,    Ø.72,     Ø.83
EXP    Ø.877,    Ø.92,     Ø.923,    Ø.93,     Ø.92
EXP    Ø.895,    Ø.9,      Ø.92,     Ø.94,     Ø.97
EXP    Ø.985,    1.Ø,      Ø.9675

      ; MACH NO.=.8
EXP   -Ø.9675,  -1.Ø,     -Ø.93,    -Ø.91,    -Ø.89
EXP   -Ø.87,    -Ø.85,    -Ø.83,    -Ø.81,    -Ø.8Ø
EXP   -Ø.79,    -Ø.81,    -Ø.75,    -Ø.69,    -Ø.47
EXP   -Ø.25,     Ø.Ø8,     Ø.35,     Ø.56,     Ø.7Ø5
EXP    Ø.81Ø,    Ø.845,    Ø.845,    Ø.85,     Ø.86
EXP    Ø.88,     Ø.9Ø,     Ø.92,     Ø.94,     Ø.96
EXP    Ø.98,     1.Ø,      Ø.9675

      ; MACH NO.=.9
EXP   -Ø.9675,  -1.Ø,     -Ø.922,   -Ø.894,   -Ø.866
EXP   -Ø.838,   -Ø.81,    -Ø.782,   -Ø.754,   -Ø.726
EXP   -Ø.698,   -Ø.67,    -Ø.665,   -Ø.66,    -Ø.54
EXP   -Ø.41,    -Ø.15,     Ø.14,     Ø.39,     Ø.64
EXP    Ø.765,    Ø.81,     Ø.83,     Ø.85,     Ø.87
EXP    Ø.885,    Ø.9Ø5,    Ø.925,    Ø.94,     Ø.96
EXP    Ø.98,     1.Ø,      Ø.9675

      ; MACH NO.=1.Ø
EXP   -Ø.9675,  -1.Ø,     -Ø.918,   -Ø.886,   -Ø.854
EXP   -Ø.822,   -Ø.79,    -Ø.758,   -Ø.726,   -Ø.694
EXP   -Ø.662,   -Ø.63,    -Ø.62,    -Ø.61,    -Ø.425
EXP   -Ø.24,    -Ø.Ø5,     Ø.2,      Ø.45,     Ø.7
EXP    Ø.8,      Ø.85,     Ø.865,    Ø.88,     Ø.895
EXP    Ø.91,     Ø.925,    Ø.94,     Ø.955,    Ø.97
EXP    Ø.985,    1.Ø,      Ø.9675
```

TABLE 1.5.2 (Cont'd)

```
                  : HIGH ANGLE MAP: AFTFMR FROM -18Ø TO 18Ø, DELTA=2
CLMRHI: EXP      Ø.Ø,        .25667,      .5133,       .77,         .755
        EXP      .74,        .725,        .71Ø,        .695,        .68
        EXP      .665,       .65,         .725,        .8,          .875
        EXP      .95,        .9175,       .885,        .8525,       .82
        EXP      .7875,      .755,        .7225,       .69,         .6575
        EXP      .625,       .5925,       .56,         .5275,       .495
        EXP      .4625,      .43,         .3975,       .365,        .3325
        EXP      .3,         .2675,       .235,        .2Ø25,       .17
        EXP      .1375,      .1Ø5,        .Ø725,       .Ø4,         .ØØ75
        EXP     -.Ø25,      -.Ø575,      -.Ø9,        -.1225,      -.155
        EXP     -.1875,     -.22,        -.2525,      -.285,       -.3175
        EXP     -.35,       -.3825,      -.415,       -.4475,      -.48
        EXP     -.5125,     -.545,       -.5775,      -.61,        -.6425
        EXP     -.675,      -.7Ø75,      -.74,        -.7725,      -.8Ø5
        EXP     -.8375,     -.87,        -.9Ø25,      -.935,       -.9675
        EXP     -1.Ø,       -.996,       -.992,       -.998,       -.984
        EXP     -.98,       -.976,       -.972,       -1.Ø7,       -.724
        EXP     -.37,       -.19,        -.39,        -.45,        -.19
        EXP      .Ø3,        .243,        .46,         .67,         .89
        EXP     1.1,        1.25,        1.1,          .98,         .9828
        EXP      .9856,      .9884,       .9912,       .994,        .997
        EXP     1.Ø,         .9675,       .935,        .9Ø25,       .87
        EXP      .8375,      .8Ø5,        .7725,       .74,         .7Ø75
        EXP      .675,       .6425,       .61,         .5775,       .545
        EXP      .5125,      .48,         .4475,       .415,        .3825
        EXP      .35,        .3175,       .285,        .2525,       .22
        EXP      .1875,      .155,        .1225,       .Ø9,         .Ø575
        EXP      .Ø25,      -.ØØ75,      -.Ø4,        -.Ø725,      -.1Ø5
        EXP     -.1375,     -.17,        -.2Ø25,      -.235,       -.2675
        EXP     -.3,        -.3325,      -.365,       -.3975,      -.43
        EXP     -.4625,     -.495,       -.5275,      -.56,        -.5925
        EXP     -.625,      -.6575,      -.69,        -.7225,      -.755
        EXP     -.7875,     -.82,        -.8525,      -.885,       -.9175
        EXP     -.95,       -.875,       -.8,         -.725,       -.65
        EXP     -.665,      -.68,        -.695,       -.71,        -.725
        EXP     -.74,       -.755,       -.77,        -.5133,      -.25667
        EXP      Ø.Ø
```

TABLE 1.5.3

BLACK HAWK MAIN ROTOR BLADE SECTION DRAG COEFFICIENT - AIRFOIL SC1095

```
                                ; ** ROTOR COEF. OF DRAG MAP **
CDMRMP: BIVUVR##                ;MAP ARGUMENT:LOOK UP ROUTINE
        AFYWMR##(17)            ;INPUT VARIABLE #1
        MACHMR##(A17)           ;INPUT VARIABLE #2
        CDMR##(A17)             ;OUTPUT VARIABLE
        CDMRLO                  ;PRIMARY (BASIC) MAP NAME
EXP  -32.Ø,32.Ø,2.Ø,^D33;LOW. LIM., UP. LIM., DELTA, # ITEMS(OCTAL)
EXP  Ø.Ø,1.Ø,.1                 ;LOW. LIM., UP. LIM., DELTA
        CDMRHI                  ;SECONDARY (HIGH ANGLE) MAP NAME
EXP -18Ø.Ø,18Ø.Ø,2.Ø            ;LOW. LIM., UP. LIM., DELTA

                ; PRIMARY MAP: AFYWMR FROM -32 TO 32,DELTA=2,MACHMR FROM Ø TO 1.
                ; MACH NO.=.Ø
CDMRLO: EXP     Ø.6975,    Ø.63,      Ø.562,     Ø.488,     Ø.417
        EXP     Ø.34,      Ø.267,     Ø.195,     Ø.12,      Ø.Ø45
        EXP     Ø.Ø18,     Ø.Ø12,     Ø.ØØ8,     Ø.ØØ775,    Ø.ØØ75
        EXP     Ø.ØØ75,    Ø.ØØ75,    Ø.ØØ8,     Ø.ØØ85,    Ø.ØØ9
        EXP     Ø.Ø11,     Ø.Ø17,     Ø.Ø26,     Ø.145,     Ø.23
        EXP     Ø.293,     Ø.345,     Ø.4,       Ø.455,     Ø.5Ø7
        EXP     Ø.56,      Ø.63,    Ø.6975

                ; MACH NO.=.1
        EXP     Ø.6975,    Ø.63,      Ø.562,     Ø.488,     Ø.417
        EXP     Ø.34,      Ø.267,     Ø.195,     Ø.12,      Ø.Ø45
        EXP     Ø.Ø18,     Ø.Ø12,     Ø.ØØ8,     Ø.ØØ775,    Ø.ØØ75
        EXP     Ø.ØØ75,    Ø.ØØ75,    Ø.ØØ8,     Ø.ØØ85,    Ø.ØØ9
        EXP     Ø.Ø11,     Ø.Ø17,     Ø.Ø26,     Ø.145,     Ø.23
        EXP     Ø.293,     Ø.345,     Ø.4,       Ø.455,     Ø.5Ø7
        EXP     Ø.56,      Ø.63,      Ø.6975

                ; MACH NO.=.2
        EXP     Ø.6975,    Ø.63,      Ø.562,     Ø.488,     Ø.417
        EXP     Ø.34,      Ø.267,     Ø.195,     Ø.12,      Ø.Ø45
        EXP     Ø.Ø18,     Ø.Ø12,     Ø.ØØ8,     Ø.ØØ775,    Ø.ØØ75
        EXP     Ø.ØØ75,    Ø.ØØ75,    Ø.ØØ8,     Ø.ØØ85,    Ø.ØØ9
        EXP     Ø.Ø11,     Ø.Ø17,     Ø.Ø26,     Ø.145,     Ø.23
        EXP     Ø.293,     Ø.345,     Ø.4,       Ø.455,     Ø.5Ø7
        EXP     Ø.56,      Ø.63,      Ø.6975

                ; MACH NO.=.3
        EXP     Ø.6975,    Ø.63,      Ø.562,     Ø.488,     Ø.417
        EXP     Ø.34,      Ø.267,     Ø.195,     Ø.12,      Ø.Ø45
        EXP     Ø.Ø18,     Ø.Ø12,     Ø.ØØ82,    Ø.ØØ79,    Ø.ØØ75
        EXP     Ø.ØØ75,    Ø.ØØ75,    Ø.ØØ8,     Ø.ØØ85,    Ø.ØØ9
        EXP     Ø.Ø11,     Ø.Ø17,     Ø.Ø26,     Ø.145,     Ø.23
        EXP     Ø.293,     Ø.345,     Ø.4,       Ø.455,     Ø.5Ø7
        EXP     Ø.56,      Ø.63,      Ø.6975

                ; MACH NO.=.4
        EXP     Ø.6975,    Ø.63,      Ø.57,      Ø.51,      Ø.448
        EXP     Ø.39,      Ø.33,      Ø.265,     Ø.2Ø8,     Ø.161
        EXP     Ø.Ø22,     Ø.Ø13,     Ø.ØØ9,     Ø.ØØ85,    Ø.ØØ8
        EXP     Ø.ØØ8,     Ø.ØØ8,     Ø.ØØ82,    Ø.ØØ85,    Ø.Ø11
        EXP     Ø.Ø14,     Ø.Ø2,      Ø.Ø98,     Ø.169,     Ø.23
        EXP     Ø.293,     Ø.345,     Ø.4,       Ø.455,     Ø.5Ø7
        EXP     Ø.56,      Ø.63,      Ø.6975
```

TABLE 1.5.3 (Cont'd)

```
        ; MACH NO.=.5
EXP     Ø.6975,   Ø.63,     Ø.564,    Ø.51,     Ø.465
EXP     Ø.4Ø8,    Ø.353,    Ø.296,    Ø.24,     Ø.183
EXP     Ø.12,     Ø.Ø67,    Ø.Ø21,    Ø.Ø1,     Ø.ØØ8
EXP     Ø.ØØ75,   Ø.ØØ75,   Ø.ØØ75,   Ø.ØØ8,    Ø.Ø11
EXP     Ø.Ø26,    Ø.Ø8,     Ø.153,    Ø.212,    Ø.262
EXP     Ø.315,    Ø.365,    Ø.416,    Ø.469,    Ø.52
EXP     Ø.569,    Ø.63,     Ø.6975

        ; MACH NO.=.6
EXP     Ø.6975,   Ø.63,     Ø.578,    Ø.525,    Ø.469
EXP     Ø.415,    Ø.361,    Ø.323,    Ø.285,    Ø.246
EXP     Ø.191,    Ø.128,    Ø.Ø7,     Ø.Ø26,    Ø.Ø125
EXP     Ø.ØØ85,   Ø.ØØ8,    Ø.ØØ85,   Ø.Ø11,    Ø.Ø28
EXP     Ø.Ø73,    Ø.122,    Ø.179,    Ø.231,    Ø.283
EXP     Ø.328,    Ø.358,    Ø.412,    Ø.467,    Ø.521
EXP     Ø.576,    Ø.63,     Ø.6975

        ; MACH NO.=.7
EXP     Ø.6975,   Ø.63,     Ø.59,     Ø.545,    Ø.5Ø4
EXP     Ø.46,     Ø.416,    Ø.373,    Ø.329,    Ø.285
EXP     Ø.242,    Ø.177,    Ø.113,    Ø.Ø6,     Ø.Ø3
EXP     Ø.Ø12,    Ø.ØØ8,    Ø.Ø1,     Ø.Ø35,    Ø.Ø82
EXP     Ø.126,    Ø.161,    Ø.24,     Ø.28,     Ø.323
EXP     Ø.365,    Ø.4Ø8,    Ø.451,    Ø.493,    Ø.535
EXP     Ø.578,    Ø.63,     Ø.6975

        ; MACH NO.=.8
EXP     Ø.6975,   Ø.63,     Ø.593,    Ø.555,    Ø.52
EXP     Ø.478,    Ø.44,     Ø.4Ø3,    Ø.364,    Ø.325
EXP     Ø.29,     Ø.225,    Ø.16,     Ø.1,      Ø.Ø65
EXP     Ø.Ø29,    Ø.Ø17,    Ø.Ø4,     Ø.Ø9,     Ø.128
EXP     Ø.17,     Ø.225,    Ø.285,    Ø.324,    Ø.361
EXP     Ø.4,      Ø.435,    Ø.47,     Ø.5Ø8,    Ø.546
EXP     Ø.583,    Ø.63,     Ø.6975

        ; MACH NO.=.9
EXP     Ø.6975,   Ø.63,     Ø.597,    Ø.563,    Ø.53
EXP     Ø.497,    Ø.463,    Ø.43,     Ø.397,    Ø.363
EXP     Ø.33,     Ø.262,    Ø.2Ø3,    Ø.149,    Ø.115
EXP     Ø.Ø66,    Ø.Ø5,     Ø.Ø8,     Ø.12,     Ø.167
EXP     Ø.21,     Ø.262,    Ø.322,    Ø.356,    Ø.39Ø
EXP     Ø.425,    Ø.459,    Ø.493,    Ø.527,    Ø 562
EXP     Ø.596,    Ø.63,     Ø.6975

        ; MACH NO.=1.Ø
EXP     Ø.6975,   Ø.63,     Ø.6Ø1,    Ø.572,    Ø 543
EXP     Ø.514,    Ø.486,    Ø.457,    Ø.428,    Ø.399
EXP     Ø.37,     Ø.297,    Ø.248,    Ø.2Ø2,    Ø.152
EXP     Ø.117,    Ø.Ø9,     Ø.1175,   Ø.1525,   Ø.2Ø3
EXP     Ø.249,    Ø.298,    Ø.37,     Ø.399,    Ø.428
EXP     Ø.457,    Ø.486,    Ø.514,    Ø.543,    Ø.572
EXP     Ø.6Ø1,    Ø.63,     Ø.6975
```

TABLE 1.5.3 (Cont'd)

```
                   ; HIGH ANGLE MAP: AFYWMR FROM -18Ø TO 18Ø, DELTA=2
CDMRHI: EXP      .Ø,          .367,        .733,        1.1,         1.Ø65
        EXP      1.Ø3,        .995,        .96,         .92,         .88
        EXP      .84,         .8,          .76,         .72,         .68
        EXP      .64,         .6875,       .735,        .7825,       .83
        EXP      .87875,      .9275,       .97625,      1.Ø25,       1.Ø7375
        EXP      1.1225,      1.17125,     1.22,        1.26875,     1.3175
        EXP      1.36625,     1.415,       1.46375,     1.5125,      1.56125
        EXP      1.61,        1.66,        1.71,        1.76,        1.81
        EXP      1.8575,      1.9Ø5,       1.9525,      2.Ø,         2.Ø2625
        EXP      2.Ø525,      2.Ø7875,     2.1Ø5,       2.Ø9875,     2.Ø925
        EXP      2.Ø8625,     2.Ø8,        2.Ø55,       2.Ø3,        2.ØØ5
        EXP      1.98,        1.92875,     1.8775,      1.82625,     1.775
        EXP      1.7Ø125,     1.6275,      1.55375,     1.48,        1.4Ø75
        EXP      1.335,       1.2625,      1.19,        1.1175,      1.Ø45
        EXP      .9725,       .9,          .8325,       .765,        .6975
        EXP      .63,         .562,        .488,        .417,        .34
        EXP      .267,        .195,        .12,         .Ø45,        .Ø18
        EXP      .Ø12,        .ØØ8,        .ØØ775,      .ØØ75,       .ØØ75
        EXP      .ØØ75,       .ØØ8,        .ØØ85,       .ØØ9,        .Ø11
        EXP      .Ø17,        .Ø26,        .145,        .23,         .293
        EXP      .345,        .4,          .455,        .5Ø7,        .56
        EXP      .63,         .6975,       .765,        .8325,       .9
        EXP      .9725,       1.Ø45,       1.1175,      1.19,        1.2625
        EXP      1.335,       1.4Ø75,      1.48,        1.55375,     1.6275
        EXP      1.7Ø125,     1.775,       1.82625,     1.8775,      1.92875
        EXP      1.98,        2.ØØ5,       2.Ø3,        2.Ø55,       2.Ø8
        EXP      2.Ø8625,     2.Ø925,      2.Ø9875,     2.1Ø5,       2.Ø7875
        EXP      2.Ø525,      2.Ø2625,     2.Ø,         1.9525,      1.9Ø5
        EXP      1.8575,      1.81,        1.76,        1.71,        1.66
        EXP      1.61,        1.56125,     1.5125,      1.46375,     1.415
        EXP      1.36625,     1.3175,      1.26875,     1.22,        1.17125
        EXP      1.1225,      1.Ø7375,     1.Ø25,       .97625,      .9275
        EXP      .87875,      .83,         .7825,       .735,        .6875
        EXP      .64,         .68,         .72,         .76,         .8
        EXP      .84,         .88,         .92,         .96,         .995
        EXP      1.Ø3,        1.Ø65,       1.1,         .733,        .367
        EXP      .Ø
```

TABLE 1.5.4

BLACK HAWK MAIN ROTOR BLADE LAG DAMPER FORCE CHARACTERISTICS

```
LDMRMP::UVSUVS##            ;MAP ARGUMENT:LOOK UP ROUTINE
        LD.MR##(A16)        ;INPUT VARIABLE
        FLD.MR##(A16)       ;OUTPUT VARIABLE
        LDMRLO              ,LOW RANGE MAP NAME
   EXP  Ø.Ø,2.Ø,Ø.1         ;LOWER LIMIT,UPPER LIMIT,DELTA
        LDMRHI              ;HIGH RANGE MAP NAME
   EXP  2.Ø,7.Ø,1.Ø         ;LOWER LIMIT,UPPER LIMIT,DELTA

                 ; LOW ANGLE MAP; LD,MR Ø TO 2.Ø , DELTA = .1
LDMRLO: EXP      Ø.Ø,     1ØØ.Ø,     23Ø.Ø,     38Ø.Ø,     6ØØ.Ø
        EXP    9ØØ.Ø,    13ØØ.Ø,    165Ø.Ø,    2Ø8Ø.Ø,    248Ø.Ø
        EXP   295Ø.Ø,    321Ø.Ø,    336Ø.Ø,    345Ø.Ø,    3525.Ø
        EXP   3565.Ø,    359Ø.Ø,    3615.Ø,    363Ø.Ø,    365Ø.Ø
        EXP   366Ø.Ø
;
                 ; HIGH ANGLE MAP: LD.MR 2.Ø TO 7.Ø , DELTA=1.Ø
LDMRHI: EXP   366Ø.Ø,    3742.Ø,    38Ø5.Ø,    3875.Ø,    394Ø.Ø
        EXP   4ØØØ.Ø
```

5.1.6 References

1. Articulated Rotor Blade Flapping Motion at Low Advance Ratios, F. D. Harris, Journal AHS, January, 1972.

2. Generalized Rotor Performance, Tanner, Watson SER-50309, 1964

3. High Speed Aerodynamics and Jet Propulsion, Volume VIII., Aerodynamic Components of Aircraft at High Speed. Princeton University Press.

4. Yawed Blade Element Rotor Performance Method, Paglino, V.M., SER-50620, September, 1969.

ORIGINAL PAGE IS
OF POOR QUALITY

SIKORSKY AIRCRAFT UNITED TECHNOLOGIES

DOCUMENT NO. SER 70452

5.2 FUSELAGE MODULE

CONTENTS

SA 29 REV. 3

5.2 Fuselage Module

5.2.1 Module Description

The effects of rotor wash on the airframe have been treated in gross terms. No attempt has been made to determine the local flow under the rotor disc and apply it to an element analysis of the fuselage. The implication of the method used is that any variations in local velocity effects have been ignored. It is considered that the technique used provides the essential effects of more interference velocity with increased rotor load, and varies as the rotor wake deflects rearward with increased forward speed.

The angles of attack and sideslip are derived from the body axes components of velocity. These comprise the components of flight path velocity, gust components and rotor downwash. The definition of the angles are those used in the wind tunnel. That is, angle of attack is the geometric angle subtended by the model relative to tunnel axis at zero yaw angle. It does not change with yaw angle. Angle of sideslip, equal to minus yaw, is defined as yaw table angle in the horizontal plane of the tunnel, irrespective of angle of attack. It should be noted that these angles are not Euler angles.

The fuselage aerodynamic characteristics are specific to the Black Hawk helicopter. They are not generalized in any way and are derived directly from wind tunnel tests. The aerodynamic coefficients in terms of ft^2 and ft^3, for forces and moments respectively, are presented as functions of angle of attack and sideslip in Section 5.2.5. These wind axes forces and moments are subsequently transformed into body axes at the fuselage center of gravity. The data obtained from wind tunnel tests up to post stall conditions must be extended to $\pm 90°$ to cover the low speed flight regimes. Near hover, the most important forces (tail off) are the vertical drag and side force. These can be estimated fairly accurately. Because of the definitions of angle of attack and sideslip the transformation equation gives invalid body axes forces and moments when these angles approach 90°.

To avoid problems during pilot-in-the-loop simulation, filters are presented which fade out the transformation and introduce fixed body axes parameters, estimated specifically for hover and low speed flight. For open loop anlaysis the longitudinal degrees-of-freedom are representative. It should be noted however, that inaccuracies will be encountered in pure side flight (i.e., rotor side wash on the fuselage does not exist). A block diagram indicating the fuselage module flow is presented on figure 2.1.1.

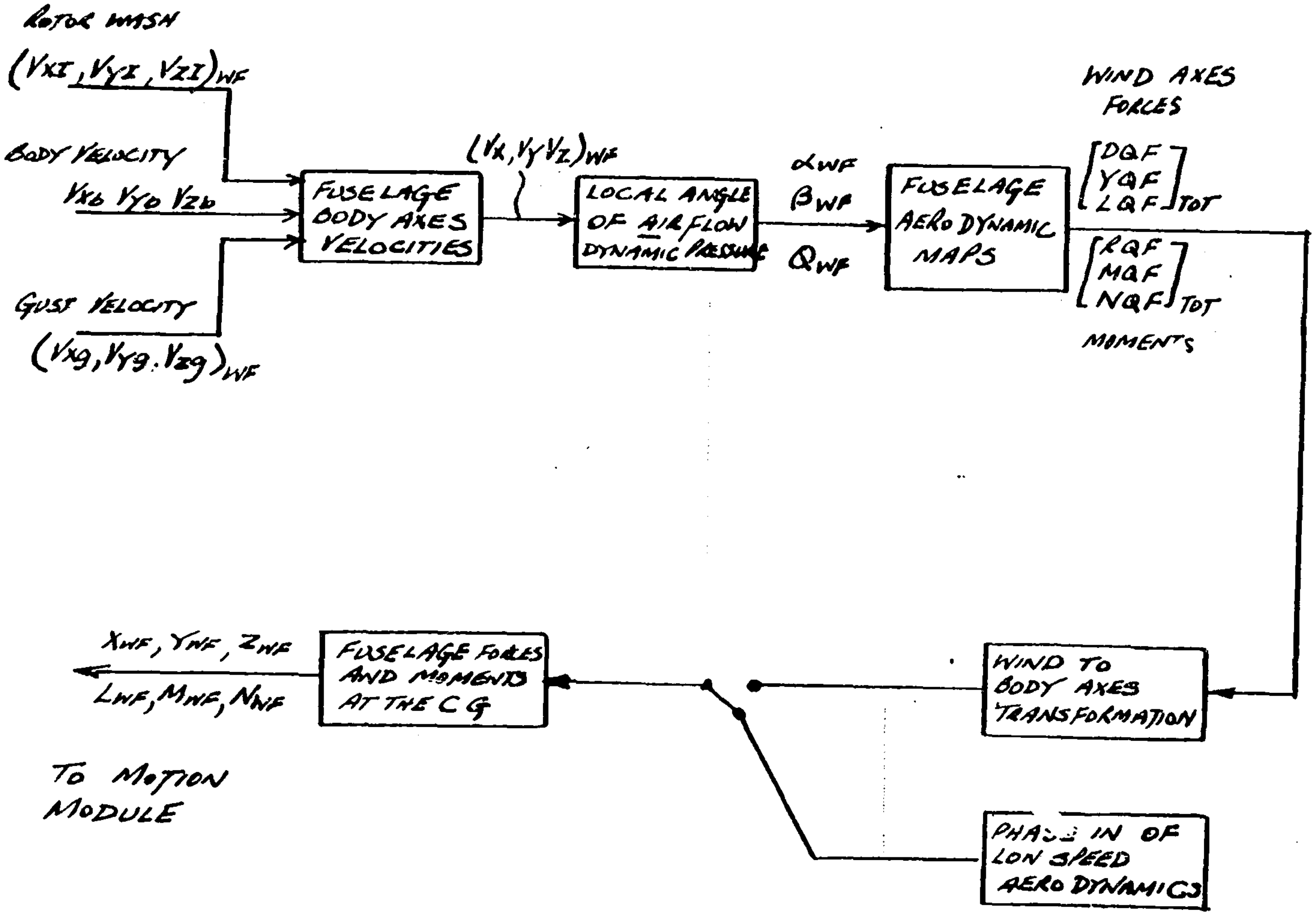

FIGURE 2.1.1

FUSELAGE EQUATION FLOW DIAGRAM

5.2.2. FUSELAGE MODULE EQUATIONS

ROTOR WASH ON THE FUSELAGE

$$VXIWF = EKXWF\,(D_{WO} \cdot \Omega_T \cdot R_T)$$

$$VYIWF = EKYWF\,(D_{WO} \cdot \Omega_T \cdot R_T)$$

$$VZIWF = -EKZWF\,(D_{WO} \cdot \Omega_T \, R_T)$$

WHERE $EKXWF = f(\chi, A_{AIFMR})$, MAP - TABLE 2.5.1
FIGURE 2.5.1

$EKYWF$ = NO INPUT DATA FOR BLACK HAWK AT THIS TIME

$EKZWF = f(\chi, A_{AIFMR})$, MAP - TABLE 2.5.2
FIGURE 2.5.2

FUSELAGE VELOCITY COMPONENTS

$$V_{XWF} = V_{Xb} + V_{XgWF} + VXIWF$$

$$V_{YWF} = V_{Yb} + V_{YgWF} + VYIWF$$

$$V_{ZWF} = V_{Zb} + V_{ZgWF} + VZIWF$$

CONTRIBUTIONS FROM ANGULAR RATES DUE TO MOUNTING POINT OFFSET FROM THE CG ARE IGNORED

ANGLES OF ATTACK AND SIDESLIP

THE FORMULATION OF THESE EQUATIONS DEPENDS ON THE CONVENTIONAL DEFINITION OF ANGLES IN THE WIND TUNNEL. α_{WF} IS MEASURED RELATIVE TO THE TUNNEL FLOOR, ψ_{WF} IS THE ANGLE OF THE TUNNEL YAW TABLE.

$$\alpha_{WF} = \tan^{-1}\left\{\frac{V_{ZWF}}{|V_{XWF}|}\right\}$$
(ALFWF) ATTACK

$$\alpha_{WWF} = \alpha_{WF} + i_{WF}$$
(ALFWWF) – NOT APPLICABLE TO BLACKHAWK

$$SNAFWF = \frac{V_{WF}}{\left(V_{XWF}^2 + V_{ZWF}^2\right)^{1/2}}$$

$$CSAFWF = \frac{V_{WF}}{\left(V_{XWF}^2 + V_{ZWF}^2\right)^{1/2}}$$

$$\beta_{WF} = \tan^{-1}\left\{\frac{V_{YWF}}{\left(V_{XWF}^2 + V_{ZWF}^2\right)^{1/2}}\right\}$$
(BETAWF) SIDESLIP

$$-\psi_{WF} = -\beta_{WF}$$
(PSIWF)

DYNAMIC PRESSURE

$$QWF = \frac{1}{2}\rho\left(V_{XWF}^2 + V_{YWF}^2 + V_{ZWF}^2\right)$$

FUSELAGE AERODYNAMIC LOADING COEFFICIENTS

$$DQFTOT = DQFMP + DDQFMP$$

$$YQFTOT = YQFMP$$

$$LQFTOT = LQFMP + DLQFMP + DLQD$$

$$RQFTOT = RQFMP$$

$$MQFTOT = MQFMP + DMQFMP + DMQD$$

$$NQFTOT = NQFMP + DNQD$$

WHERE

$DQFMP = f(\alpha_{WF})$, TABLE 2.5.3, FIGURE 2.5.3

$DDQFMP = f(|\psi_{WF}|)$, TABLE 2.5.4, FIGURE 2.5.4

$YQFMP = \frac{\psi_{WF}}{|\psi_{WF}|} \cdot f(|\psi_{WF}|)$, TABLE 2.5.5, FIGURE 2.5.5

$LQFMP = f(\alpha_{WF})$, TABLE 2.5.6, FIGURE 2.5.6

$DLQFMP = f(\psi_{WF})$, TABLE 2.5.7, FIGURE 2.5.7

$RQFMP = \frac{\psi_{WF}}{|\psi_{WF}|} f(|\psi_{WF}|)$, TABLE 2.5.8, FIGURE 2.5.8

$MQFMP = f(\alpha_{WF})$, TABLE 2.5.9, FIGURE 2.5.9

$DMQFMP = \frac{\psi_{WF}}{|\psi_{WF}|} \cdot f(|\psi_{WF}|)$ TABLE 2.5.10, FIGURE 2.5.10

$NQFMP = f(\psi_{WF})$, TABLE 2.. 11, FIGURE 2.5.11

GEOMETRY

$$F_{WT} = \left(\frac{FSCGB - FSWF}{12}\right)$$

$$W_{WT} = \left(\frac{WLCGB - WLWF}{12}\right)$$

$$B_{WT} = \left(\frac{BLCGB - BLWF}{12}\right)$$

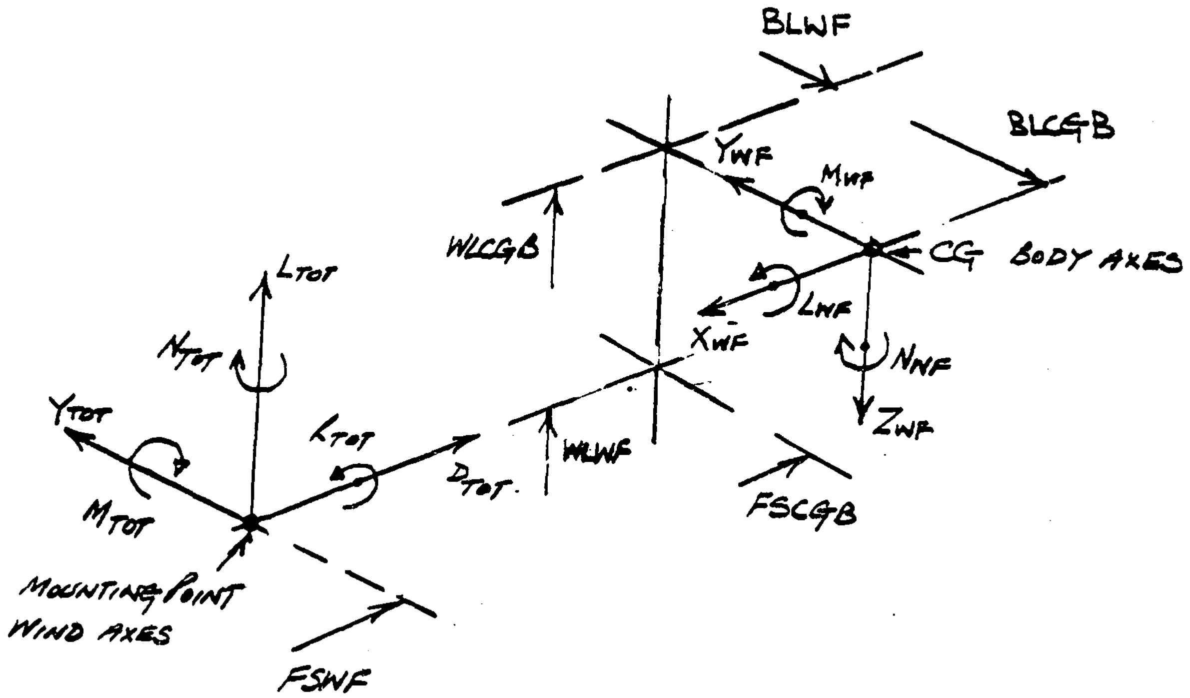

SIDESLIP RESOLUTION COEFFICIENTS

SNBTWF } DERIVED FROM SINCOS (β_{WF}) ROUTINE
CSBTWF }

TRANSFORMATION OF WIND AXES FORCES AND MOMENTS INTO BODY AXES

NOTE α_{WF}, β_{WF} ARE NOT EULER ANGLES.

$$\begin{bmatrix} XWF' \\ YWF' \\ ZWF' \end{bmatrix} = \begin{bmatrix} (\cos\alpha_{WF}\cos\beta_{WF}), & (\cos\alpha_{WF}\sin\beta_{WF}), & (-\sin\alpha_{WF}) \\ (\sin\beta_{WF}) & , (-\cos\beta_{WF}), & 0 \\ (\sin\alpha_{WF}\cos\beta_{WF}), & (\sin\alpha_{WF}\sin\beta_{WF}), & (\cos\alpha_{WF}) \end{bmatrix} \begin{bmatrix} -DQFTOT * QWF \\ -YQFTOT * QWF \\ -LQFTOT * QWF \end{bmatrix}$$

$$\begin{bmatrix} LWF' \\ MWF' \\ NWF' \end{bmatrix} = \begin{bmatrix} LWFWF \\ MWFWF \\ NWFWF \end{bmatrix} + \begin{bmatrix} -Y_{WF}.W_{WT} + Z_{WF}.B_{WT} \\ -Z_{WF}'.F_{WT} + X_{WF}'.W_{WT} \\ +Y_{WF}.F_{WT} - X_{WF}.B_{WT} \end{bmatrix}$$

WHERE

$$\begin{bmatrix} LWFWF \\ MWFWF \\ NWFWF \end{bmatrix} = \begin{bmatrix} \text{SAME MATRIX} \\ \text{AS ABOVE} \end{bmatrix} \begin{bmatrix} RQFTOT * QWF \\ -MQFTOT * QWF \\ NQFTOT * QWF \end{bmatrix}$$

LOW SPEED FILTER OF FUSELAGE AERODYNAMICS

THIS FILTER IS INTENDED FOR USE WITH PILOT-IN-THE LOOP SIMULATION AND IS AN ATTEMPT TO ELIMINATE PROBLEMS OF HIGH α_{WF} AND β_{WF} OPERATION

* IF $|V_{XWF}| > 25$ FT/SEC $(XYZLMN)_{WF} = (XYZLMN)'_{WF}$

IF $|V_{XWF}| \leq 25$ FT/SEC.

$$^{*}X_{WF} = \left|\frac{V_{XWF}}{25}\right| X_{WF}' - \frac{\alpha_{WF}}{|\alpha_{WF}|}\left\{1 - \left|\frac{V_{XWF}}{25}\right|\right\} \cdot X_{LS}\, q_{WF}$$

$$^{*}Y_{WF} = \left|\frac{V_{XWF}}{25}\right| Y_{WF}' - \frac{V_{YWF}}{|V_{YWF}|}\left\{1 - \left|\frac{V_{XWF}}{25}\right|\right\} \cdot Y_{LS}\, q_{WF}$$

$$^{*}Z_{WF} = \left|\frac{V_{XWF}}{25}\right| Z_{WF}' - \frac{\alpha_{WF}}{|\alpha_{WF}|}\left\{1 - \left|\frac{V_{XWF}}{25}\right|\right\} Z_{LS}\, q_{WF}$$

$$^{*}L_{WF} = \left|\frac{V_{XWF}}{25}\right| L_{WF}' - \frac{V_{YWF}}{|V_{YWF}|}\left\{1 - \left|\frac{V_{XWF}}{25}\right|\right\} L_{LS}\, q_{WF}$$

$$^{*}M_{WF} = \left|\frac{V_{XWF}}{25}\right| M_{WF}' - \frac{\alpha_{WF}}{|\alpha_{WF}|}\left\{1 - \left|\frac{V_{XWF}}{25}\right|\right\} M_{LS}\, q_{WF}$$

$$^{*}N_{WF} = \left|\frac{V_{XWF}}{25}\right| N_{WF}' - \frac{V_{YWF}}{|V_{YWF}|}\left\{1 - \left|\frac{V_{XWF}}{25}\right|\right\} N_{LS}\, q_{WF}$$

* THESE EQUATIONS ARE NOT BEING EXECUTED ON PDP10

ORIGINAL PAGE IS
OF POOR QUALITY

SIKORSKY AIRCRAFT UNITED TECHNOLOGIES

DOCUMENT NO. SER 70452

5.2.3 FUSELAGE MODULE INPUT/OUTPUT DATA TRANSFER

INPUT TRANSFER	
PARAMETER	ORIGIN MODULE
BLCGB	MAIN ROTOR
FSCGB	
WLCGB	
DWSHMR	
CHIPMR	
A1FMR	
OMGTMR	
RMR	
VXGWF	GUST
VYGWF	
VZGWF	
VXB	MOTION
VYB	
VZB	

OUTPUT TRANSFER	
PARAMETER	DESTINATION MODULE
ALFWF	EMPENNAGE
BETAWF	
ALFNF	TAIL ROTOR
BETANF	
XWF	MOTION
YWF	
ZWF	
LWF	
MWF	
NWF	

5.2.4 Notation for the Fuselage Module

SYMBOL USED IN EQUATIONS	PROGRAM MNEMONIC	UNITS	DESCRIPTION
V_{XWF}	VXWF	FT/SEC	Total velocity components at the fuselage center of gravity
V_{YWF}	VYWF	FT/SEC	
V_{ZWF}	VZWF	FT/SEC	
V_{XIWF}	VXIWF	FT/SEC	Rotor wash interference on the fuselage.
V_{YIWF}	VYIWF	FT/SEC	
V_{ZIWF}	VZIWF	FT/SEC	
EK_{XWF}	EKXWF	-	Rotor wash interference factors
EK_{YWF}	EKYWF	-	
EK_{ZWF}	EKYWF	-	
D_{WO}	DWSHMR	-	Main rotor uniform downwash.
Ω_T	OMGTMR	RADS/SEC	Rotor speed
R_T	RMR	FT	Rotor radius
q_{WF}	QWF	LB/FT^2	Dynamic pressure at the body
α_{WF}	ALFWF	DEG	Body axis angle of attack
$\lvert\alpha_{WF}\rvert$	AFABWF	DEG	ABS (ALFWF)
α_{WWF}	ALFWWF	DEG	Wing angle of attack
β_{WF}	BETAWF	DEG	Sideslip angle
ψ_{WF}	PSIWF	DEG	W/T model yaw angle (=-BETAWF)
$\lvert\psi_{WF}\rvert$	PSABWF	DEG	ABS (PSIWF)
-	SNAFWF		SIN(ALFWF)
-	CSAFWF		COS(ALFWF)
-	SNBTWF		SIN(BETAWF)
-	CSBTWF		COS(BETAWF)

SA 29 REV. G

5.2.4 (Cont'd) Notation for the Fuselage Module

SYMBOL USED IN EQUATIONS	PROGRAM MNEMONIC	UNITS	DESCRIPTION
DQFMP	DQFMP	FT^2	Drag coefficient from angle of attack
YQFMP	YQFMP	FT^2	Side force coefficient from sideslip
LQFMP	LWFMP	FT^2	Lift coefficient from angle of attack
RQFMP	RQFMP	FT^3	Rolling moment coefficient from sideslip
MQFMP	MQFMP	FT^3	Pitching moment coefficent from angle of attack
NQFMP	NQFMP	FT^3	Yawing moment coefficient from sideslip
DDQFMP	DDQFMP	FT^2	Deltat drag coefficient from sideslip
DLQFMP	DLWFMP	FT^2	Delta lift coefficient from sideslip
DMQFMP	DMQFMP	FT^3	Delta pitching moment coefficient from sideslip
DQFTOT	DQFTOT	FT^2	Total components of aerodynamic coefficients at the wind tunnel mounting point in wind axes.
YQFTOT	YQFTOT	FT^2	
LQFTOT	LQFTOT	FT^2	
RQFTOT	RQFTOT	FT^3	
MQFTOT	MQFTOT	FT^3	
NQFTOT	NQFTOT	FT^3	
FSCGB	FSCGB	INS	Fuselage station for the fuselage C.G.
WLCGB	WLCGB	INS	Waterline station for the fuselage C.G.
FSWF	FSWF	INS	Fuselage station for tunnel mounting point.

5.2.4 (Cont'd) Notation for the Fuselage Module

SYMBOL USED IN EQUATIONS	PROGRAM MNEMONIC	UNITS	DESCRIPTION
WLWF	WLWF	INS	Waterline station for tunnel mounting point.
F_{WT}	-	FT	Fuselage longitudinal mounting point arm.
W_{WT}	-	FT	Fuselage vertical mounting point arm.
B_{WT}	-	FT	Fuselage lateral mounting point arm.
X_{WF}'	XWF'	LB	Fuselage aerodynamic component loads in body axes at the C.G.
Y_{WF}'	YWF'	LB	
Z_{WF}'	ZWF'	LB	
L_{WF}'	LWF'	FT LB	
M_{WF}'	MWF'	FT LB	
N_{WF}'	NWF'	FT LB	
X_{WF}		LB	Fuselage aerodynamic component loads in body axes at the C.G. modified by low speed phasing.
Y_{WF}		LB	
Z_{WF}		LB	
L_{WF}		FT LB	
M_{WF}		FT LB	
N_{WF}		FT LB	
V_{XgWF}	VXGWF	FT/SEC	GUST VELOCITIES AT THE FUSELAGE
V_{YgWF}	VYGWF	FT/SEC	
V_{ZgWF}	VZGWF	FT/SEC	

5.2.5 BLACK HAWK FUSELAGE INPUT DATA

INPUT CONSTANTS

FSWF = 345.5 ins
WLWF = 234.0 ins
BLWF = 0.0 ins
I_{WF} = 0.0

TABLE 2.5.1

INPLANE COMPONENT OF ROTOR WASH ON THE FUSELAGE

```
EXWFMP::BIV##                        ;MAP ARGUMENT:LOOK UP ROUTINE
   EXP   CHIPMR##,AA1FMR##           ;INPUT VARIABLE #1, INPUT VARIABLE #2
         EKXWF##                     ;OUTPUT VARIABLE
         EXWFLO                      ;LOW ANGLE MAP NAME
   EXP   Ø.Ø,1ØØ.Ø,1Ø.Ø,13           ;LOW LIM,UPPER LIM,DELTA,#ENTRYS(OCT)-CHIPMR
   EXP   -6.Ø,6.Ø,6.Ø                ;LOW LIM,UPPER LIM,DELTA-AA1FMR


              ; LOW ANGLE MAP CHIPMR Ø TO 1ØØ (DEL=1Ø) AA1FMR -6,Ø,6
              ; AA1FMR=-6
EXWFLO:EXP       Ø.Ø8,        Ø.18,        Ø.3,        Ø.43,        Ø.55
       EXP       Ø.66,        Ø.79,        Ø.9,        1.Ø3,        Ø.55
                 Ø.Ø

              ; AA1FMR=Ø
       EXP       Ø.Ø,         Ø.1,         Ø.21,       Ø.32,        Ø.42
       EXP       Ø.54,        Ø.66,        Ø.8,        Ø.94,        Ø.5
                 Ø.Ø

              ; AA1FMR=6
       EXP      -Ø.12,        Ø.Ø2,        Ø.Ø8,       Ø.18,        Ø.28
       EXP       Ø.4,         Ø.53,        Ø.67,       Ø.82,        Ø.4
                 Ø.Ø
```

TABLE 2.5.2

DOWNWASH FROM THE MAIN ROTOR ONTO THE FUSELAGE

```
EZWFMP::BIV##                        ;MAP ARGUMENT:LOOK UP ROUTINE
   EXP   CHIPMR##,AA1FMR##           ;INPUT VARIABLE #1, INPUT VARIABLE #2
         EKZWF##                     ;OUTPUT VARIABLE
         EZWFLO                      ;LOW ANGLE MAP NAME
   EXP   Ø.Ø,1ØØ.Ø,1Ø.Ø,13           ;LOW LIM,UPPER LIM,DELTA,#ENTRYS(OCT)-CHIPMR
   EXP   -6.Ø,6.Ø,6.Ø                ;LOW LIM,UPPER LIM,DELTA-AA1FMR

              ; LOW ANGLE MAP CHIPMR Ø TO 1ØØ (DEL=1Ø) AA1FMR -6,Ø,6
              ; AA1FMR=-6
EZWFLO:EXP       1.11,        1.Ø9,        1.Ø8,       1.Ø65,       1.Ø5
       EXP       1.Ø4,        1.Ø2,        1.Ø1,       1.Ø,         Ø.88
                 Ø.6

              ; AA1FMR=Ø
       EXP       1.12,        1.12,        1.12,       1.12,        1.12
       EXP       1.12,        1.12,        1.12,       1.11,        Ø.96
                 Ø.6

              ; AA1FMR=6
       EXP       1.15,        1.15,        1.15,       1.15,        1.16
       EXP       1.17,        1.18,        1.22,       1.16,        Ø.98
                 Ø.6
```

TABLE 2.5.3

FUSELAGE DRAG COEFFICIENT DUE TO ANGLE OF ATTACK

```
DQFMP::UVRUVR##                ;MAP ARGUMENT:LOOK UP ROUTINE
       ALFWF##                 ;INPUT VARIABLE
       DQF##                   ;OUTPUT VARIABLE
       DQFLO                   ;LOW ANGLE MAP NAME
  EXP  -3Ø.Ø,3Ø.Ø,5.Ø          ;LOWER LIMIT,UPPER LIMIT,DELTA-LOW ANGLE
       DQFHI                   ;HIGH ANGLE MAP NAME
  EXP  -9Ø.Ø,9Ø.Ø,1Ø.Ø         ;LOWER LIMIT,UPPER LIMIT,DELTA-HIGH ANGLE

          ; LOW ANGLE MAP: ALFWF -3Ø TO 3Ø , DELTA=5
DQFLO: EXP    45.Ø8,     37.38,     31.68,     27.48,     25.Ø6
       EXP    23.58,     23.58,     25.Ø8,     27.58,     31.28
       EXP    36.58,     43.Ø8,     51.Ø8

          ; HIGH ANGLE MAP: ALFWF -9Ø TO 9Ø , DELTA=1Ø
DQFHI: EXP    15Ø.Ø,     145.Ø,     133.Ø,     114.Ø,     88.Ø
       EXP    61.Ø,      45.Ø8,     31.68,     25.Ø6,     23.58
       EXP    27.58,     36.58,     51.Ø8,     66.Ø,      84.Ø
       EXP    11Ø.Ø,     132.Ø,     145.Ø,     15Ø.Ø
```

TABLE 2.5.4

INCREMENTAL FUSELAGE DRAG COEFFICIENT DUE TO SIDESLIP

```
DDQFMP::UVRUVR##               ;MAP ARGUMENT:LOOK UP ROUTINE
        PSABWF##               ;INPUT VARIABLE
        DDQF##                 ;OUTPUT VARIABLE
        DDQFLO                 ;LOW ANGLE MAP NAME
   EXP  Ø.Ø,3Ø.Ø,5.Ø           ;LOWER LIMIT,UPPER LIMIT,DELTA-LOW ANGLE
        DDQFHI                 ;HIGH ANGLE MAP NAME
   EXP  3Ø.Ø,9Ø.Ø,1Ø.Ø         ;LOWER LIMIT,UPPER LIMIT,DELTA-HIGH ANGLE

          ; LOW ANGLE MAP: PSI(ABS) Ø TO 3Ø, DELTA=5
DDQFLO: EXP   Ø.Ø,       1.Ø,       4.Ø,       9.Ø,       16.3
        EXP   28.Ø,      38.5

          ; HIGH ANGLE MAP: PSI(ABS) 3Ø TO 9Ø, DELTA=1Ø
DDQFHI: EXP   38.5,      76.5,      113.5,     141.5,     164.5
        EXP 169.5,       17Ø.5
```

TABLE 2.5.5

FUSELAGE SIDE FORCE COEFFICIENT DUE TO SIDESLIP

```
YQFMP::UVSUVS##                ;MAP ARGUMENT:LOOK UP ROUTINE
       PSIWF##                 ;INPUT VARIABLE
       YQF##                   ;OUTPUT VARIABLE
       YQFLO                   ;LOW ANGLE MAP NAME
  EXP  Ø.Ø,3Ø.Ø,5.Ø            ;LOWER LIMIT,UPPER LIMIT,DELTA-LOW ANGLE
       YQFHI                   ;HIGH ANGLE MAP NAME
  EXP  3Ø.Ø,9Ø.Ø,1Ø.Ø          ;LOWER LIMIT,UPPER LIMIT,DELTA-HGIH ANGLE

          ; LOW ANGLE MAP: PSIWF Ø TO 3Ø, DELTA=5  Y(PSI)=-Y(-PSI)
YQFLO: EXP    Ø.Ø,       11.Ø,      23.Ø,      35.Ø,      5Ø.Ø
       EXP    65.Ø,      72.Ø

          ; HIGH ANGLE MAP: PSIWF 3Ø TO 9Ø, DELTA=1Ø  Y(PSI)=-Y(-PSI)
YQFHI: EXP    72.Ø,      92.Ø,      1Ø3.Ø,     1ØØ.Ø,     84.Ø
       EXP    64.Ø,      37.Ø
```

TABLE 2.5.6

FUSELAGE LIFT COEFFICIENT DUE TO ANGLE OF ATTACK

```
LQFMP::UVRUVR##             ;MAP ARGUMENT:LOOK UP ROUTINE
       ALFWF##              ;INPUT VARIABLE
       LQF##                ;OUTPUT VARIABLE
       LQFLO                ;LOW ANGLE MAP NAME
   EXP -3Ø.Ø,3Ø.Ø,5.Ø       ;LOWER LIMIT,UPPER LIMIT,DELTA-LOW ANGLE
       LQFHI                ;HIGH ANGLE MAP NAME
   EXP -9Ø.Ø,9Ø.Ø,1Ø.Ø      ;LOWER LIMIT,UPPER LIMIT,DELTA-HIGH ANGLE

          ; LOW ANGLE MAP: ALFWF -3Ø TO 3Ø , DELTA=5
LQFLO: EXP   -7Ø.Ø,    -52.Ø,    -35.Ø,    -25.Ø,    -13.Ø
       EXP    -5.Ø,      1.Ø,     1Ø.Ø,     2Ø.Ø,     25.Ø
       EXP    3Ø.Ø,     34.Ø,     37.Ø

          ; HIGH ANGLE MAP: ALFWF -9Ø TO 9Ø , DELTA=1Ø
LQFHI: EXP   -24.Ø,    -54.Ø,    -72.Ø,    -81.Ø,    -85.Ø
       EXP   -83.Ø,    -7Ø.Ø,    -35.Ø,    -13.Ø,      1.Ø
       EXP    2Ø.Ø,     3Ø.Ø,     37.Ø,     43.Ø,     48.Ø
       EXP    5Ø.Ø,     48.Ø,     39.Ø,     22.Ø
```

TABLE 2.5.7

INCREMENTAL FUSELAGE LIFT COEFFICIENT DUE TO SIDESLIP

```
DLQFMP::UVR##               ;MAP ARGUMENT:LOOK UP ROUTINE
        PSIWF##             ;INPUT VARIABLE
        DLQF##              ;OUTPUT VARIABLE
        DLQFLO              ;LOW ANGLE MAP NAME
    EXP -3Ø.Ø,3Ø.Ø,5.Ø      ;LOWER LIMIT,UPPER LIMIT,DELTA-LOW ANGLE

          ; LOW ANGLE MAP: PSIWF -3Ø TO 3Ø, DELTA=5
DLQFLO: EXP   3Ø.Ø,     2Ø.Ø,     12.Ø,      7.Ø,      3.Ø
        EXP   2.Ø,       Ø.Ø,      2.Ø,      5.Ø,     1Ø.Ø
        EXP   15.Ø,     22.Ø,     3Ø.Ø
```

TABLE 2.5.8

FUSELAGE ROLLING MOMENT COEFFICIENT DUE TO SIDESLIP

```
RQFMP::UVSUVS##             ;MAP ARGUMENT:LOOK UP ROUTINE
       PSIWF##              ;INPUT VARIABLE
       RQF##                ;OUTPUT VARIABLE
       RQFLO                ;LOW ANGLE MAP NAME
   EXP Ø.Ø,3Ø.Ø,5.Ø         ;LOWER LIMIT,UPPER LIMIT,DELTA-LOW ANGLE
       RQFHI                ;HIGH ANGLE MAP NAME
   EXP 3Ø.Ø,9Ø.Ø,1Ø.Ø       ;LOWER LIMIT,UPPER LIMIT,DELTA-HGIH ANGLE

          ; LOW ANGLE MAP: PSIWF Ø TO 3Ø, DELTA=5  R(PSI)=-R(-PSI)
RQFLO: EXP    Ø.Ø,       Ø.Ø,      Ø.Ø,    -3Ø.Ø,    -75.Ø
       EXP  -12Ø.Ø,   -11Ø.Ø

          ; HIGH ANGLE MAP: PSIWF 3Ø TO 9Ø, DELTA=1Ø  R(PSI)=-R(-PSI)
RQFHI: EXP  -11Ø.Ø,   -1Ø6.Ø,   -1Ø3.Ø,   -1Ø1.Ø,   -1ØØ.Ø
       EXP  -1ØØ.Ø,   -1ØØ.Ø
```

TABLE 2.5.9

FUSELAGE PITCHING MOMENT COEFFICIENT DUE TO ANGLE OF ATTACK

```
MQFMP::UVRUVR##              ;MAP ARGUMENT:LOOK UP ROUTINE
       ALFWF##               ;INPUT VARIABLE
       MQF##                 ;OUTPUT VARIABLE
       MQFLO                 ;LOW ANGLE MAP NAME
   EXP -3Ø.Ø,3Ø.Ø,5.Ø        ;LOWER LIMIT,UPPER LIMIT,DELTA-LOW ANGLE
       MQFHI                 ;HIGH ANGLE MAP NAME
   EXP -9Ø.Ø,9Ø.Ø,1Ø.Ø       ;LOWER LIMIT,UPPER LIMIT,DELTA-HGIH ANGLE

            ; LOW ANGLE MAP: ALFWF -3Ø TO 3Ø , DELTA=5
MQFLO: EXP  -74Ø.Ø,    -7ØØ.Ø,    -63Ø.Ø,    -52Ø.Ø,    -38Ø.Ø
       EXP  -23Ø.Ø,     -9Ø.Ø,      1Ø.Ø,     1ØØ.Ø,     29Ø.Ø
       EXP   45Ø.Ø,     6ØØ.Ø,     75Ø.Ø

            ; HIGH ANGLE MAP: ALFWF -9Ø TO 9Ø , DELTA=1Ø
MQFHI: EXP  -2ØØ.Ø,    -47Ø.Ø,    -645.Ø,    -73Ø.Ø,    -76Ø.Ø
       EXP  -76Ø.Ø,    -74Ø.Ø,    -63Ø.Ø,    -38Ø.Ø,     -9Ø.Ø
       EXP   1ØØ.Ø,     45Ø.Ø,     75Ø.Ø,     81Ø.Ø,     825.Ø
       EXP   78Ø.Ø,     65Ø.Ø,     47Ø.Ø,     2ØØ.Ø
```

TABLE 2.5.10

INCREMENTAL FUSELAGE PITCHING MOMENT DUE TO SIDESLIP

```
            ; ** BLACK HAWK FUSELAGE DEL PITCH MOM VS PSIWF(ABS)
DMQFMP::UVR##                ;MAP ARGUMENT:LOOK UP ROUTINE
        PSABWF##             ;INPUT VARIABLE
        DMQF##               ;OUTPUT VARIABLE
        DMQFLO               ;LOW RANGE MAP NAME
    EXP Ø.Ø,3Ø.Ø,5.Ø         ;LOWER LIMIT,UPPER LIMIT,DELTA-LOW ANGLE MAP

            ; LOW ANGLE MAP: PSI(ABS) Ø TO 3Ø, DELTA=5
DMQFLO:EXP    Ø.Ø,      1Ø.Ø,      2Ø.Ø,      5Ø.Ø,      9Ø.Ø
       EXP  13Ø.Ø,     18Ø.Ø
```

TABLE 2.5.11

FUSELAGE YAWING MOMENT COEFFICIENT DUE TO SIDESLIP

```
NQFMP::UVRUVR##              ;MAP ARGUMENT:LOOK UP ROUTINE
       PSIWF##               ;INPUT VARIABLE
       NQF##                 ;OUTPUT VARIABLE
       NQFLO                 ;LOW ANGLE MAP NAME
   EXP -3Ø.Ø,3Ø.Ø,5.Ø        ;LOWER LIMIT,UPPER LIMIT,DELTA-LOW ANGLE
       NQFHI                 ;HIGH ANGLE MAP NAME
   EXP -9Ø.Ø,9Ø.Ø,1Ø.Ø       ;LOWER LIMIT,UPPER LIMIT,DELTA-HIGH ANGLE

            ; LOW ANGLE MAP: PSIWF -3Ø TO 3Ø, DELTA=5
NQFLO: EXP  -14Ø.Ø,    -19Ø.Ø,    -24Ø.Ø,    -22Ø.Ø,    -18Ø.Ø
       EXP  -1ØØ.Ø,       Ø.Ø,     1ØØ.Ø,     18Ø.Ø,     22Ø.Ø
       EXP   24Ø.Ø,     19Ø.Ø,     14Ø.Ø

            ; HIGH ANGLE MAP: PSIWF -9Ø TO 9Ø, DELTA=1Ø
NQFHI: EXP   44Ø.Ø,     392.Ø,     332.Ø,     259.Ø,     16Ø.Ø
       EXP    4Ø.Ø,    -14Ø.Ø,    -24Ø.Ø,    -18Ø.Ø,       Ø.Ø
       EXP   18Ø.Ø,     24Ø.Ø,     14Ø.Ø,      59.Ø,     -3Ø.Ø
       EXP  -125.Ø,    -22Ø.Ø,    -32Ø.Ø,    -42Ø.Ø
```

INPLANE COMPONENT OF ROTOR WASH ON THE FUSELAGE

MAP NAME: EXWFMP
MAP TYPE: BIV
INPUT VARIABLE(S): CHIPMA AA1FMA
OUTPUT VARIABLE: EKXWF

PRIMARY MAP:

0.00	LOWER LIMIT	-6.00
100.00	UPPER LIMIT	6.00
10.00	DELTA	6.00

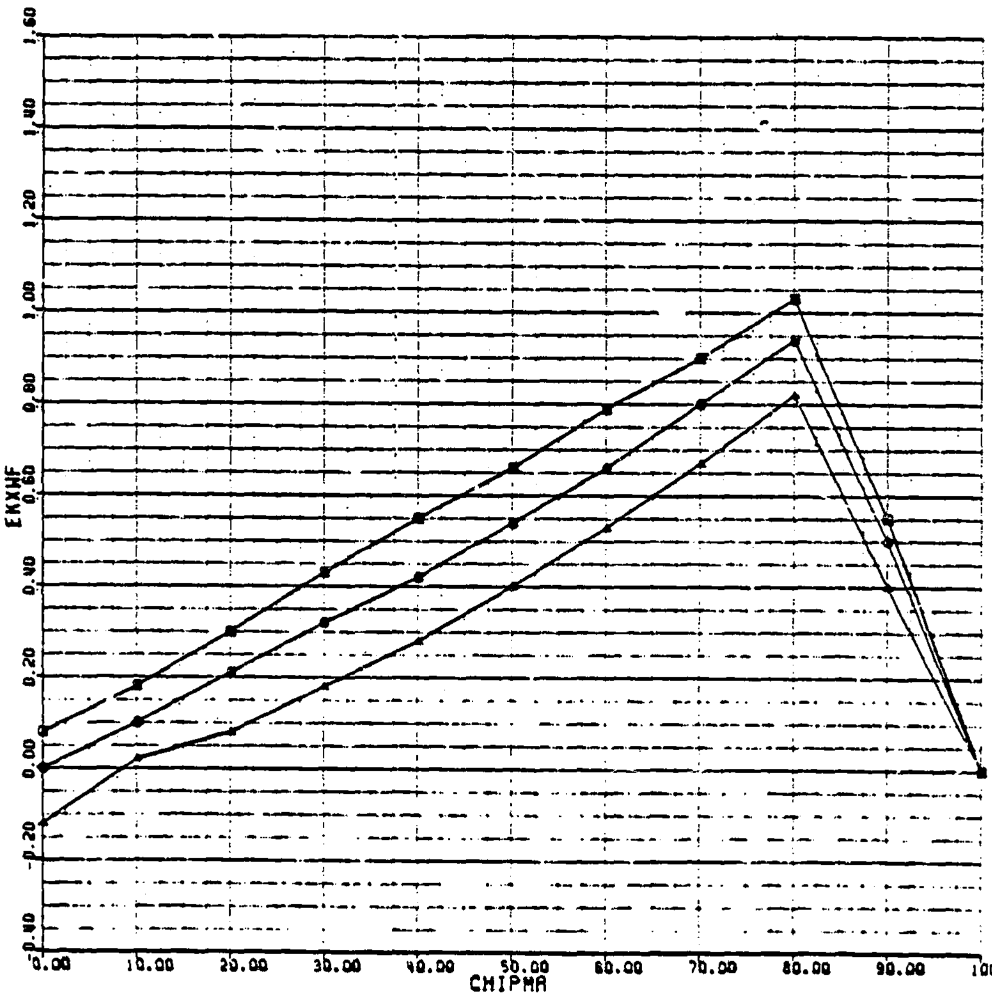

FIGURE 2.5.1

DOWNWASH FROM THE MAIN ROTOR ONTO THE FUSELAGE

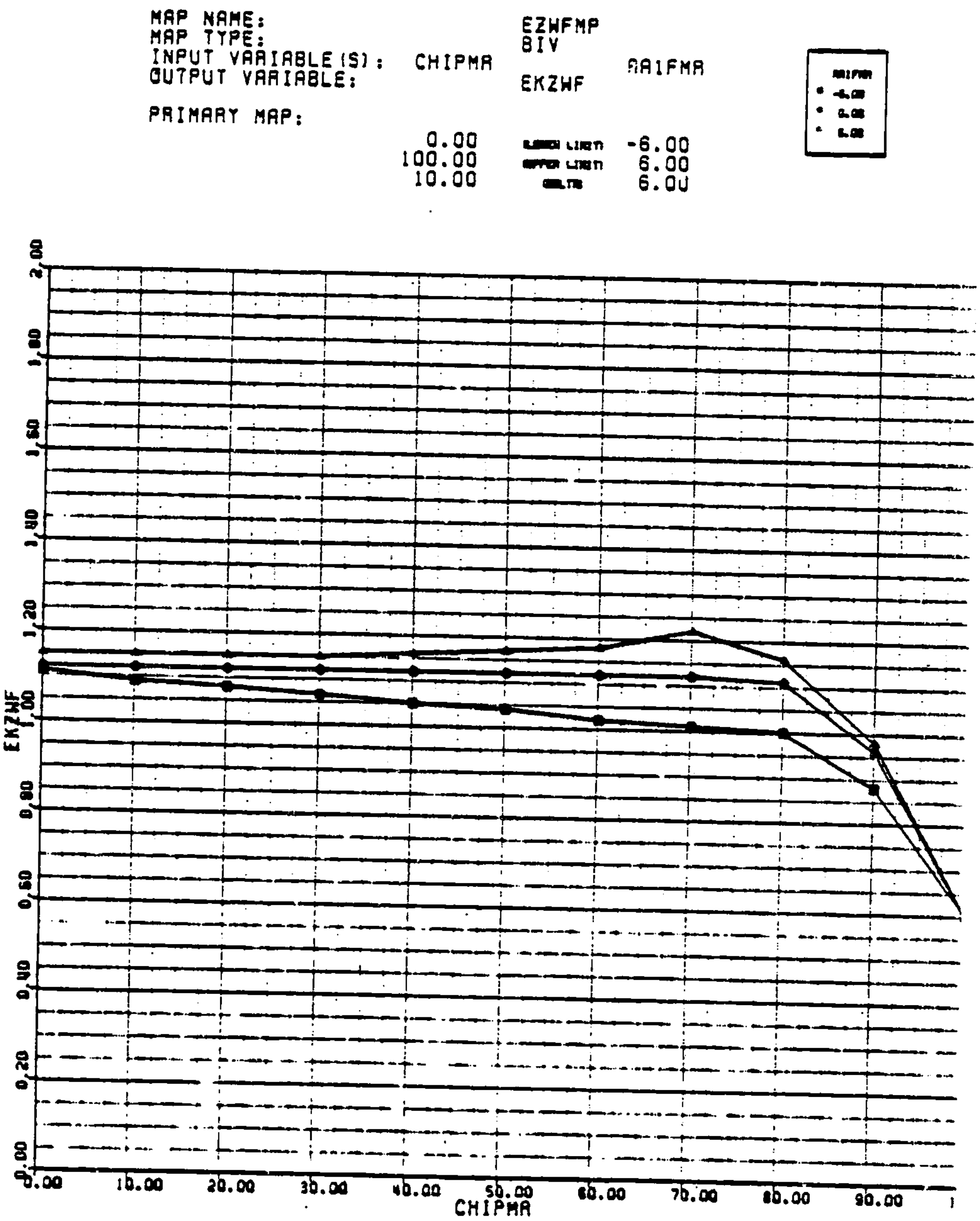

FIGURE 2.5.2

FUSELAGE DRAG COEFFICIENT DUE TO ANGLE OF ATTACK

BLACKHAWK - NASA STUDY 23-SEP-80 DQFMP (1/2)

MAP NAME:		DQFMP
MAP TYPE:		UVAUVA
INPUT VARIABLE(S):	ALFWF	
OUTPUT VARIABLE:		DQF
PRIMARY MAP:	-30.00	(LOWER LIMIT)
	30.00	(UPPER LIMIT)
	5.00	(DELTA)
SECONDARY MAP:	-90.00	(LOWER LIMIT)
	90.00	(UPPER LIMIT)
	10.00	(DELTA)

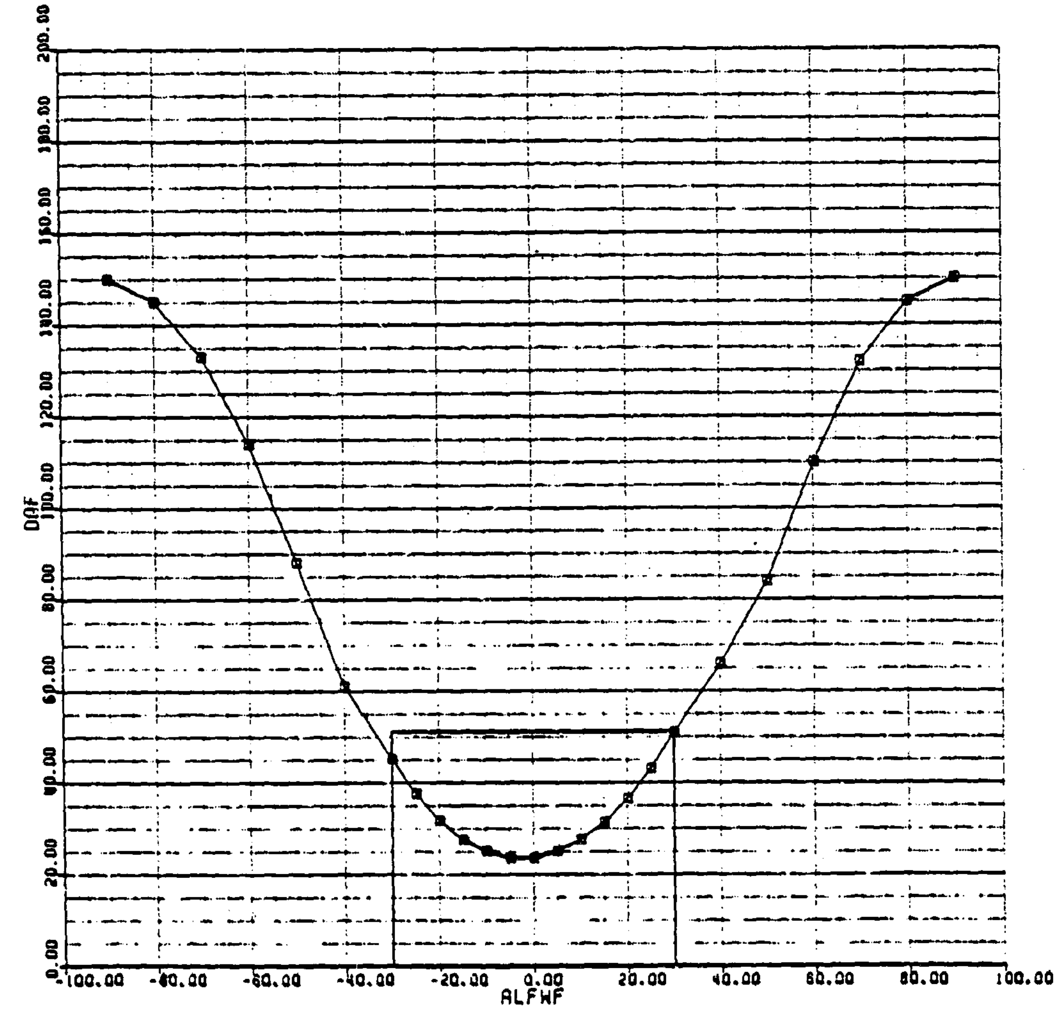

FIGURE 2.5.3(a)

SIKORSKY AIRCRAFT Division of UNITED TECHNOLOGIES

SER-70452

FUSELAGE DRAG COEFFICIENT DUE TO ANGLE OF ATTACK (cont'd)

BLACKHAWK - NASA STUDY 23-SEP-80 DQFMP (2/2)

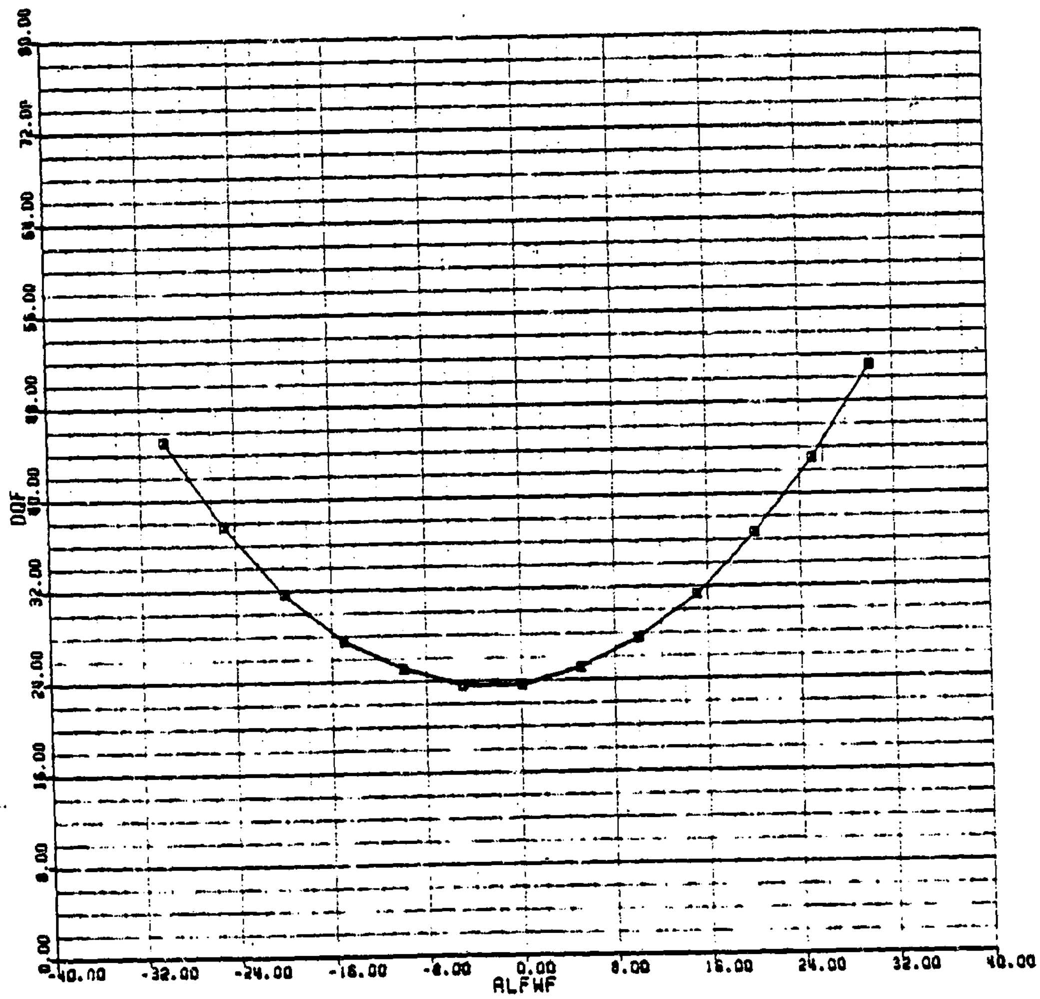

FIGURE 2.5.3(b)

INCREMENTAL FUSELAGE DRAG COEFFICIENT DUE TO SIDESLIP

BLACKHAWK - NASA STUDY 23-SEP-80 DDQFMP (1/2)

MAP NAME: DDQFMP
MAP TYPE: UVAUVA
INPUT VARIABLE(S): PSABWF
OUTPUT VARIABLE: DDQF

PRIMARY MAP:
0.00 (LOWER LIMIT)
30.00 (UPPER LIMIT)
5.00 (DELTA)

SECONDARY MAP:
30.00 (LOWER LIMIT)
90.00 (UPPER LIMIT)
10.00 (DELTA)

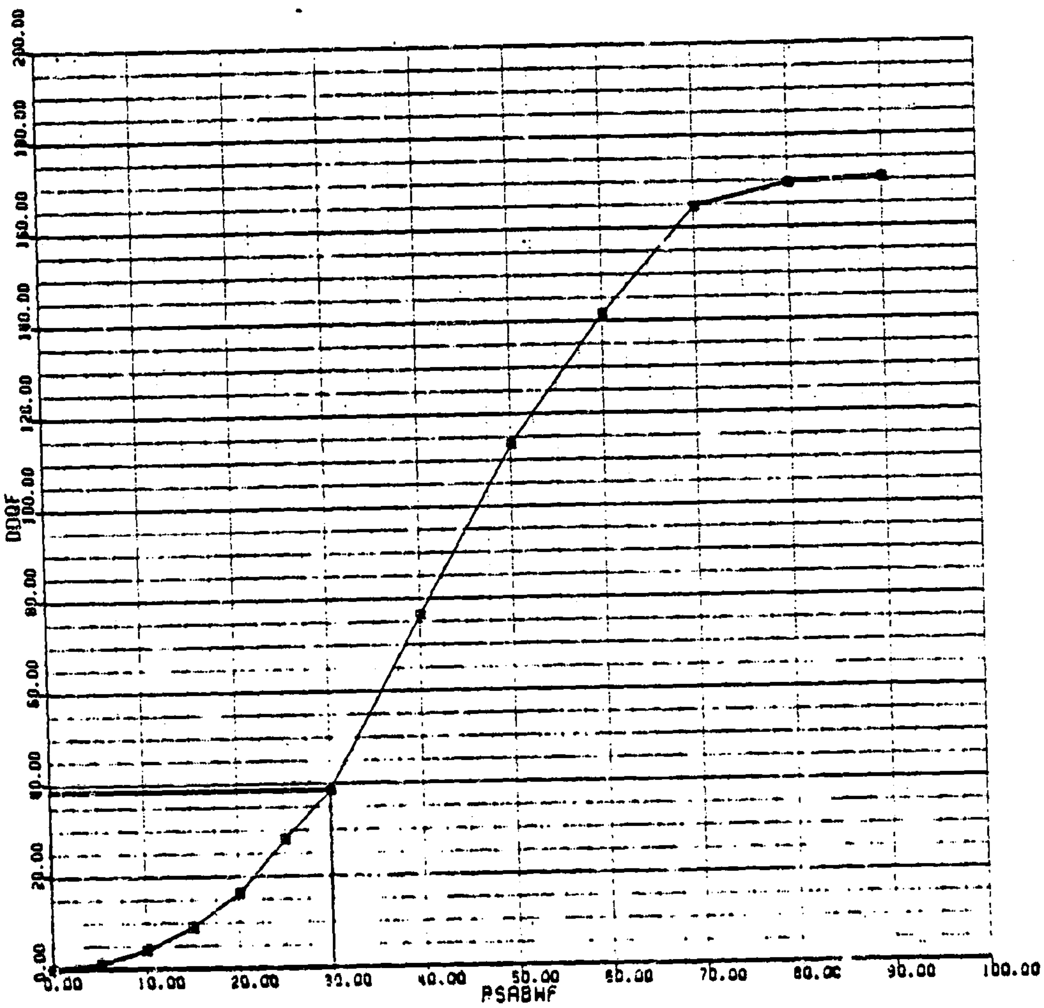

FIGURE 2.5.4(a)

INCREMENTAL FUSELAGE DRAG COEFFICIENT DUE TO SIDESLIP (Cont'd)

BLACKHAWK - NASA STUDY 23-SEP-80 DDQFMP (2/2)

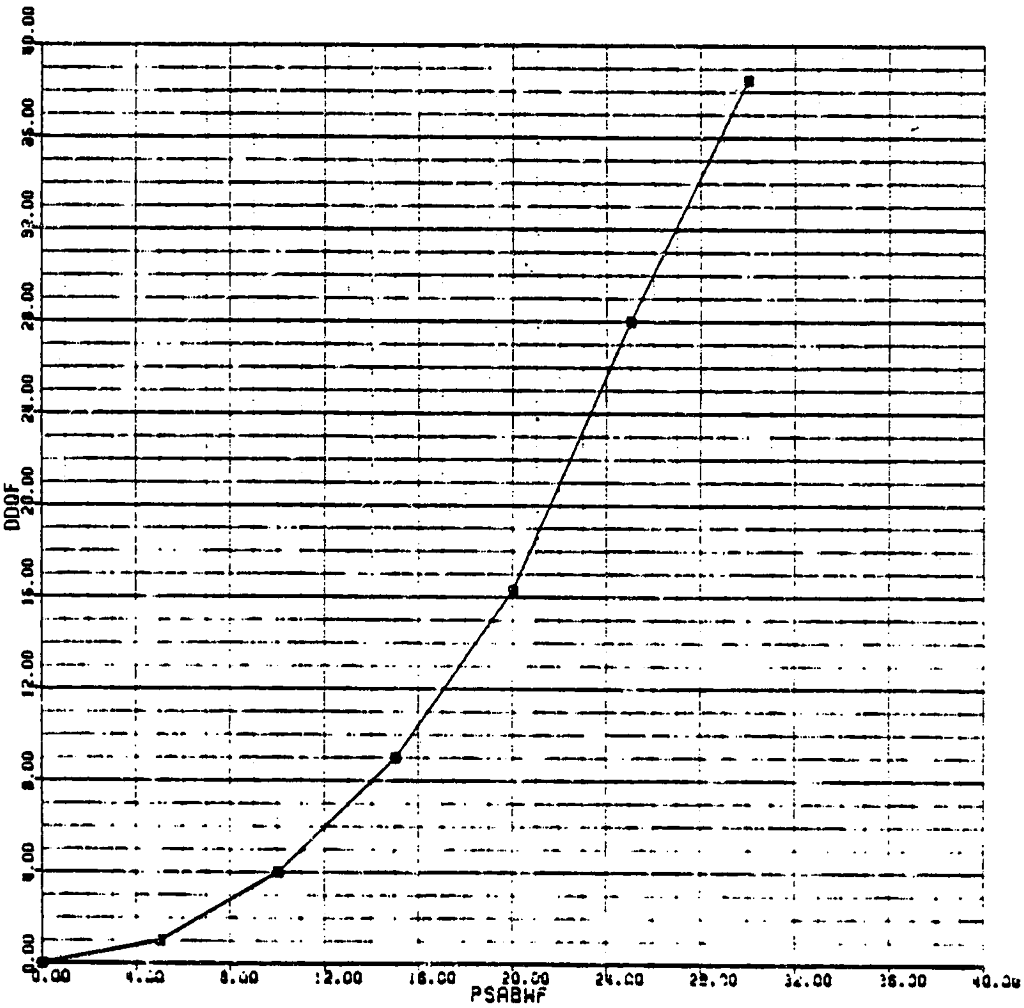

FIGURE 2.5.4(b)

ORIGINAL PAGE IS
OF POOR QUALITY

SIKORSKY AIRCRAFT Division of UNITED TECHNOLOGIES

SER 70452

FUSELAGE SIDEFORCE COEFFICIENT DUE TO SIDESLIP

BLACKHAWK - NASA STUDY 23-SEP-80 YQFMP (1/2)

MAP NAME:		YQFMP
MAP TYPE:		UVSUVS
INPUT VARIABLE(S):	PSIWF	
OUTPUT VARIABLE:		YQF
PRIMARY MAP:		
	-30.00	LOWER LIMIT
	30.00	UPPER LIMIT
	5.00	DELTA
SECONDARY MAP:		
	-90.00	LOWER LIMIT
	90.00	UPPER LIMIT
	10.00	DELTA

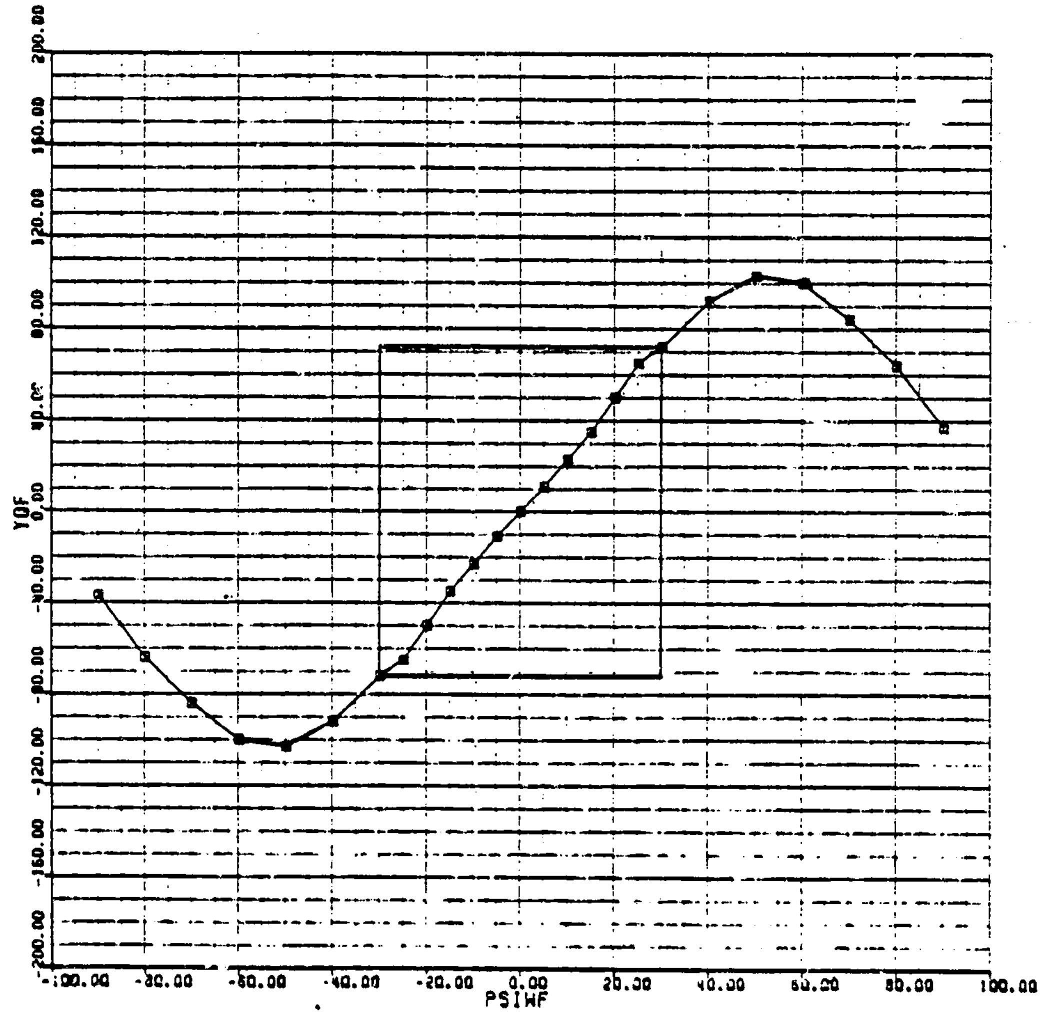

FIGURE 2.5.5(a)

FUSELAGE SIDEFORCE COEFFICIENT DUE TO SIDESLIP (cont'd)

BLACKHAWK - NASA STUDY 23-SEP-80 YQFMP (2/2)

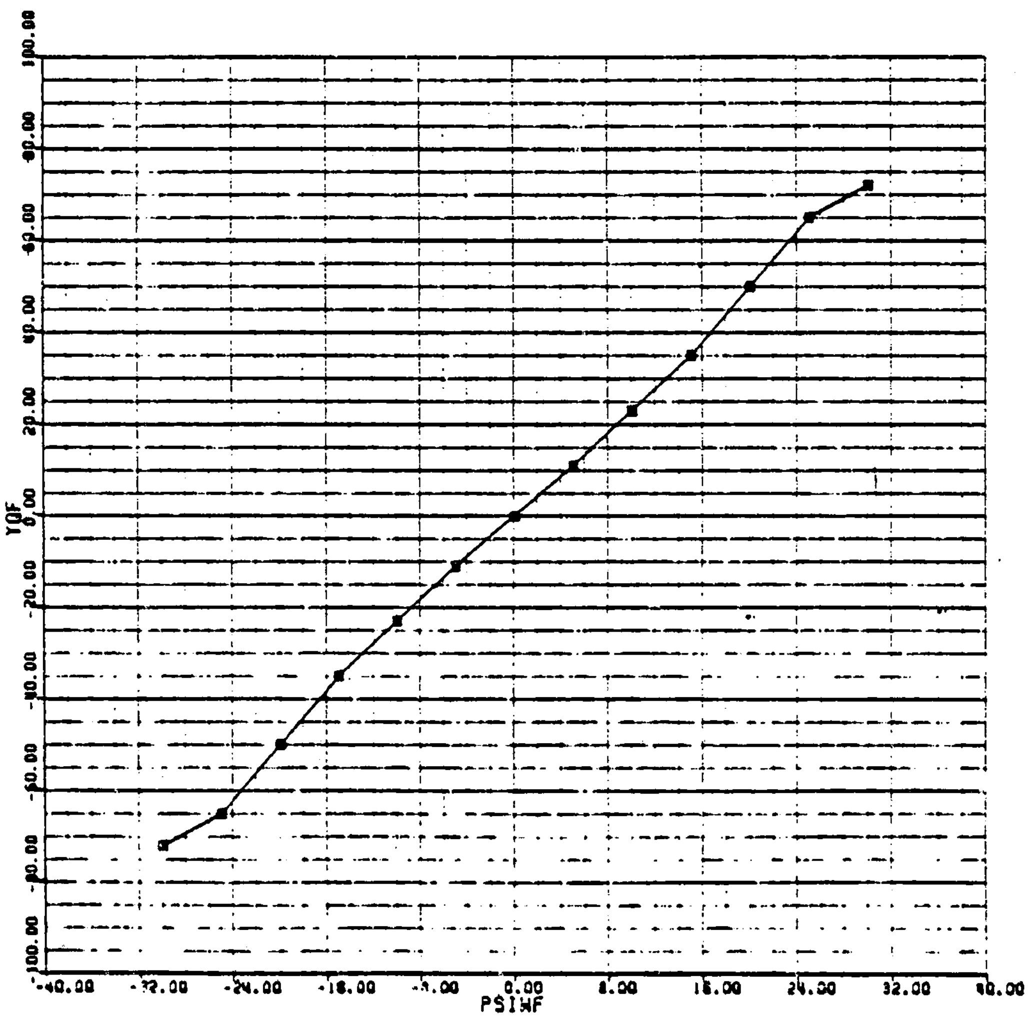

FIGURE 2.5.5(b)

FUSELAGE LIFT COEFFICIENT DUE TO ANGLE OF ATTACK

BLACKHAWK - NASA STUDY   23-SEP-80   LQFMP   (1/2)

MAP NAME: LQFMP
MAP TYPE: UVAUVA
INPUT VARIABLE(S): ALFWF
OUTPUT VARIABLE: LQF

PRIMARY MAP:
-30.00 (LOWER LIMIT)
30.00 (UPPER LIMIT)
5.00 (DELTA)

SECONDARY MAP:
-90.00 (LOWER LIMIT)
90.00 (UPPER LIMIT)
10.00 (DELTA)

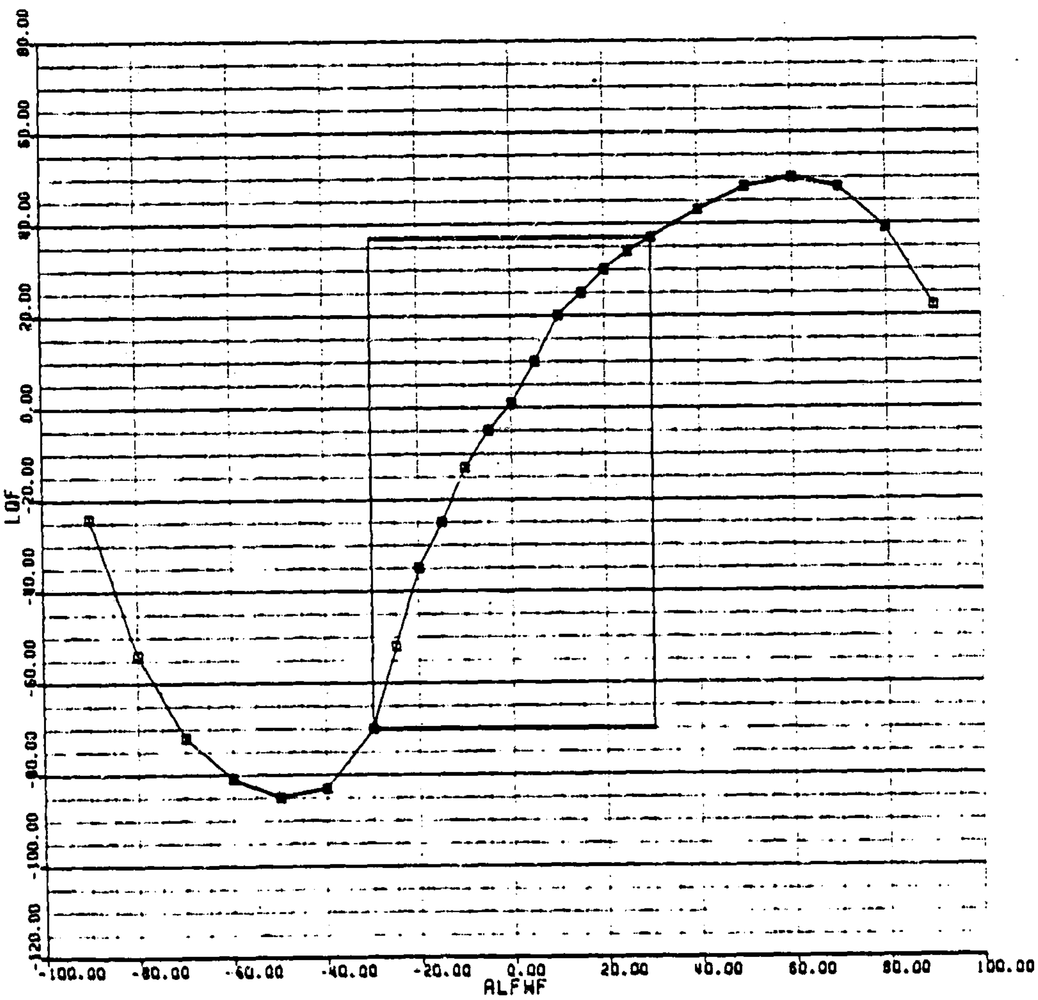

FIGURE 2.5.6(a)

FUSELAGE LIFT COEFFICIENT DUE TO ANGLE OF ATTACK (Cont'd)

BLACKHAWK - NASA STUDY 23-SEP-80 LQFMP (2/2)

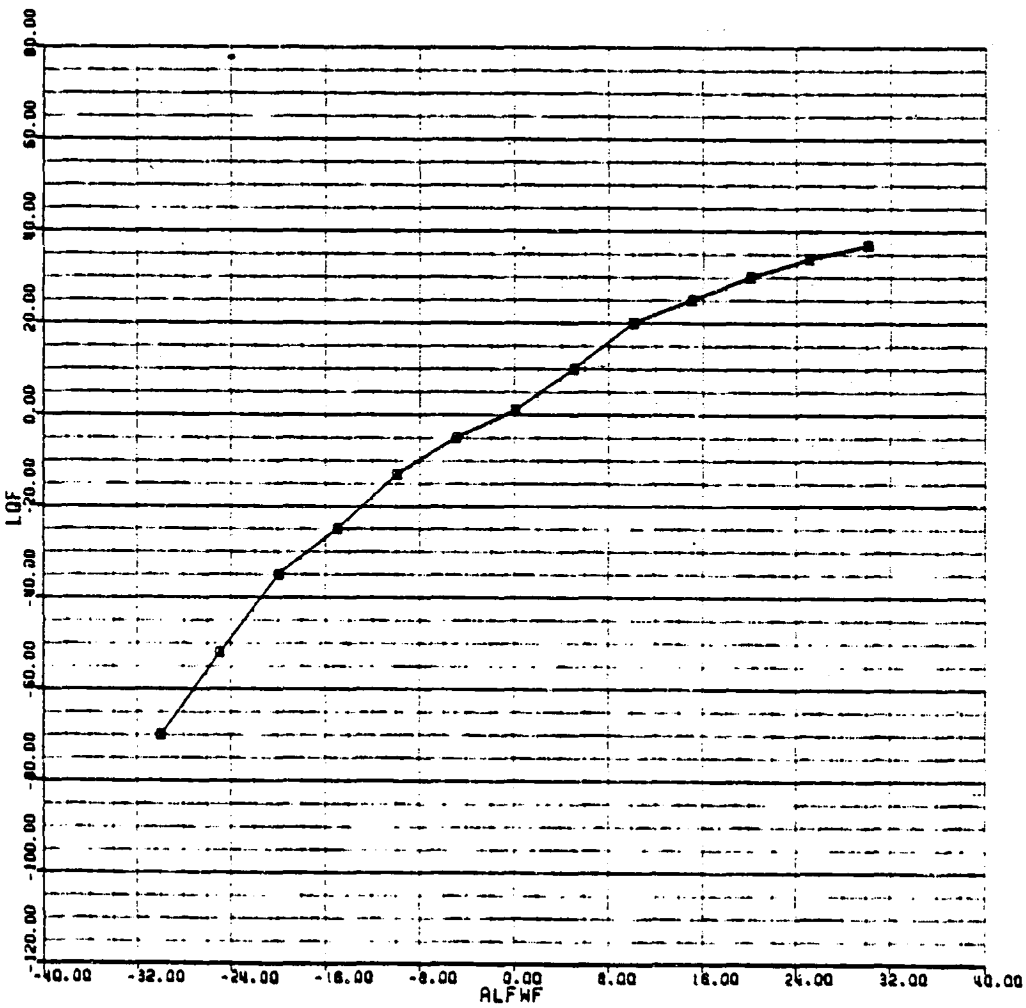

FIGURE 2.5.6(b)

INCREMENTAL FUSELAGE LIFT COEFFICIENT DUE TO SIDESLIP

```
MAP NAME:                        DLQFMP
MAP TYPE:                        UVA
INPUT VARIABLE(S):  PSIWF
OUTPUT VARIABLE:                 DLQF

PRIMARY MAP:
                      -30.00     LOWER LIMIT
                       30.00     UPPER LIMIT
                        5.00
```

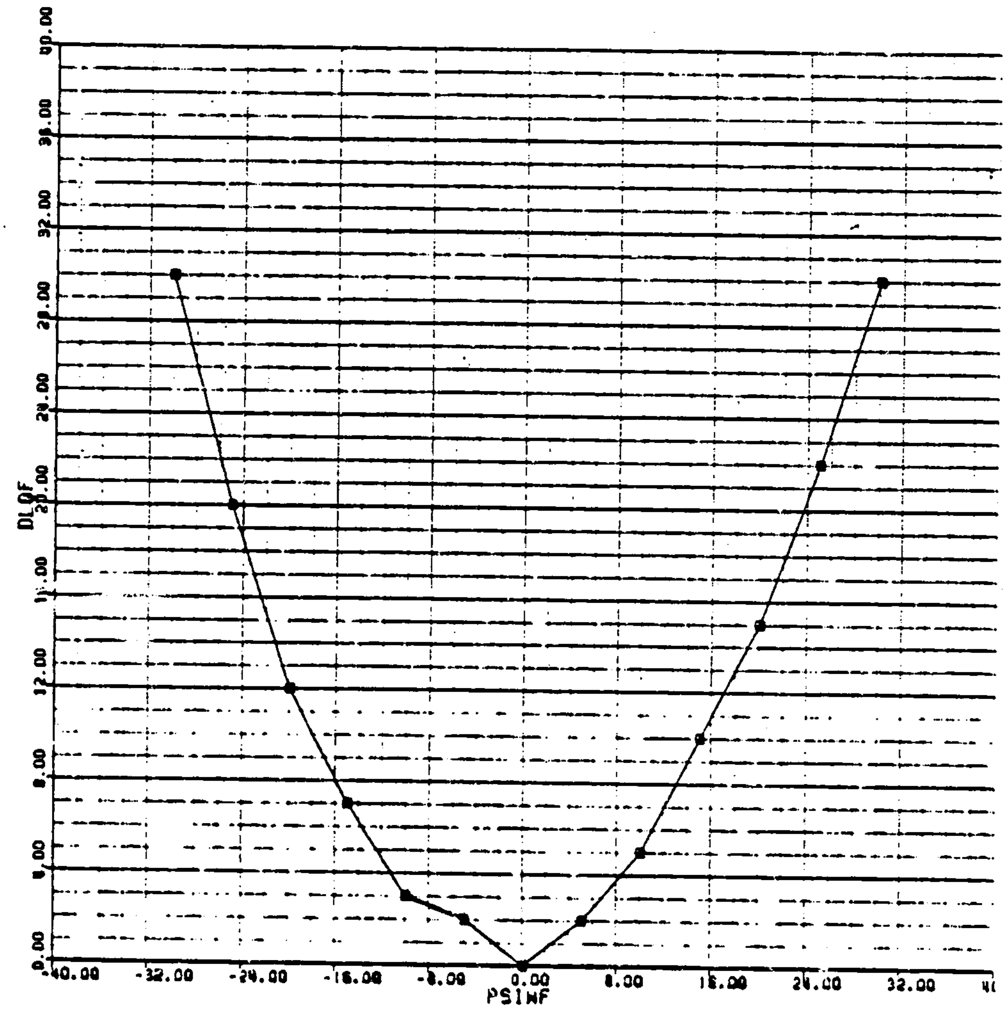

FIGURE 2.5.7

FUSELAGE ROLLING MOMENT COEFFICIENT DUE TO SIDESLIP

BLACKHAWK - NASA STUDY   23-SEP-80   AQFMP   (1/2)

MAP NAME: AQFMP
MAP TYPE: UVSUVS
INPUT VARIABLE(S): PSIWF
OUTPUT VARIABLE: AQF

PRIMARY MAP:

-30.00	(LOWER LIMIT)
30.00	(UPPER LIMIT)
5.00	(DELTA)

SECONDARY MAP:

-90.00	(LOWER LIMIT)
90.00	(UPPER LIMIT)
10.00	(DELTA)

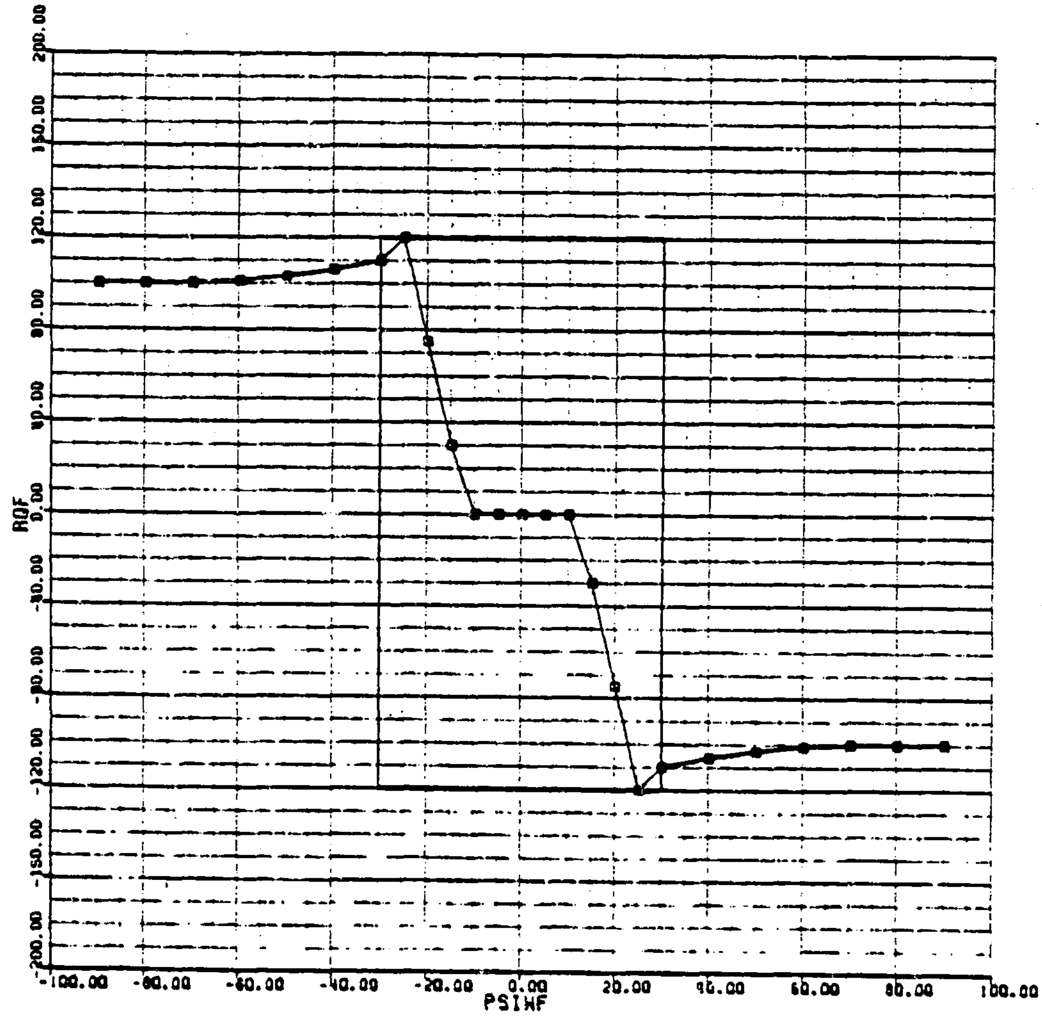

FIGURE 2.5.8(a)

FUSELAGE ROLLING MOMENT COEFFICIENT DUE TO SIDESLIP (Cont'd)

BLACKHAWK - NASA STUDY 23-SEP-80 AQFMP (2/2)

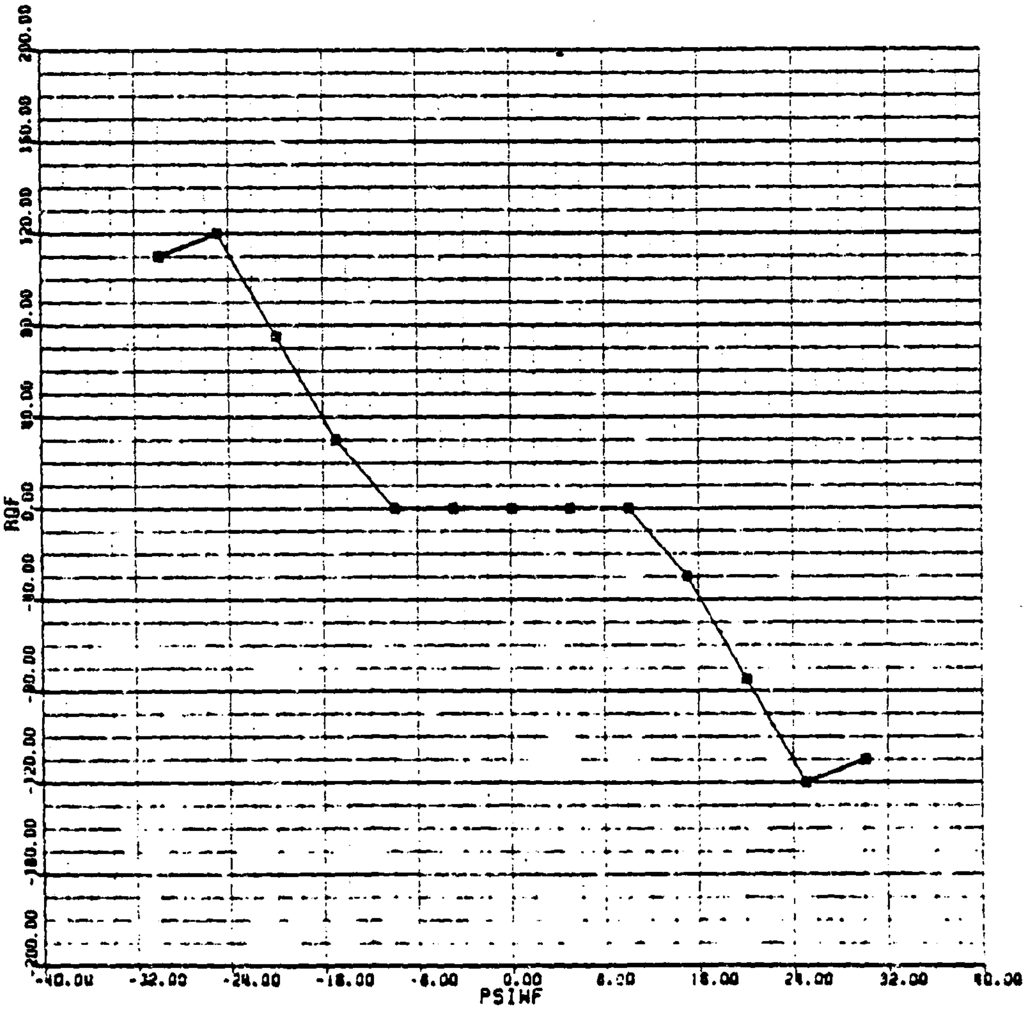

FIGURE 2.5.8(b)

ORIGINAL PAGE IS
OF POOR QUALITY

FUSELAGE PITCHING MOMENT COEFFICIENT DUE TO ANGLE OF ATTACK

BLACKHAWK - NASA STUDY 23-SEP-80 MQFMP (1/2)

MAP NAME: MQFMP
MAP TYPE: UVRUVR
INPUT VARIABLE(S): ALFWF
OUTPUT VARIABLE: MQF

PRIMARY MAP:
-30.00 (LOWER LIMIT)
30.00 (UPPER LIMIT)
5.00 (DELTA)

SECONDARY MAP:
-90.00 (LOWER LIMIT)
90.00 (UPPER LIMIT)
10.00 (DELTA)

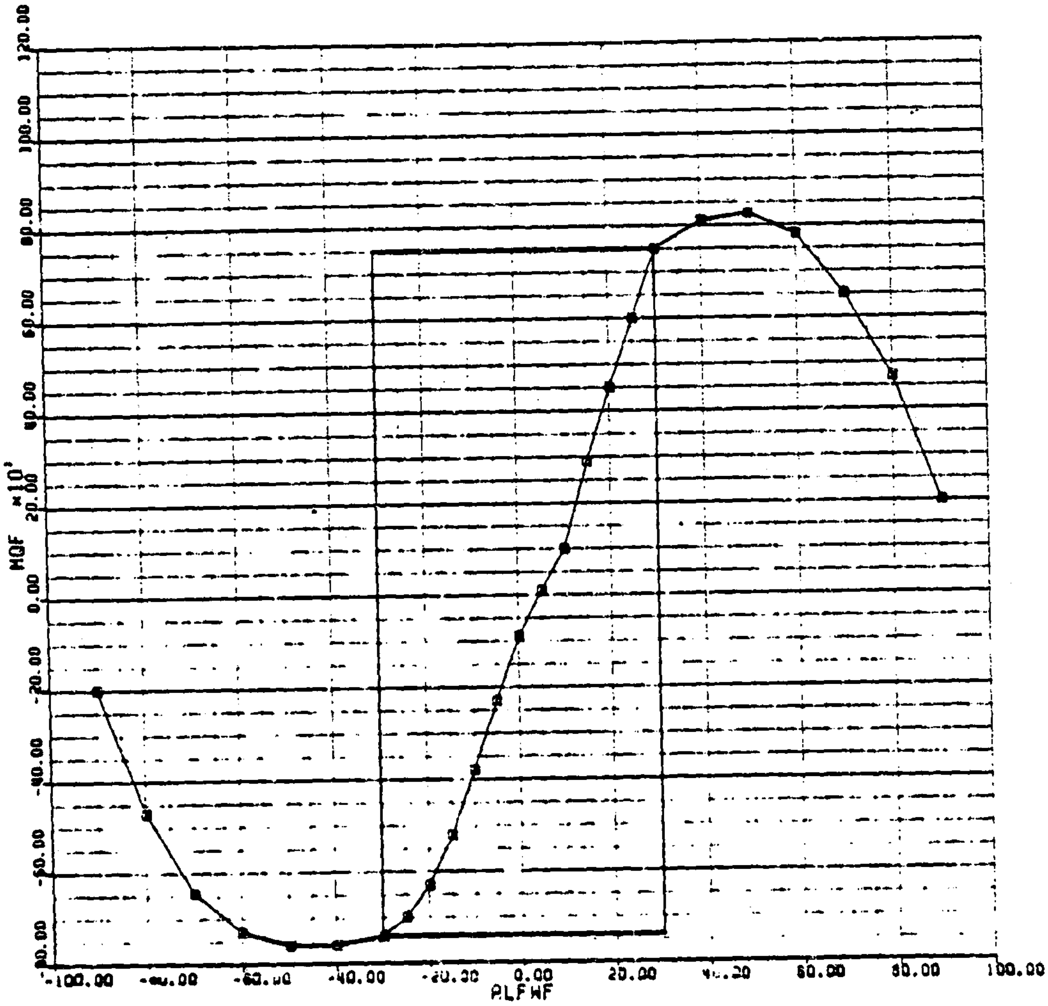

FIGURE 2.5.9(a)

FUSELAGE PITCHING MOMENT COEFFICIENT DUE TO ANGLE OF ATTACK (Cont'd)

BLACKHAWK - NASA STUDY 23-SEP-80 MQFMP (2/2)

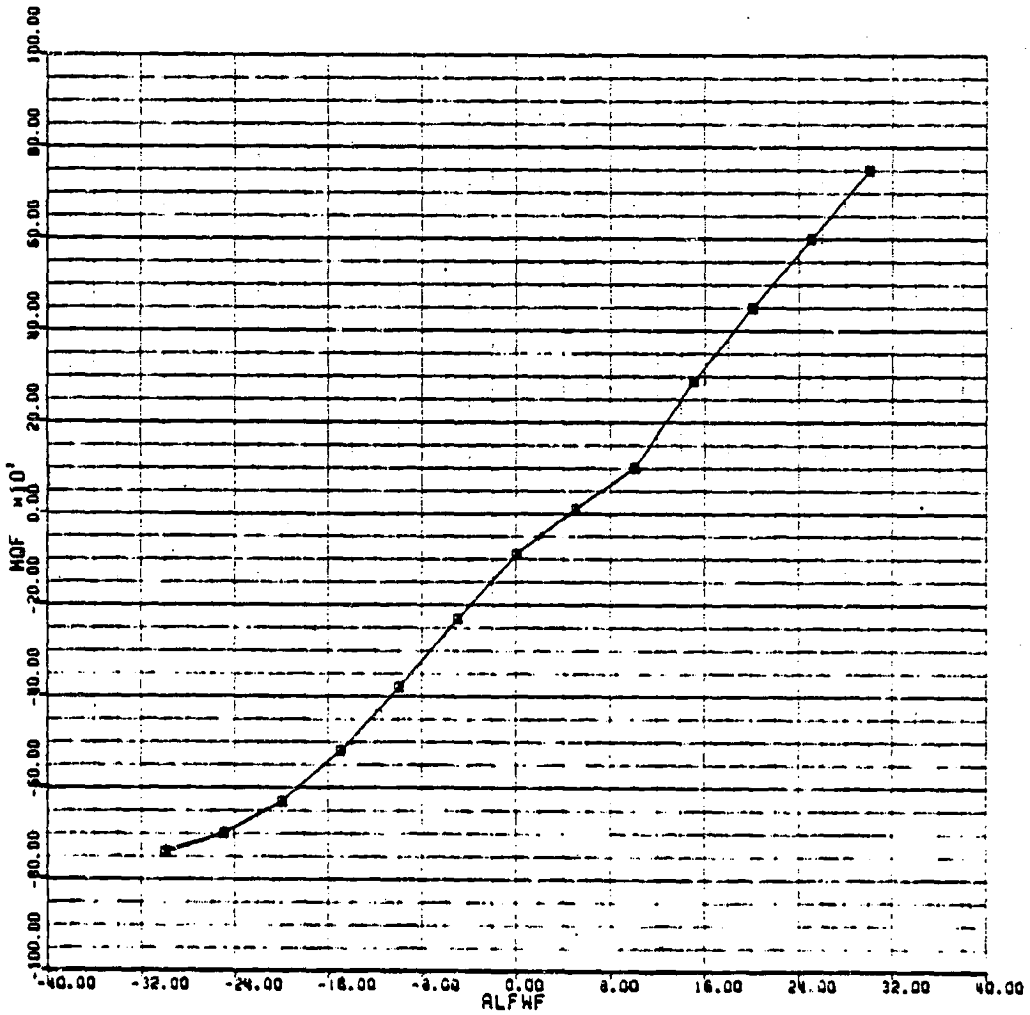

FIGURE 2.5.9(b)

INCREMENTAL FUSELAGE PITCHING MOMENT DUE TO SIDESLIP

MAP NAME:		DMQFMP
MAP TYPE:		UVA
INPUT VARIABLE(S):	PSABWF	
OUTPUT VARIABLE:		DMQF

PRIMARY MAP:

0.00	(LOWER LIMIT)
30.00	(UPPER LIMIT)
5.00	(DELTA)

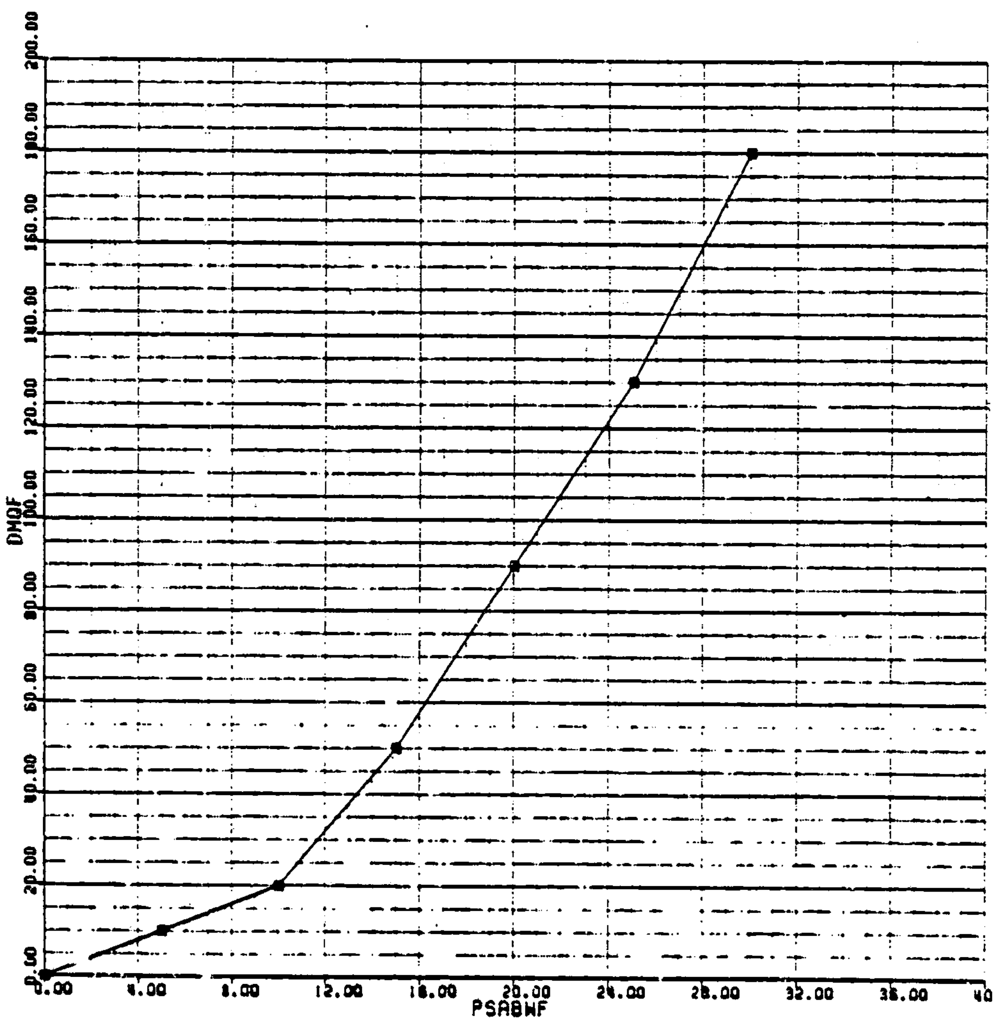

FIGURE 2.5.10

FUSELAGE YAWING MOMENT COEFFICIENT DUE TO SIDESLIP

BLACKHAWK - NASA STUDY 23-SEP-80 NQFMP (1/2)

MAP NAME: NQFMP
MAP TYPE: UVAUVA
INPUT VARIABLE(S): PSIWF
OUTPUT VARIABLE: NQF

PRIMARY MAP:
-30.00 (LOWER LIMIT)
30.00 (UPPER LIMIT)
5.00 (DELTA)

SECONDARY MAP:
-90.00 (LOWER LIMIT)
90.00 (UPPER LIMIT)
10.00 (DELTA)

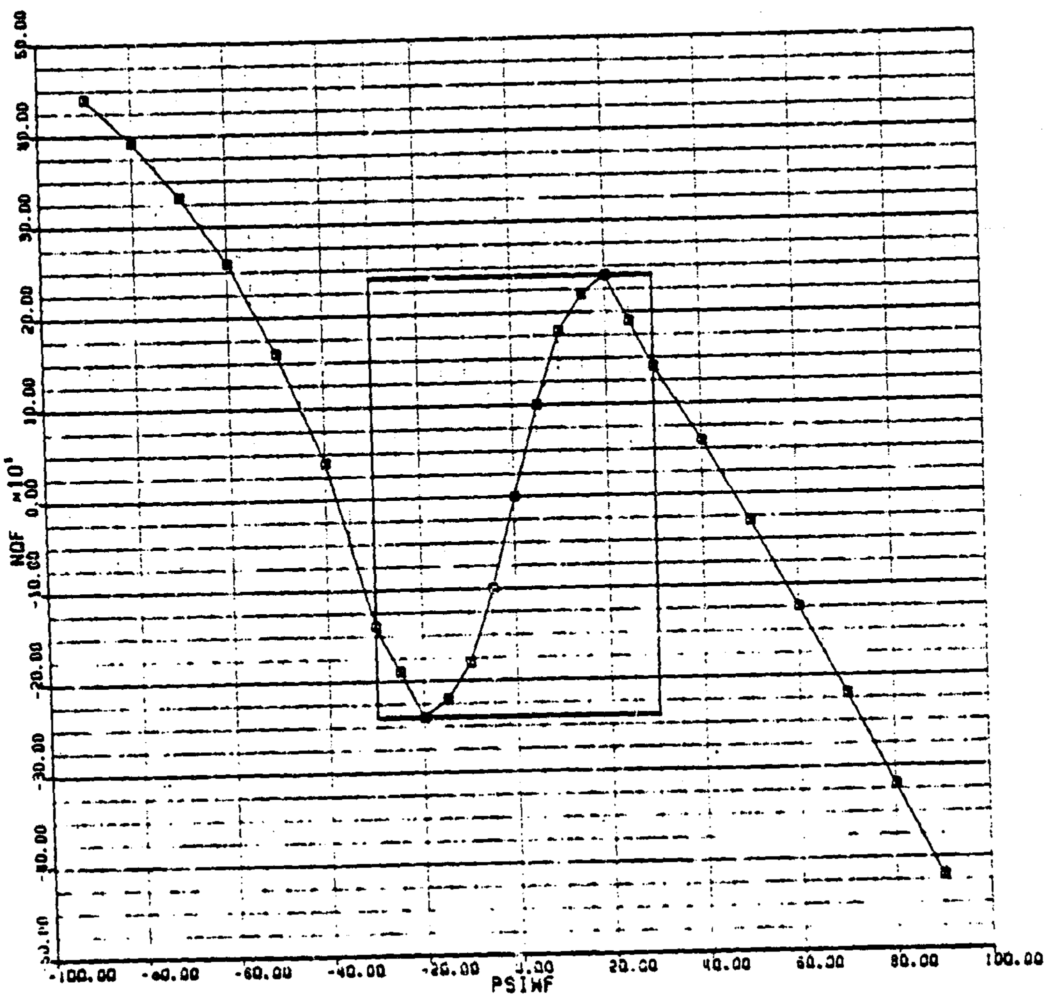

FIGURE 2.5.11(a)

FUSELAGE YAWING MOMENT COEFFICIENT DUE TO SIDESLIP (Cont'd)

BLACKHAWK - NASA STUDY 23-SEP-80 NOFMP (2/2)

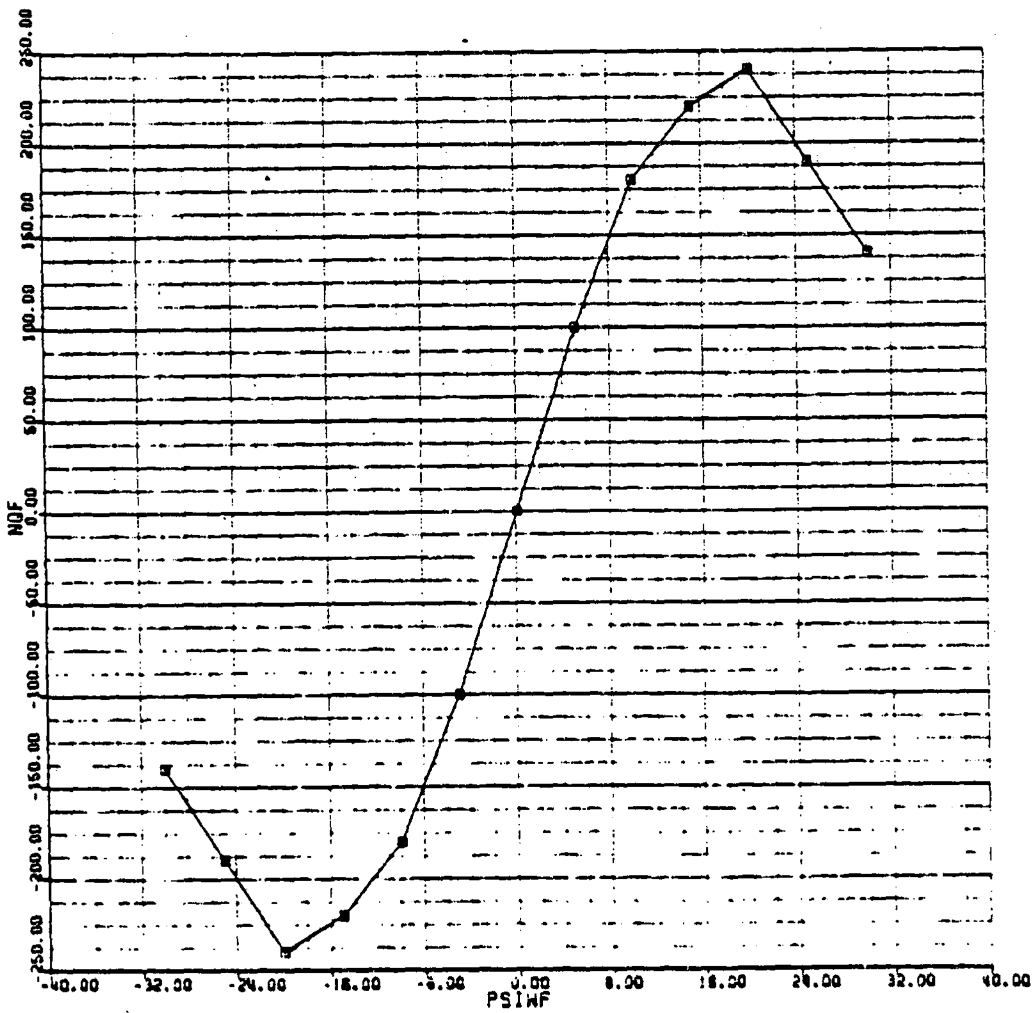

FIGURE 2.5.11(b)

ORIGINAL PAGE IS
OF POOR QUALITY

SIKORSKY AIRCRAFT UNITED TECHNOLOGIES

DOCUMENT NO. SER 70452

5.3 EMPENNAGE MODULE

SA 29 REV. 6

5.3 Empennage Module

5.3.1 Module Description

This module calculates the aerodyanmic forces on the horizontal and vertical tail surfaces resulting from the local airflow. The velocities are derived at, and the aerodynamic forces assummed to act at, the panel center of pressure. Aerodynamic forces are developed in the local flow wind axes system and subsequently transferred to the body axes system at the fuselage CG as defined on Figure 3.1.1. The overall module equation flow is shown in block diagram form on Figure 3.1.2.

The tail can experience aerodynamic interference effects from many sources. Components of flow from the main rotor and fuselage are define at present in this module. However, the equations are formulated to allow easy insertion of other components. Three components of rotor wash are developed as a function of rotor wake skew angle and blade longitudinal flapping. Tail dynamic pressure blockage and downwash from the forebody are developed as a function of angle of attack and sideslip. Small downwash/sidewash angles are assumed and the velocity delayed to account for the time taken by the airflow to reach the tail.

The total velocity components for the tail are made up of contributions from the basic body axes translational and angular velocities, gust effects, rotor wash, fuselage downwash and sidewash. Dynamic pressure loss is introduced by factoring the components of the free stream flow. The actual total dynamic pressure at the tail is calculated from the resultant velocity vector. This allows a more representative definition of dynamic pressure at low speeds where downwash from the rotor predominates the flow at the tail. The lift and drag forces at the tail are obtained from isolated tail data and are a function of tail total angle of attack. In the case of the vertical tail, angle of attack has the same connotation as sideslip. The lift and drag forces in local wind axes are resolved into body axes at the tail. (Moments from the tail about its own axis are not accounted for.) Finally, the component forces at the empennage are transferred to the CG together with the corresponding moments.

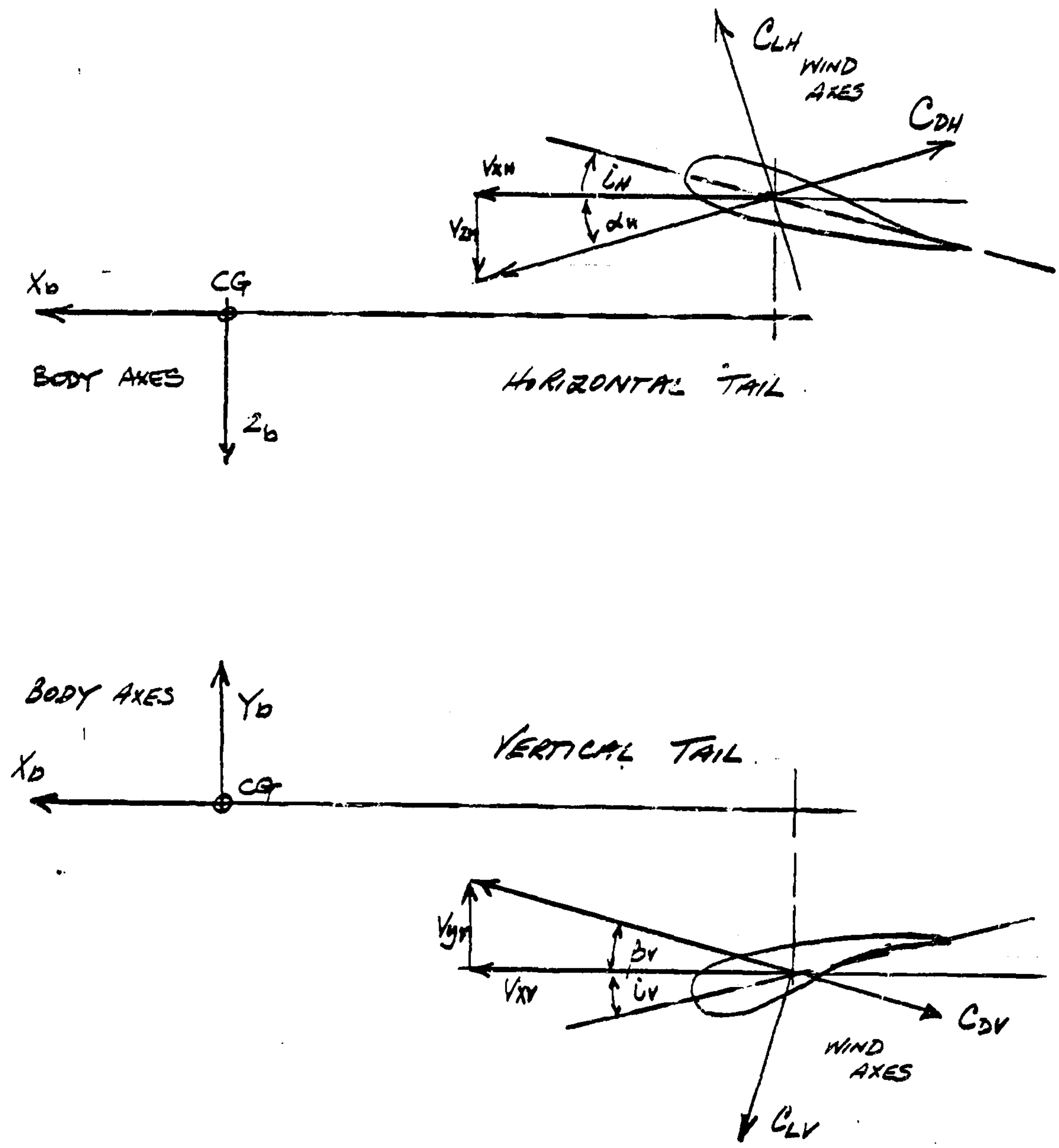

EMPENNAGE AXES SYSTEM

Figure 3.1.1

ORIGINAL PAGE IS OF POOR QUALITY

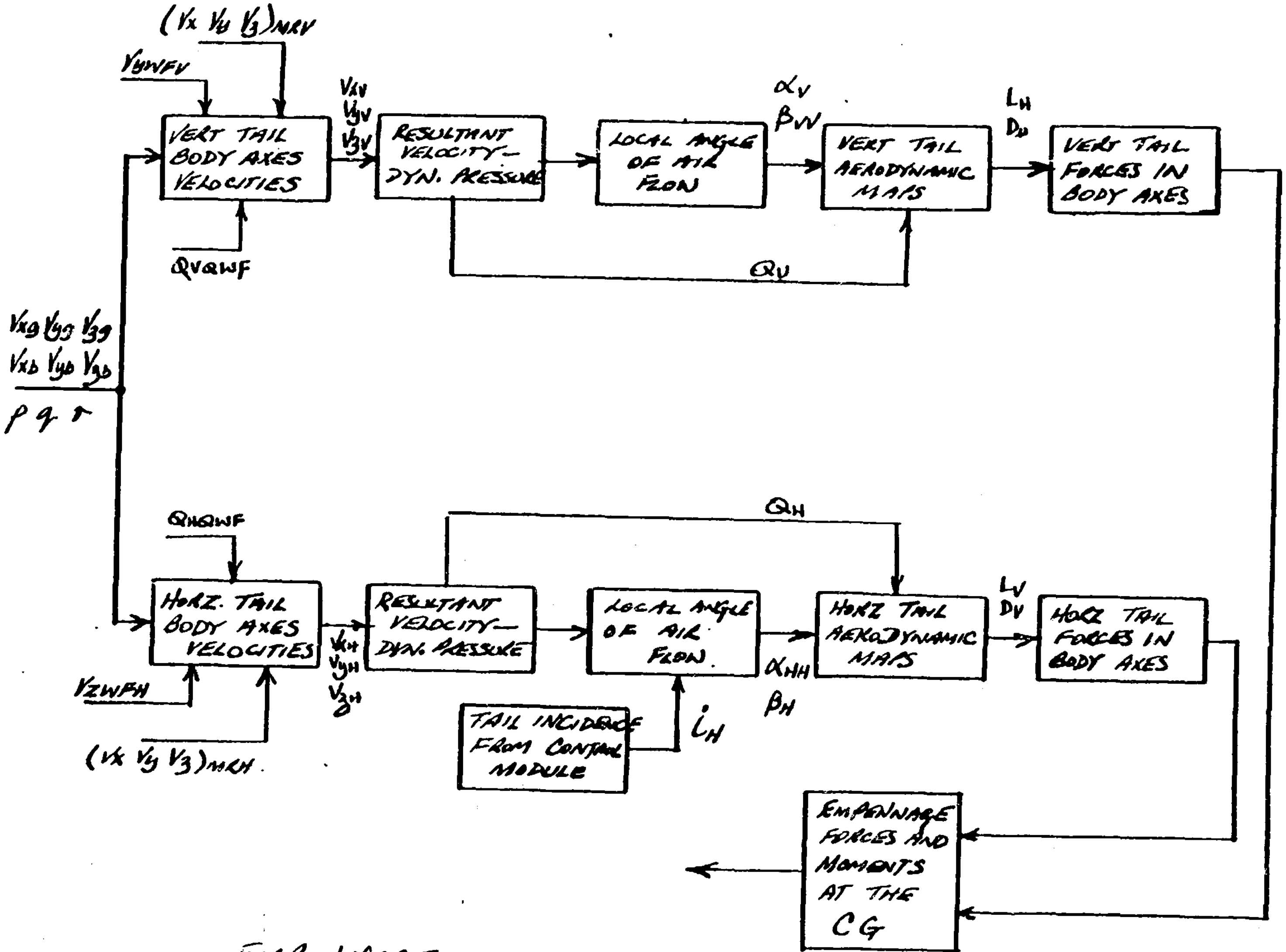

EMPENNAGE EQUATION FLOW

Figure 3.1.2

5.3.2 EMPENNAGE MODULE EQUATIONS

HORIZONTAL TAIL PANEL

GEOMETRY

$$F_{HT1} = \frac{(FSH1 - FSCGb)}{12}$$

$$W_{HT1} = \frac{(WLH1 - WLCGb)}{12}$$

$$B_{HT1} = \frac{(BLH1 - BLCGb)}{12}$$

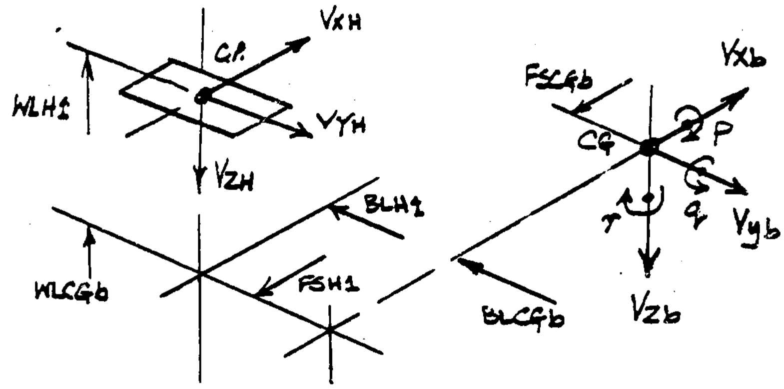

INTERFERENCE VELOCITIES

— FROM THE MAIN ROTOR

$EKXH1 = f(\chi_{PMR}, a_{1FMR})$, MAP – EXH1MP TABLE 3.5.1 FIGURE 3.5.1

$V_{XMRH1} = D_{WSHMR}\ \Omega_T R_T\ EKXH1$

$EKYH1 = f(\chi_{PMR}, a_{1FMR})$, NO INPUT FOR BLACK HAWK AT THIS TIME

$V_{YMRH1} = D_{WSHMR}\ \Omega_T R_T \cdot EKYH1$

$EKZH1 = f(\chi_{PMR}, a_{1FMR})$, MAP – EZH1MP TABLE 3.5.2 FIGURE 3.5.2

$V_{ZMRH1} = -D_{WSHMR} \cdot \Omega_T R_T \cdot EKZH1$

— FROM THE FUSELAGE

DYNAMIC PRESSURE RATIO

$$QH1QWF = f(\alpha_{WF}) \quad , \text{ MAP-QH1MP}$$

$$KQH1 = (QH1QWF)^{1/2}$$

TABLE 3.5.3
FIGURE 3.5.3

DOWNWASH COMPONENT

$$EpsH1 = f(\alpha_{WF}) \quad , \text{ MAP-EPH1MP}$$

$$VZWFH1 = -\frac{Vxb}{57.3} \cdot EpsH1 \cdot K_{QH1}$$

TABLE 3.5.4
FIGURE 3.5.4

$$EpsH1 \text{ DELAYED BY } \left(\frac{FSH1 - FSCGb}{12 * Vxb}\right) \text{ SECS}$$

TOTAL INTERFERENCE VELOCITIES

$$VXIH1 = VXMRH1$$

$$VYIH1 = VYMRH1$$

$$VZIH1 = VZMRH1 + VZWFH1$$

LOCAL VELOCITY AT THE HORIZONTAL TAIL PANEL

$$V_{XH1} = (V_{Xb} + V_{XgH1}) K_{QH1} - q\, W_{HT1} + r\, B_{HT1} + V_{XIH1}$$

$$V_{YH1} = (V_{Yb} + V_{YgH1}) K_{QH1} + p\, W_{HT1} - r\, F_{HT1} + V_{YIH1}$$

$$V_{ZH1} = (V_{Zb} + V_{ZgH1}) K_{QH1} + q\, F_{HT1} - p\, B_{HT1} + V_{ZIH1}$$

DYNAMIC PRESSURE AT THE HORIZONTAL TAIL

$$Q_{H1} = \frac{1}{2}\rho \left(V_{XH1}^2 + V_{YH1}^2 + V_{ZH1}^2 \right)$$

LOCAL ANGLE OF THE FLOW AT THE HORIZONTAL TAIL

$$\sin \alpha_{H1} = \frac{V_{ZH1}}{(V_{XH1}^2 + V_{ZH1}^2)^{1/2}}$$

$$\cos \alpha_{H1} = \frac{V_{XH1}}{(V_{XH1}^2 + V_{ZH1}^2)^{1/2}}$$

$$\alpha_{H1} = \tan^{-1} \left\{ \frac{V_{ZH1}}{|V_{XH1}|} \right\}$$

$$\alpha_{HH1} = i_{H1} + \alpha_{H1}$$

$$\beta_{H1} = \tan^{-1} \left\{ \frac{V_{YH1}}{(V_{XH1}^2 + V_{ZH1}^2)^{1/2}} \right\}$$

$\left.\begin{array}{l}\sin \beta_{H1} \\ \cos \beta_{H1}\end{array}\right\}$ DERIVED FROM SINCOS (β_{H1}) ROUTINE

HORIZONTAL TAIL LIFT AND DRAG COEFFICIENTS

$C_{LH1} = f(\alpha_{HH1})$, MAP – CLH1MP, TABLE 3.5.5 FIGURE 3.5.5

$C_{DH1} = f(|\alpha_{HH1}|)$, MAP – CDH1MP, TABLE 3.5.6, FIGURE 3.5.6

BODY AXES FORCES AND MOMENTS ABOUT THE CG

$$\begin{bmatrix} X_{H1} \\ Y_{H1} \\ Z_{H1} \end{bmatrix} = \begin{bmatrix} (\cos\alpha_{H1} \cos\beta_{H1}) & (\cos\alpha_{H1} \sin\beta_{H1}) & (-\sin\alpha_{H1}) \\ (\sin\beta_{H1}) & (-\cos\beta_{H1}) & 0 \\ (\sin\alpha_{H1} \cos\beta_{H1}) & (\sin\alpha_{H1} \sin\beta_{H1}) & (\cos\alpha_{H1}) \end{bmatrix} \begin{bmatrix} -Q_{H1} \cdot S_{AH1} \cdot C_{DH1} \\ 0 \\ -Q_{H1} \cdot S_{AH1} \cdot C_{LH1} \end{bmatrix}$$

$$L_{H1} = Y_{H1}(W_{HT1}) - Z_{H1}(B_{HT1})$$

$$M_{H1} = -X_{H1}(W_{HT1}) + Z_{H1}(F_{HT1})$$

$$N_{H1} = -Y_{H1}(F_{HT1}) + X_{H1}(B_{HT1})$$

SA 29 REV. 6

VERTICAL TAIL PANEL

GEOMETRY

$$FYT1 = \left(\frac{FSVT1 - FSCGb}{12}\right)$$

$$WVT1 = \left(\frac{WLVT1 - WLCGb}{12}\right)$$

$$BYT1 = \left(\frac{BLVT1 - BLCGb}{12}\right)$$

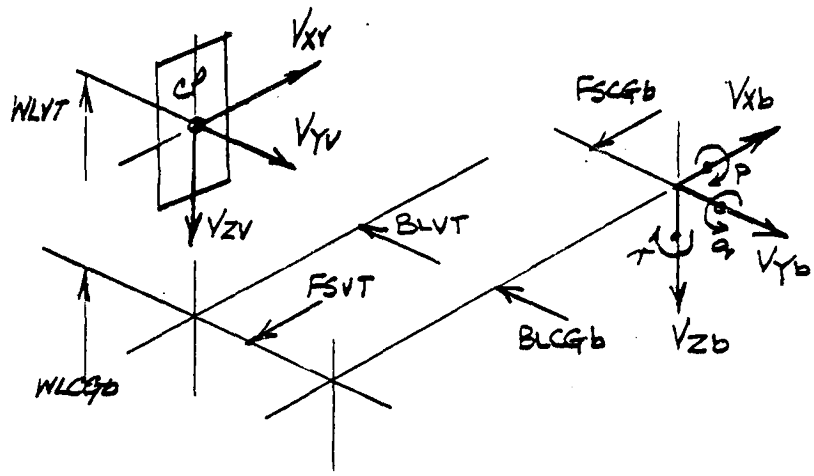

INTERFERENCE VELOCITIES

— FROM THE MAIN ROTOR , SAME AS HORIZONTAL TAIL FOR BLACK HAWK

$EKXV1 = f(\chi_{PMR}, a_{1FMR})$, MAP-EXH1MP
TABLE 3.5.1
FIGURE 3.5.1

$VXMRV1 = DWSHMR\ \Omega_T R_T\ EKXV1$

$EKYV1 = f(\chi_{PMR}, a_{1FMR})$, NO INPUT FOR BLACK HAWK AT THIS TIME

$VYMRV1 = DWSHMR\ \Omega_T R_T\ EKYV1$

$EKZV1 = f(\chi_{AMR}, a_{1FMR})$, MAP-EZH1MP
TABLE 3.5.2
FIGURE 3.5.2

$VZMRV1 = DWSHMR\ \Omega_T R_T\ EKZV1$

SA 29 REV. G

- FROM THE FUSELAGE

DYNAMIC PRESSURE RATIO

$$QV1QWF = f(|\psi_{WF}|)$$, MAP - QV1MP

$$KQV1 = (QV1QWF)^{1/2}$$

TABLE 3.5.7
FIGURE 3.5.7

SIDEWASH COMPONENT

$$S_{IGV1} = f(\psi_{WF})$$, MAP - SGV1MP

$$VYWFV1 = -\frac{Vxb}{57.3} \cdot S_{IGV1} \cdot KQV1$$

TABLE 3.5.8
FIGURE 3.5.8

S_{IGV1} DELAYED BY $\left(\frac{FSV1 - FSCGb}{12 * Vxb}\right)$ SECS

TOTAL INTERFERENCE VELOCITIES

$$VXIV1 = VXMRV1$$

$$VYIV1 = VYMRV1 + VYWFV1$$

$$VZIV1 = VZMRV1$$

LOCAL VELOCITIES AT THE VERTICAL TAIL PANEL

$$V_{XV1} = (V_{xb} + V_{xgv1}) K_{QV1} - q(W_{VT1}) + r(B_{VT1}) + V_{xIV1}$$

$$V_{YV1} = (V_{yb} + V_{ygv1}) K_{QV1} - r(F_{VT1}) + p(W_{VT1}) + V_{yIV1}$$

$$V_{ZV1} = (V_{zb} + V_{zgv1}) K_{QV1} + q(F_{VT1}) - p(B_{VT1}) + V_{zIV1}$$

DYNAMIC PRESSURE AT THE VERTICAL TAIL

$$Q_{V1} = \frac{1}{2}\rho\left(V_{xv1}^2 + V_{yv1}^2 + V_{zv1}^2\right)$$

LOCAL ANGLES OF THE FLOW AT THE VERTICAL TAIL

$$\sin\alpha_{V1} = \frac{V_{ZV1}}{\left(V_{XV1}^2 + V_{ZV1}^2\right)^{1/2}}$$

$$\cos\alpha_{V1} = \frac{V_{XV1}}{\left(V_{XV1}^2 + V_{ZV1}^2\right)^{1/2}}$$

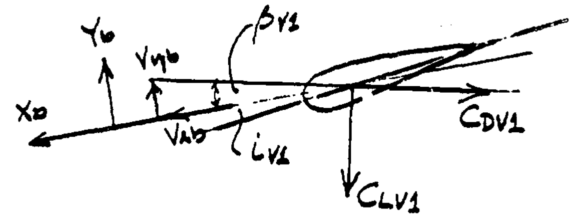

$$\alpha_{V1} = \tan^{-1}\left\{\frac{V_{ZV1}}{|V_{XV1}|}\right\}$$

$$\beta_{V1} = \tan^{-1}\left\{\frac{V_{yV1}}{\left(V_{XV1}^2 + V_{ZV1}^2\right)^{1/2}}\right\}$$

$$\beta_{VV1} = i_{V1} + \beta_{V1}$$

$\left.\begin{array}{l}\sin\beta_{V1}\\ \cos\beta_{V1}\end{array}\right\}$ DERIVED FROM SINCOS(β_{V1}) ROUTINE

SA 29 REV. G

VERTICAL TAIL LIFT AND DRAG COEFFICIENTS

$C_{LV1} = f(\beta_{VV1})$, MAP-CLV1MP, TABLE 3.5.9, FIGURE 3.5.9

$C_{DV1} = f(\beta_{VV1})$, MAP-CDV1MP, TABLE 3.5.10, FIGURE 3.5.10

BODY AXES FORCES AND MOMENTS ABOUT THE CG

$$\begin{bmatrix} X_{V1} \\ Y_{V1} \\ Z_{V1} \end{bmatrix} = \begin{bmatrix} (\cos\alpha_{V1}\cos\beta_{V1}) & (\cos\alpha_{V1}\sin\beta_{V1}) & (-\sin\alpha_{V1}) \\ (\sin\beta_{V1}) & (-\cos\beta_{V1}) & 0 \\ (\sin\alpha_{V1}\cos\beta_{V1}) & (\sin\alpha_{V1}\sin\beta_{V1}) & (\cos\alpha_{V1}) \end{bmatrix} \begin{bmatrix} -C_{DV1}.S_{AV1}.Q_{V1} \\ C_{LV1}.S_{AV1}.Q_{V1} \\ 0 \end{bmatrix}$$

$$L_{V1} = Y_{V1}(W_{VT1}) - Z_{V1}(B_{VT1})$$

$$M_{V1} = Z_{V1}(F_{VT1}) - X_{V1}(W_{VT1})$$

$$N_{V1} = -Y_{V1}(F_{VT1}) + X_{V1}(B_{VT1})$$

$$X_T = \sum_{i=1}^{n}(X_{H_i} + X_{V_i})$$

$$Y_T = \sum_{i=1}^{n}(Y_{H_i} + Y_{V_i})$$

$$Z_T = \sum_{i=1}^{n}(Z_{H_i} + Z_{V_i})$$

$$L_T = \sum_{i=1}^{n}(L_{H_i} + L_{V_i})$$

$$M_T = \sum_{i=1}^{n}(M_{H_i} + M_{V_i})$$

$$N_T = \sum_{i=1}^{n}(N_{H_i} + N_{V_i})$$

5.3.3 EMPENNAGE MODULE INPUT/OUTPUT DATA TRANSFER

INPUT TRANSFER	
PARAMETER	ORIGIN MODULE
FSCGB	MAIN ROTOR
WLCGB	
BLCGB	
DWSHMR	
CHIPMR	
ALFMR	
OMGTMR	
RMR	
ALFWF	FUSELAGE
BETAWF	
IHT	FLIGHT CONTROL
IVT	
VXGH1	GUST
VYGH1	
VZGH1	
VXGV1	
VYGV1	
VZGV1	
VXB	MOTION
VYB	
VZB	
P	
Q	
R	

OUTPUT TRANSFER	
PARAMETER	DESTINATION MODULE
XT	MOTION
YT	
ZT	
LT	
MT	
NT	

5.3.4 NOTATION FOR THE EMPENNAGE MODULE

SYMBOL USED IN EQUATIONS	PROGRAM MNEMONIC	UNITS	DESCRIPTION
FSH1	FSH1	INS	Fuselage station for horizontal tail C.P.
FSCGb	FSCGB	INS	Fuselage station for CG
F_{HT1}	KH	FT	
WLH1	WLH1	INS	Waterline station for horizontal tail C.P.
WLCGb	WLCGB	INS	Waterline station for CG
W_{HT1}	KH+1	FT	
B_{LH1}	B_{LH1}	INS	Buttline station for Horizontal tail C.P.
BLCGb	BLCGB	INS	Buttline station for CG
B_{HT}	KH+2	FT	
E_{KXH1}	EKXH1	ND	Rotor wash factors
EK_{TH1}	EKYH1	ND	
EK_{ZH1}	EKZH1	ND	
χ_{PMR}	CHIPMR	DEG	Rotor Wake Skew angle
a_{1FMR}	AALFMR	DEG	Rotor longitudinal flapping
D_{WSHMR}	DWSHMR	ND	Rotor uniform downwash
Ω_T	OMGTMR	RADS/SEC	Trim rotor speed
R_T	RMR	FT	Rotor radius
V_{XMRH1}	VXMRH1	FT/SEC	Rotor interference velocity at the Horizontail tail.
V_{YMRH1}	VYMRH1	FT/SEC	
V_{ZMRH1}	VXMRH1	FT/SEC	
Q_{H1QWF}	QH1QWF	ND	Horizontal tail dynamic pressure ratio
α_{WF}	ALFWF	DEG	Fuselage angle of attack.
ψ_{WF}	PSIWF	DEG	Fuselage heading
β_{WF}	BETAWF	DEG	Fuselage sideslip.

5.3.4 (Continued) NOTATION FOR THE EMPENNAGE MODULE

SYMBOL USED IN EQUATIONS	PROGRAM MNEMONIC	UNITS	DESCRIPTION
K_{QH1}	KQH1	ND	
E_{PSH1}	EPSH1	DEG	Downwash angle
V_{Xb}	VXB	FT/SEC	Fuselage X axis velocity
V_{ZWFH1}	VZWFH1	FT/SEC	Fuse/Tail downwash velocity
V_{XIH1}	VXIH1	FT/SEC	Horizontal tail total interference velocity
V_{YIH1}	VYIH1	FT/SEC	
V_{ZIH1}	VZIH1	FT/SEC	
P	P	RADS/SEC	Body axes angular rates.
q	q	RADS/SEC	
r	r	RADS/SEC	
V_{XH1}	VXH1	FT/SEC	Total velocity at the horizontal tail.
V_{YH1}	VYH1	FT/SEC	
V_{ZH1}	VZH1	FT/SEC	
V_{XGH1}	VXGH1	FT/SEC	Gust velocity at the horizontal tail.
V_{YGH1}	VYGH1	FT/SEC	
V_{ZGH1}	VZGH1	FT/SEC	
ρ	RHO	$SLUG/FT^3$	Air density.
Q_{H1}	QH1	LB/FT^2	Dynamic pressure at the horizontal tail
α_{H1}	ALFH1	DEG	Body axis angle of attack
α_{HH1}	ALFHH1	DEG	Total tail angle of attack
β_{H1}	BETH1	DEG	Sideslip angle

5.3.4 (Continued) NOTATION FOR THE EMPENNAGE MODULE

SYMBOL USED IN EQUATIONS	PROGRAM MNEMONIC	UNITS	DESCRIPTION
V_{XMRV1}	VXMRV1	FT/SEC	Rotor interference velocities
V_{YMRV1}	VYMRV1	FT/SEC	
V_{ZMRV1}	VZMRV1	FT/SEC	
S_{IGV1}	SIGV1	DEG	Fuselage sidewash angle
V_{YWFV1}	VYWFV1	FT/SEC	Fuselage sidewash velocity
V_{XV1}	VXV1	FT/SEC	Total velocity at the vertical tail.
V_{YV1}	VYV1	FT/SEC	
V_{ZV1}	VZV1	FT/SEC	
V_{XGV1}	VXGV1	FT/SEC	Gust velocity at the vertical tail.
V_{YGV1}	VYGV1	FT/SEC	
V_{ZGV1}	VZGV1	FT/SEC	
V_{XIV1}	VXIV1	FT/SEC	Inteference velocity at the vertical tail.
V_{YIV1}	VYIV1	FT/SEC	
V_{ZIV1}	VZIV1	FT/SEC	
Q_{V1}	QV1	LB/FT^2	Dynamic pressure at the vertical tail.
α_{V1}	AFVF1	DEG	Angle of attack
β_{V1}	BETV1	DEG	Sideslip
β_{VV1}	BETVV1	DEG	Total sideslip angle
-	SNAFV1	-	SIN(ALFV1)
-	CSAFV1	-	COS(ALFV1)
-	SNBTV1	-	SIN(BETV1)
-	CSBTV1	-	COS(BETV1)

5.3.4 (Continued) NOTATION FOR THE EMPENNAGE MODULE

SYMBOL USED IN EQUATIONS	PROGRAM MNEMONIC	UNITS	DESCRIPTION
-	SNAFHL	-	SIN(ALFH1)
-	CSAFH1	-	COS(ALFH1)
-	SNBTH1	-	SIN(BETH1)
-	SCPTH1	-	COS(BETH1)
C_{LH1}	CLH1	ND	Coef of lift
C_{DH1}	CDH1	ND	Coef of drag.
X_{H1}	XH1	LB	Horizontal tail forces and moments
Y_{H1}	YH1	LB	
Z_{H1}	ZH1	LB	
L_{H1}	LH1	FT LB	
M_{H1}	MH1	FT LB	
N_{H1}	NH1	FT LB	
FSV1	FSVT1	INS	Fuselage Station for the vertical tail C.P.
FVT1	KV	FT	Waterline Station for the vertical
WLV1	WLVT1	INS	tail C.P.
BLV1	BLVT1	INS	Buttline Station for the vertical
B_{VT1}	KV+2	FT.	tail C.P.
E_{KXV1}	EKXV1	-	Rotor wash factors
E_{KYV1}	EKYV1	-	
E_{KZV1}	EKZV1	-	

5.3.4 (Continued) NOTATION FOR THE EMPENNAGE MODULE

SYMBOL USED IN EQUATIONS	PROGRAM MNEMONIC	UNITS	DESCRIPTION
Q_{V1QWF}	QV1QWF	-	Dynamic pressure ratio, ratio
K_{QV1}	KWV1	-	SQRT (dynamic pressure ratio)
C_{LV1}	CLV1	ND	Coef of lift
C_{DV1}	CDV1	ND	Coef of drag
X_{V1}	XV1	LB	Vertical tail forces and moments
Y_{V1}	YV1	LB	
Z_{V1}	ZV1	LB	
L_{V1}	LV1	FT LB	
M_{V1}	MV1	FT LB	
N_{V1}	NV1	FT LB	
X_T	-	LB	Total Empennage forces and moments
Y_T	-	LB	
Z_T	-	LB	
L_T	-	FT LB	
M_T	-	FT LB	
N_T	-	FT LB	

5.3.5 BLACK HAWK EMPENNAGE INPUT DATA

INPUT CONSTANTS

FSH1 = 700.1 ins
WLH1 = 244.0 ins
BLH1 = 0
SAH1 = 45.0
IH1 = CALCULATED IN THE CONTROL SYSTEM

FSV1 = 695.0
WLV1 = 273.0
BLV1 = 0.0
SAV1 = 32.3
IV1 = 0.0

TABLE 3.5.1

MAIN ROTOR INPLANE WASH AT THE HORIZONTAL TAIL

```
EXH1MP::BIV##                     ;MAP ARGUMENT:LOOK UP ROUTINE
   EXP   CHIPMR##,AA1FMR##        ;INPUT VARIABLE #1, INPUT VARIABLE #2
         EKXH1##                  ;OUTPUT VARIABLE
         EXH1LO                   ;LOW ANGLE MAP NAME
   EXP   Ø.Ø,1ØØ.Ø,1Ø.Ø,13        ;LOW LIM,UPPER LIM,DELTA,#ENTRYS(OCT)-CHIPMR
   EXP   -6.Ø,6.Ø,6.Ø             ;LOW LIM,UPPER LIM,DELTA-AA1FMR

           ; LOW ANGLE MAP CHIPMR Ø TO 1ØØ (DEL=1Ø) AA1FMR -6,Ø,6
           ; AA1FMR=-6

EXH1LO:EXP     Ø.Ø,      -Ø.2,     Ø.Ø5,     Ø.3,      Ø.54
       EXP     Ø.3,       1.Ø4,    1.3,      1.55,     Ø.8
               Ø.Ø

           ; AA1FMR=Ø
       EXP    -Ø.4,      -Ø.6,    -Ø.2,      Ø.12,     Ø.36
       EXP     Ø.6,       Ø.83,    1.Ø6,     1.3,      Ø.66
               Ø.Ø

           ; AA1FMR=6
       EXP    -Ø.56,     -Ø.8,    -Ø.74,    -Ø.32,     Ø.Ø4
       EXP     Ø.32,      Ø.6,     Ø.86,     1.12,     Ø.54
               Ø.Ø
```

TABLE 3.5.2

MAIN ROTOR DOWNWASH AT THE HORIZONTAL TAIL

```
EZH1MP::BIV##                     ;MAP ARGUMENT:LOOK UP ROUTINE
   EXP   CHIPMR##,AA1FMR##        ;INPUT VARIABLE #1, INPUT VARIABLE #2
         EKZH1##                  ;OUTPUT VARIABLE
         EZH1LO                   ;LOW ANGLE MAP NAME
   EXP   Ø.Ø,1ØØ.Ø,1Ø.Ø,13        ;LOW LIM,UPPER LIM,DELTA,#ENTRYS(OCT)-CHIPMR
   EXP   -6.Ø,6.Ø,6.Ø             ;LOW LIM,UPPER LIM,DELTA-AA1FMR

           ; LOW ANGLE MAP CHIPMR Ø TO 1ØØ (DEL=1Ø) AA1FMR -6,Ø,6
           ; AA1FMR=-6
EZH1LO:EXP    -Ø.13,      Ø.8,     1.8,      1.82,     1.86
       EXP     1.88,      1.91,    1.94,     1.69,     1.42
               1.14

           ; AA1FMR=Ø
       EXP     Ø.4,       Ø.94,    1.84,     1.91,     1.98
       EXP     2.Ø4,      2.Ø8,    2.14,     1.89,     1.62
               1.35

           ; AA1FMR=6
       EXP     Ø.78,      1.36,    1.91,     1.98,     2.Ø6
       EXP     2.14,      2.21,    2.28,     2.16,     1.96
               1.56
```

TABLE 3.5.3

DYNAMIC PRESSURE LOSS AT THE HORIZONTAL TAIL

```
QHIMP::UVR##                            ;MAP ARGUMENT:LOOK UP ROUTINE
       ALFWF##                          ;INPUT VARIABLE
       QHIQWF##                         ;OUTPUT VARIABLE
       QHILO                            ;LOW ANGLE MAP NAME
   EXP -3Ø.Ø,3Ø.Ø,5.Ø                   ;LOWER LIMIT, UPPER LIMIT, DELTA

          ; LOW ANGLE MAP ALFHHI -3Ø TO 3Ø DELTA=5
QHILO:  EXP    1.Ø,       1.Ø,       Ø.95,      Ø.76,      Ø.76
        EXP    Ø.76,      Ø.75,      Ø.76,      Ø.76,      Ø.82
        EXP    Ø.91,      1.Ø,       1.Ø
```

TABLE 3.5.4

FUSELAGE DOWNWASH AT THE HORIZONTAL TAIL

```
EPHIMP::UVRUVR##                        ;MAP ARGUMENT:LOOK UP ROUTINE
        ALFWF##                         ;INPUT VARIABLE
        EPSHI##                         ;OUTPUT VARIABLE
        EPHILO                          ;LOW ANGLE MAP NAME
   EXP  -3Ø.Ø,3Ø.Ø,5.Ø                  ;LOWER LIMIT,UPPER LIMIT,DELTA-LOW ANGLE
        EPHIHI                          ;HIGH ANGLE MAP NAME
   EXP  -9Ø.Ø,9Ø.Ø,1Ø.Ø                 ;LOWER LIMIT,UPPER LIMIT,DELTA-HIGH ANGLE

          ; LOW ANGLE MAP ALFHHI -3Ø TO 3Ø DELTA=5
EPHILO: EXP    1.8,       1.4,       1.1,       Ø.8,       Ø.55
        EXP    Ø.5,       Ø.45,      Ø.4,       Ø.38,      Ø.33
        EXP    Ø.19,      -Ø.12,     -Ø.4

          ; HIGH ANGLE MAP ALFHHI -9Ø TO 9Ø DELTA=1Ø
EPHIHI: EXP    Ø.Ø,       Ø.25,      Ø.7,       1.2,       1.6
        EXP    1.9,       1.8,       1.1,       Ø.55,      Ø.45
        EXP    Ø.38,      Ø.19,      -Ø.4,      -Ø.7,      -Ø.75
        EXP    -Ø.65,     -Ø.45,     -Ø.15,     Ø.Ø
```

TABLE 3.5.5

HORIZONTAL TAIL LIFT COEFFICIENT DUE TO ANGLE OF ATTACK

```
          ; S=45 FT**2 ,ASPECT RATIO=4.6 ,ØØ14 AIRFOIL
CLHIMP::UVSUVS##                        ;MAP ARGUMENT:LOOK UP ROUTINE
        ALFHHI##                        ;INPUT VARIABLE
        CLHI##                          ;OUTPUT VARIABLE
        CLHILO                          ;LOW ANGLE MAP NAME
   EXP  Ø.Ø,3Ø.Ø,5.Ø                    ;LOWER LIMIT,UPPER LIMIT,DELTA-LOW ANGLE
        CLHIHI                          ;HIGH ANGLE MAP NAME
   EXP  3Ø.Ø,9Ø.Ø,1Ø.Ø                  ;LOWER LIMIT,UPPER LIMIT,DELTA-HIGH ANGLE

          ; LOW ANGLE MAP ALFHHI Ø TO 3Ø,DELTA=5 CL(ALF)=-CL(-ALF)
CLHILO: EXP    Ø.Ø,       Ø.356,     Ø.71,      1.Ø3,      Ø.95
        EXP    Ø.795,     Ø.745

          ; HIGH ANGLE MAP ALFHHI 3Ø TO 9Ø,DELTA=1Ø CL(ALF)=-CL(-ALF)
CLHIHI: EXP    Ø.745,     Ø.847,     Ø.847,     Ø.745,     Ø.558
        EXP    Ø.294,     Ø.Ø
```

TABLE 3.5.6

HORIZONTAL TAIL DRAG COEFFICIENT DUE TO ANGLE OF ATTACK

```
CDH1MP::UVRUVR##              ;MAP ARGUMENT:LOOK UP ROUTINE
        AFAHH1##              ;INPUT VARIABLE
        CDH1##                ;OUTPUT VARIABLE
        CDH1LO                ;LOW ANGLE MAP NAME
    EXP Ø.Ø,3Ø.Ø,5.Ø          ;LOWER LIMIT,UPPER LIMIT,DELTA
        CDH1HI                ;HIGH ANGLE MAP NAME
    EXP 3Ø.Ø,9Ø.Ø,1Ø.Ø        ;LOWER LIMIT,UPPER LIMIT,DELTA

        ; LOW ANGLE MAP ALFHH1 Ø TO 3Ø,DELTA=5 CD(ALF)=CD(-ALF)
CDH1LO: EXP    Ø.Ø1,     Ø.Ø22,     Ø.Ø4,     Ø.19,     Ø.36
        EXP    Ø.37,     Ø.43

        ; HIGH ANGLE MAP ALFHH1 3Ø TO 9Ø,DELTA=1Ø CD(ALF)=CD(-ALF)
CDH1HI: EXP    Ø.43,     Ø.531,     Ø.7Ø2,     Ø.888,     1.Ø5
        EXP    1.161,    1.2
```

TABLE 3.5.7

DYNAMIC PRESSURE LOSS AT THE VERTICAL TAIL

```
QV1MP:: UVR##                 ;MAP ARGUMENT:LOOK UP ROUTINE
        PSABWF##              ;INPUT VARIABLE
        QP3QWF##              ;OUTPUT VARIABLE
        QP3LO                 ;LOW ANGLE MAP NAME
    EXP Ø.Ø,3Ø.Ø,5.Ø,7        ;LOWER LIMIT, UPPER LIMIT, DELTA, NO OF ENTRYS(PSABWF)

        ; LOW ANGLE MAP PSI(ABS.) Ø TO 3Ø DELTA=5

        EXP    Ø.62,     Ø.64,     Ø.66,     Ø.72,     Ø.79
        EXP    Ø.88,     1.ØØ
```

TABLE 3.5.8

FUSELAGE SIDEWASH AT THE VERTICAL TAIL

```
SGV1MP::UVSUVS##              ;MAP ARGUMENT:LOOK UP ROUTINE
        PSIWF##               ;INPUT VARIABLE
        SIGP3##               ;OUTPUT VARIABLE
        SGP3LO                ;LOW ANGLE MAP NAME
    EXP Ø.Ø,3Ø.Ø,5.Ø          ;LOWER LIMIT, UPPER LIMIT, DELTA-LOW ANGLE
        SGP3HI                ;HIGH ANGLE MAP NAME
    EXP Ø.Ø,9Ø.Ø,3Ø.Ø         ;LOWER LIMIT, UPPER LIMIT, DELTA-HIGH ANGLE

        ; LOW ANGLE MAP PSIWF Ø TO 3Ø DELTA=5
        EXP    Ø.Ø,      -Ø.4,      -Ø.6,     Ø.8,      1.4
        EXP    Ø.6,      Ø.2

        ; HIGH ANGLE MAP PSIWF Ø TO 9Ø DELTA=3Ø
        EXP    Ø.Ø,      Ø.2,       Ø.Ø,      Ø.Ø
```

TABLE 3.5.9

VERTICAL TAIL LIFT COEFFICIENT DUE TO SIDESLIP

```
                 ; S=32.3 FT**2  ,ASPECT RATIO =1.92 ,ØØ21 MOD AIRFOIL
CLV1MP::UVRUVR##                 ;MAP ARGUMENT:LOOK UP ROUTINE
        BETVV1##                 ;INPUT VARIABLE
        CLV1##                   ;OUTPUT VARIABLE
        CLV1LØ                   ;LOW ANGLE MAP NAME
    EXP -3Ø.Ø,3Ø.Ø,5.Ø           ;LOWER LIMIT,UPPER LIMIT,DELTA-LOW ANGLE
        CLV1HI                   ;HIGH ANGLE MAP NAME
    EXP -9Ø.Ø,9Ø.Ø,1Ø.Ø          ;LOWER LIMIT,UPPER LIMIT,DELTA-HIGH ANGLE

                 ; LOW ANGLE MAP BETVV1 -3Ø TO 3Ø,DELTA=5
CLV1LØ:EXP       -1.ØØ,      -1.ØØ,      -Ø.93,      -Ø.73,      -Ø.5


       EXP       -Ø.28,      -Ø.Ø6,       Ø.16,       Ø.38,       Ø.61
       EXP        Ø.82,       Ø.89,       Ø.89

                 ; HIGH ANGLE MAP BETVV1 -9Ø TO 9Ø,DELTA=1Ø
CLV1HI:EXP       -Ø.Ø,       -Ø.12,      -Ø.28,      -Ø.46,      -Ø.66
       EXP       -Ø.88,      -1.ØØ,      -Ø.93,      -Ø.5,       -Ø.Ø6
       EXP        Ø.38,       Ø.82,       Ø.89,       Ø.8,        Ø.63
       EXP        Ø.48,       Ø.32,       Ø.17,       Ø.Ø
```

TABLE 3.5.10

VERTICAL TAIL DRAG COEFFICIENT DUE TO SIDESLIP

```
CDV1MP::UVRUVR##                 ;MAP ARGUMENT:LOOK UP ROUTINE
        BETVV1##                 ;INPUT VARIABLE
        CDV1##                   ;OUTPUT VARIABLE
        CDV1LO                   ;LOW ANGLE MAP NAME
    EXP -3Ø.Ø,3Ø.Ø,5.Ø           ;LOWER LIMIT,UPPER LIMIT,DELTA-LOW ANGLE
        CDV1HI                   ;HIGH ANGLE MAP NAME
    EXP -9Ø.Ø,9Ø.Ø,1Ø.Ø          ;LOWER LIMIT,UPPER LIMIT,DELTA-HIGH ANGLE

                 ; LOW ANGLE MAP BETVV1 -3Ø TO 3Ø,DELTA=5
CDV1LO: EXP       Ø.36,       Ø.265,      Ø.174,      Ø.118,      Ø.Ø66
        EXP       Ø.Ø33,      Ø.Ø18,      Ø.Ø21,      Ø.Ø44,      Ø.Ø92
        EXP       Ø.162,      Ø.248,      Ø.355

                 ; HIGH ANGLE MAP BETVV1 -9Ø TO 9Ø,DELTA=5
CDV1HI: EXP       1.1,        1.Ø25,      Ø.965,      Ø.875,      Ø.745
        EXP       Ø.575,      Ø.36,       Ø.174,      Ø.Ø66,      Ø.Ø18
        EXP       Ø.Ø44,      Ø.162,      Ø.355,      Ø.58,       Ø.75
        EXP       Ø.875,      Ø.965,      1.Ø2,       1.Ø8
```

MAIN ROTOR INPLANE WASH AT THE HORIZONTAL TAIL

MAP NAME: EXHIMP
MAP TYPE: BIV
INPUT VARIABLE(S): CHIPMA AA1FMA
OUTPUT VARIABLE: EKXH1

PRIMARY MAP:

0.00	LOWER LIMIT	-6.00
100.00	UPPER LIMIT	6.00
10.00	DELTA	6.00

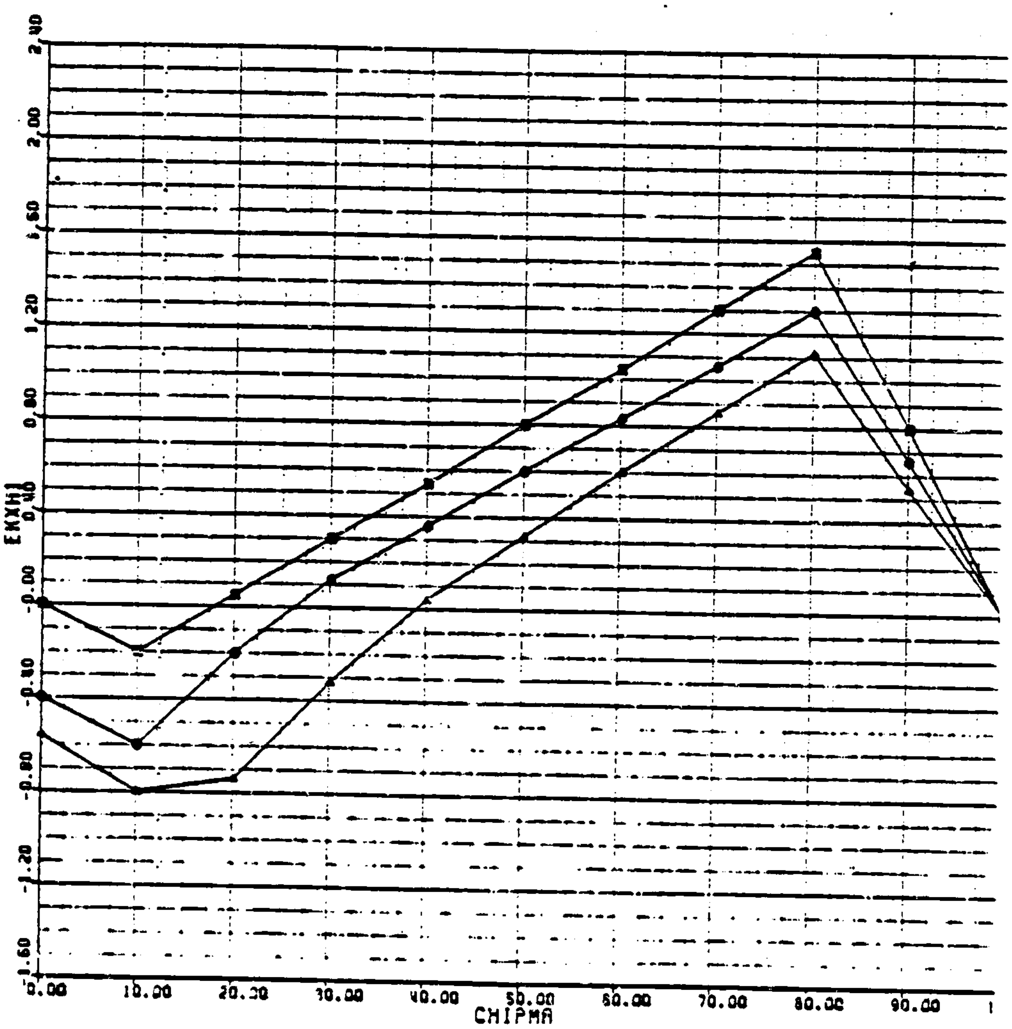

FIGURE 3.5.1

MAIN ROTOR DOWNWASH AT THE HORIZONTAL TAIL

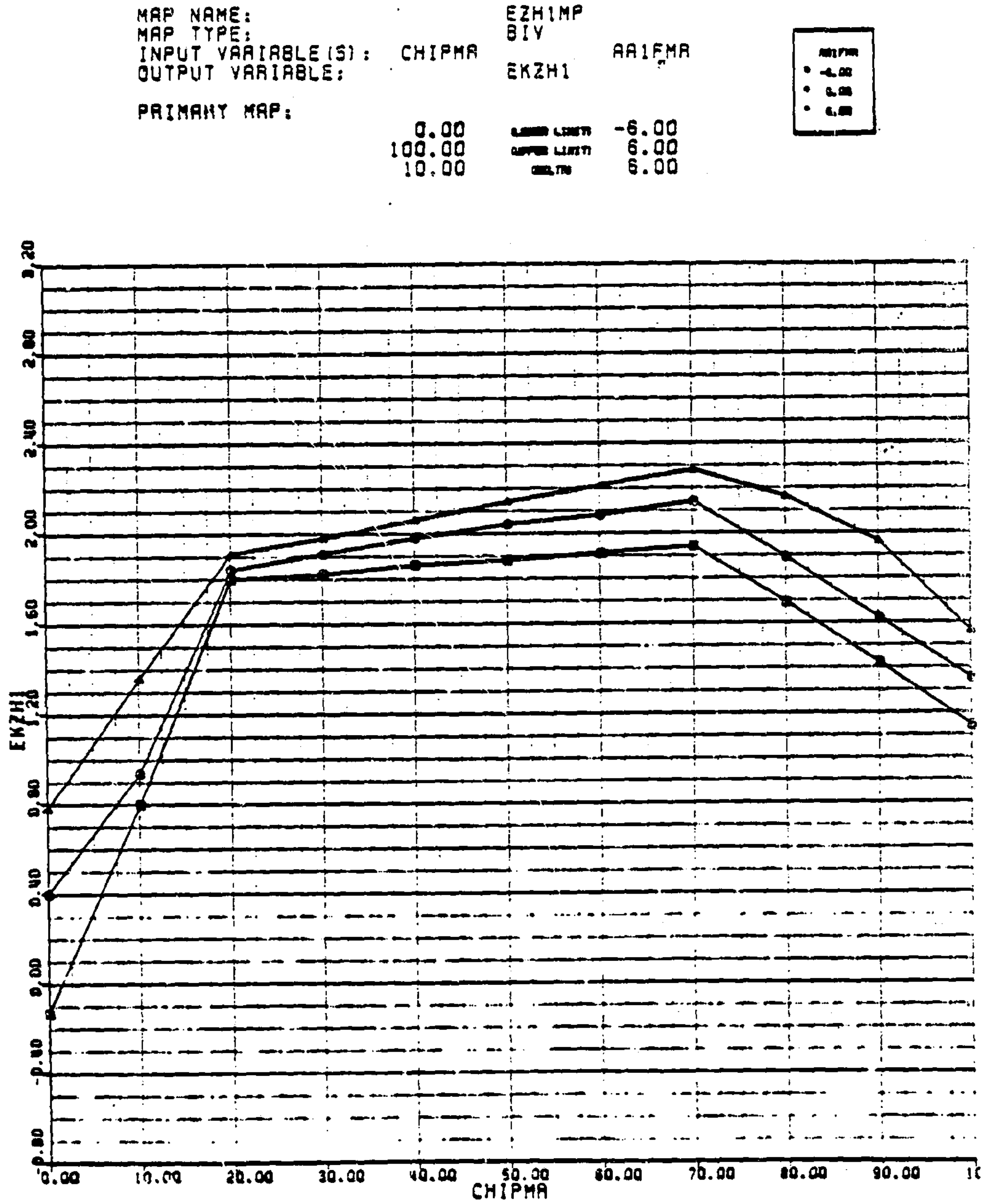

FIGURE 3.5.2

DYNAMIC PRESSURE LOSS AT THE HORIZONTAL TAIL

MAP NAME: QHIMP
MAP TYPE: UVA
INPUT VARIABLE(S): ALFWF
OUTPUT VARIABLE: QHIQWF

PRIMARY MAP:
-30.00 LOWER LIMIT
30.00 UPPER LIMIT
5.00 DELTA

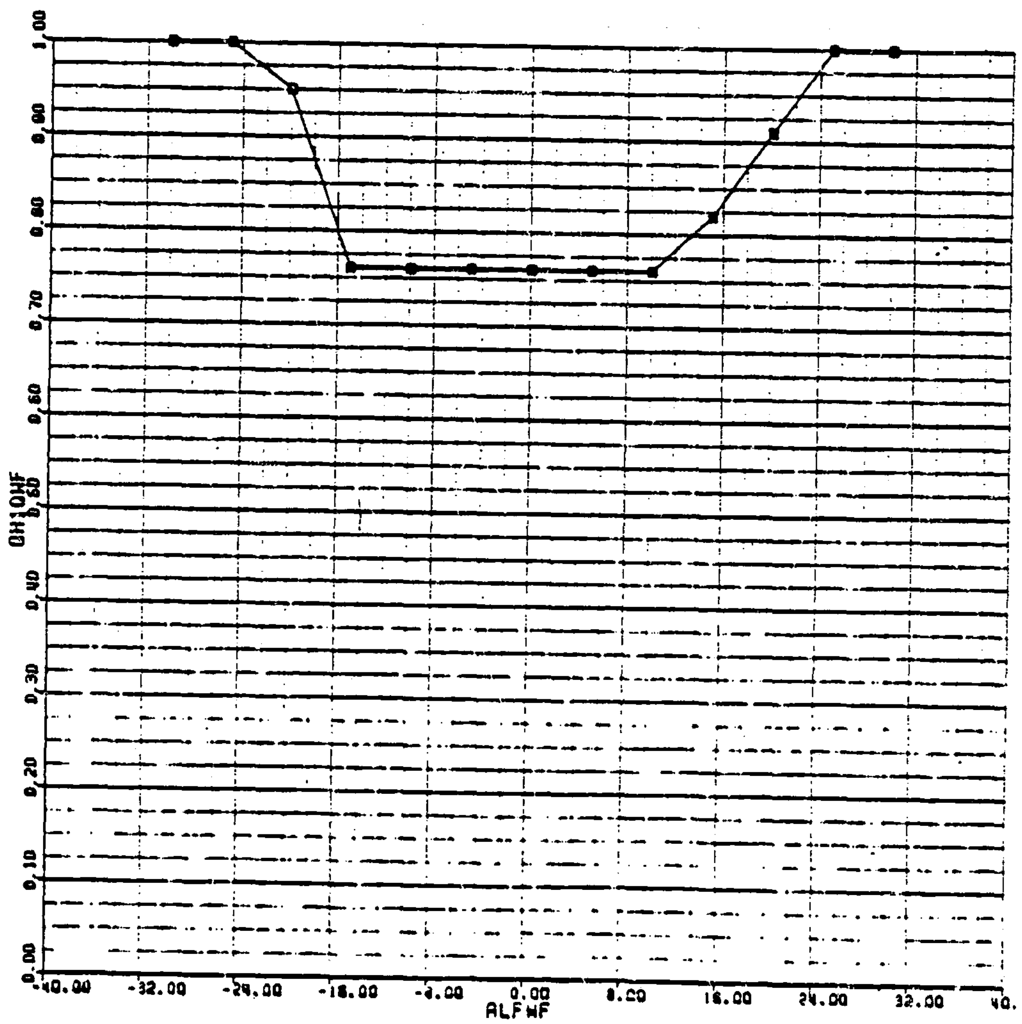

FIGURE 3.5.3

FUSELAGE DOWNWASH AT THE HORIZONTAL TAIL

BLACKHAWK - NASA STUDY 23-SEP-80 EPHIMP (1/2)

MAP NAME: EPHIMP
MAP TYPE: UVAUVA
INPUT VARIABLE(S): ALFWF
OUTPUT VARIABLE: EPSH1

PRIMARY MAP:
-30.00 (LOWER LIMIT)
30.00 (UPPER LIMIT)
5.00 (DELTA)

SECONDARY MAP:
-90.00 (LOWER LIMIT)
90.00 (UPPER LIMIT)
10.00 (DELTA)

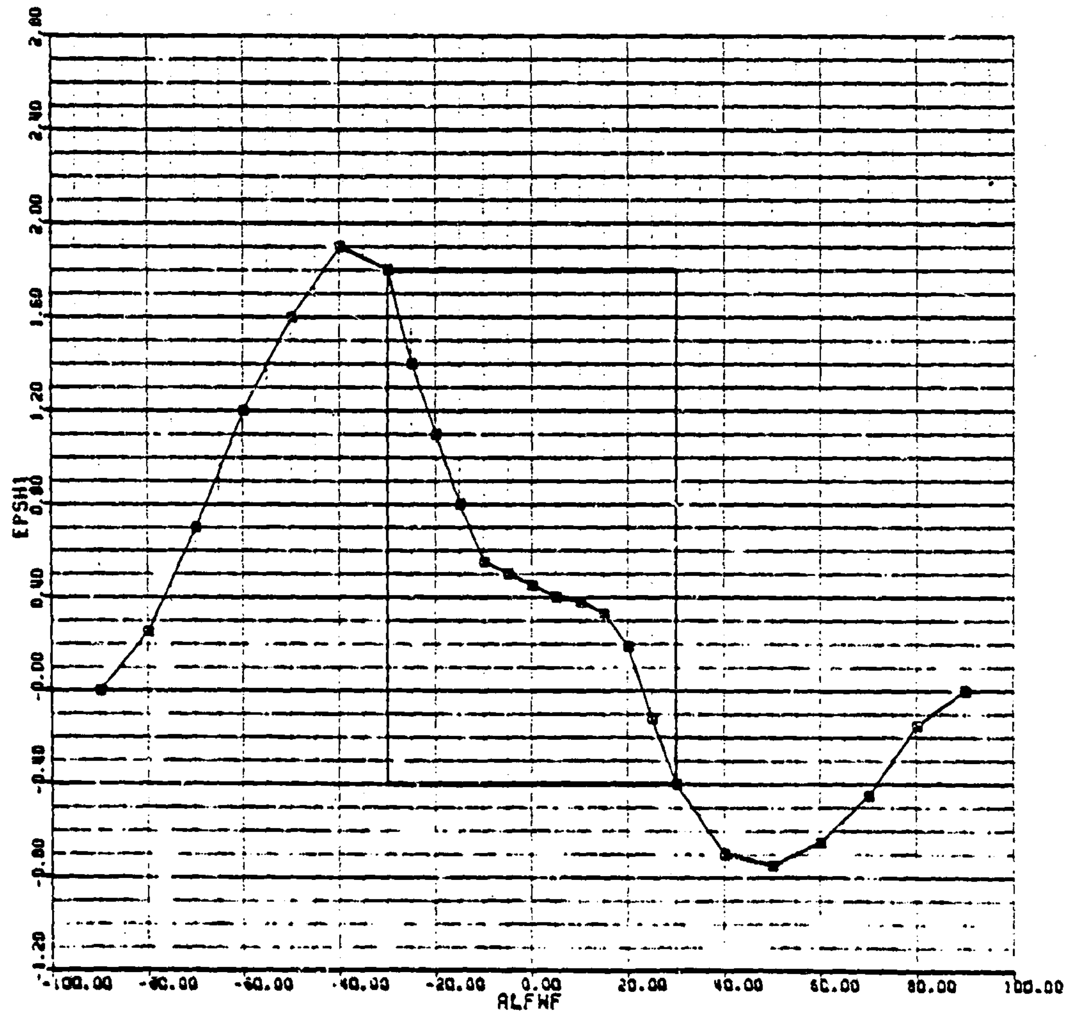

FIGURE 3.5.4(a)

FUSELAGE DOWNWASH AT THE HORIZONTAL TAIL (Cont'd)

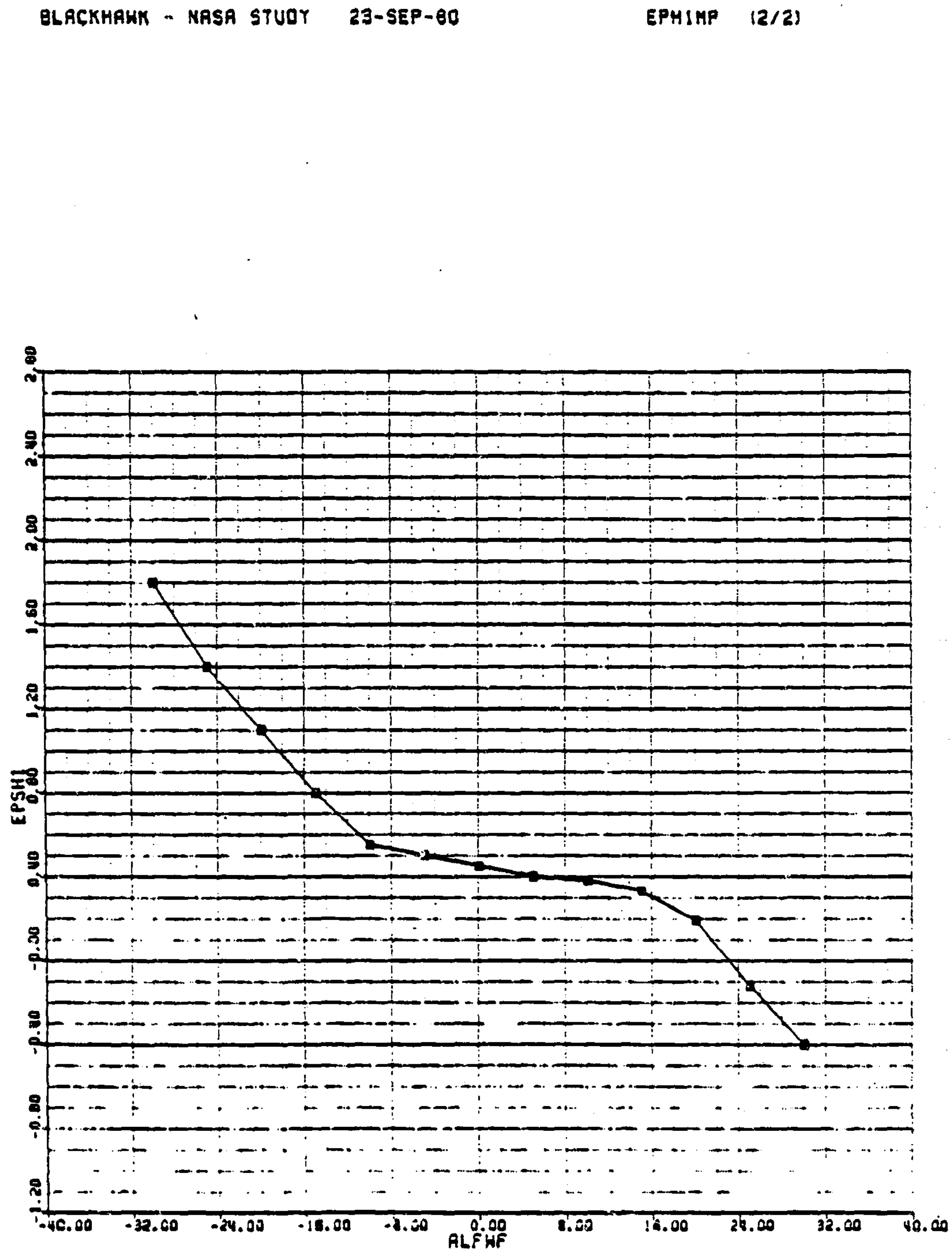

FIGURE 3.5.4(b)

HORIZONTAL TAIL LIFT COEFFICIENT DUE TO ANGLE OF ATTACK

BLACKHAWK - NASA STUDY 29-SEP-80 CLHIMP (1/2)

MAP NAME: CLH1MP
MAP TYPE: UVSUVS
INPUT VARIABLE(S): ALFHH1
OUTPUT VARIABLE: CLH1

PRIMARY MAP:
-30.00 (LOWER LIMIT)
30.00 (UPPER LIMIT)
5.00 (DELTA)

SECONDARY MAP:
-90.00 (LOWER LIMIT)
90.00 (UPPER LIMIT)
10.00 (DELTA)

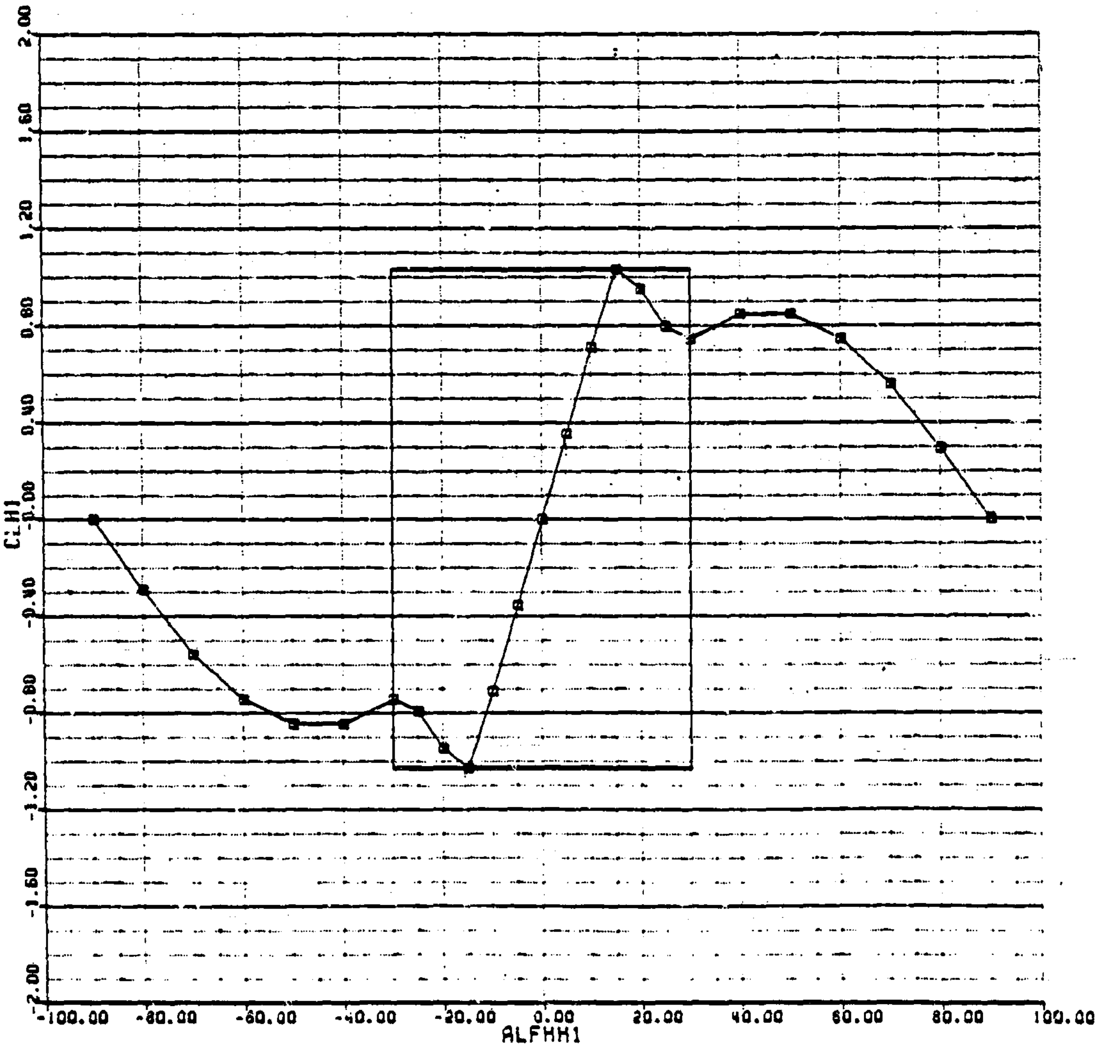

FIGURE 3.5.5(a)

HORIZONTAL TAIL LIFT COEFFICIENT DUE TO ANGLE OF ATTACK (Cont'd)

BLACKHAWK - NASA STUDY 29-SEP-80 CLH1NP (2/2)

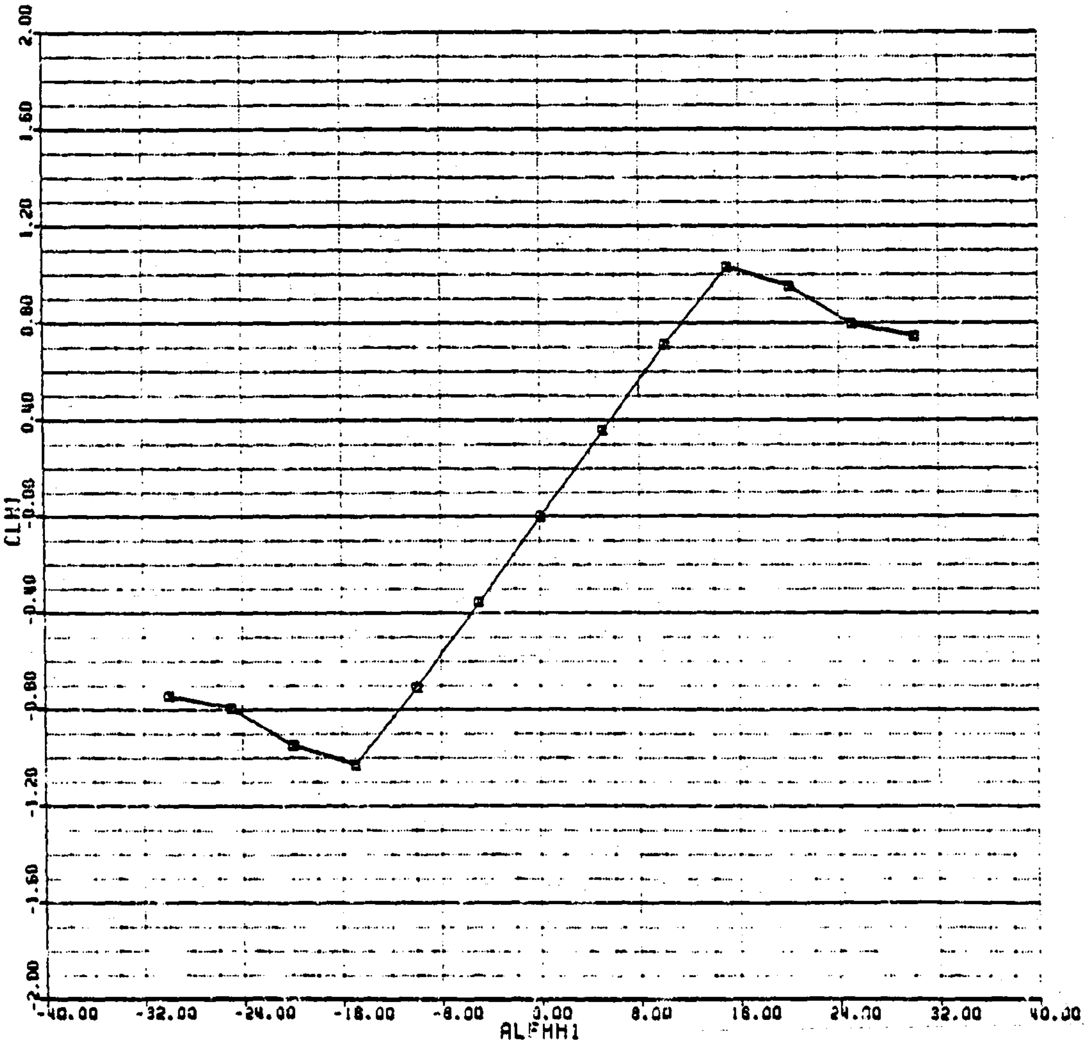

FIGURE 3.5.5(b)

HORIZONTAL TAIL DRAG COEFFICIENT DUE TO ANGLE OF ATTACK

BLACKHAWK - NASA STUDY 23-SEP-80 CDH1MP (1/2)

MAP NAME: CDH1MP
MAP TYPE: UVAUVA
INPUT VARIABLE(S): AFAHH1
OUTPUT VARIABLE: CDH1

PRIMARY MAP:
0.00 LOWER LIMIT
30.00 UPPER LIMIT
5.00 DELTA

SECONDARY MAP:
30.00 LOWER LIMIT
90.00 UPPER LIMIT
10.00 DELTA

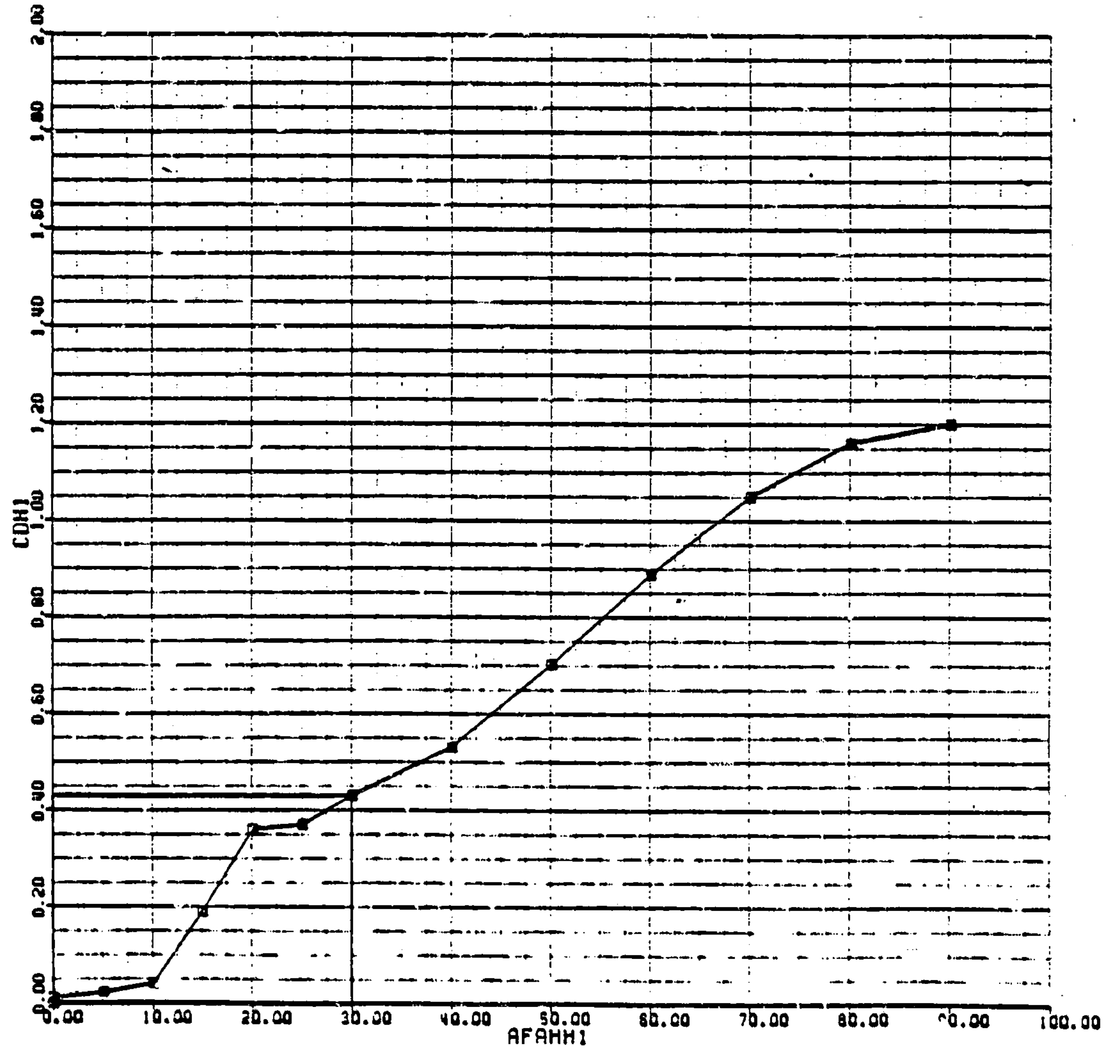

FIGURE 3.5.6(a)

HORIZONTAL TAIL DRAG COEFFICIENT DUE TO ANGLE OF ATTACK (Cont'd)

BLACKHAWK - NASA STUDY 23-SEP-80 CDHIMP (2/2)

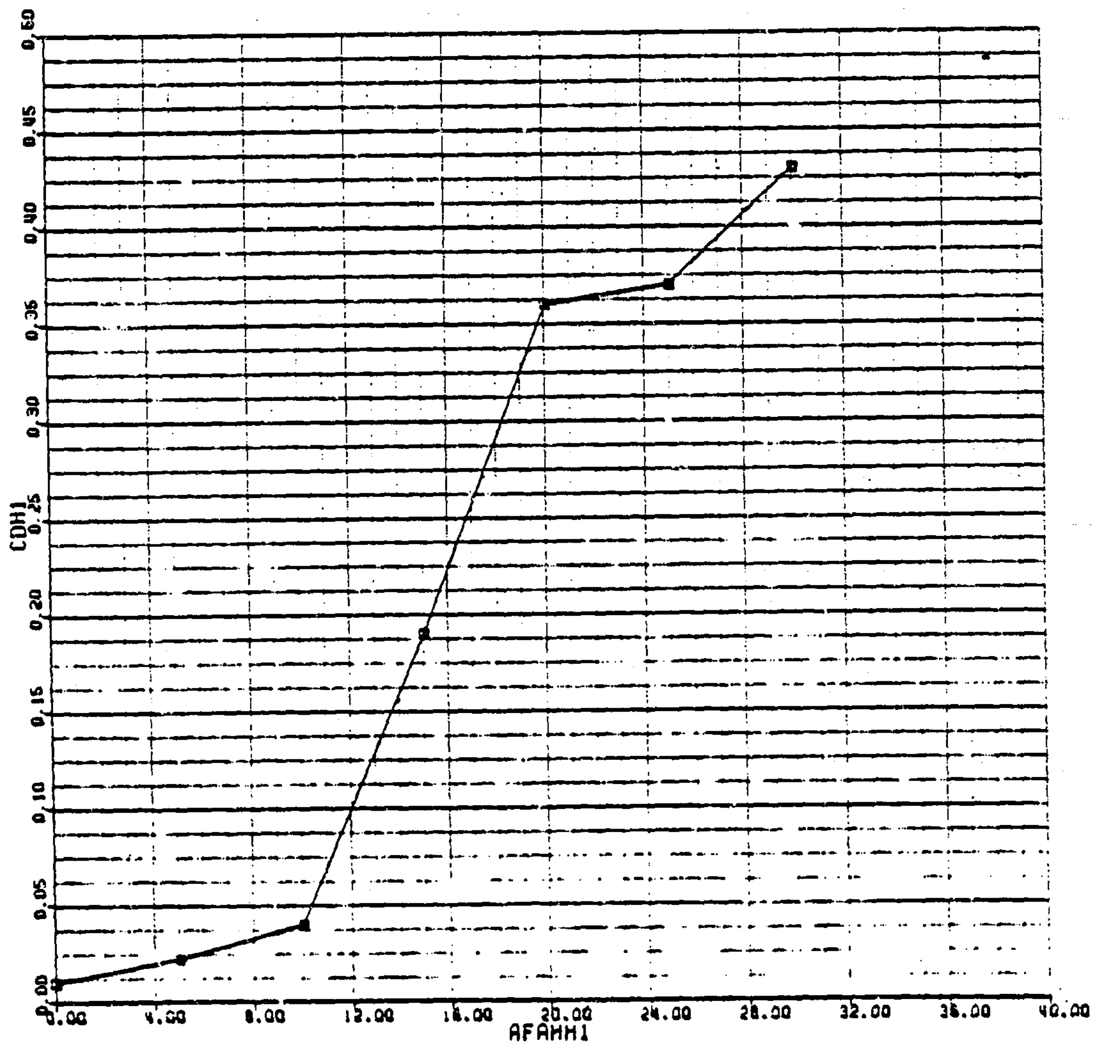

FIGURE 3.5.6(b)

DYNAMIC PRESSURE LOSS AT THE VERTICAL TAIL

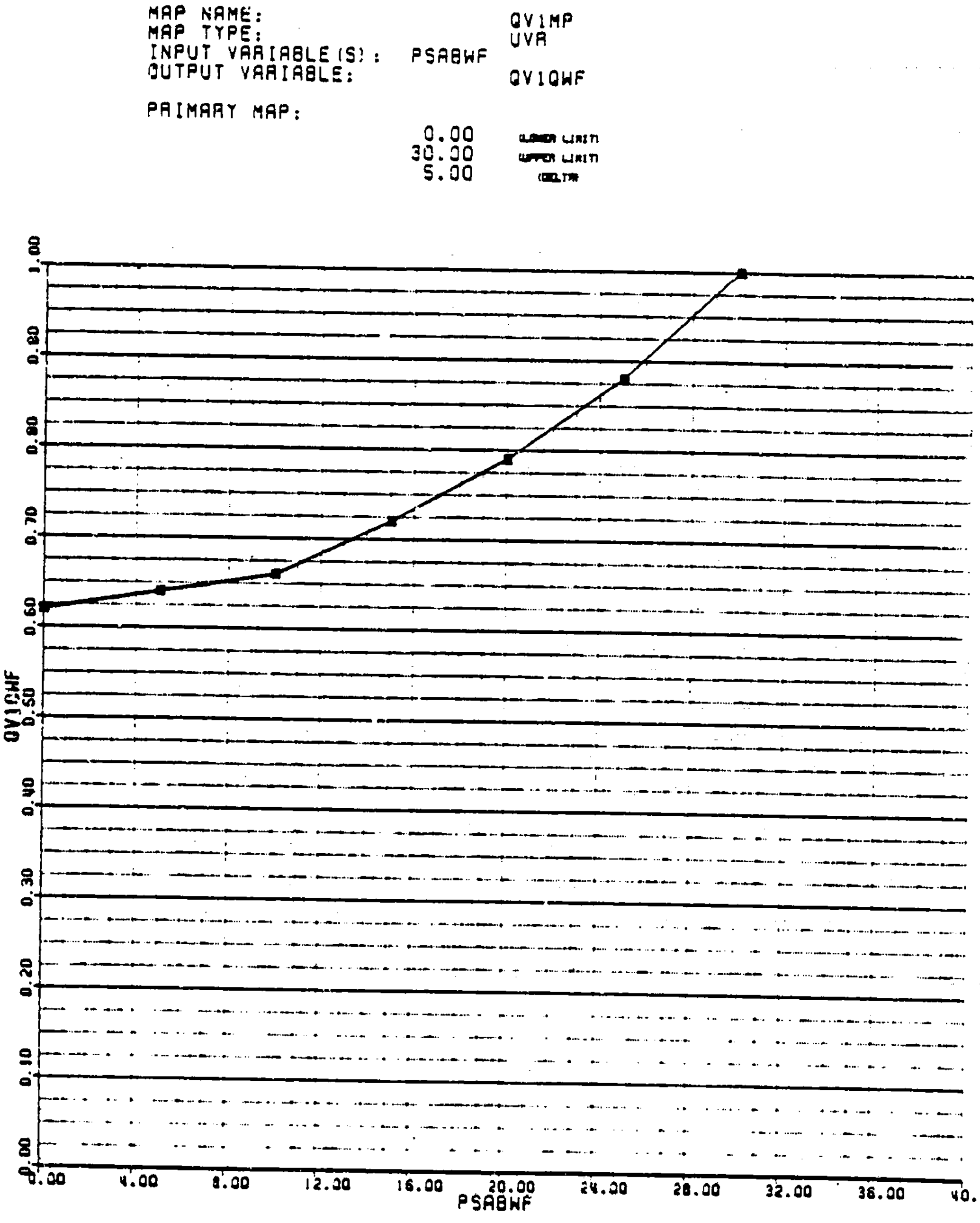

FIGURE 3.5.7

FUSELAGE SIDEWASH AT THE VERTICAL TAIL

BLACKHAWK - NASA STUDY   25-SEP-80   SGV1MP (1/2)

MAP NAME: SGV1MP
MAP TYPE: UVAUVA
INPUT VARIABLE(S): PSIWF
OUTPUT VARIABLE: SIGV1

PRIMARY MAP:
-30.00 (LOWER LIMIT)
30.00 (UPPER LIMIT)
5.00 (DELTA)

SECONDARY MAP:
-90.00 (LOWER LIMIT)
90.00 (UPPER LIMIT)
30.00 (DELTA)

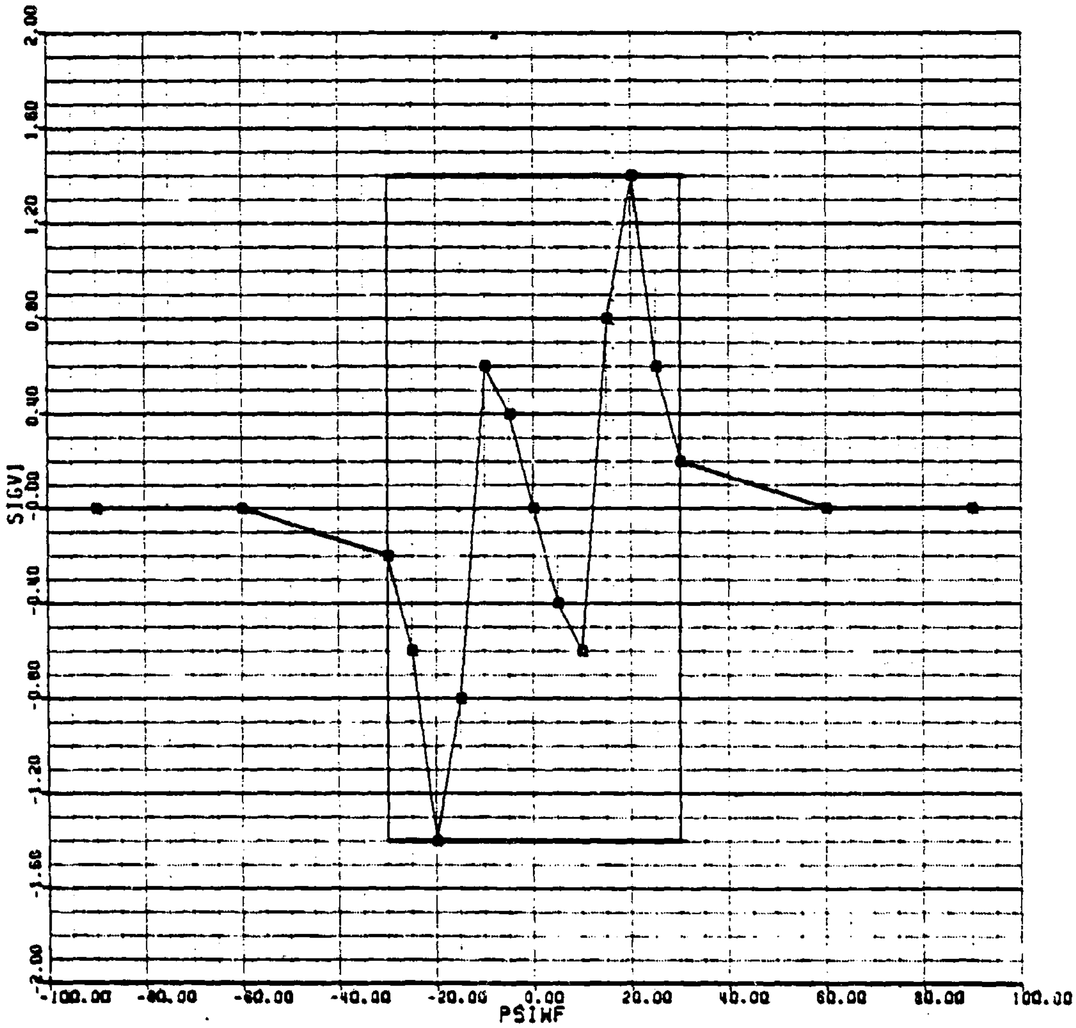

FIGURE 3.5.8(a)

FUSELAGE SIDEWASH AT THE VERTICAL TAIL (Cont'd)

BLACKHAWK - NASA STUDY 25-SEP-80 SGV1MP (2/2)

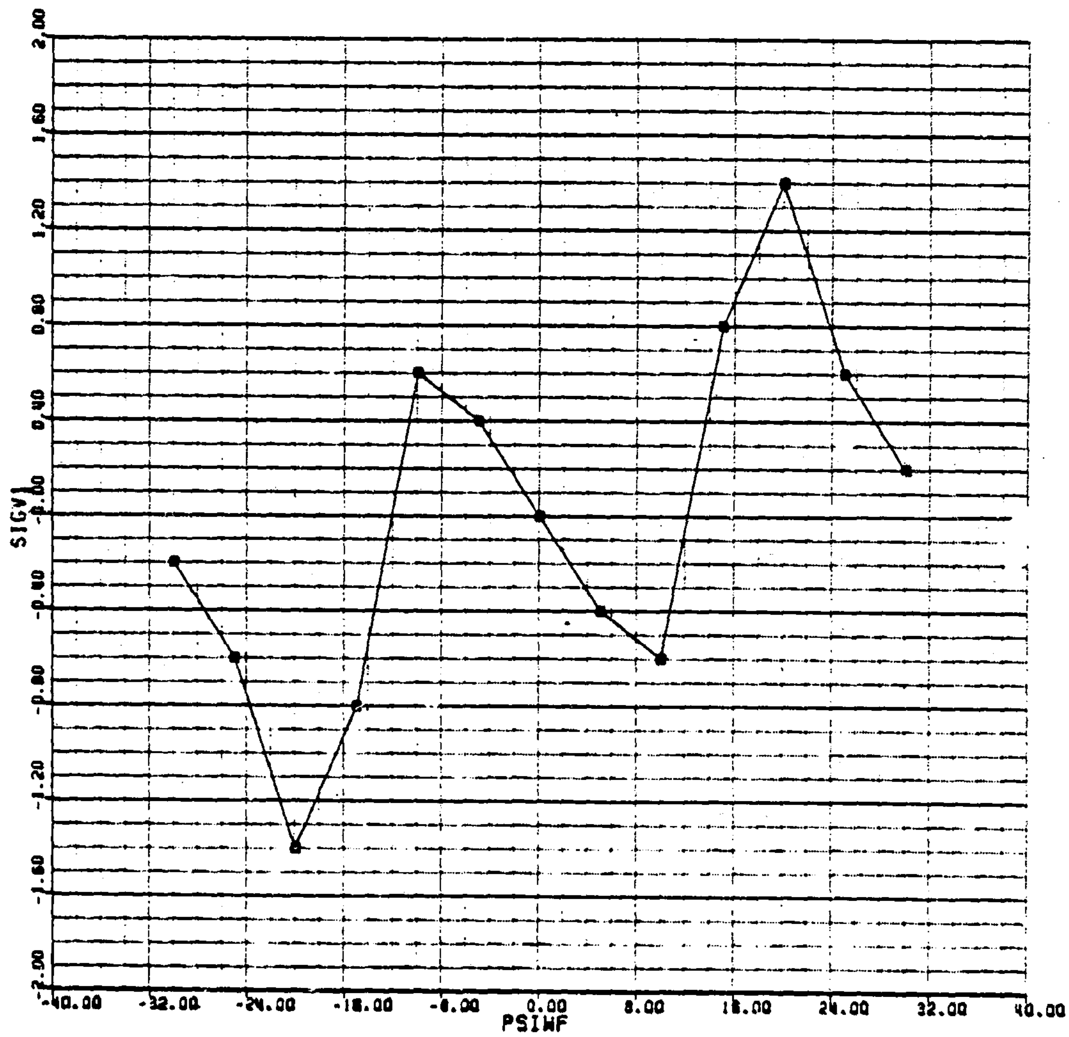

FIGURE 3.5.8(b)

VERTICAL TAIL LIFT COEFFICIENT DUE TO SIDESLIP

BLACKHAWK - NASA STUDY 25-SEP-80 CLV1MP (1/2)

MAP NAME:		CLV1MP
MAP TYPE:		UVAUVA
INPUT VARIABLE(S):	BETVV1	
OUTPUT VARIABLE:		CLV1
PRIMARY MAP:		
	-30.00	(LOWER LIMIT)
	30.00	(UPPER LIMIT)
	5.00	(DELTA)
SECONDARY MAP:		
	-90.00	(LOWER LIMIT)
	90.00	(UPPER LIMIT)
	10.00	(DELTA)

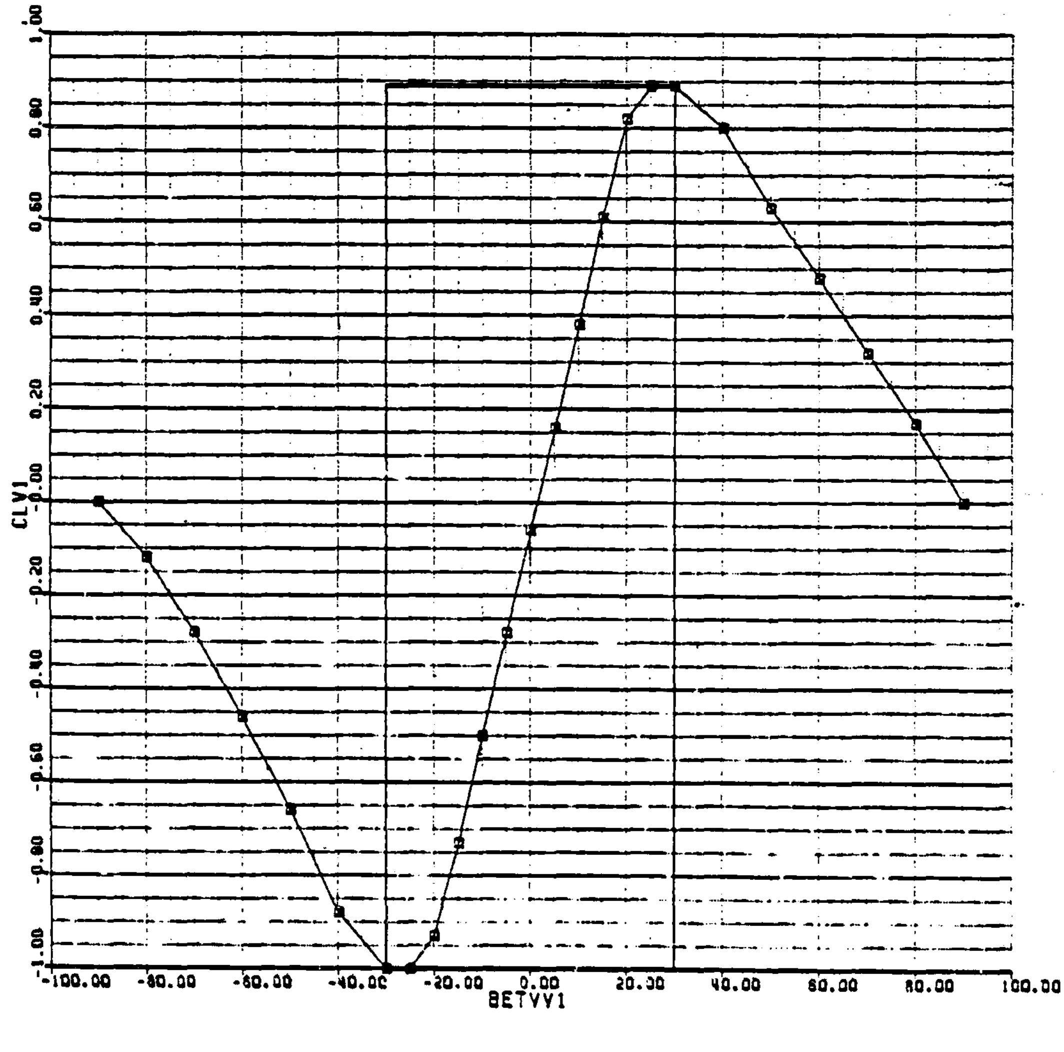

FIGURE 3.5.9(a)

VERTICAL TAIL LIFT COEFFICIENT DUE TO SIDESLIP (Cont'd)

BLACKHAWK - NASA STUDY 23-SEP-80 CLVIMP (2/2)

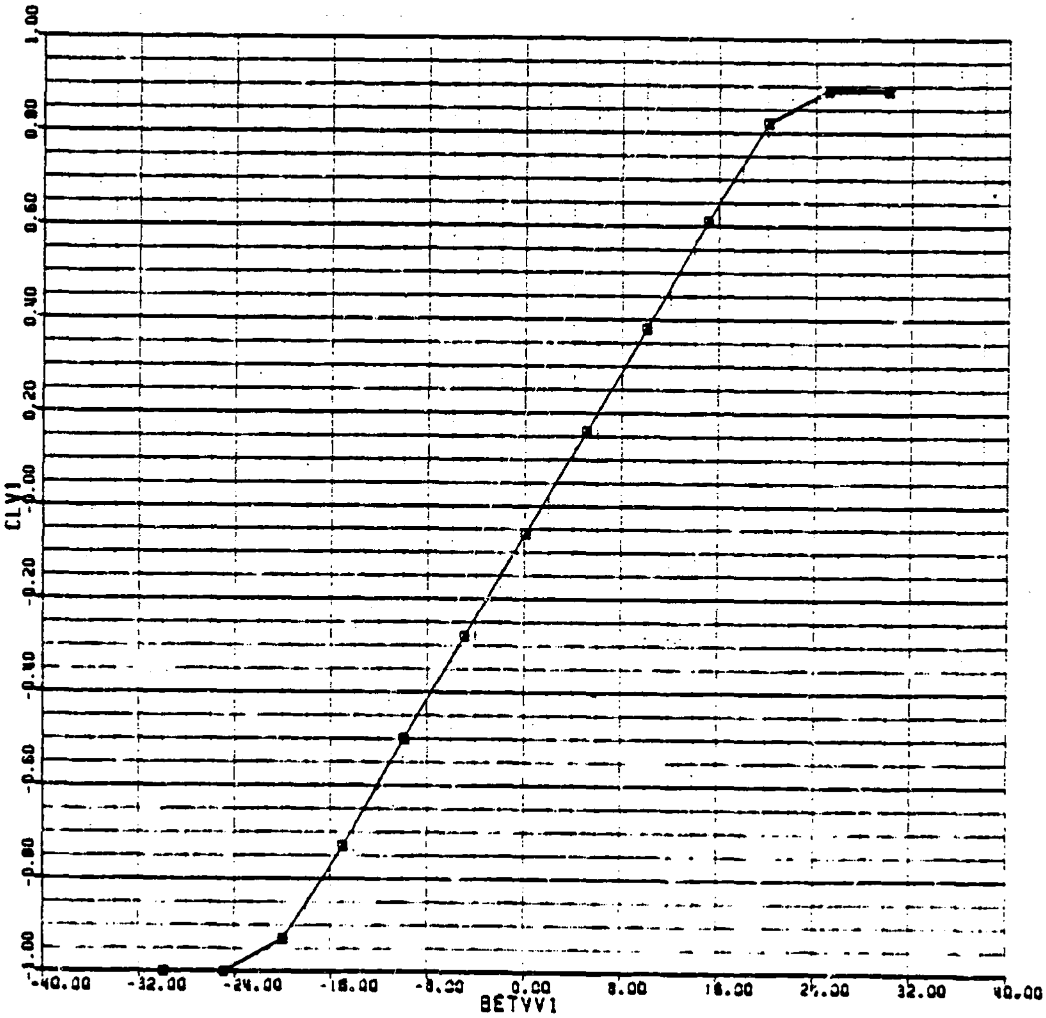

FIGURE 3.5.9(b)

VERTICAL TAIL DRAG COEFFICIENT DUE TO SIDESLIP

BLACKHAWK - NASA STUDY 23-SEP-80 CDV1MP (1/2)

MAP NAME: CDV1MP
MAP TYPE: UVAUVA
INPUT VARIABLE(S): BETVV1
OUTPUT VARIABLE: CDV1

PRIMARY MAP:
-30.00 (LOWER LIMIT)
30.00 (UPPER LIMIT)
5.00 (DELTA)

SECONDARY MAP:
-90.00 (LOWER LIMIT)
90.00 (UPPER LIMIT)
10.00 (DELTA)

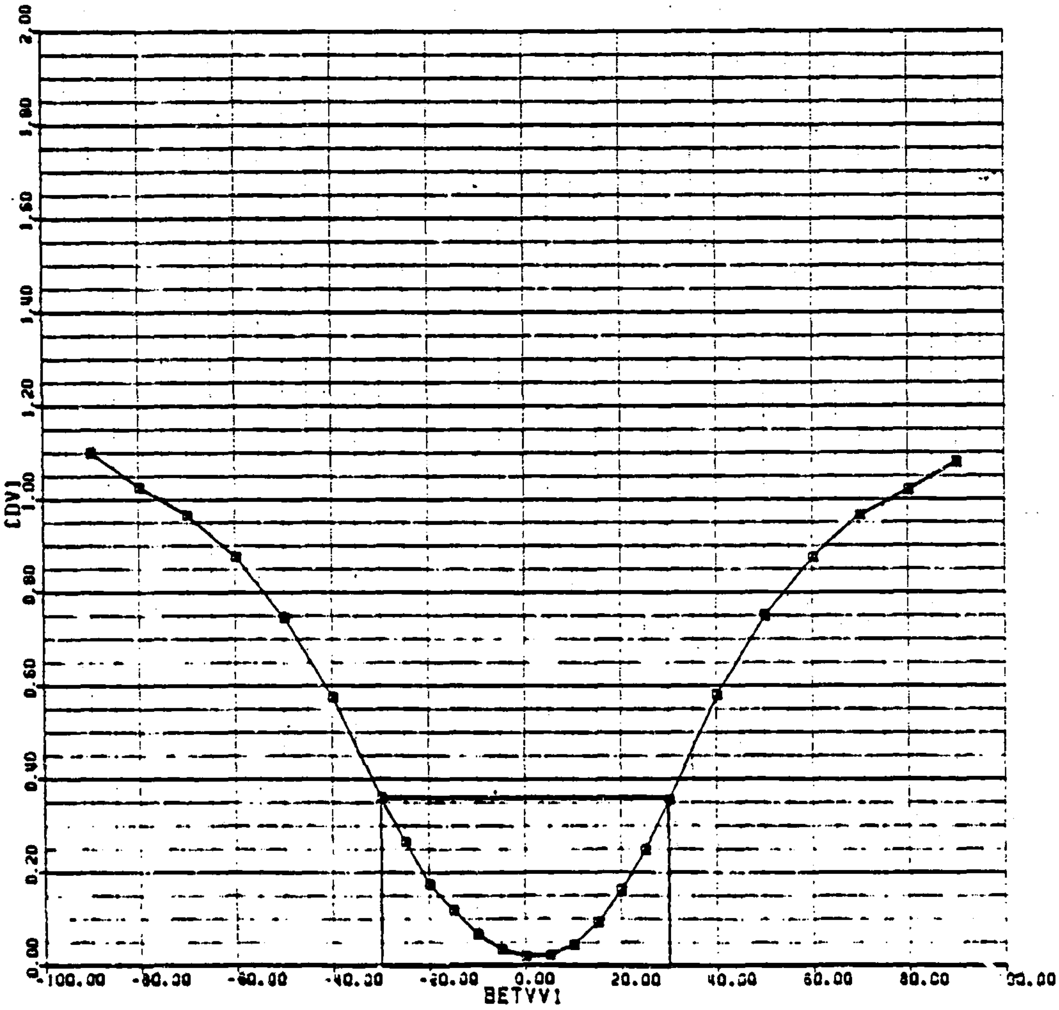

FIGURE 3.5.10(a)

VERTICAL TAIL DRAG COEFFICIENT DUE TO SIDESLIP (Cont'd)

BLACKHAWK - NASA STUDY 25-SEP-80 CDV1MP (2/2)

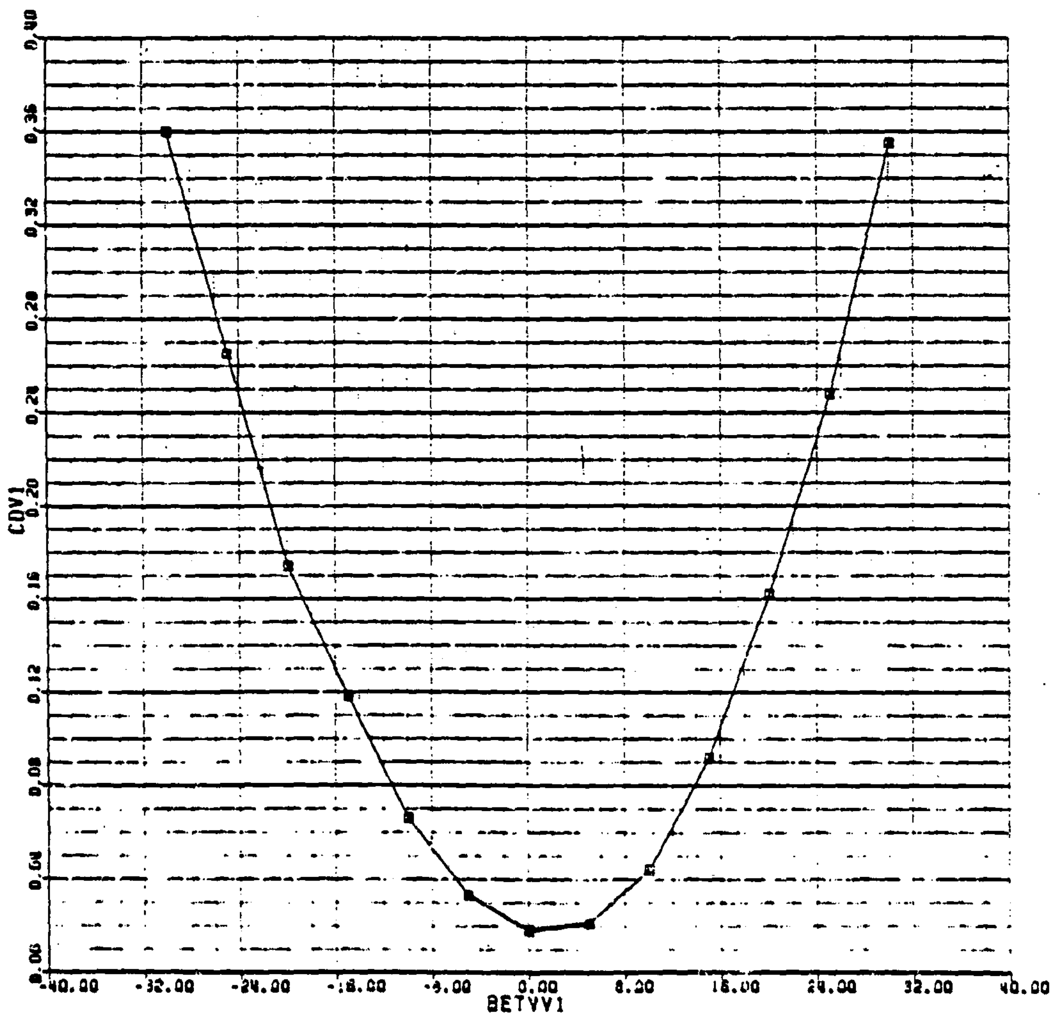

FIGURE 3.5.10(b)

5.4 TAIL ROTOR MODULE

5.4 Tail Rotor Module

5.4.1 Module Description

This module calculates the forces and moments at the center of gravity which are generated by a canted tail rotor. This rotor is represented basically by a simplified, closed form, Bailey Solution as developed in Reference 4.6.1. All terms in tip speed ratio (μ) greater than squared have been eliminated. In order to obtain the actual tail rotor collective pitch value, (θ_{TR}) , the Bailey equations have been modified to account for δ_3 (pitch-flap coupling). This reduces the blade pitch which is impressed by the control system.

The airflow impinging on the tail rotor is developed from the free stream, rotor wash and fuselage sidewash, together with body angular rate effects. The total components of velocity are resolved through the cant angle into the tail rotor shaft axes system.

The Bailey theory equation is normally presented as the thrust coefficient in terms of the 't' coefficients. It should be noted that the equations have been manipulated to obtain an expression for downwash. This was found to be necessary to obtain an unconditionally stable solution. It is important that program flow follows the equation flow for a stable tail rotor solution (Figure 4.1.1).

A blockage factor K_{TRBLK} is applied to the final thrust output to account for the proximity of the vertical tail. This correction is empirical and based on flight test data of other helicopters.

This simplified tail rotor model only calculates thrust. No account of H force is included in the final tail rotor force outputs. The tail rotor thrust is finally resolved into force and moments in body axes, at the center of gravity.

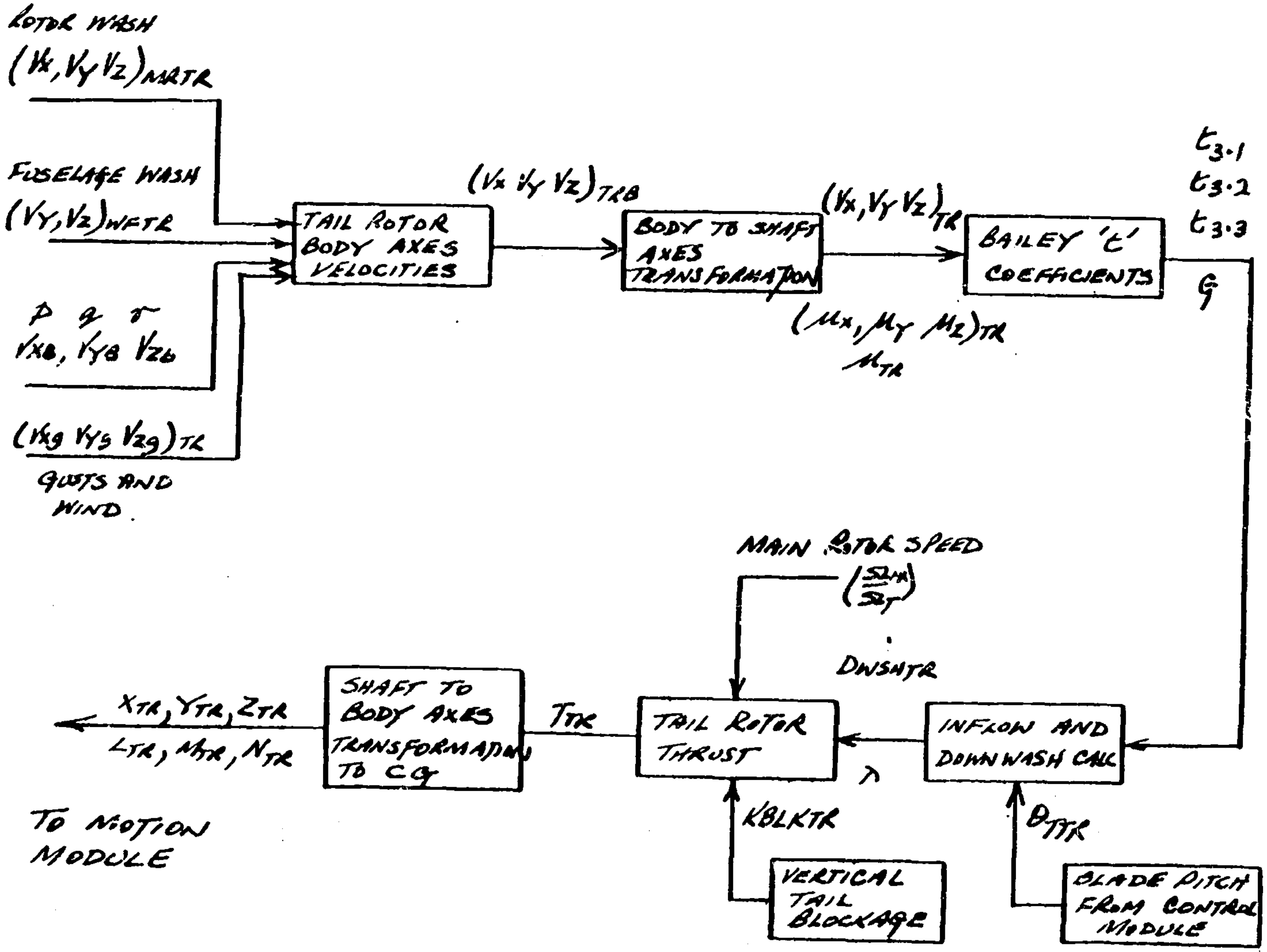

TAIL ROTOR EQUATION FLOW DIAGRAM

FIGURE 4.1.1

5.4.2 TAIL ROTOR MODULE EQUATIONS

GEOMETRY

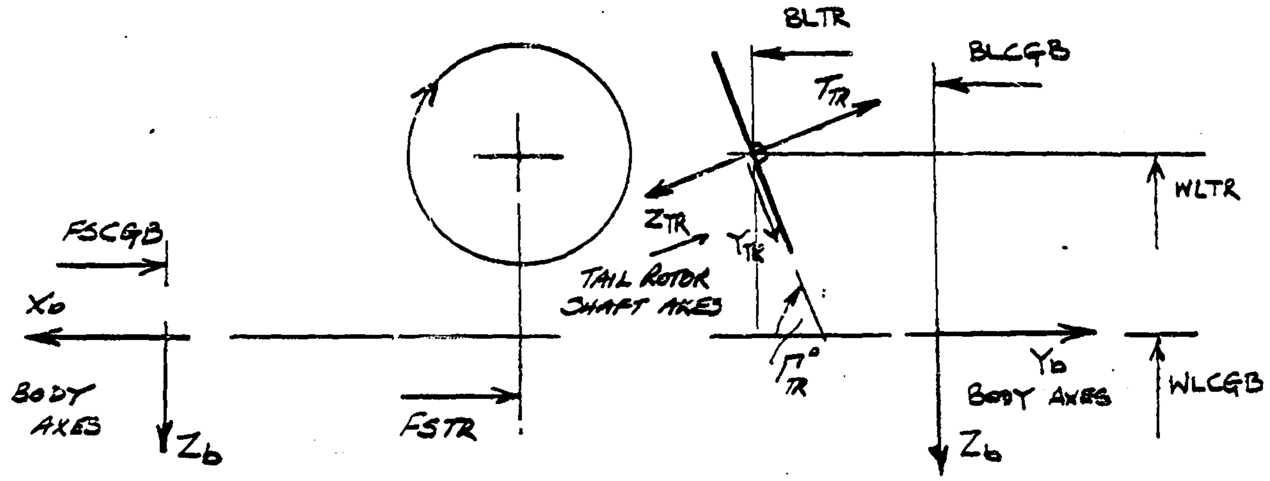

$$F_{TR} = \frac{(FSTR - FSCGb)}{12}$$

$$W_{TR} = \frac{(WLTR - WLCGb)}{12}$$

$$B_{TR} = \frac{(BLTR - BLCGb)}{12}$$

INTERFERENCE VELOCITIES

- FROM THE MAIN ROTOR , SAME AS HORIZONTAL TAIL FOR BLACKHAWK

$$EKXTR = f(\chi_{AMR}, a_{1FMR})$$, MAP-EXH1MP TABLE 3.5.1 FIGURE 3.5.1

$$VXMRTR = DWSHMR \cdot \Omega_T R_T \; EKXTR$$

$E_{KYTR} = f(\chi_{PMR}, a_{1FMR})$ NO INPUT

$V_{YMRTR} = D_{NSHMR} \cdot \Omega_T l_T E_{KYTR}$

$E_{KZTR} = f(\chi_{PMR}, a_{1FMR})$, MAP-EZH1MP TABLE 3.5.2 FIGURE 3.5.2

$V_{ZMRTR} = -D_{NSHMR} \cdot \Omega_T R_T E_{KZTR}$

– FROM THE FUSELAGE

DYNAMIC PRESSURE RATIO

$Q_{TRQWF} = f(|\psi_{HF}|)$, MAP- QV1MP TABLE 3.5.7 FIGURE 3.5.7

$K_{QTR} = (Q_{TRQWF})^{1/2}$

SIDEWASH COMPONENT

$S_{IGTR} = f(\psi_{HF})$, MAP - SGV1MP TABLE 3.5.8 FIGURE 3.5.8

$V_{YWFTR} = -\frac{V_{Xb}}{57.3} S_{IGTR} K_{QTR}$

S_{IGTR} DELAYED BY $\left(\frac{FSTR - FSCG_b}{12 * V_{Xb}}\right)$, SEC

DOWNWASH COMPONENT

$EPSTR = f(\alpha_{WF})$

$V_{ZWFTR} = -\frac{V_{Xb}}{57.3} \cdot EPSTR\ K_{QTR}$, MAP- EPH1MP TABLE 3.5.4 FIGURE 3.5.4

EPSTR DELAYED BY $\left(\frac{FSTR - FSCG_b}{12 * V_{Xb}}\right)$, SEC

SIKORSKY AIRCRAFT UNITED TECHNOLOGIES

DOCUMENT NO. SER 70452

TOTAL INTERFERENCE VELOCITIES

$$V_{XITR} = V_{XMRTR}$$

$$V_{YITR} = V_{YMRTR} + V_{YWFTR}$$

$$V_{ZITR} = V_{ZMRTR} + V_{ZWFTR}$$

TAIL ROTOR VELOCITIES IN THE BODY AXES

$$V_{XTRB} = (V_{Xb} + V_{XgTR}) K_{QTR} - q(W_{TR}) + r(B_{TR}) + V_{XITR}$$

$$V_{YTRB} = (V_{Yb} + V_{YgTR}) K_{QTR} - r(F_{TR}) + p(W_{TR}) + V_{YITR}$$

$$V_{ZTRB} = (V_{Zb} + V_{ZgTR}) K_{QTR} + q(F_{TR}) - p(B_{TR}) + V_{ZITR}$$

TAIL ROTOR VELOCITIES IN THE SHAFT AXES

$$V_{XTR} = V_{XTRB}$$

$$V_{YTR} = V_{YTRB} \cos \Gamma_{TR} + V_{ZTRB} \sin \Gamma_{TR}$$

$$V_{ZTR} = -V_{YTRB} \sin \Gamma_{TR} + V_{ZTRB} \cos \Gamma_{TR}$$

$$\mu_{XTR} = V_{XTR} / (\Omega R)_{TR}$$

$$\mu_{YTR} = V_{YTR} / (\Omega R)_{TR}$$

$$\mu_{ZTR} = V_{ZTR} / (\Omega R)_{TR}$$

$$\mu_{TR} = (\mu_{XTR}^2 + \mu_{YTR}^2)^{1/2}$$

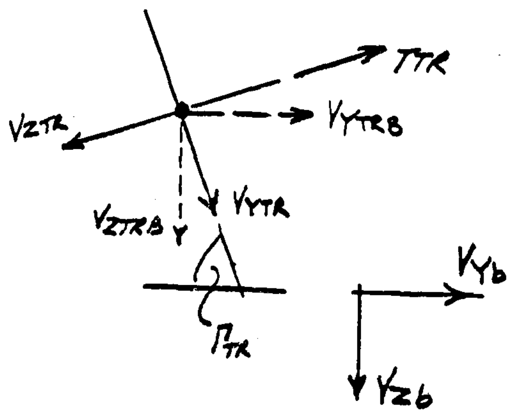

BAILEY COEFFICIENTS

$$t_{3.1} = \frac{B^2}{2} + \frac{\mu_{TR}^2}{4}$$

$$t_{3.2} = \frac{B^3}{3} + \frac{B}{2} \cdot \mu_{TR}^2$$

$$t_{3.3} = \frac{B^4}{4} + \frac{B^2}{4} \mu_{TR}^2$$

$$G = \frac{A_{TR}}{2} \left[\frac{bc}{\pi R}\right]_{TR}$$

TAIL ROTOR BLADE PITCH

$$\theta_{TR} = \frac{1}{57.3} \left[\theta_{TTR} - T_{TR_{(t-1)}} \left(\frac{\partial a_0}{\partial T_{TR}} \right) \cdot \tan \delta_3 + B_{IASTR} \right]$$

TAIL ROTOR INFLOW

$$D_{WSHTR_{(t)}} = G \frac{\left[\mu_{ZTR} (t_{3.1}) + \theta_{TR} (t_{3.2}) + \frac{T_{WSTTR}}{57.3} (t_{3.3}) \right]}{2 \left(\mu_{TR}^2 + \lambda_{TR_{(t-1)}}^2 \right)^{1/2} + G (t_{3.1})}$$

$$\lambda_{TR_t} = \mu_{ZTR} - D_{WSHTR_{(t)}}$$

ROTOR THRUST

$$T_{TR} = 2\rho\pi R_{TR}^4 \, DWSHTR \left(\mu_{TR}^2 + \lambda_{TR}^2\right)^{1/2} \Omega_{TR}^2 \left(\frac{\Omega_{MR}}{\Omega_T}\right)^2 \cdot KBLKTR$$

WHERE KBLKTR IS THE VERTICAL TAIL BLOCKAGE FACTOR

IF $V_{KT} \geq VBYTTR$, SET $KBLKTR = 1.0$

IF $V_{KT} < VBYTTR$

$$\text{SET } KBLKTR = (1 - KBVTTR)\frac{V_{KT}^2}{(VBYTTR)^2} + KBVTTR.$$

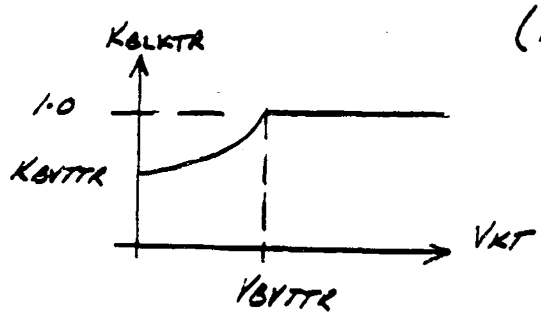

TAIL ROTOR FORCES AND MOMENTS AT THE CG IN BODY AXES

$$X_{TR} = -(C_{DTR})\tfrac{1}{2}\rho(V_{XTR})^2$$

$$Y_{TR} = T_{TR}\sin\Gamma_{TR}$$

$$Z_{TR} = -T_{TR}\cos\Gamma_{TR}$$

$$L_{TR} = Y_{TR}(W_{TR}) - Z_{TR}(B_{TR})$$

$$M_{TR} = Z_{TR}(F_{TR}) - X_{TR}(W_{TR})$$

$$N_{TR} = X_{TR}(B_{TR}) - Y_{TR}(F_{TR})$$

ORIGINAL PAGE IS
OF POOR QUALITY

5.4.3 TAIL ROTOR MODULE INPUT/OUTPUT DATA TRANSFER

INPUT TRANSFER

PARAMETER	ORIGIN MODULE
FSCGB	MAIN ROTOR
WLCGB	
DWSHMR	
CHIPMR	
A1FMR	
OMGTMR	
RMR	
OMRMR	
ALFWF	FUSELAGE
BETAWF	
THETTR	FLIGHT CONTROL
VXGTR	GUST
VYGTR	
VZGTR	
VXB	MOTION
VYB	
VZB	
P	
Q	
R	
VKT	

OUTPUT TRANSFER

PARAMETER	DESTINATION MODULE
XTR	MOTION
YTR	
ZTR	
LTR	
MTR	
NTR	

SA 29 REV. 6

5.4.4 NOTATION FOR THE TAIL ROTOR MODULE

SYMBOL USED IN EQUATIONS	PROGRAM MNEMONIC	UNITS	DESCRIPTION
F_{STR}	FSTR	INS	Fuselage station for tail rotor
F_{SCGB}	FSCGB	INS	Fuselage station for CG
F_{TR}	KTR	FT	Tail rotor longitudinal arm
W_{LTR}	WLTR	INS	Waterline station for tail rotor
W_{LCGB}	WLCGB	INS	Waterline station for CG
W_{TR}	KTR+1	FT	Tail rotor vertical arm
B_{LTR}	BLTR	INS	Buttline station for tail rotor
B_{LCGB}	BLCGB	INS	Buttline station for the CG
B_{TR}	KTR+2	FT	Tail rotor lateral arm
χ_{PMR}	CHIPMR	DEG	Rotor Wake Skew Ang .
a_{1FMR}	AA1FMR	DEG	Longitudinal main rotor flapping
D_{WSHMR}	DWSHMR	ND	Uniform downwash at the main rotor
Ω_T	OMGTMR	RADS/SEC	Trimmed rotor speed
R_T	RMR	FT	Main rotor radius
E_{KXTR}	EKXTR	ND	Main rotor wash factors
E_{KYTR}	EKYTR	ND	
E_{KZTR}	EKZTR	ND	
V_{XMRTR}	VXMRTR	FT/SEC	Main rotor wash at the tail rotor
V_{YMRTR}	VYMRTR	FT/SEC	
V_{ZMRTR}	VZMRTR	FT/SEC	
α_{WF}	ALFAWF	DEG	Fuselage angle of attack
ψ_{WF}	PSIWF	DEG	Fuselage yaw attitude
Q_{TRQWF}	QTRQWF	-	Dynamic Pressure ratio at the tail rotor
K_{QTR}	KQTR	-	----
S_{IGTR}	SIGTR	DEG	Fuselage sidewash at the tail rotor

SA 29 REV. 6

5.4.4 (Cont'd) NOTATION FOR THE TAIL ROTOR MODULE

SYMBOL USED IN EQUATIONS	PROGRAM MNEMONIC	UNITS	DESCRIPTION
V_{xb}	VXB	FT/SEC	Body axes velocities
V_{yb}	VYB	FT/SEC	
V_{zb}	VZB	FT/SEC	
V_{YWFTR}	VYWFTR	FT/SEC	Fuselage sidewash velocity
V_{XITR}	VXITR	FT/SEC	Total interference velocities at the tail rotor
V_{YITR}	VYITR	FT/SEC	
V_{ZITR}	VZITR	FT/SEC	
V_{XGTR}	VXGTR	FT/SEC	Body axes gust velocities
V_{YGTR}	VYGTR	FT/SEC	
V_{ZGTR}	VZGTR	FT/SEC	
p	p	RADS/SEC	Body axes angular rates
q	q	RADS/SEC	
r	r	RADS/SEC	
V_{XTRB}	VXTRB	FT/SEC	Total velocities at the tail rotor in body axes.
V_{YTRB}	VYTRB	FT/SEC	
V_{ZTRB}	VZTRB	FT/SEC	
V_{XTR}	VXTR	FT/SEC	Total velocities at the tail rotor in shaft axes.
V_{YTR}	VYTR	FT/SEC	
V_{ZTR}	VZTR	FT/SEC	
Γ_{TR}	GAMTR	DEG	Tail rotor cant angle
Ω_{TR}	OMEGTR	RADS/SEC	Tail rotor trim speed
R_{TR}	RTR	FT	Tail rotor radius
μ_{XTR}	MUXTR	ND	Shaft axes velocities normalized by rotor tip speed.
μ_{YTR}	MUYTR	ND	
μ_{ZTR}	MUZTR	ND	
μ_{TR}	MUTR	ND	

5.4.4 (Cont'd) NOTATION FOR THE TAIL ROTOR MODULE

SYMBOL USED IN EQUATIONS	PROGRAM MNEMONIC	UNITS	DESCRIPTION
$t_{3.1}$			Bailey Coefficients
$t_{3.2}$			
$t_{3.3}$			
B	BTLTR	-	Blade tip loss factor
G			Constant
A_{TR}	ATR	1/RADS	Blade section lift curve Slope (2D)
b_{TR}	BTR	-	Actual number of blades on the tail rotor
C_{TR}	CHRDTR	FT	Blade Chord for the Tail rotor
θ_{TTR}	THETTR	DEG	Tail rotor commanded blade pitch
T_{TR}	TTR	LB	Tail Rotor Thrust
ao/T_{TR}	DELTTR	-	Rate of change of coning with thrust
δ_3	DEL3TR	DEG	Flapping hinge offset angle
B_{1ASTR}	B1ASTR	DEG	Blade pitch correction to linear twist
θ_{TR}	-	DEG	Actual Blade pitch
D_{WSHTR}	DWSHTR	-	Uniform downwash at the tail rotor disc
T_{WSTTR}	TWSTTR	DEG/R_{TR}	Linear blade twist
λ_{TR}	LAMBTR	-	Tail rotor inflow
Ω_{MR}	OMGMR	RADS/SEC	Actual rotor speed
K_{BLKTR}	KBLKTR	-	Tail rotor blockage from vertical tail
V_{BVTTR}	VBVTTR		Airspeed breakpoint for blockage factor
C_{DTR}	CDTR	FT^2	Tail rotor drag
ρ	RHO	$SLUGS/FT^3$	Air density
X_{TR}	XTR	LB	Tail rotor forces at the CG in body axes
Y_{TR}	YTR	LB	
Z_{TR}	ZTR	LB	

5.4.4 (Cont'd) NOTATION FOR THE TAIL ROTOR MODULE

SYMBOL USED IN EQUATIONS	PROGRAM MNEMONIC	UNITS	DESCRIPTION
L_{TR}	LTR	FT LB	Tail rotor moments at the CG in body axes
M_{TR}	MTR	FT LB	
N_{TR}	NTR	FT LB	
V_{KT}	VKT	KNOTS	Flight Path airspeed

5.4.5 BLACK HAWK TAIL ROTOR INPUT DATA

INPUT CONSTANTS

FS_{TR}	=	732.0	INS
WL_{TR}	=	324.7	INS
BL_{TR}	=	−14.0	INS
R_{TR}	=	5.5	FT
Ω_{TR}	=	124.62	RADS/SEC
b_{TR}	=	4	−
TWSTTR	=	−18	DEG/R
Γ_{TR}	=	70.0	DEG
δ_{3TR}	=	35.0	DEG
C_{TR}	=	·81	FT
A_{TR}	=	5·73	1/RAD
B	=	·92	−
C_{DTR}	=	0	−
$\left(\frac{\partial a_0}{\partial T_{TR}}\right)$	=	·001455	DEG/lb
KBVTTR	=	·796	
VBVTTR	=	30	KNOTS
BIASTR	=	6.0	DEG

5.4.6 References

1. Simplified Theoretical Method of Determining the Characteristics of a Lifting Rotor in Forward Flight, Bailey, NACA Report 716

5.5 FLIGHT CONTROL SYSTEM MODULE

CONTENTS

FIGURES

5.5 FLIGHT CONTROL SYSTEM MODULE

5.5.1 Flight Control Simulation Module Description

The simulation of the flight control system is presented entirely in terms of block diagrams indicating the transfer function between signals. The Background information presented in Section 3.5 of Volume II complements this description of the control system simulation. An overview of the control system simulation nomenclature, for the various elements, is presented on Figure 5.1.1. The block diagrams, subsequently presented, are aligned with the flow of this figure. It will be noted in studying this section, that the bandwidth of some control system components is wide. This leads to time constants of some of the transfer functions being small. For completeness these components have been retained in the model, thus making it necessary to provide a test for cycle time in the corresponding algorithms to ensure unity gain if cycle time is large relative to the function's time constant.

(a) Sensors - The transfer functions for the sensors are presented in Figure 5.1.2.

(b) Stability Augmentation System (SAS) - The simulation definitions for pitch, roll and yaw SAS channels are shown on Figures 5.1.3 (a), (b), and (c) respectively. Each figure incorporates the representation of the digital and analog SAS channels. In general, the helicopter motion sensed by the gyroscopes is passed through signal conditioning filters before being shaped by the SAS networks. The signal is then processed through a washout, if required, and the 2:1 gain change switch. The switch definition is - ON/ON, both channels working at gain 1.0, ON/OFF, digital channel only working at gain 2.0, OFF/ON, analog channel only working at gain 2.0. Finally, the signal is restricted in amplitude by a 5% authority limit. In the case of the digital channel, the signal is passed through a zero order hold to account for update delays. A switch in the yaw channel inhibits the lagged rate term at speeds above 60 knots and introduces lagged lateral acceleration for aid in turn coordination.

The following logic applies for all control system channels:

In the IC Mode: 1. Outputs of all synchronizers are zero.
2. Outputs of all integraters are zero or have defined initial values.

In the Compute Mode: The logic is defined on the block diagrams.

(c) Pitch Bias Actuator (PBA) - The PBA representation is presented on Figure 5.1.4. The input signals are derived as indicated. It should be noted that the pitch rate signal is picked off downstream of the signal conditioning. The three input signals are limited, passed through a gain and summed to obtain the signal output to the PBA actuator. The actuator travel is restricted by a ± 3%/sec rate limit and a ± 15% authority limit. Because the PBA algorithm is computed by the digital computer, the simulation includes a zero order hold.

(d) Flight Path Stabilization (FPS) - The simulation representation of the pitch, roll, and yaw Flight Path Stabilization channels are presented on Figures 5.1.5 (a), (b) and (c) respectively. The synchronization elements in the model must track during the simulation trimming phase and in the IC mode. During the compute mode, they must track with the FPS off. The FPS shaping networks are relatively straightforward, however, a degree of complication is introduced by the automatic turn coordination capability. On the helicopter the turn switch is enabled by several channels of complex logic. For this simulation it is recommended that the switch be enabled by one path only.

FPS ON, VXBIKT $>$ 60 kts, plus trim release pressed, plus $\emptyset_b > 2^o$

Exit is by feet on the pedals and trim release pressed. For analysis purposes the turn switch can be enabled as required. Since the FPS is computed in the digital computer, the final output to the trim actuator is passed through a zero order hold. The trim actuator has 100% authority within certain control force constraints and is rate limited at 10%/sec.

(e) Mechanical Control System - In addition to its function as a mixing unit for control coupling, this area in the simulation is used to bring together the various elements of the control system computed upstream. The representations of the four primary controls, main rotor collective blade pitch, lateral cyclic blade pitch, longitudinal cyclic blade pitch and tail rotor collective pitch are shown on Figures 5.1.6 (a), (b), (c) and (d) respectively. The longitudinal cyclic pitch channel will be used for purposes of discussion. The outputs from the digital and analog SAS channels are summed and processed through the SAS actuator dynamics, resulting in actuator travel in inches (XBILS). This is summed with the PBA (XBBAS), the FPS (XBOLS) and the pilot control stick input (XB+2). The trimming algorithm input (XB+1) is added in the simulation at this point for cases where trim is accomplished using the control sticks. The resultant linkage motion is converted into equivalent degrees of longitudinal cyclic before being summed with coupled motion from other controls in the mixing unit. The output from the mixing unit B1SMIX is modified by the primary servo dynamics giving the final longitudinal cyclic impressed on the main rotor. Additional inputs are added at this point for use in analysis. Travel limits for the rotor head are given on page 5.5.20.

(f) Stabilator - The representation of the analog network controlling the stabilator is presented on figure 5.1.7. The network provides for the feedback of velocity, collective stick, lateral acceleration and pitch rate scheduled as a function of forward speed. The output from the network is passed through the dynamics of the limited rate tail servo. For the simulation provision is made for ar alternative input (STBSET) for use in analysis.

ORIGINAL PAGE IS OF POOR QUALITY

OVERVIEW OF THE CONTROL SYSTEM SIMULATION

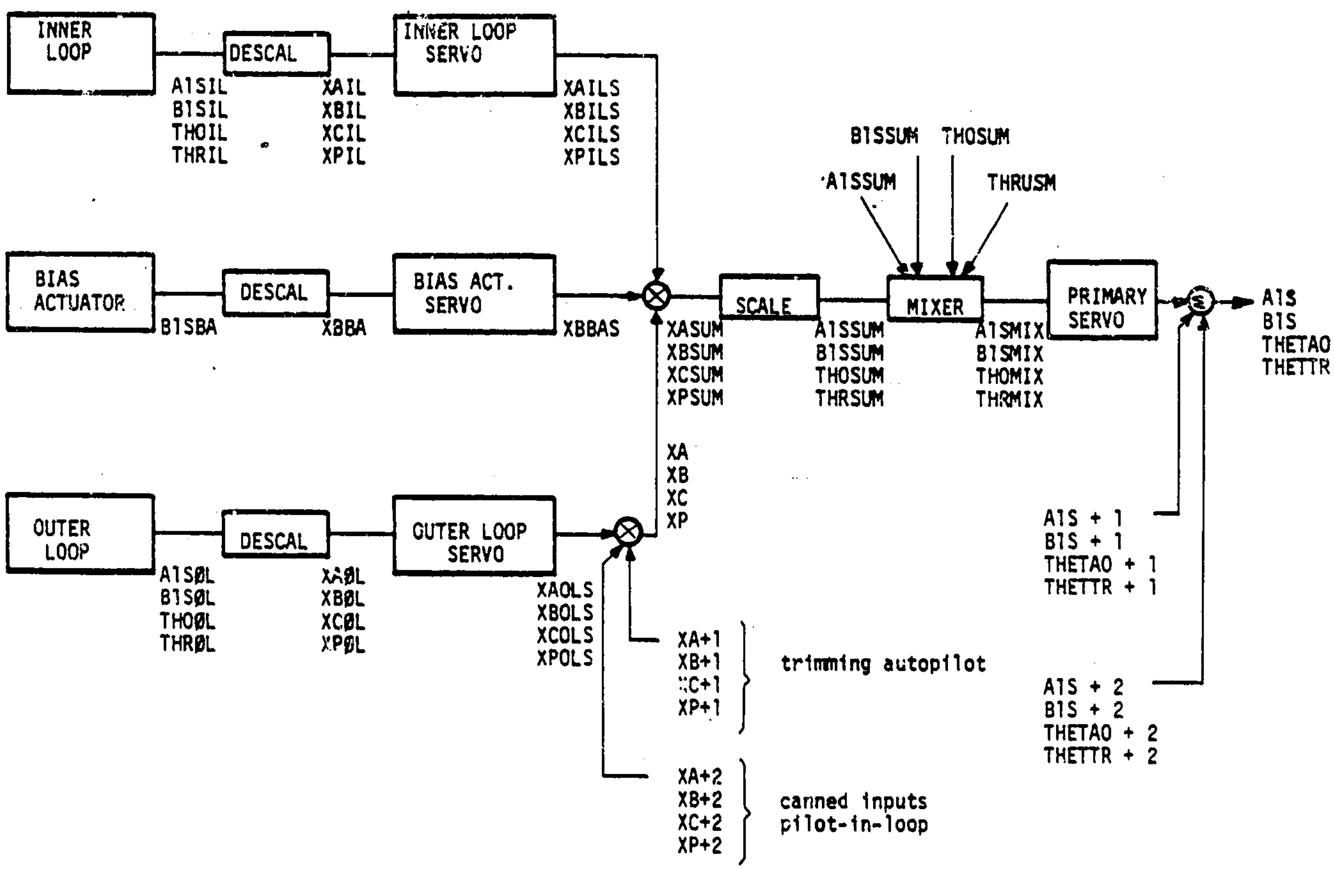

FIGURE 5.1.1

BLACK HAWK HELICOPTER MOTION SENSORS

ATTITUDE GYROS

PITCH THETAB, DEG

ROLL PHIB, DEG

YAW PSIB, DEG

AIRSPEED VXBIKT, KNOTS

RATE GYROS

$$\begin{array}{lll} \text{PITCH}, & \text{QSENSR}, & \\ \text{ROLL}, & \text{PSENSR}, & = \\ \text{YAW}, & \text{RSENSR}, & \end{array} \frac{\begin{array}{c}\text{QDEG},\\ \text{PDEG},\\ \text{RDEG},\end{array}}{(.00014S^2 + .016S + 1)}$$

LATERAL ACCELERATION

$$\text{Y.SENS} = \frac{\text{AYPS1}}{(.0254S^2 + .233S + 1)}$$

FIGURE 5.1.2

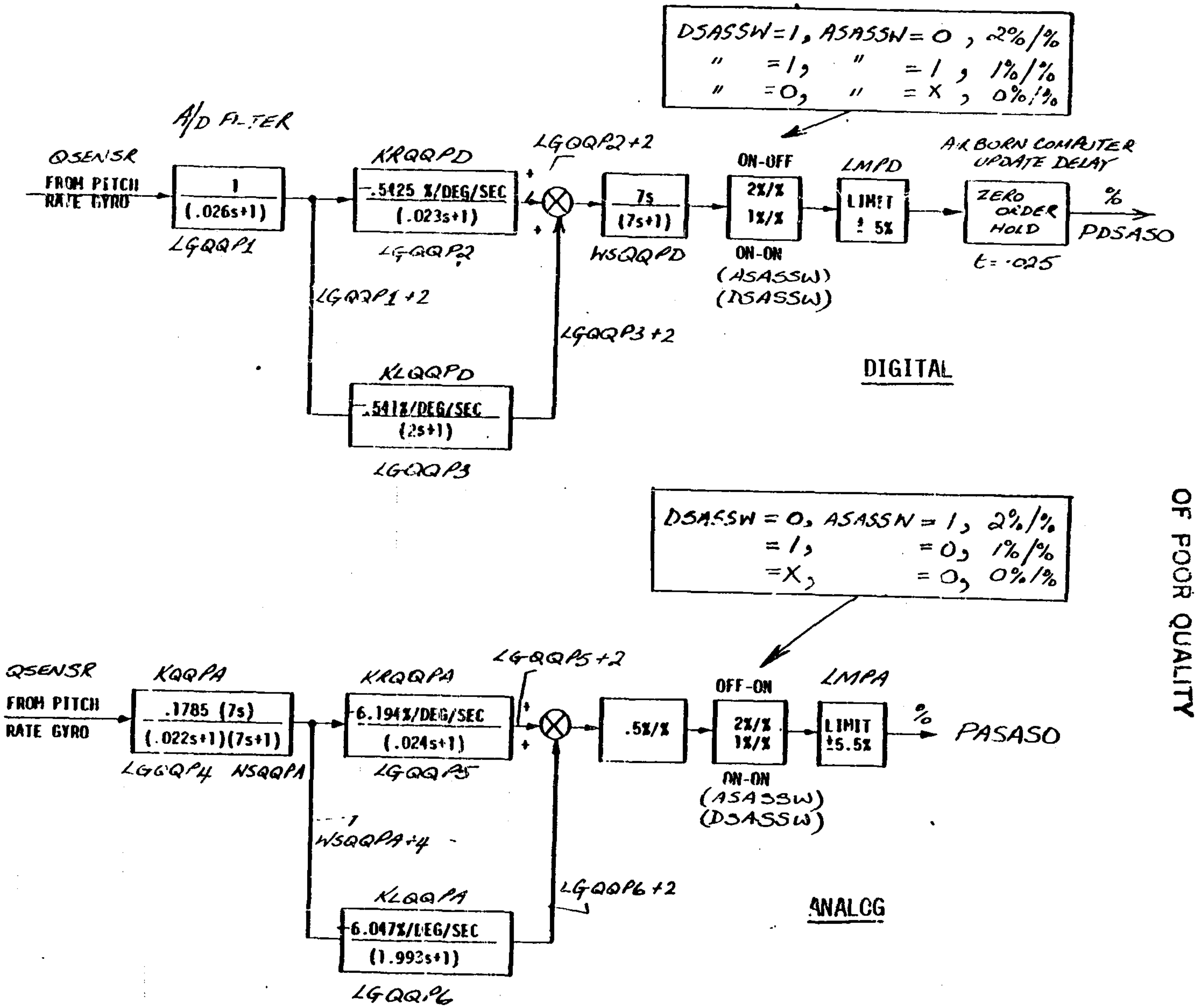

BLACK HAWK PITCH SAS CHANNELS

FIGURE 5.1.3(a)

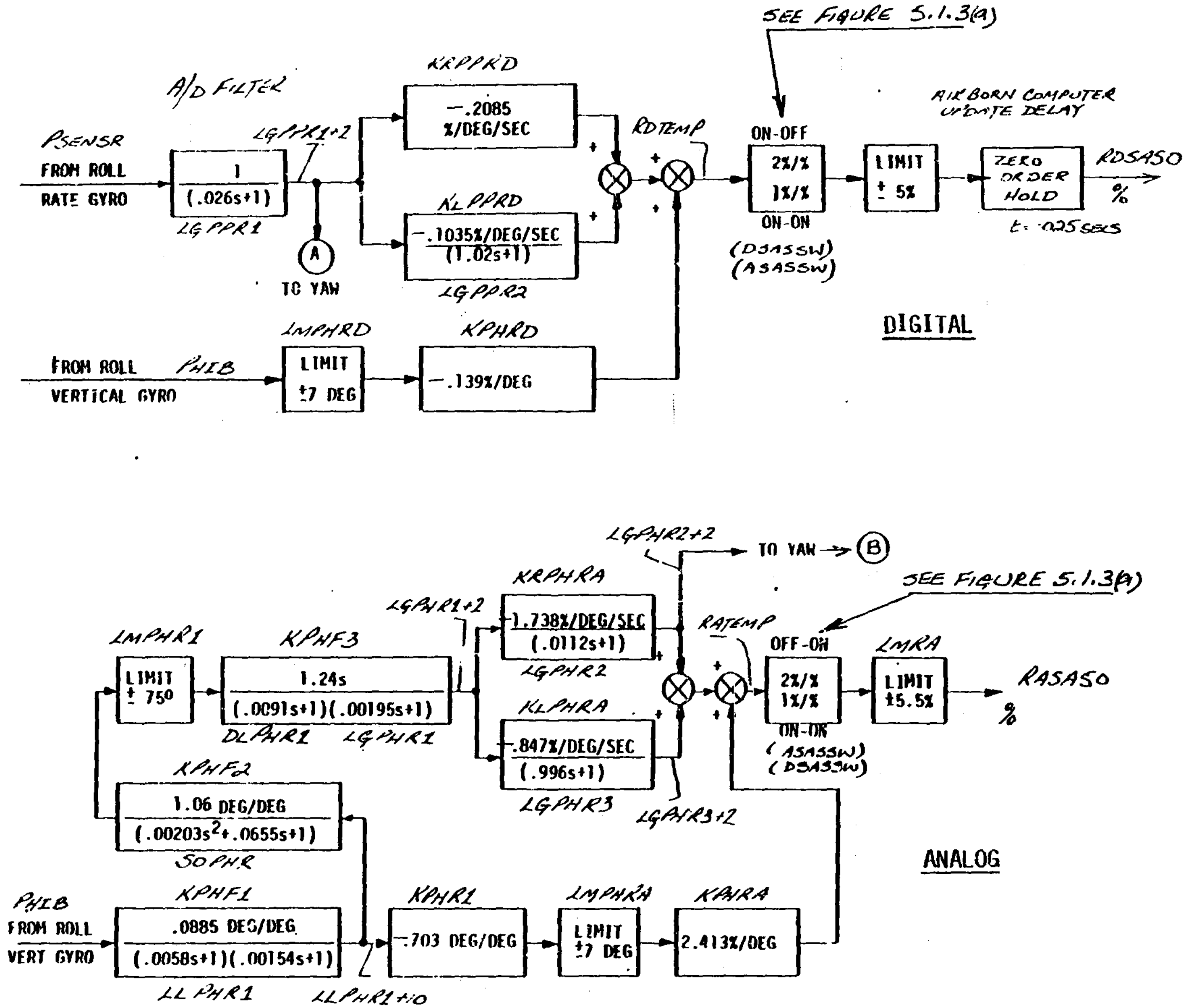

BLACK HAWK ROLL SAS CHANNELS

FIGURE 5.1.3(b)

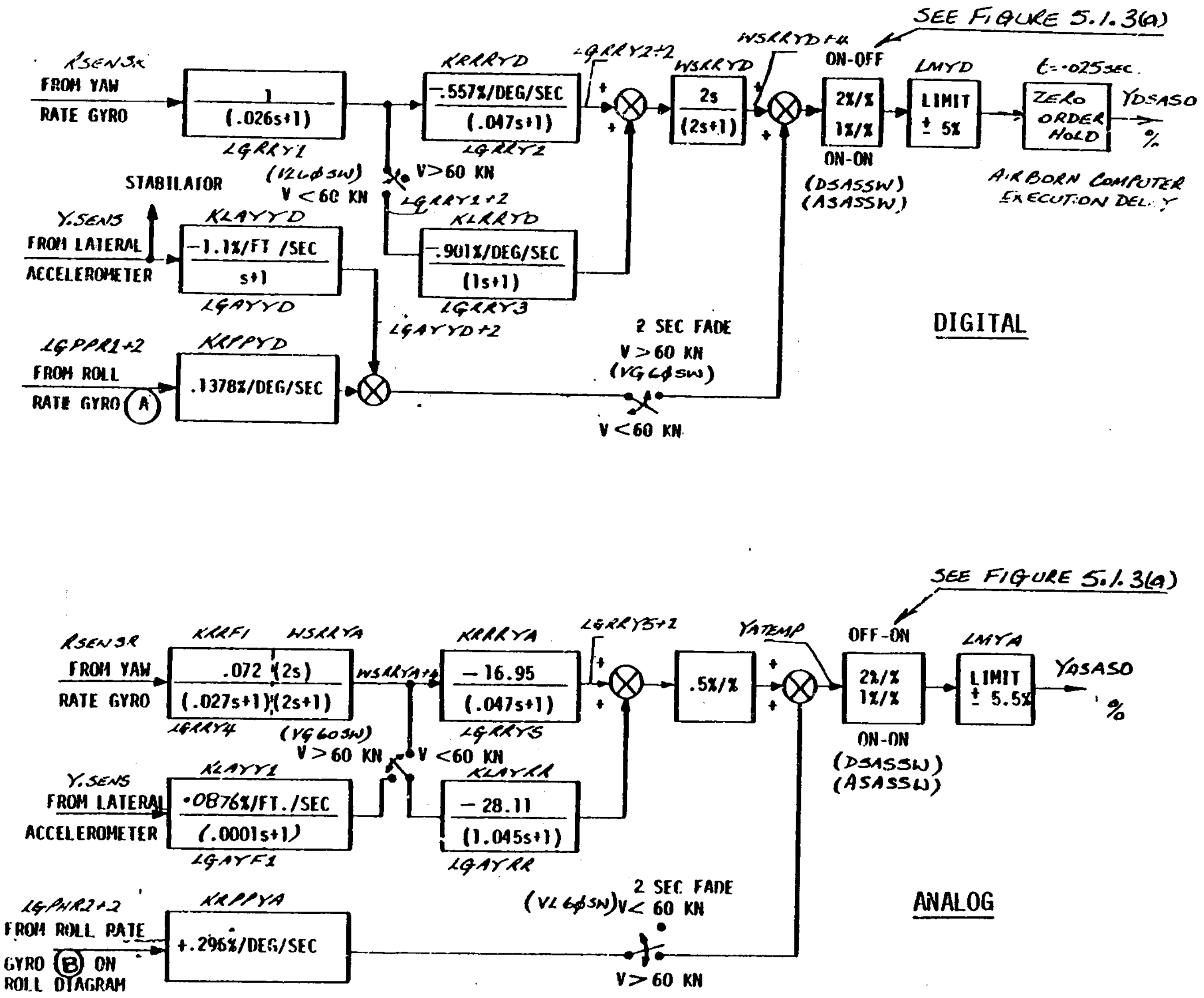

BLACK HAWK YAW SAS CHANNELS

FIGURE 5.1.3(c)

ORIGINAL PAGE IS
OF POOR QUALITY

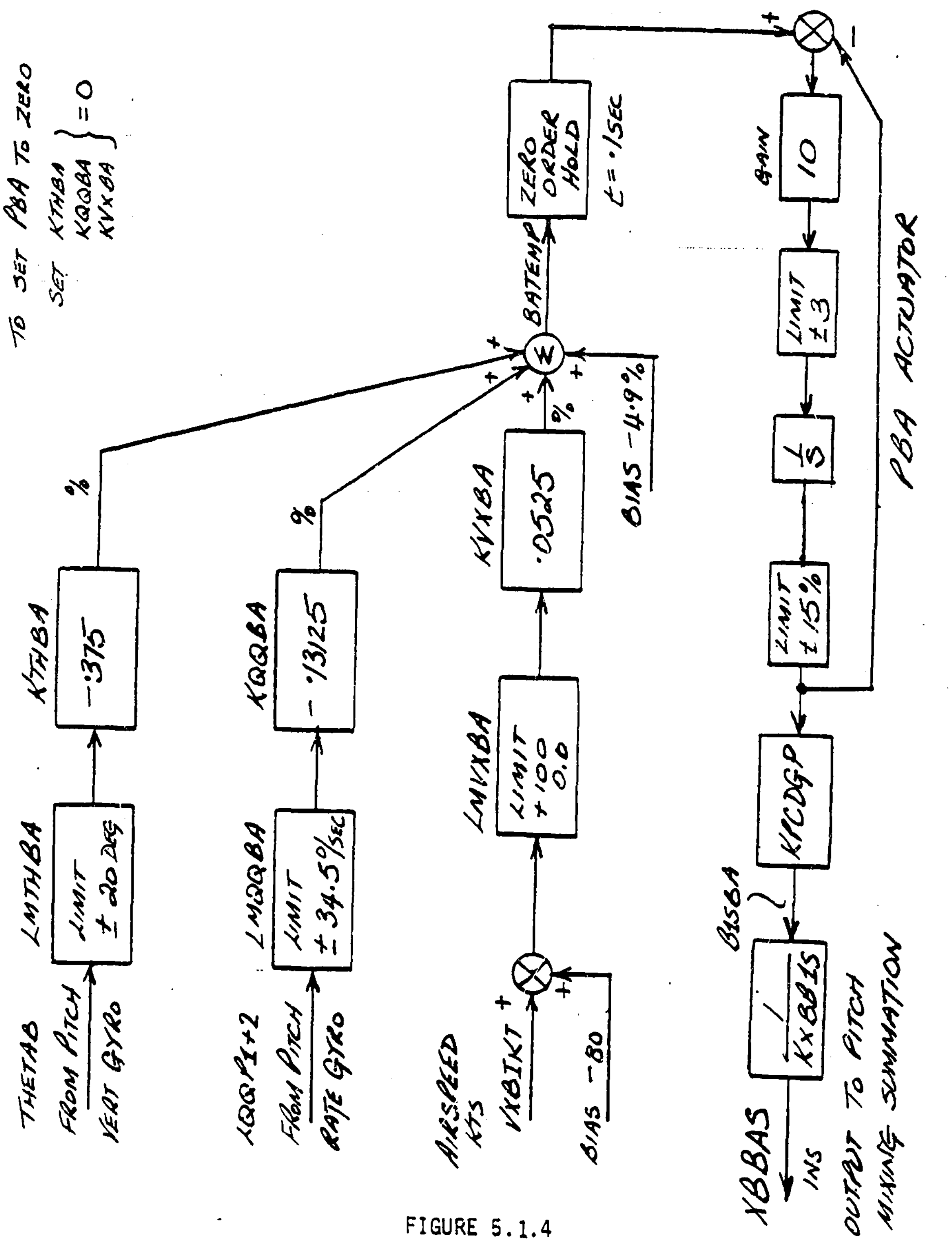

BLACK HAWK PITCH BIAS ACTUATOR

FIGURE 5.1.4

ORIGINAL PAGE IS OF POOR QUALITY

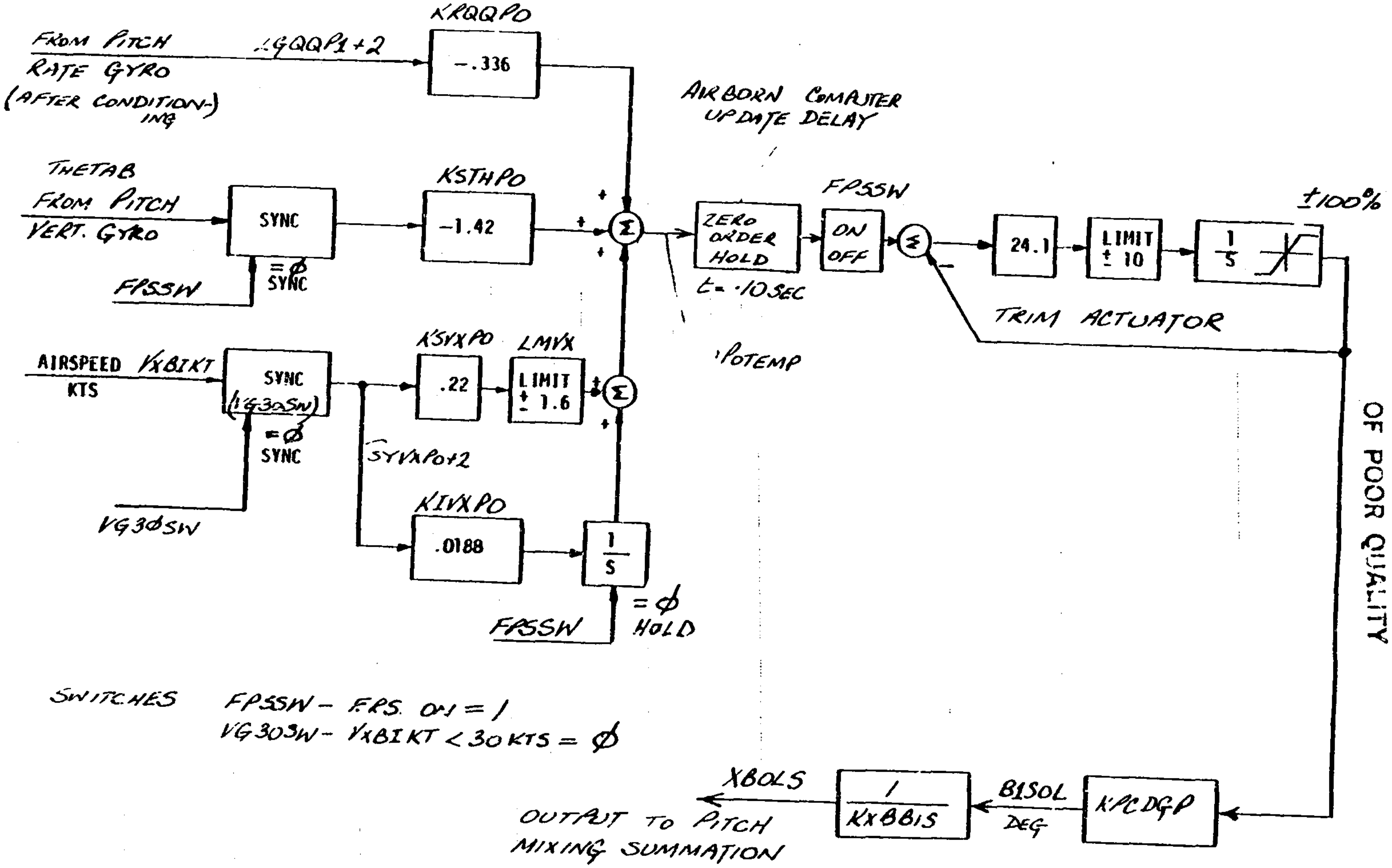

BLACK HAWK PITCH FPS CHANNEL

FIGURE 5.1.5(a)

ORIGINAL PAGE IS OF POOR QUALITY

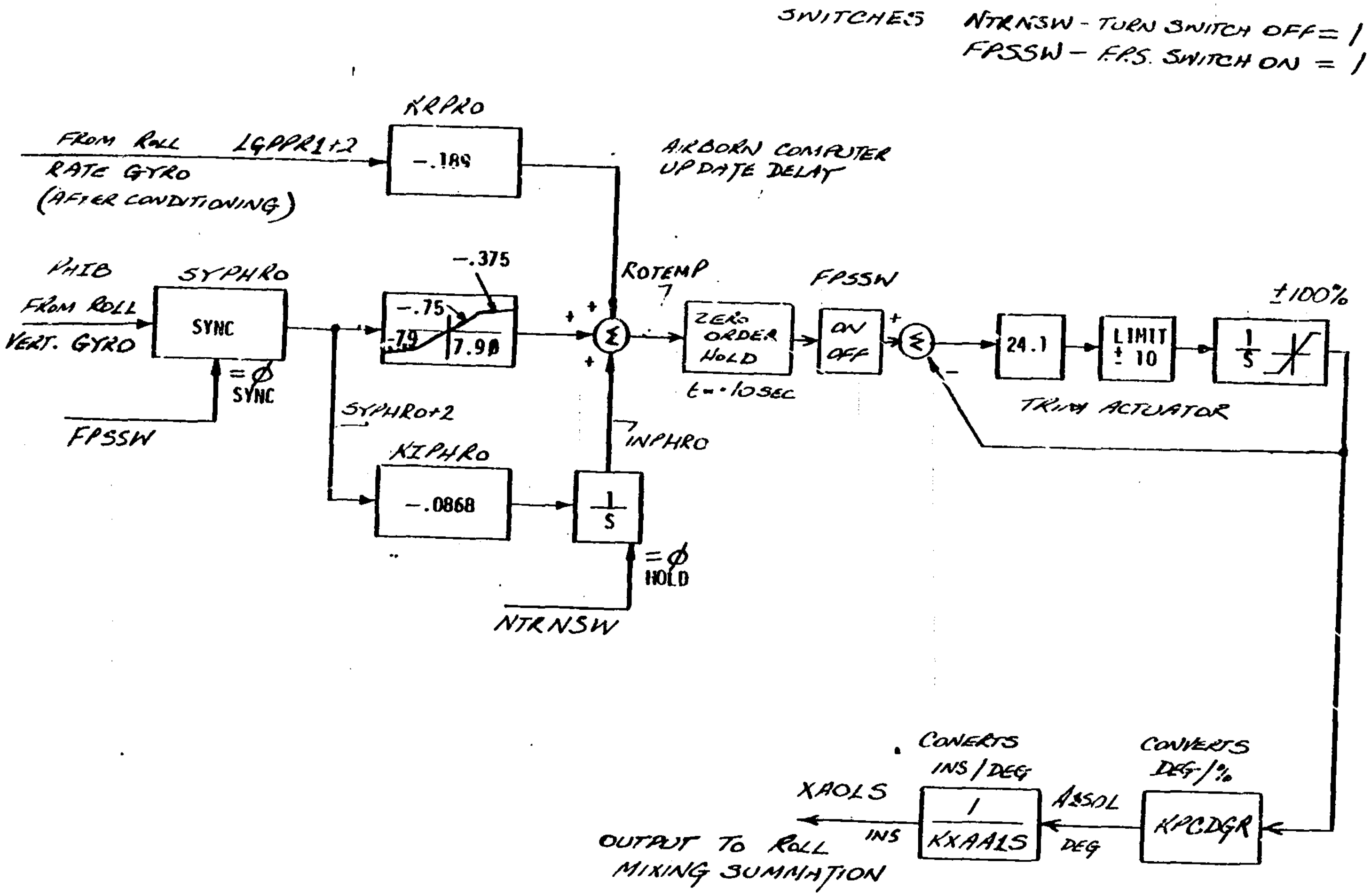

BLACK HAWK ROLL FPS CHANNEL

FIGURE 5.1.5(b)

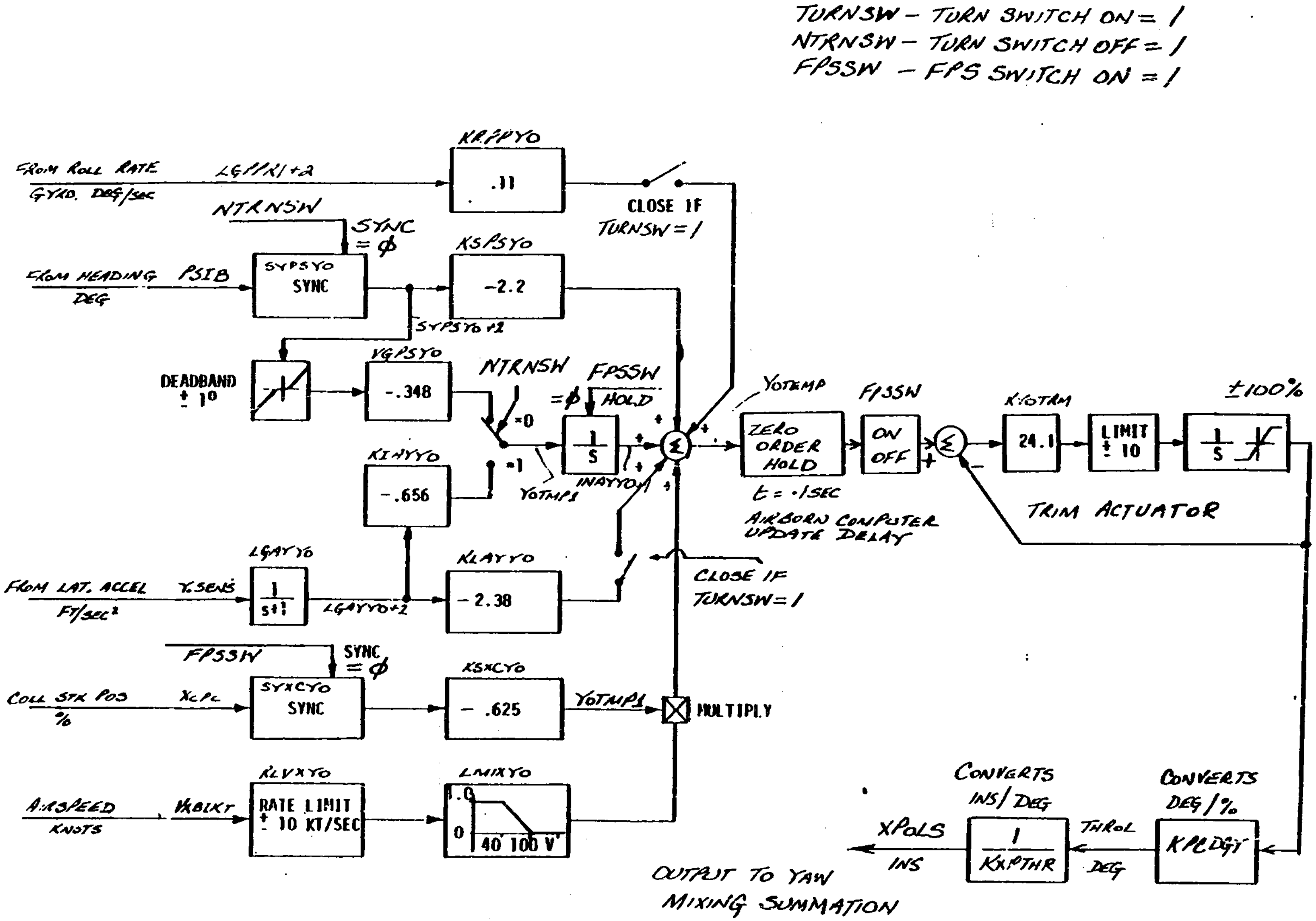

BLACK HAWK YAW FPS CHANNEL

FIGURE 5.1.5(c)

ORIGINAL PAGE IS OF POOR QUALITY

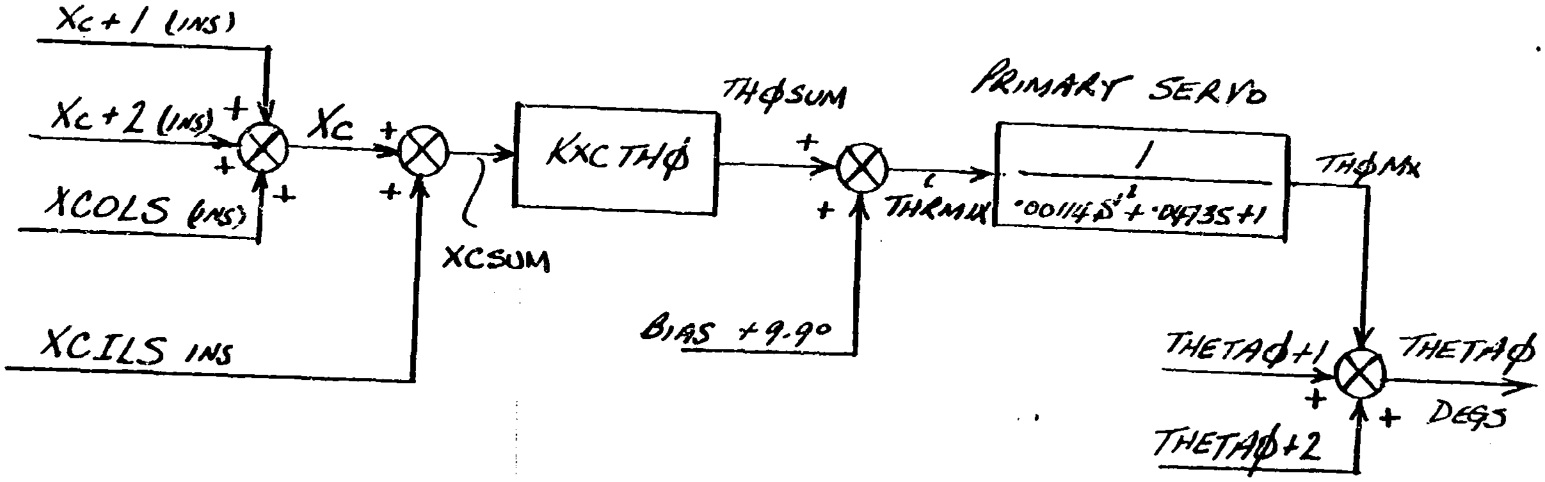

BLACK HAWK COLLECTIVE CONTROL

FIGURE 5.1.6(a)

FIGURE 5.1.6(b)

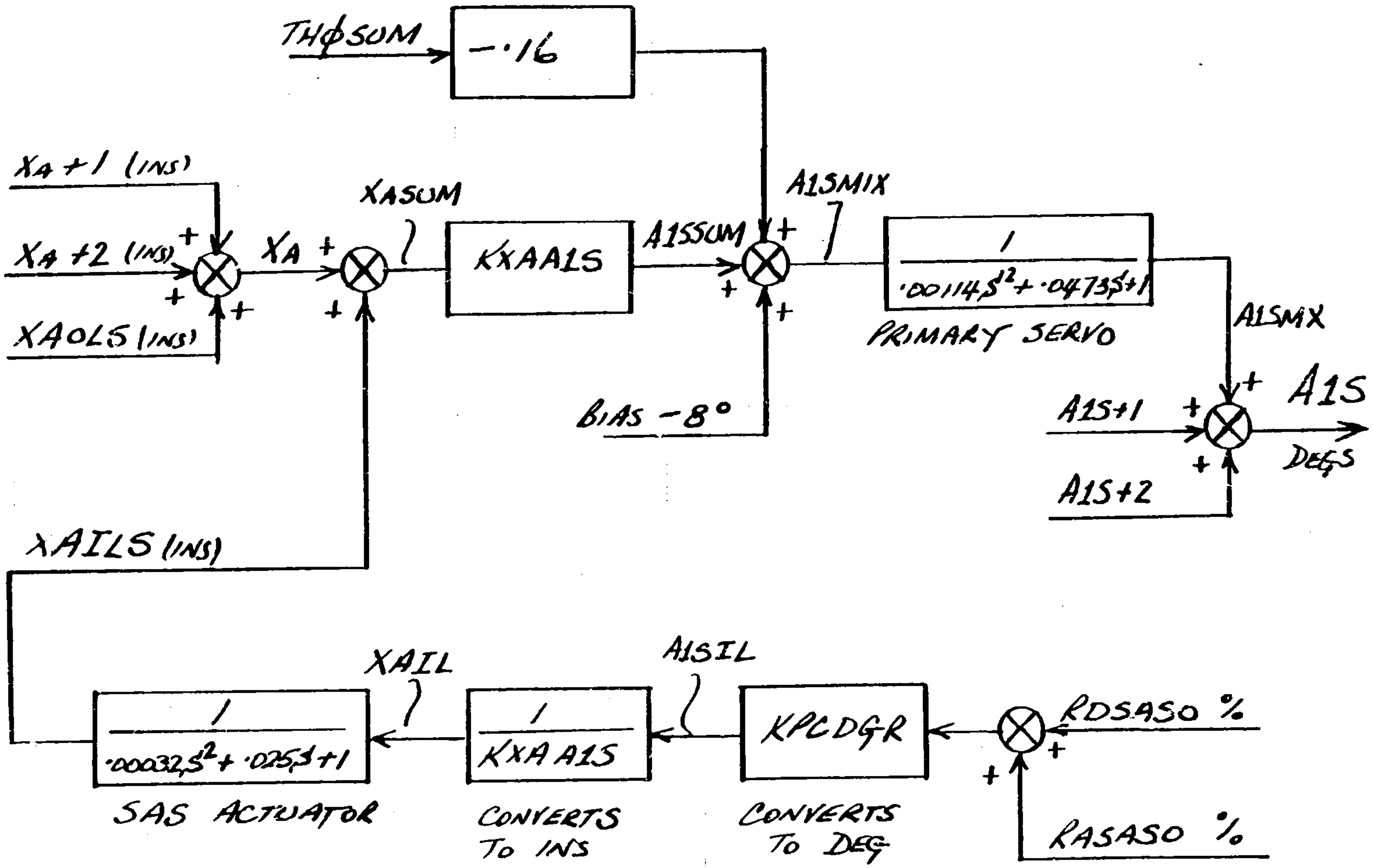

BLACK HAWK LATERAL CYCLIC CONTROL

FIGURE 5.1.6(c)

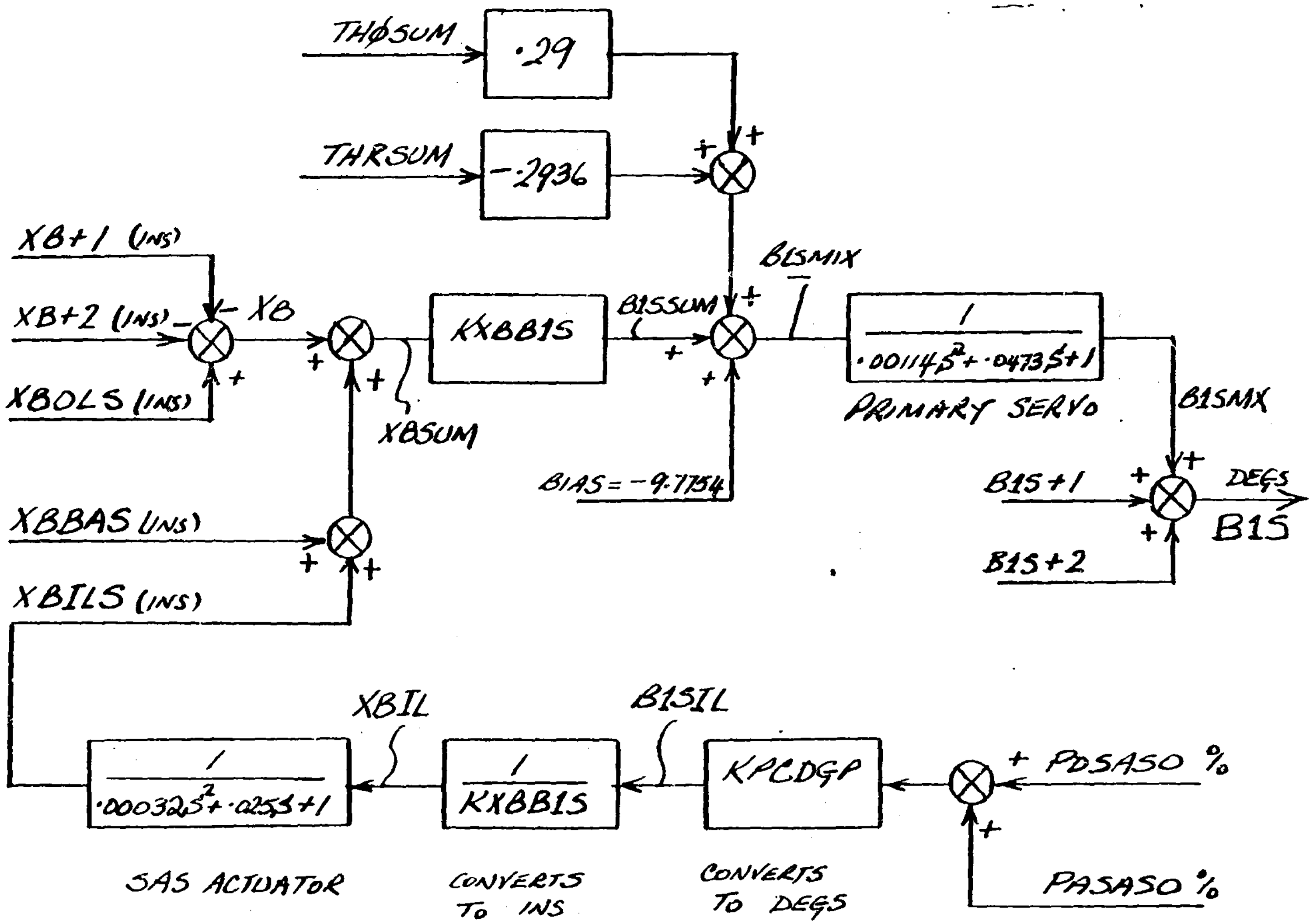

BLACK HAWK LONGITUDINAL CYCLIC CONTROL

FIGURE 5.1.6(d)

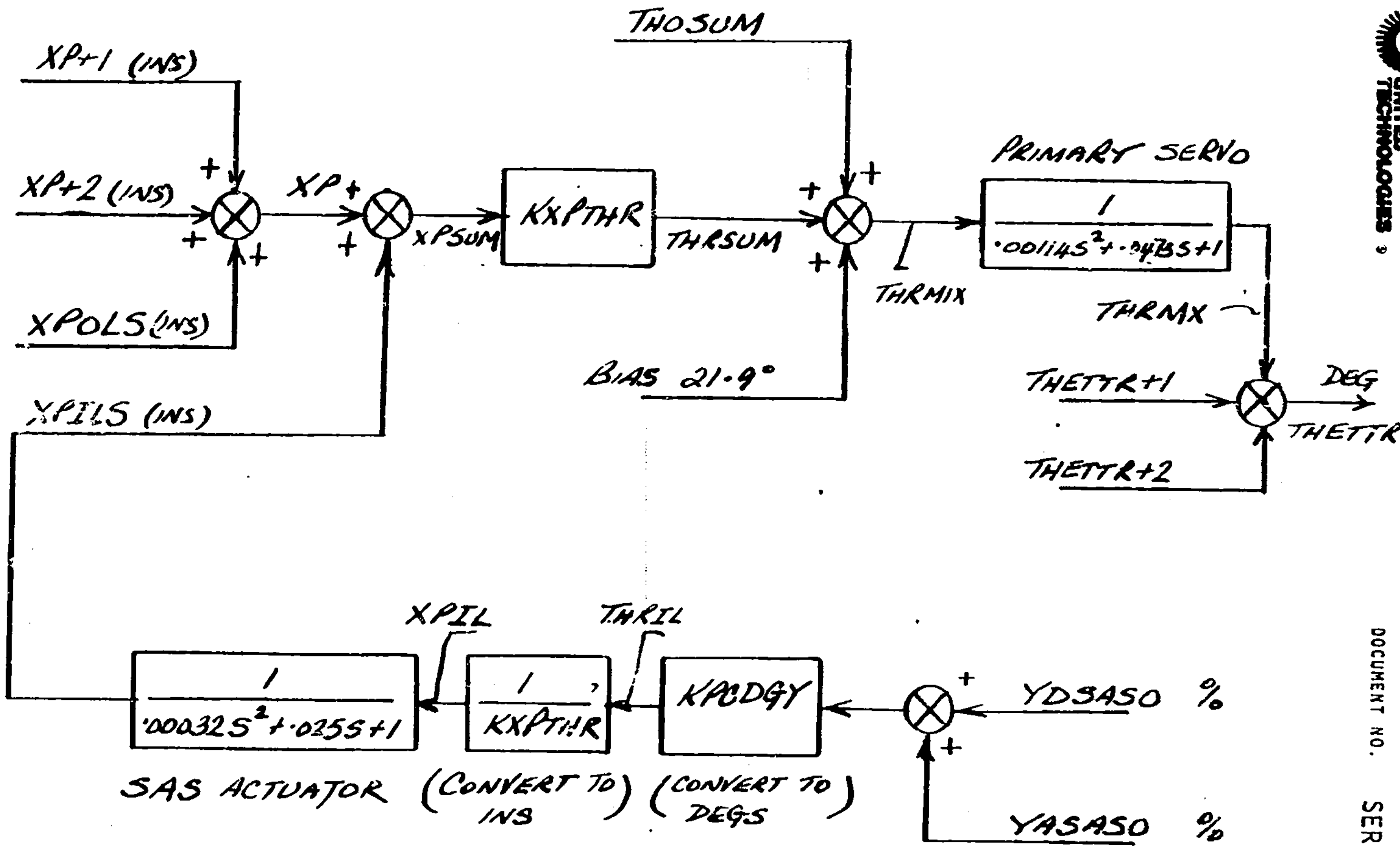

BLACK HAWK TAIL ROTOR COLLECTIVE CONTROL

DOCUMENT NO. SER 70452

SA 29 REV. 6

SA 29 REV. 6

BLACK HAWK STABILATOR CONTROL SYSTEM

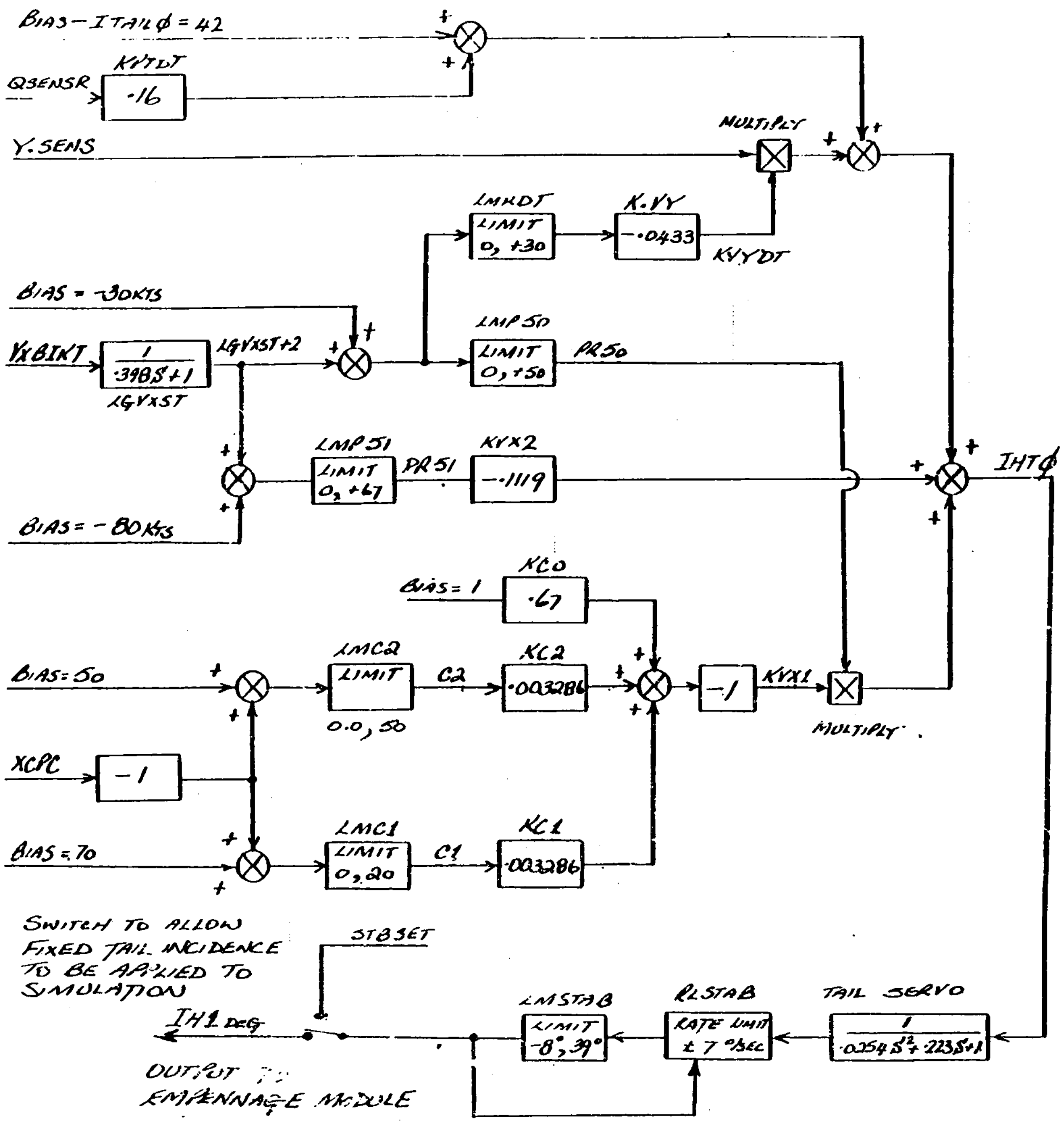

FIGURE 5.1.7

ORIGINAL PAGE IS OF POOR QUALITY

5.5.3 FLIGHT CONTROLS MODULE INPUT/OUTPUT DATA TRANSFER

INPUT TRANSFER	
PARAMETER	ORIGIN MODULE
QDEG	MOTION
PDEG	
RDEG	
THETAB	
PHIB	
PSIB	
VXBIKT	
AYPS1	
XA+1	TRIMMER
XB+1	
XC+1	
XP+1	
XA+2	COCKPIT
XB+2	
XC+2	
XP+2	

OUTPUT TRANSFER	
PARAMETER	DESTINATION MODULE
A1S	MAIN ROTOR
B1S	
THETAØ	
IHT	EMPENNAGE
IVT	
THETTR	TAIL ROTOR

3

SA 29 REV. 6

5.5.4 BLACK HAWK CONTROL SYSTEM GENERAL INPUT

KPCDGP	=	−.283	PITCH DEG/%
KPCDGR	=	.16	ROLL DEG/%
KPCDGY	=	−.298	YAW DEG/%
KPCDGC	=	.16	COLL DEG/%
KXBB1S	=	−2.83	LONG DEG/INCH
KXAA1S	=	1.60	LAT DEG/INCH
KXPTHR	=	−5.539	DIR DEG/INCH
KXCTHφ	=	1.60	COLL DEG/INCH

ROTOR HEAD BLADE PITCH TRAVEL LIMITS

FOR GENERAL ANALYTICAL INVESTIGATION HEAD TRAVEL LIMITS ARE INHIBITING. HOWEVER, FOR PILOTED SIMULATION EVALUATION, THE FOLLOWING LIMITS SHOULD BE INTRODUCED TO PROPERLY DEFINE THE RIGGING.

UPPER LIMIT, DEG	LOWER LIMIT, DEG
A1SUL = 8.0	A1SLL = −8.0
B1SUL = 16.3	B1SLL = −12.5
THφUL = 25.9	THφLL = 9.9
THRUL = 36.5	THRLL = 4.5

SEE VOLUME II FOR FURTHER DETAILS

5.6 ENGINE/FUEL CONTROL MODULE

CONTENTS

5.6 ENGINE/FUEL CONTROL MODULE

5.6.1 Module Description

This engine/fuel control model is basically a linearized representation with coefficients which vary as a function of engine operating condition. This model adequately provides for closing the rotor shaft speed loop throughout the normal operating envelope of the helicopter. However, maneuvers which result in significant rotor speed excursions may result in discrepancies in the simulation. All the usual restrictions and assumptions of linear simulation are applicable and should be observed. In an analysis mode deviations from trim are not large, but for pilot-in-the-loop operation some means of continuously synchronizing the steady state engine torque must be developed. This engine module should not be used for engine performance evaluation.

The elements of the model are shown on the simplified block diagram of Figure 6.1.1. They comprise the control interface with Gen. Hel., fuel control, gas turbine, power turbine, and rotor shaft speed degree-of-freedom interface with the Gen. Hel. rotor. This model which derives total S.H.P. at the rotor shaft by appropriately factoring the output from one engine is applicable for evaluations in the governed range. A transmission clutch is represented allowing disconnect of the rotor drive at zero torque required by the rotor. This allows autorotations and recoveries to be executed.

Initialization of the engine/fuel control module is accomplished by using the steady state engine performance required to trim the helicopter simulation in free flight.

A basic background to the complete T.700 engine/fuel control system is given in references 6.6.1 and 6.6.2. A detailed block diagram of the simulation is given in Figure 6.1.2.

The basic engine control system operation is through the interaction of the Electrical (ECU, Figure 6.1.3), and Hydromechanical (HMU) control units. In general, the HMU provides for gas generator speed control and rapid response to power demand. The ECU trims the HMU to satisfy the requirements of the load so as to maintain rotor speed. The Load Demand Spindle (LDS) is a function of collective pitch setting and provides compensation to reduce rotor transient droop. Any steady state errors resulting from inconsistent collective positioning are trimmed by the ECU. In the simulation, this is trimmed by the difference between actual gas generator speed (from steady performance data and that resulting from the collective setting). These characteristics are implemented in the simulation.

In general, isochronous governing of the rotor speed is maintained by developing an error relative to the reference speed and commanding more or less power to stabilize at the required speed. Basically, this process involves the speed error demanding a change in gas generator speed (N_{GG}) via the shaping of the ECU electrical network, Figure 6.1.3. This signal is summed with the LDS input in the HMU, and compared with the actual gas generator speed. The subsequent error, commands changes in fuel flow leading to a higher or lower gas turbine speed and changes in the gas flow. This in turn provides increased or decreased power at the driveshaft from the power turbine. In the simulation, torque output from one engine (Qpt) is derived from three sources. From direct changes in fuel flow, from changes in gas generator speed and as a result of changes in power turbine speed. These increments are summed to obtain a total change in engine torque from trim and subsequently factored by the number of operating engines and engine/rotor gearing ratio, to obtain engine torque output to the rotor shaft.

The interface with the main program is presented on Figures 6.1.1 and 6.1.2. The rotor can be visualized in simple terms as a damper responding to changes in rotor speed. However, the significant effect of the rotor relates to the changes in torque loading as a result of control inputs and changing states. Rotor shaft accelerations result from torque differences in output from the power turbine and torque required by the rotor. The simulation is initialized at trim such that the rotor is at the input speed and $\Delta Q=0$. A clutch is modelled, Figure 6.1.4, which will disengage the rotor from the engine at a zero rotor torque level. When Gen Hel is being executed in combination with the engine, total engine torque must replace rotor torque as a reaction in the airframe equations.

ENGINE/FUEL CONTROL/DRIVE REPRESENTATION

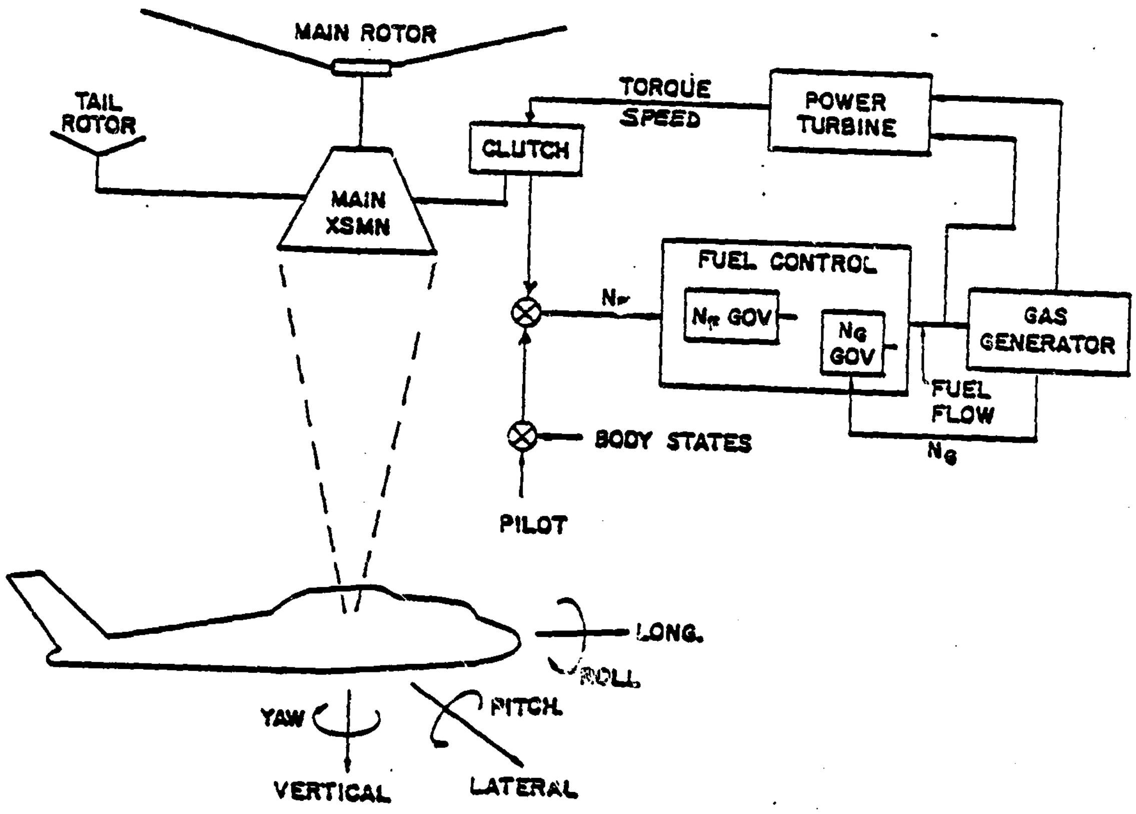

FIGURE 6.1.1

ENGINE/FUEL CONTROL MODULE

SIKORSKY AIRCRAFT UNITED TECHNOLOGIES

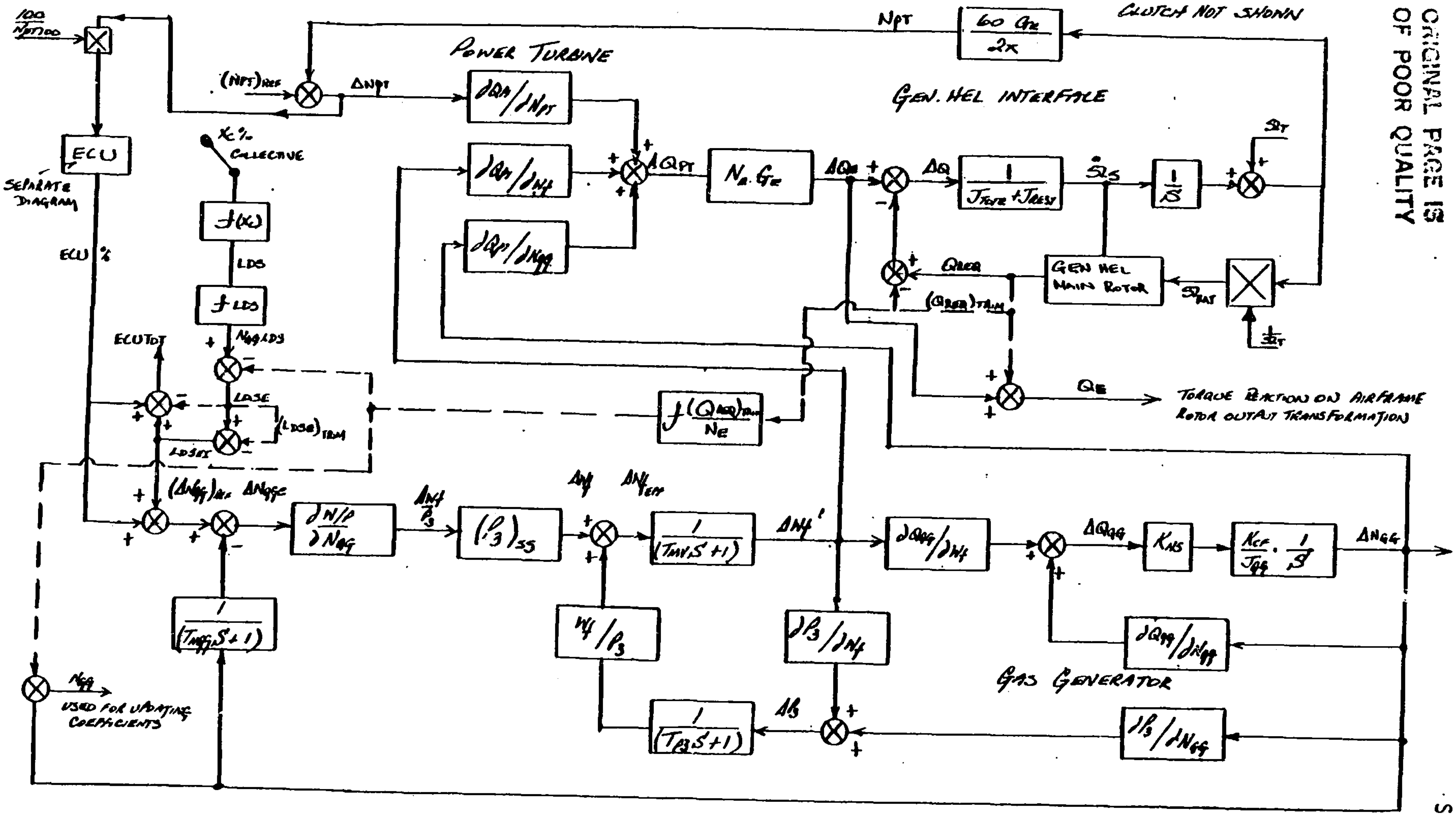

FIGURE 6.1.2

5.5.5

ORIGINAL PAGE IS OF POOR QUALITY

SER 70452

FUEL CONTROL
ELECTRIC CONTROL UNIT

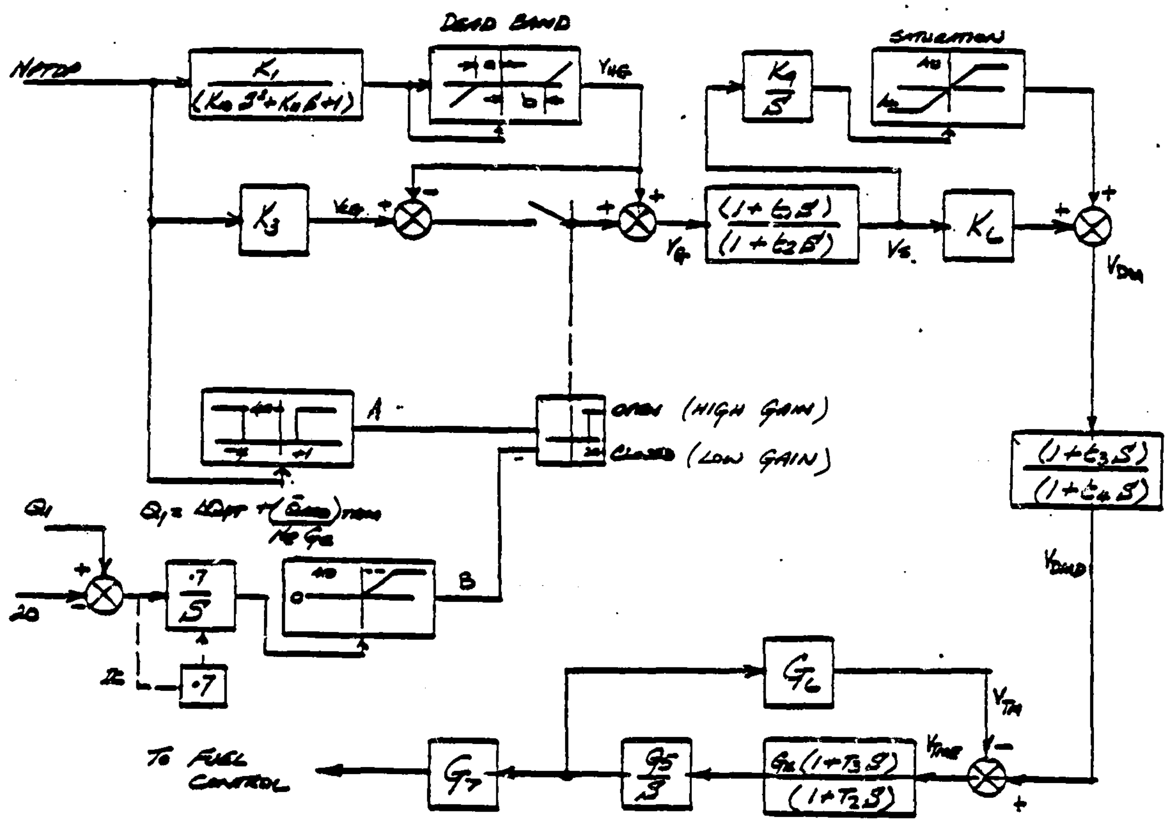

FIGURE 6.1.3

ROTOR DEGREE OF FREEDOM

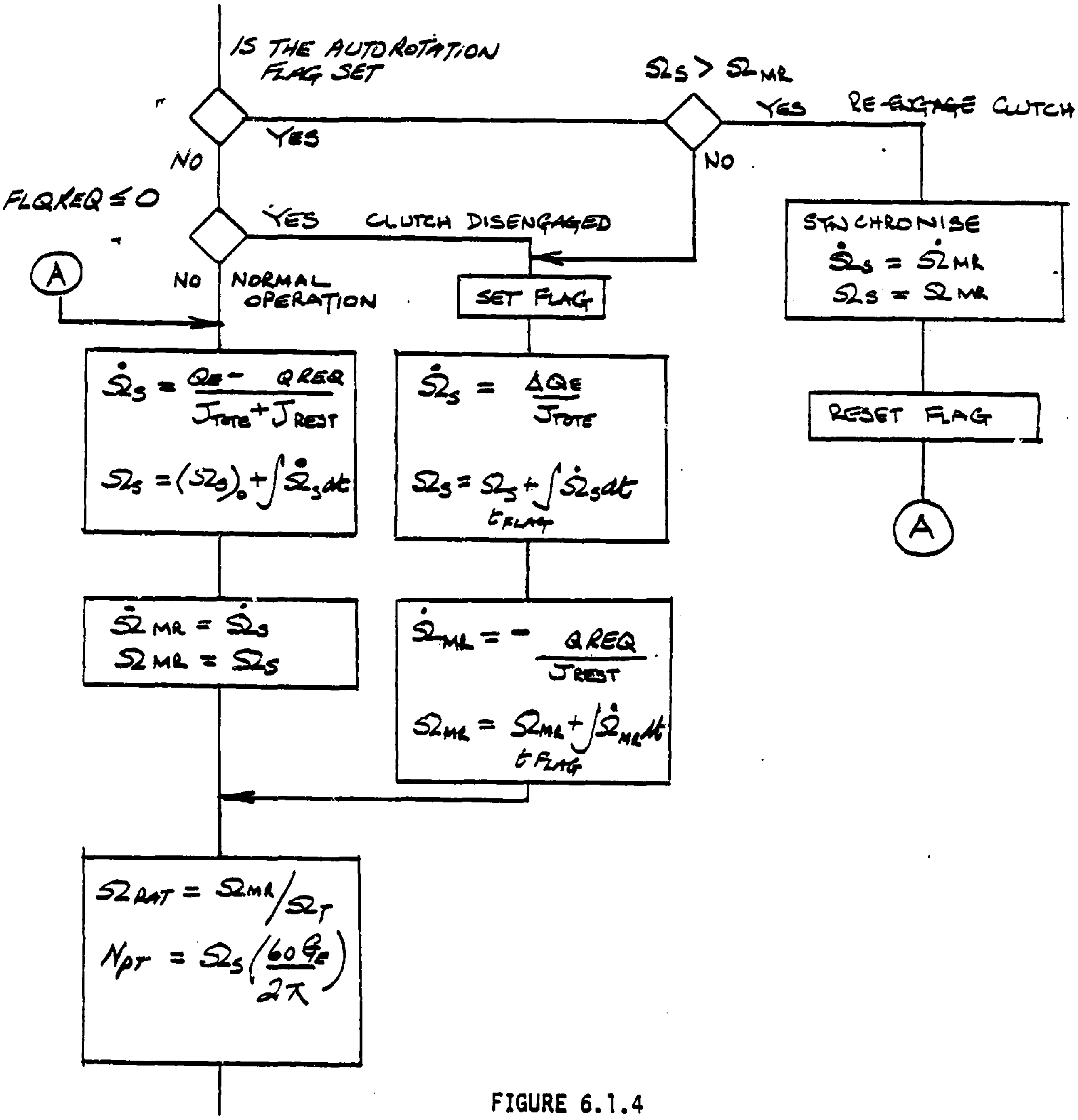

FIGURE 6.1.4

5.6.2 ENGINE/FUEL CONTROL MODULE EQUATIONS

ENGINE/FUEL CONTROL SELECTION LOGIC

A SOFTWARE SWITCH SHOULD BE PROVIDED TO SELECT THE ENGINE/FUEL CONTROL MODULE

IF THE ENGINE FUEL CONTROL SWITCH IS NOT SET DO NOT EXECUTE THIS MODULE, RETURN TO MAIN PROGRAM

SET $\Omega_{MR} = \Omega_T$

$Q_E = Q_{MR}$

IF THE ENGINE/FUEL CONTROL SWITCH IS SET EXECUTE THE FOLLOWING EQUATIONS.

THE FOLLOWING EQUATIONS ARE EXECUTED IN THE TRIMMING MODE

TOTAL TORQUE REQUIRED TO TRIM

$$(\bar{Q}_{REQ})_{TRIM} = Q_{TRIM}\,(1+K_Q) \qquad , \text{QRQTRM}$$

WHERE

$$Q_{TRIM} = \left(\frac{K_{FRQ}-1}{K_{FRQ}}\right) Q_{TRIM_{(t-1)}} + \frac{1}{K_{FRQ}} \cdot Q_{HMR_t}$$

GAS GENERATOR SPEED FOR TRIM

$$(N_{GG})_{TRIM} = f\left(\frac{Q_{REQ}}{N_E}\right)_{TRIM} \qquad , \text{GGSS}$$

FROM TABLE 6.5.1, FIGURE 6.5.1

LOAD DEMAND SPINDLE (LDS) OUTPUT

$$NGGLDS = f(LDSCAM, X_C) \qquad , \text{NGGLDS}$$

FROM FIGURES 6.5.2, 6.5.3 TABLES 6.5.2, 6.5.3

WHERE $X_C = (X_{C+1}) + (X_{C+2})$

ELECTRONIC CONTROL UNIT (ECU) BIAS AT TRIM

$$(LDSE)_{TRIM} = (NGGLDS)_{TRIM} - (N_{GG})_{TRIM} \qquad , \text{LDSTRM}$$

SA 29 REV. 6

FUEL FLOW AT TRIM

$$(TOTFUL)_{TRIM} = f\,(N_{GG})_{TRIM}$$ per engine , SUM 2

FROM TABLE 6.5.4, FIGURE 6.5.4

REFERENCE POWER TURBINE SPEED

$$(N_{PT})_{REF} = \Omega_{S_0} * \left(\frac{60\, G_E}{2\pi}\right) \text{ RPM}$$, NPTREF

WHERE $\Omega_{SO} = \Omega_T$ UNLESS HELICOPTER IS TRIMMED IN AUTOROTATION WITH SPLIT NEEDLES

$$(N_{PTP})_{REF} = (N_{PT})_{REF} \left(\frac{100}{N_{PT100}}\right) \%$$, NPTRFP

SA 29 REV. 6

THE FOLLOWING EQUATIONS ARE EXECUTED IN THE COMPUTE MODE - INITIALISE / UPDATE ALL TIME VARYING COEFFICIENTS

$$FLQREQ = \frac{Q_{HMR}(1+K_Q)}{(.3S+1)}$$

$$QREQ = Q_{HMR}(1+K_Q)$$

<u>LOAD DEMAND SPINDLE OUTPUT (LDS)</u>

$$N_{GGLDS} = f(LDSCAM, X_C) \quad , LDS$$

FROM TABLES 6.5.2, 3 FIGURES 6.5.2, 3

LDS INCREMENTAL INPUT FROM TRIM.

$$LDSEI = N_{GGLDS} - (N_{GG})_{TRIM} - (L_{DSE})_{TRIM}$$

<u>ELECTRICAL CONTROL UNIT</u>

POWER TURBINE SPEED ERROR

$$N_{PTDP} = (N_{PTDP})_{REF} - N_{PT(G-1)} \cdot \frac{100}{(N_{PT100})}$$

SPEED ERROR SHAPING

$$I_{DB1}(S) = N_{PTDP} \frac{K_1}{(K_{10}S^2 + K_{11}S + 1)} \quad , IDB1$$

$$\begin{array}{llll} IF & I_{DB1} \le -a & V_{HG} = I_{DB1} + a & , V_{HG} \\ & I_{DB1} \ge b & V_{HG} = I_{DB1} - b & \\ & -a < I_{DB1} < b & V_{HG} = 0 & \end{array}$$

IE DEAD BAND

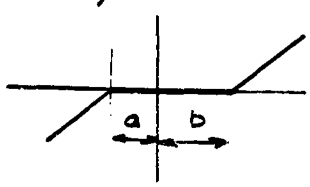

$$V_{LG} = N_{PTDP} \cdot K_3 \qquad , VLG$$

ERROR SIGNAL TRANSFER LOGIC

IF $A \geq 20$ OR $B \geq 20$ (SWITCH OPEN)

$$V_G = V_{HG} \qquad , VGVG$$

OTHERWISE (SWITCH CLOSED)

$$V_G = V_{LG} + V_Q$$

WHERE

IF $-4 \leq N_{PTDP} \leq 1$, $A = 0$

IF $N_{PTD} < -4$ OR $N_{PTDP} > 1$, $A = 40$

$$Q_{INT} = \frac{\cdot 7}{S} \left\{ \Delta Q_{PT_{(t-1)}} + \frac{(\bar{Q}_{REQ})_{TRIM}}{N_E \cdot G_E} - 20 \right\} \qquad , QINT$$

IF $0 \leq Q_{INT} \leq 40$, $B = Q_{INT}$, BBBBB
IF $Q_{INT} < 0$, $B = 0$
IF $Q_{INT} > 40$, $B = 40$

<u>NOTE</u> THAT QINT MUST BE INITIALISED AT TRIM VALUE OF QINT ie. $\Delta Q_{PT_{(t-1)}} = 0$

$$V_S(S) = \left(\frac{1 + t_1 S}{1 + t_2 S}\right) V_G \qquad , \; VSVS$$

$$V_{SS}(S) = \frac{K_4}{S} \cdot V_S \qquad , \; VSS$$

IF $V_{SS} > A_U$ SET $V_{SS} = A_U$

IF $V_{SS} < A_L$ SET $V_{SS} = A_L$

$$V_{DM} = V_{SS} + K_6 V_S \qquad , \; VDM$$

$$V_{DMD}(S) = \frac{(1 + t_3 S)}{(1 + t_4 S)} \cdot V_{DM} \qquad , \; VDMD$$

$$M(S) = (V_{DMD} - V_{TM})\, G_4 \frac{(1 + T_3 S)}{(1 + T_2 S)} \qquad , \; MAMA$$

WHERE $V_{TM} = G_6 \, INS_{(t-1)}$

$$INS(S) = M \frac{G_5}{S} \qquad , \; INS$$

$$ECU(S) = G_7 \; INS \qquad , \; ECU$$

TOTAL ECU OUTPUT

$$ECU_{TOT} = ECU(S) + LDSEI - (LDSE)_{TRIM} \quad , \text{ ECUOUT}$$

GAS GENERATOR REFERENCE SPEED CHANGE REQUIRED.

$$\Delta N_{gg\,Ref} = ECU(S) + LDSEI \quad , \text{ GGRPMR}$$

GAS GENERATOR SPEED ERROR

$$\Delta N_{ggE} = (\Delta N_{gg})_{REF} - \frac{\Delta N_{gg(t-1)}}{(T_{NGG}\,S + 1)} \quad , \text{ GGRPME}$$

INCREMENTAL FUEL FLOW DEMANDED

$$\Delta W_f = \left[P_3\right]_{SS} \cdot \left(\frac{\partial W_f/P_3}{\partial N_{gg}}\right) \Delta N_{ggE} \quad , \text{ FUEL}$$

$(P_3)_{SS}$ FROM TABLE 6.55, FIGURE 6.5.5

SA 29 REV. 6

GAS GENERATOR SECTION

CHANGE IN COMPRESSOR DISCHARGE PRESSURE

$$\Delta P_3 = \left[\frac{\partial P_3}{\partial W_f}\right] \cdot \Delta W'_{f(t-1)} + \left[\frac{\partial P_3}{\partial N_{GG}}\right] \cdot \Delta N_{GG(t-1)}$$

$\frac{\partial P_3}{\partial W_f}, \frac{\partial P_3}{\partial N_{GG}}$ FROM TABLE 6.5.6, FIGURES 6.5.6 6.5.7

EFFECTIVE INCREMENTAL FUEL FLOW DEMANDED

$$\Delta W_{f_{EFF}}(S) = \Delta W_f + \left\{\left[\frac{\Delta W_f}{\Delta P_3}\right] \Delta P_3\right\} \frac{1}{(T_{P3} S + 1)} \qquad \text{, INCWF}$$

$\frac{\Delta W_f}{\Delta P_3}$ FROM TABLE 6.5.6, FIGURE 6.5.8

ACTUAL METERED FUEL FLOW

$$\Delta W'_f(S) = \frac{\Delta W_{f_{EFF}}}{(T_{MV} S + 1)} \qquad \text{, ACTWF}$$

TOTAL FUEL FLOW (OUTPUT ONLY)

$$TOT_{FUL} = (TOTFUL)_{TRIM} + \Delta W'_f \qquad \text{, TOTFUL}$$

GAS GENERATOR ACCELERATING TORQUE

$$\Delta Q_{GG} = \left[\frac{\partial Q_{GG}}{\partial W_f}\right] \cdot \Delta W'_f + \left[\frac{\partial Q_{GG}}{\partial N_{GG}}\right] \cdot \Delta N_{GG(t-1)} \qquad \text{, GGQD}$$

$\frac{\partial Q_{GG}}{\partial W_f}, \frac{\partial Q_{GG}}{\partial N_{GG}}$ FROM TABLE 6.5.6, FIGURES 6.5.9, 6.5.10

INCREMENTAL CHANGE IN GAS GENERATOR SPEED FROM TRIM

$$\Delta N_{GG} = K_{HS} \cdot \left(\frac{K_{CF}}{J_{GG}}\right) \int \Delta Q_{GG}\, dt \qquad , \text{GGRPMD}$$

ACTUAL GAS GENERATOR SPEED (FOR UPDATING TIME VARYING COEFFICIENTS)

$$N_{GG} = (N_{GG})_{TRIM} + \Delta N_{GG} \qquad , \text{GGRPM}$$

POWER TURBINE SECTION

$$\Delta N_{PT} = N_{PTDP} * \left(\frac{N_{PT100}}{100}\right)$$

POWER TURBINE TORQUE PER ENGINE FROM TRIM

$$\Delta Q_{PT} = \left[\frac{\partial Q_{PT}}{\partial W_f}\right] \cdot \Delta W_f' + \left[\frac{\partial Q_{PT}}{\partial N_{PT}}\right] \cdot \Delta N_{PT} + \left[\frac{\partial Q_{PT}}{\partial N_{GG}}\right] \cdot \Delta N_{GG} \qquad , \text{PTQ}$$

$\frac{\partial Q_{PT}}{\partial W_f}$, $\frac{\partial Q_{PT}}{\partial N_{PT}}$, $\frac{\partial Q_{PT}}{\partial N_{GG}}$ FROM TABLE 6.5.6, FIGURES 6.5.11
6.5.12
6.5.13

TOTAL INCREMENTAL TORQUE OUTPUT

(AT ROTOR SPEED)

$$\Delta Q_E = N_E \cdot G_E \cdot \Delta Q_{PT} \qquad , \text{QE}$$

TOTAL TORQUE OUTPUT

$$Q_E = \Delta Q_E + (\bar{Q}_{REQ})_{TRIM} \qquad , \text{QHEG}$$

THIS IS THE TORQUE REACTION ON THE AIRFRAME

ROTOR SPEED DEGREE OF FREEDOM

NORMAL OPERATION

$$\dot{\Omega}_S = \frac{Q_E - QREQ}{(J_{TOTE} + J_{REST})}$$

$$\Omega_S = \Omega_{S_0} + \int \dot{\Omega}_S \, dt$$

WHERE $\Omega_{S_0} = \Omega_T$

THEN

$$\dot{\Omega}_{MR} = \dot{\Omega}_S$$

$$\Omega_{MR} = \Omega_S$$

$$\Omega_{RAT} = \Omega_{MR} / \Omega_T$$

$$N_{PT} = \Omega_S \cdot \left(\frac{60 \, G_E}{2\pi} \right)$$

$$N_{PTP} = N_{PT} \left(\frac{100}{N_{PT100}} \right)$$

CLUTCH DISENGAGEMENT

IF ROTOR CLUTCH WAS ENGAGED ON THE PREVIOUS PROGRAM PASS, AND

IF $FLQREQ \leq 0$

DISENGAGE THE CLUTCH AND SET FLAG

THEN.

$$\dot{\Omega}_S = \frac{\Delta Q_E}{J_{TOTE}}$$

$$\Omega_S = \Omega_{S_{t\,FLAG}} + \int \dot{\Omega}_S \, dt.$$

$$\dot{\Omega}_{MR} = - \frac{QREQ}{J_{REST}}$$

$$\Omega_{MR} = \Omega_{MR_{t\,FLAG}} + \int \dot{\Omega}_{MR} \, dt$$

$\Omega_{S_{t\,FLAG}}$, $\Omega_{MR_{t\,FLAG}}$ ARE THE VALUES OF Ω_S AND Ω_{MR} WHEN THE DISENGAGE FLAG IS SET.

CLUTCH ENGAGEMENT

IF THE ROTOR CLUTCH WAS DISENGAGED ON THE PREVIOUS PROGRAM PASS, AND

IF $\Omega_S \geqslant \Omega_{MR}$, RE-ENGAGED THE CLUTCH
RESET FLAG

SYNCHRONISE $\dot{\Omega}_{S_t} = \dot{\Omega}_{MR_t}$

$$\Omega_{S_t} = \Omega_{MR_t}$$

CONTINUE AS FOR NORMAL OPERATION

5.6.3 ENGINE MODULE INPUT/OUTPUT DATA TRANSFER

INPUT TRANSFER	
PARAMETER	ORIGIN MODULE
QHMR	MAIN ROTOR
XC+1	TRIMMER
XC+2	COCKPIT

OUTPUT TRANSFER	
PARAMETER	DESTINATION MODULE
OMR.MR OMR MR QHBEG	MAIN ROTOR

5.6.4 NOTATION FOR THE ENGINE/FUEL CONTROL MODULE

SYMBOL USED IN EQUATIONS	PROGRAM MNEMONIC	UNITS	DESCRIPTION
$(\bar{Q}_{REQ})_{TRIM}$	QRQTRM	lb FT	Total torque required at trim.
Q_{TRIM}	QTRIM	lb FT	Filtered torque required by the main rotor.
K_Q	KTRQ	-	Factor to account for tail rotor torque plus losses
Q_{MR}	QHMR	lb FT	Actual rotor torque required.
N_{GG}	GGRPM	% RPM	Gas generator speed
$(N_{GG})_{TRIM}$	GGSS	% RPM	Gas generator speed at trim.
N_E	NETOT	-	Number of engines.
N_{GGLDS}	NGGLDS	% RPM	Load demand spindle output.
L_{DSCAM}	LDS	DEG	Load demand spindle rotation.
X_C	XCPC	% COLL	Collective stick position.
$(L_{DSE})_{TRIM}$	LDSTRM	% RPM	Synchronized LDS output at trim.
$(TOTFUL)_{TRIM}$	SUM2	LB/HR	Total fuel flow.
$(N_{PT})_{REF}$	NPTREF	RPM	Power turbine reference speed, RPM. (Set by sync with rotor speed at trim).
N_{PT100}	NPT100	RPM	100% power turbine speed
L_{DSEI}			LDS incremental input from trim.
N_{PTD}	NPTDP	% RPM	Power turbine speed error.
N_{PT}	NPT	% RPM	Actual power turbine speed.
Q_{TRIM}	QTRIM	lb FT	Filtered Rotor Torque
FLQREQ	FLQREQ	lb FT	Filtered Rotor Torque used in the clutch model.

NOTATION FOR THE ENGINE/FUEL CONTROL MODULE

SYMBOL USED IN EQUATIONS	PROGRAM MNEMONIC	UNITS	DESCRIPTION
I_{DB1}	IDB1		Electronic Control Unit Shaping Network Variables
V_{HG}	VHG		
V_{LG}	VLG		
V_G	VGVG		
Q_{INT}	QINT		
B	BBBBB		
V_S	VSVS		
V_{SS}	VSS		
V_{DM}	VDM		
V_{DMD}	VDMD		
M	MAMA		
V_{TM}	VTM		
I_{NS}	INS		
E_{CU}	ECU	% RPM	Incremental ECU output
G_E	GER	-	Power turbine to rotor gearing.
ECU_{TOT}	ECUTOT	% RPM	Total ECU output
$K_{1----11}$	$K_{1----11}$	-	ECU gain constants
t_{1----4}		SECS	ECU time constants
T_2, T_3		SECS	ECU time constants
a, b,		-	ECU dead band definition
A, B		-	ECU logic variables
G_{4---7}		-	ECU gain constants
$\Delta N_{GG\ REF}$	GGRPMR	% RPM	Demanded change in G.G. reference speed.

5.6.4 (Cont'd.)

NOTATION FOR THE ENGINE/FUEL CONTROL MODULE

SYMBOL USED IN EQUATIONS	PROGRAM MNEMONIC	UNITS	DESCRIPTION
L_{DSEI}		% RPM	Increment in LDS output from trim.
ΔN_{GGE}	GGRPME	% RPM	G.G. speed error.
T_{NGG}	TNGG	SEC.	SPD servo time constant
ΔW_f	FUEL	LB/HR	Incremental fuel flow demanded
$\Delta W_f'$	ACT WF	LB/HR	Actual metered increment in fuel flow.
ΔP_3	P3D		Change in compressor discharge pressure.
T_{P3}	TP3	SEC.	Lag in fuel feedback loop.
ΔW_{Eff}	INCWf	LB/HR	Compensated demand in fuel flow
T_{MV}	TMV	SEC.	Fuel metering valve time constant
ΔQ_{GG}	GGQD	LB/FT	Gas generator accelerating torque
ΔN_{GG}	GGRPMD	% RPM	Incremental change in gas generator speed.
K_{CF}		-	Conversion factor.
J_{GG}		SLUGS FT^2	Inertia of G.G. rotor.
ΔQ_{PT}	PTQ	LB FT	P.T. incremental torque output per engine.
ΔQ_E	PTE	LB FT	P.T. incremental torque output (at rotor speed)
Q_E	QHEG	LB FT	P.T. total torque output
$\dot{\Omega}_S$	OSHAF.	$RADS/SEC^2$	Rotor shaft acceleration
Ω_S	OSHAFT	RADS/SEC	Actual shaft speed.
Ω_{SO}	OMSFO	RADS/SEC	Initial shaft speed.
Δ NPT	NPTD		Incremental P.T. Speed From Ref.

SA 29 REV. G

NOTATION FOR THE ENGINE/FUEL CONTROL MODULE

SYMBOL USED IN EQUATIONS	PROGRAM MNEMONIC	UNITS	DESCRIPTION
Ω_o	OMMRO	RADS/SEC	Trim rotor speed.
$\dot{\Omega}_{MR}$	OMRAT.	RADS/SEC^2	Rotor hub acceleration
Ω_{MR}	OMGRR.	RADS/SEC	Rotor hub speed.
Ω_{RAT}		-	Rotor speed relative to trim.
J_{TOTE}	JTOTE	SLUGS FT^2	Inertia upstream of clutch
J_{REST}	JREST	SLUGS FT^2	Inerta downstream of clutch less blades
K_{HS}	KHS		Gas generator heat sink factor

5.6.5 BLACKHAWK / T700 ENGINE MODULE INPUT DATA

INPUT CONSTANTS

$K_Q = .1$

$K_{FRQ} = 15$

$N_E = 2$

$G_E = 76.0216$

Ω_T FROM ROTOR MODULE

$N_{PT100} = 20{,}000$ RPM

$K_1 = 3.0$ V/%

$K_3 = .6$ V/%

$K_4 = .059$ V/FT lb

$K_6 = .2$ V/V

$K_9 = .08$ V/V-SEC.

$K_{10} = .020408$

$K_{11} = .1$

$a = 0.4$ V

$b = 0.8$ V

$t_1 = .55$ SEC

$t_2 = .107$ SEC

$t_3 = .08$ SEC

$t_4 = 1.58$ SEC

$A_U = 0$

$A_L = -3.5$

$G_4 = 564$ ma/V

$G_5 = .0159$ ins/ma

$G_6 = 56$ V/ins

$G_7 = 336$ %/in

$T_2 = .2$ SEC

$T_3 = .04$ SEC

$T_{NGG} = .02$ SEC

$\dfrac{\partial W_f/P_3}{\partial N_{GG}} = .25$

$T_{P3} = .01$

$\dfrac{K_{GF}}{J_{GG}} = .479$ % RPM / FT lb

$K_{HS} = .65$

$J_{TOTE} = 690.6$ SLUGS FT^2

$J_{REST} = 943.9$ SLUGS FT^2

$N_{GG100} = 44700$ RPM

$T_{MV} = .004$ SEC.

INPUT FUNCTIONS

TABLE 6.5.1 STEADY STATE ENGINE PERFORMANCE

$(\bar{Q}_{REQ})_{TRIM}/N_E$ lb FT	$(N_{gg})_{TRIM}$ % RPM
0	70
6000	84.6
12000	89.9
18000	94.0
24 000	97.2
30 000	100.1
36 000	102.6

TABLE 6.5.2 COLLECTIVE/STATIC DROOP COMPENSATION RIGGING

X_C %	∠DS DEGS
0	0
10	8.5
20	17.0
30	25.5
40	34.0
50	42.6
60	51.0
70	59.5
80	68.0
90	76.5
100	85.0

TABLE 6.5.3 LOAD DEMAND SPINDLE CAM OUTPUT

LDS DEGS	NGGLDS %
0	78.6
20	85.0
40	91.3
60	97.8
80	100.0
100	100.0

NGG = 100% @ LDS = 67°

TABLE 6.5.4 STEADY FUEL FLOW REQUIRED

$(NGG)_{SS}$ %	$(TOTFUL)_{SS}$ lb/hr
65	120
70	140
75	166
80	210
85	280
90	390
95	575
100	790

TABLE 6.5.5 DISCHARGE PRESSURE FOR STEADY CONDITIONS

N_{gg} %	$(P_3)_{ss}$ lb/ins^2
70	69
75	78
80	94
85	118
90	149
95	184
100	226

TABLE 6.5.6 TIME VARYING COEFFICIENTS

N_{gg} %	$\frac{\partial P_3}{\partial W_f}$	$\frac{\partial P_3}{\partial N_{gg}}$	$\frac{\Delta W_f}{\Delta P_3}$	$\frac{\partial Q_{gg}}{\partial W_f}$	$\frac{\partial Q_{gg}}{\partial N_{gg}}$
UNITS	$\frac{lb/in^2}{lb/hr}$	$\frac{lb/in^2}{\% RPM}$	$\frac{lb/hr}{lb/in^2}$	$\frac{Ft\ lb}{lb/hr}$	$\frac{Ft\ lb}{\%}$
70	·051	5·10	2.60	·29	-1.10
75	·071	4·30	2.50	·285	-2.1
80	·078	3·97	2.40	·283	-3.1
85	·072	4·20	2.32	·273	-4.3
90	·089	4.73	2.49	·261	-5.65
95	·080	4·97	2.75	·200	-7.20
100	·075	1·71	3.20	·173	-4.62

TABLE 6.5.6 (CONTINUED)

N_{gg} %	$\frac{\partial Q_{PT}}{\partial W_f}$	$\frac{\partial Q_A}{\partial N_{PT}}$	$\frac{\partial Q_{PT}}{\partial N_{gg}}$
UNITS	$\frac{\text{Ft lb}}{\text{lb/hr}}$	$\frac{\text{Ft lb}}{\text{RPM}}$	$\frac{\text{Ft lb}}{\text{\% RPM}}$
70	.24	.0045	0
75	.325	.0065	4.8
80	.358	.0086	7.0
85	.363	.0094	8.3
90	.387	.0107	9.9
95	.380	.0132	11.8
100	.331	.0151	5.5

BLACK HAWK STEADY STATE ENGINE PERFORMANCE

MAP NAME: MAPA1
MAP TYPE: UVA
INPUT VARIABLE(S): QRQTRM/ENGINE
OUTPUT VARIABLE: GGSS

PRIMARY MAP:
0.00 (LOWER LIMIT)
36000.00 (UPPER LIMIT)
5000.00 (DELTA)

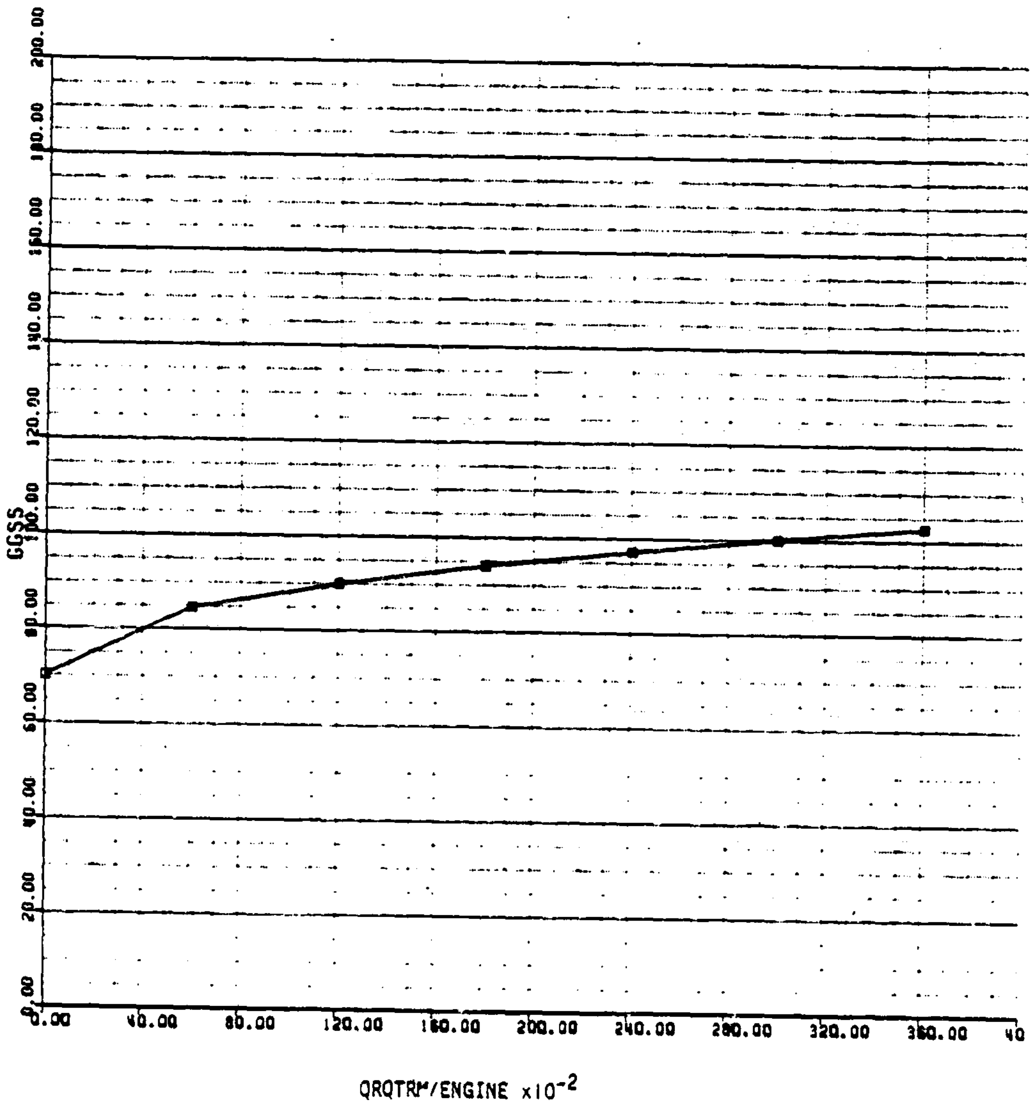

FIGURE 6.5.1

BLACK HAWK COLLECTIVE STATIC DROOP
COMPENSATOR RIGGING

MAP NAME: MAPC1
MAP TYPE: UVA
INPUT VARIABLE(S): AO
OUTPUT VARIABLE: LOS

PRIMARY MAP:
0.00 LOWER LIMIT
100.00 UPPER LIMIT
10.00 DELTA

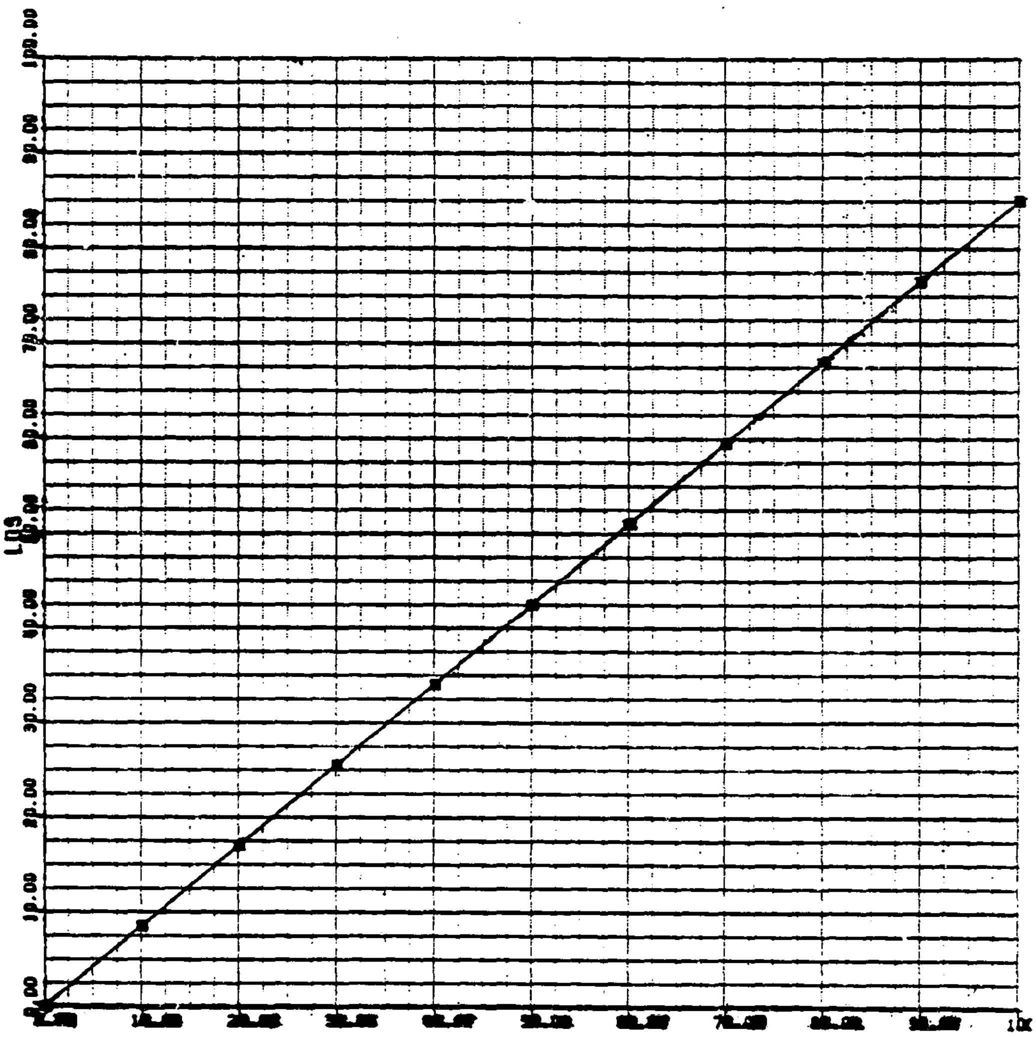

X_c, %

FIGURE 6.5.2

BLACK HAWK - LOAD DEMAND SPINDLE CAM OUTPUT

MAP NAME:		MAPC2
MAP TYPE:		UVA
INPUT VARIABLE(S):	LDS	
OUTPUT VARIABLE:		NGGLDS
PRIMARY MAP:		
	0.00	(LOWER LIMIT)
	100.00	(UPPER LIMIT)
	20.00	(DELTA)

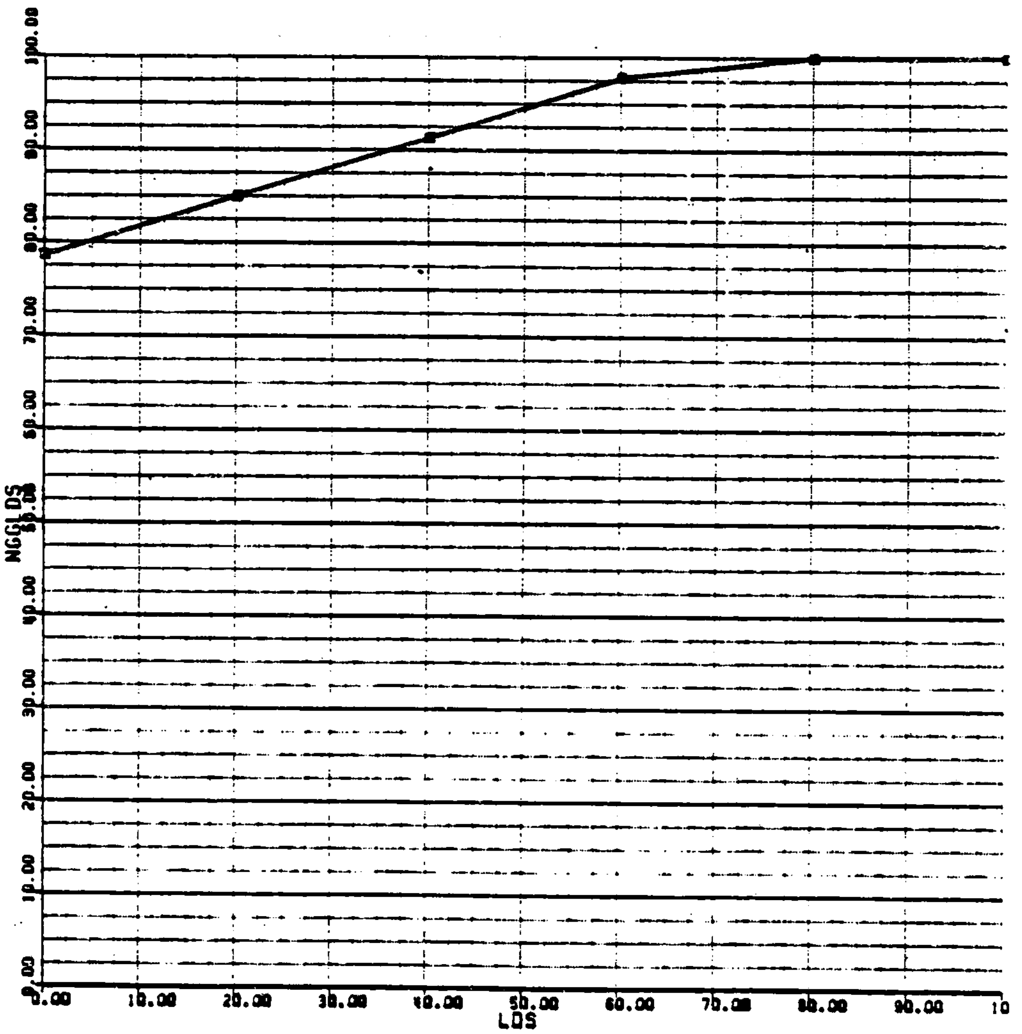

FIGURE 6.5.3

BLACK HAWK-ENGINE STEADY STATE FUEL FLOW REQUIRED

MAP NAME: MAP92
MAP TYPE: UVA
INPUT VARIABLE(S): GGSS
OUTPUT VARIABLE: SUM2

PRIMARY MAP:

70.00	(LOWER LIMIT)
100.00	(UPPER LIMIT)
5.00	(DELTA)

$(TOTFUL)_{SS} \sim (NGG)_{SS\%}$

$(TOTFUL)_{SS}$

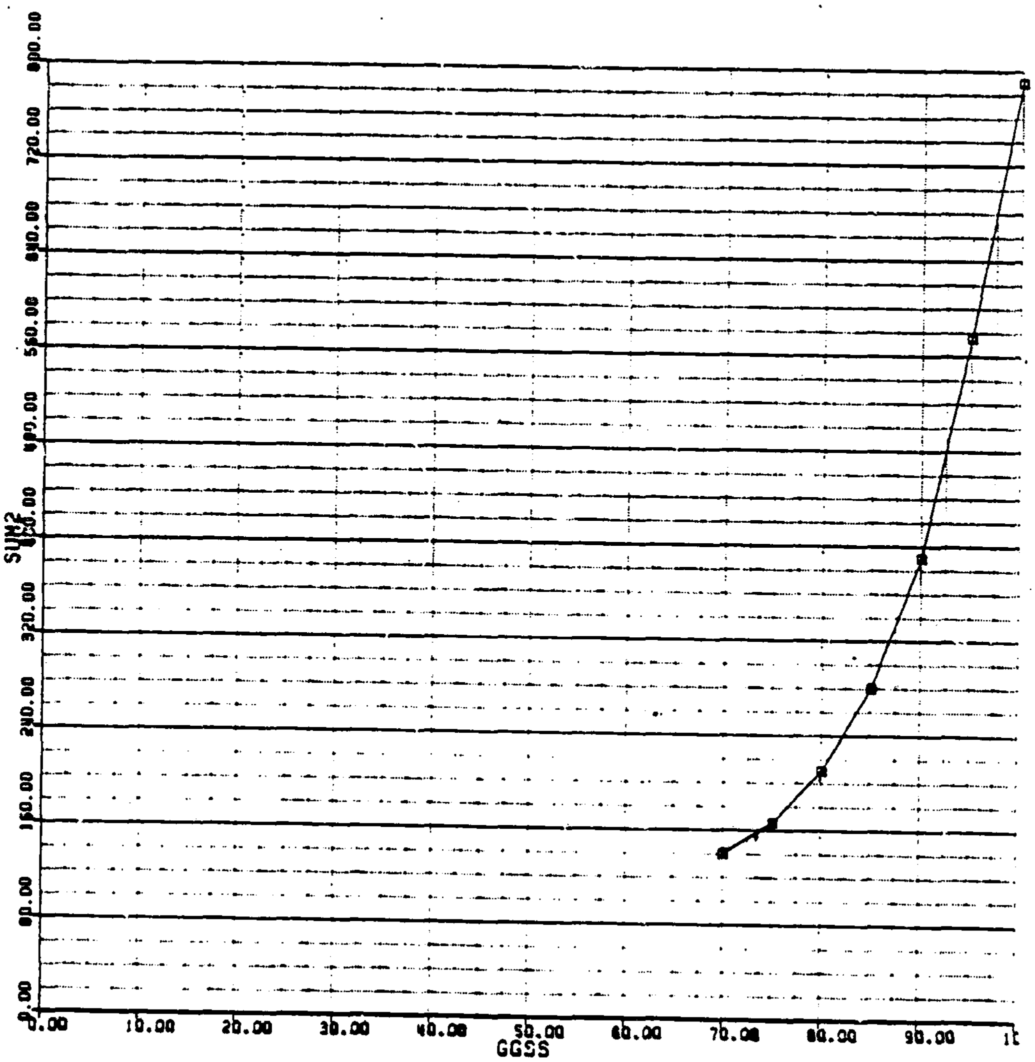

FIGURE 6.5.4

ORIGINAL PAGE IS
OF POOR QUALITY

BLACK HAWK - ENGINE DISCHARGE PRESSURE FOR STEADY CONDITIONS

MAP NAME:		MAP82
MAP TYPE:		UVR
INPUT VARIABLE(S):	GGRPM	
OUTPUT VARIABLE:		KFUN+2
PRIMARY MAP:		
	70.00	LOWER LIMIT
	100.00	UPPER LIMIT
	5.00	DELTA

$(P_3)_{SS}$

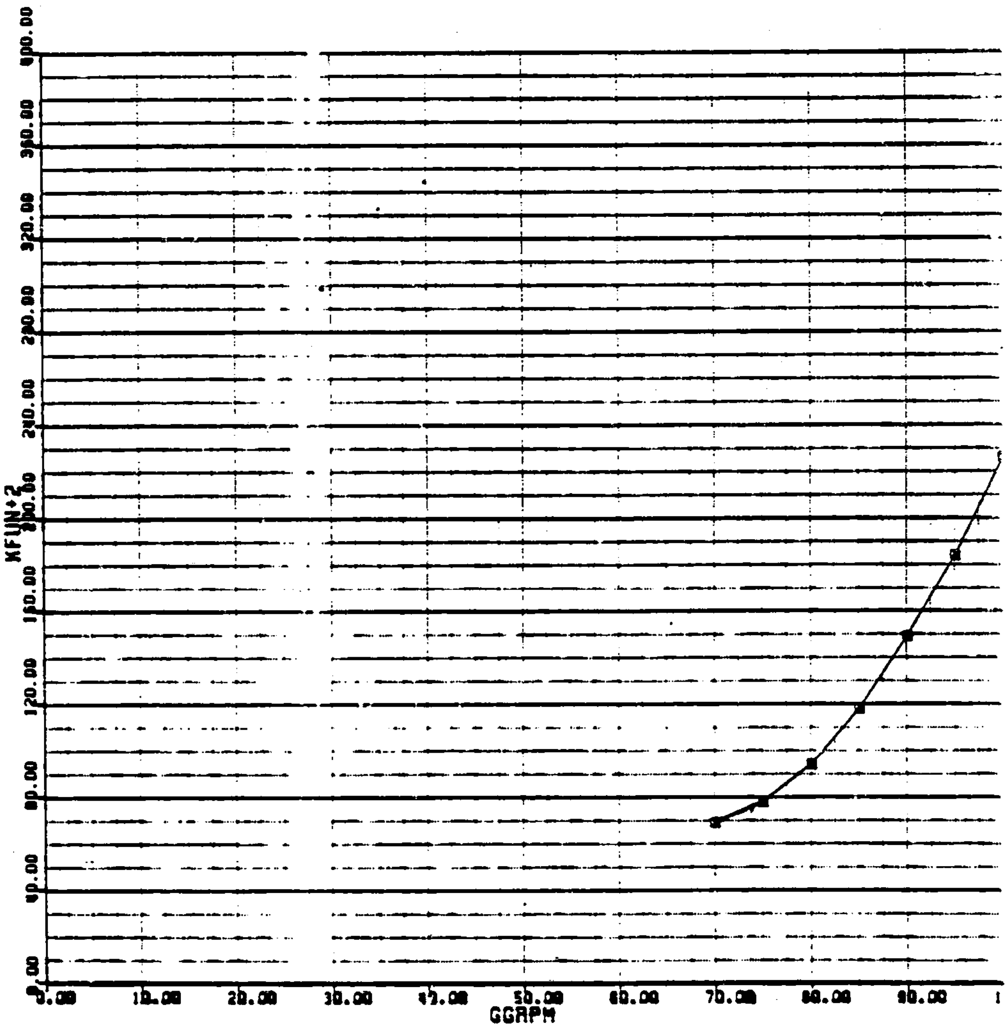

FIGURE 6.5.5

BLACK HAWK - ENGINE TIME VARYING COEFFICIENT

$\frac{\partial P_3}{\partial W_F}$

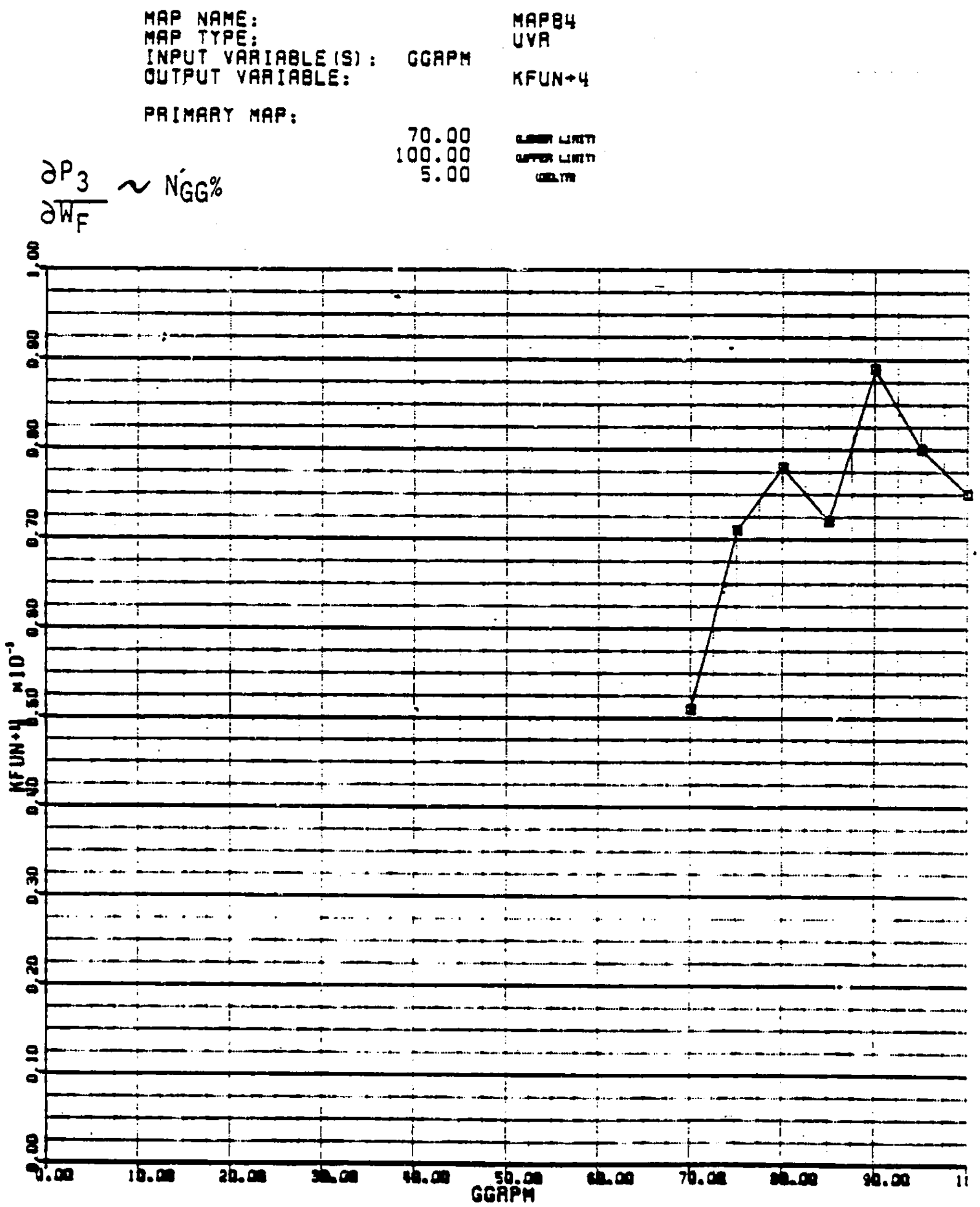

FIGURE 6.5.6

BLACK HAWK - ENGINE TIME VARYING COEFFICIENT

$\frac{\partial P_3}{\partial N_{GG}}$

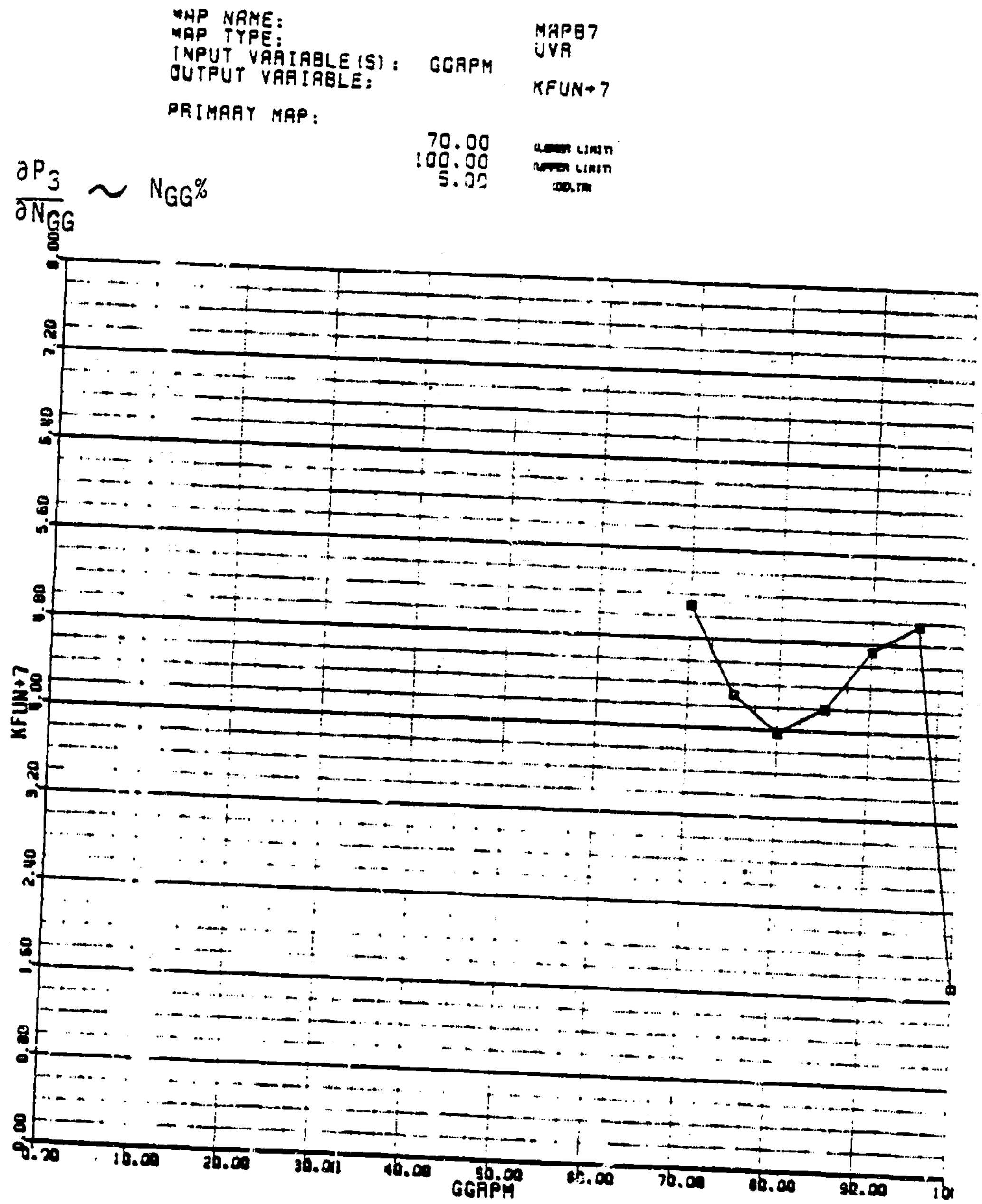

FIGURE 6.5.7

BLACK HAWK - ENGINE TIME VARYING COEFFICIENT

$\frac{\Delta W_F}{\Delta P_3} \sim N_{GG}\%$

MAP NAME: MAP83
MAP TYPE: UVA
INPUT VARIABLE(S): GGRPM
OUTPUT VARIABLE: KFUN+3

PRIMARY MAP:
70.00 (LOWER LIMIT)
100.00 (UPPER LIMIT)
5.00 (DELTA)

$\frac{\Delta W_F}{\Delta P_3}$

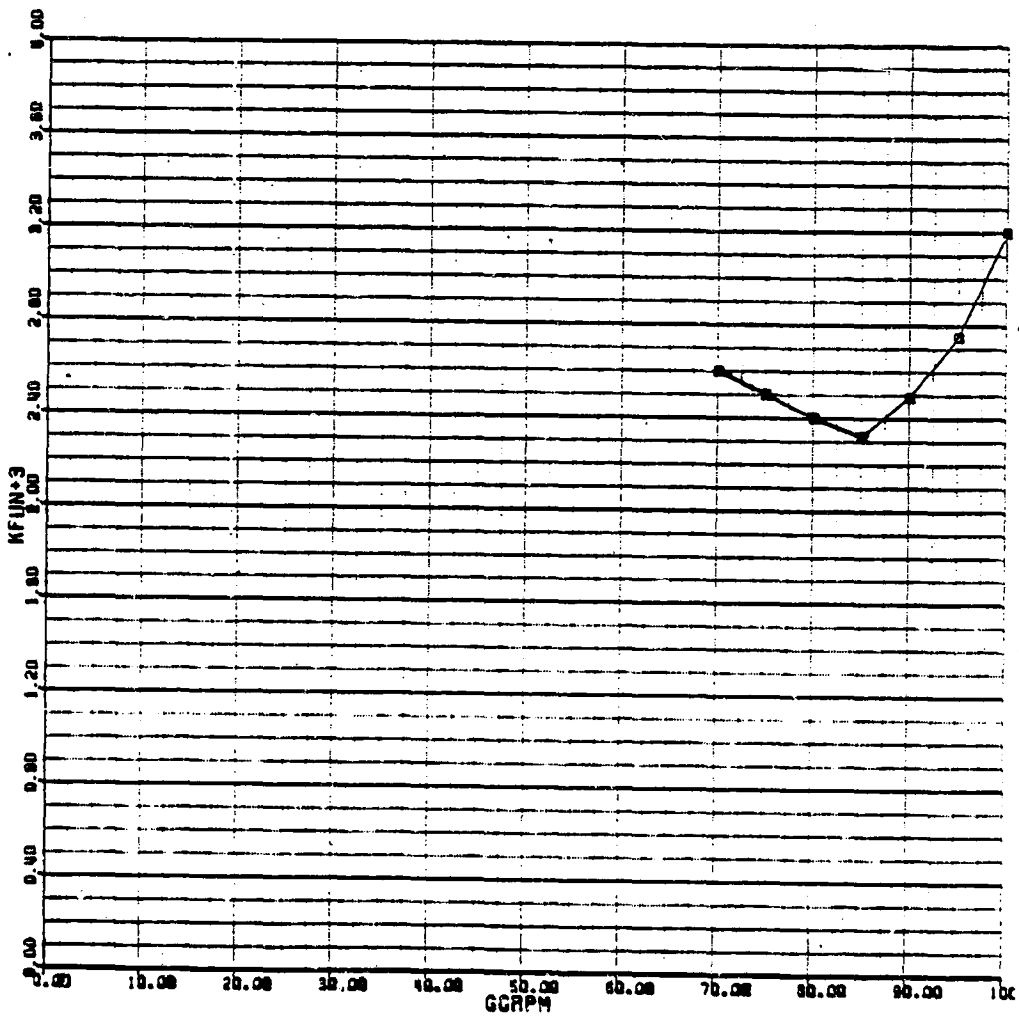

FIGURE 6.5.8

BLACK HAWK - ENGINE TIME VARYING COEFFICIENT

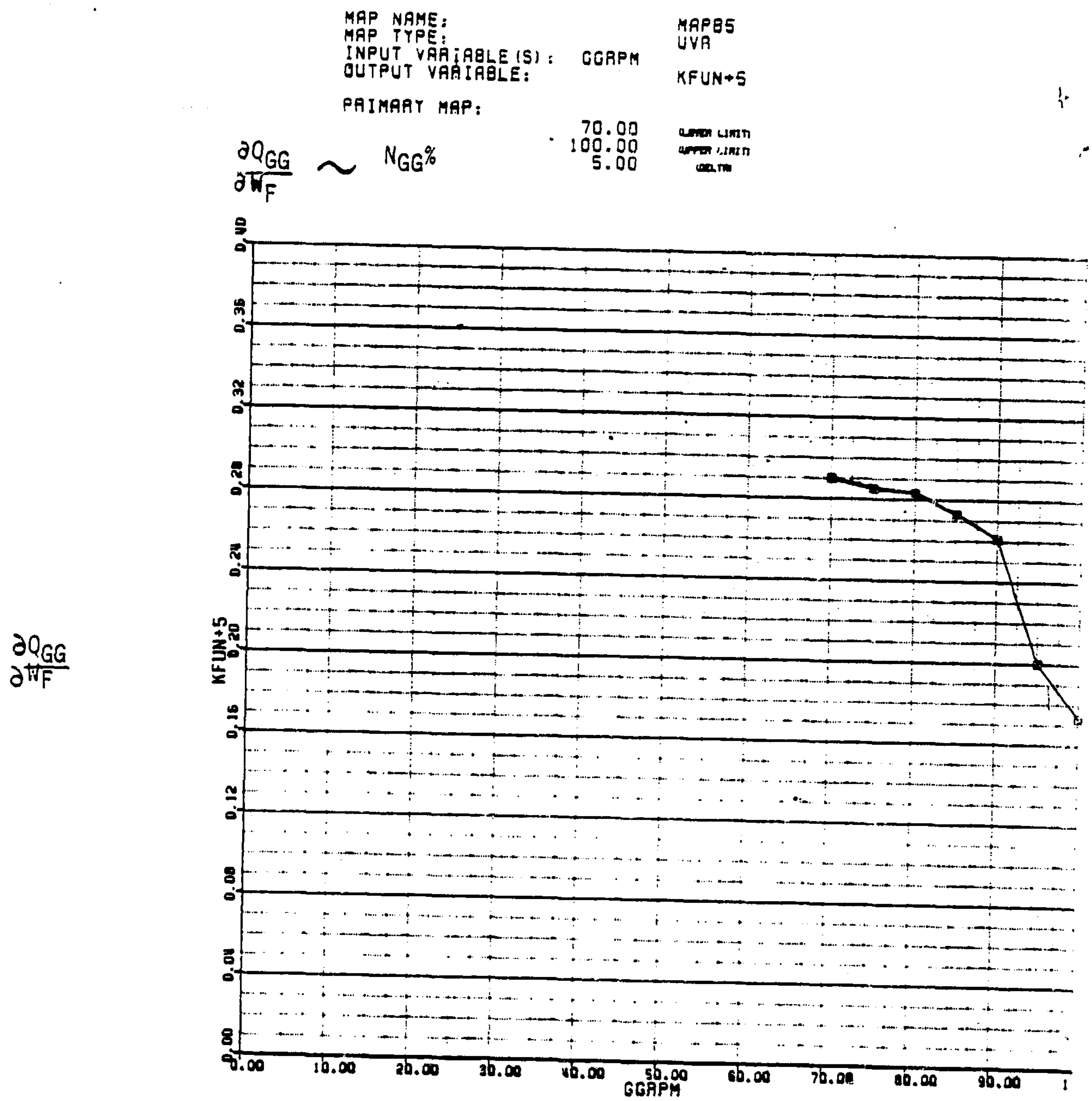

FIGURE 6.5.9

BLACK HAWK - ENGINE TIME VARYING COEFFICIENT

MAP NAME: MAPB6
MAP TYPE: UVA
INPUT VARIABLE(S): GGRPM
OUTPUT VARIABLE: KFUN+6

PRIMARY MAP:
70.00 LOWER LIMIT
100.00 UPPER LIMIT
5.00 DELTA

$\frac{\partial Q_{GG}}{\partial N_{GG}} \sim N_{GG}\%$

$\frac{\partial Q_{GG}}{\partial N_{GG}}$

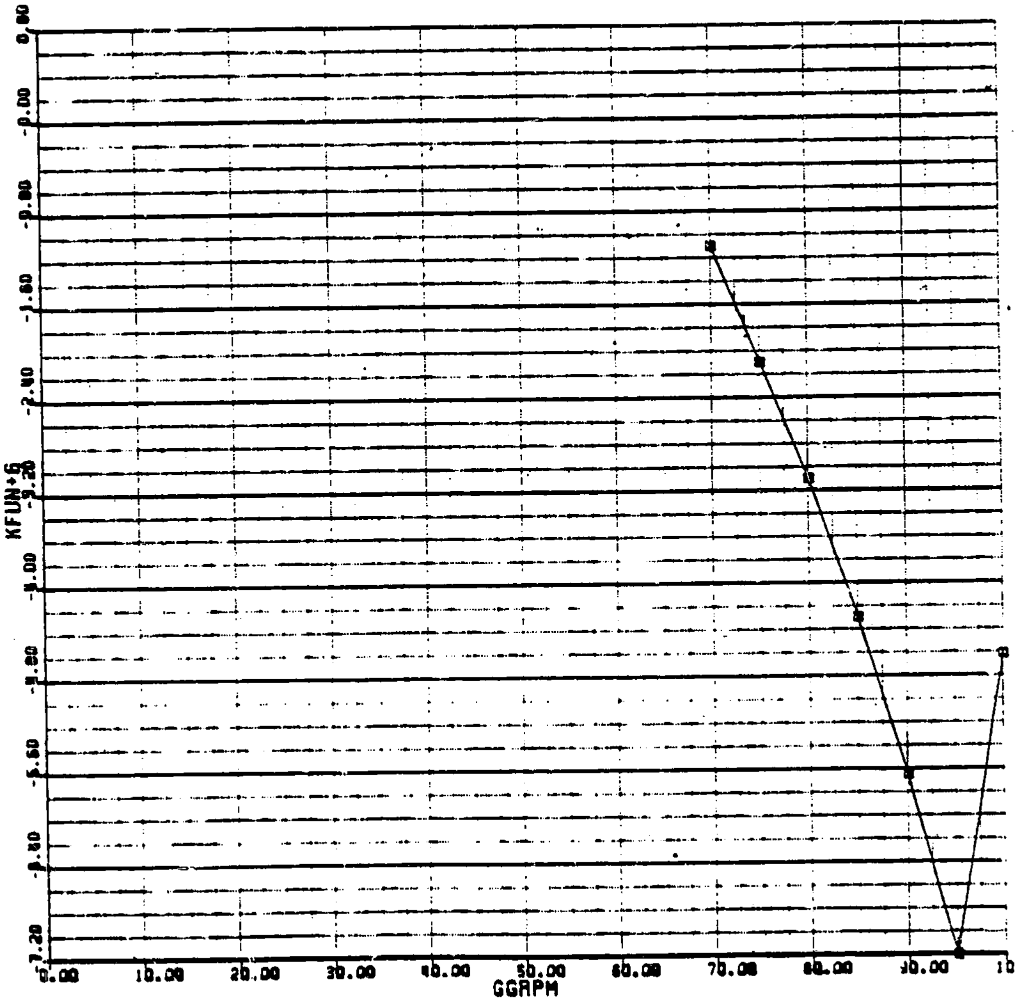

FIGURE 6.5.10

BLACK HAWK - ENGINE TIME VARYING COEFFICIENT

MAP NAME: MAP88
MAP TYPE: UVA
INPUT VARIABLE(S): GGRPM
OUTPUT VARIABLE: KFUN+8

PRIMARY MAP:

70.00 (LOWER LIMIT)
100.00 (UPPER LIMIT)
5.00 (DELTA)

$\frac{\partial Q_{PT}}{\partial W_F} \sim N_{GG}\%$

$\frac{\partial Q_{PT}}{\partial W_F}$

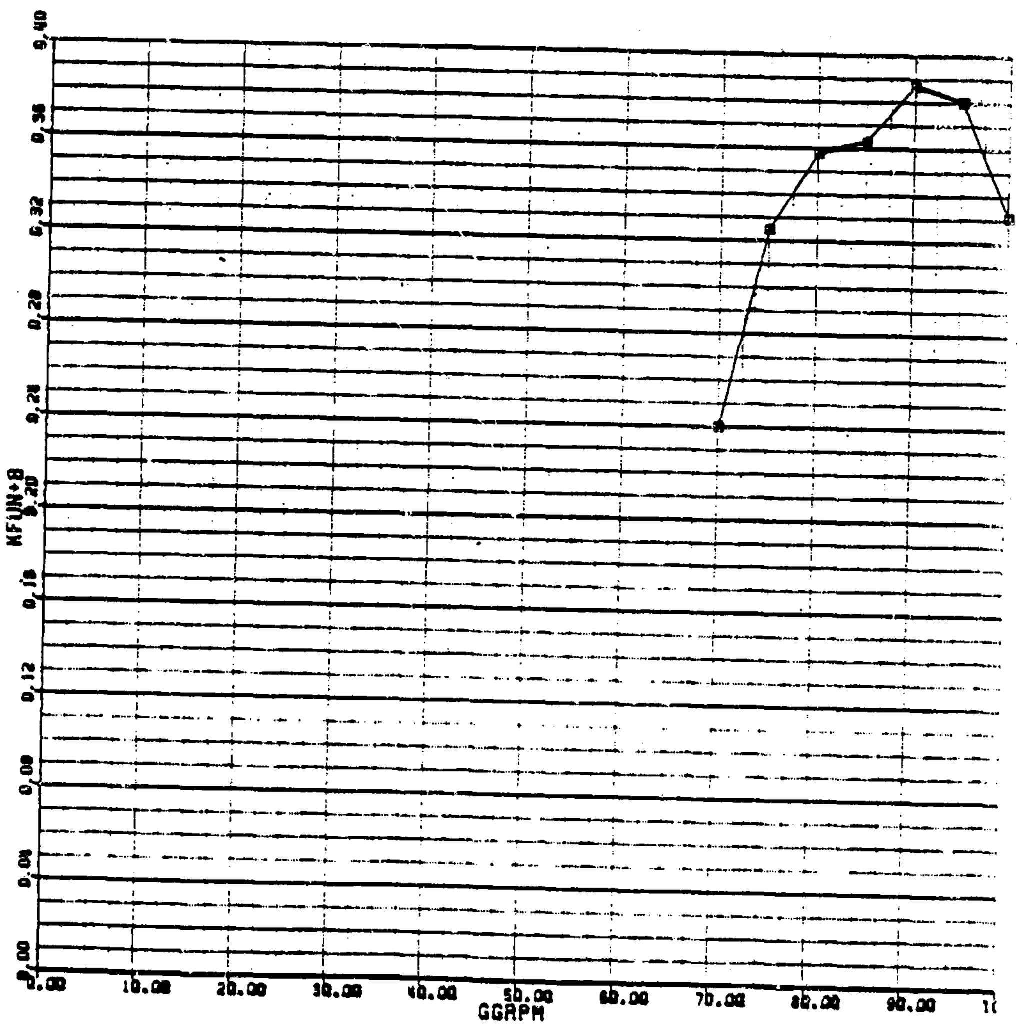

FIGURE 6.5.11

BLACK HAWK - ENGINE TIME VARYING COEFFICIENT

MAP NAME: MAP810
MAP TYPE: UVA
INPUT VARIABLE(S): GGRPM
OUTPUT VARIABLE: KFUN*10

PRIMARY MAP:
70.00 (LOWER LIMIT)
100.00 (UPPER LIMIT)
5.00 (DELTA)

$\frac{\partial Q_{PT}}{\partial N_{PT}} \sim N_{GG}\%$

$\frac{\partial Q_{PT}}{\partial N_{PT}}$

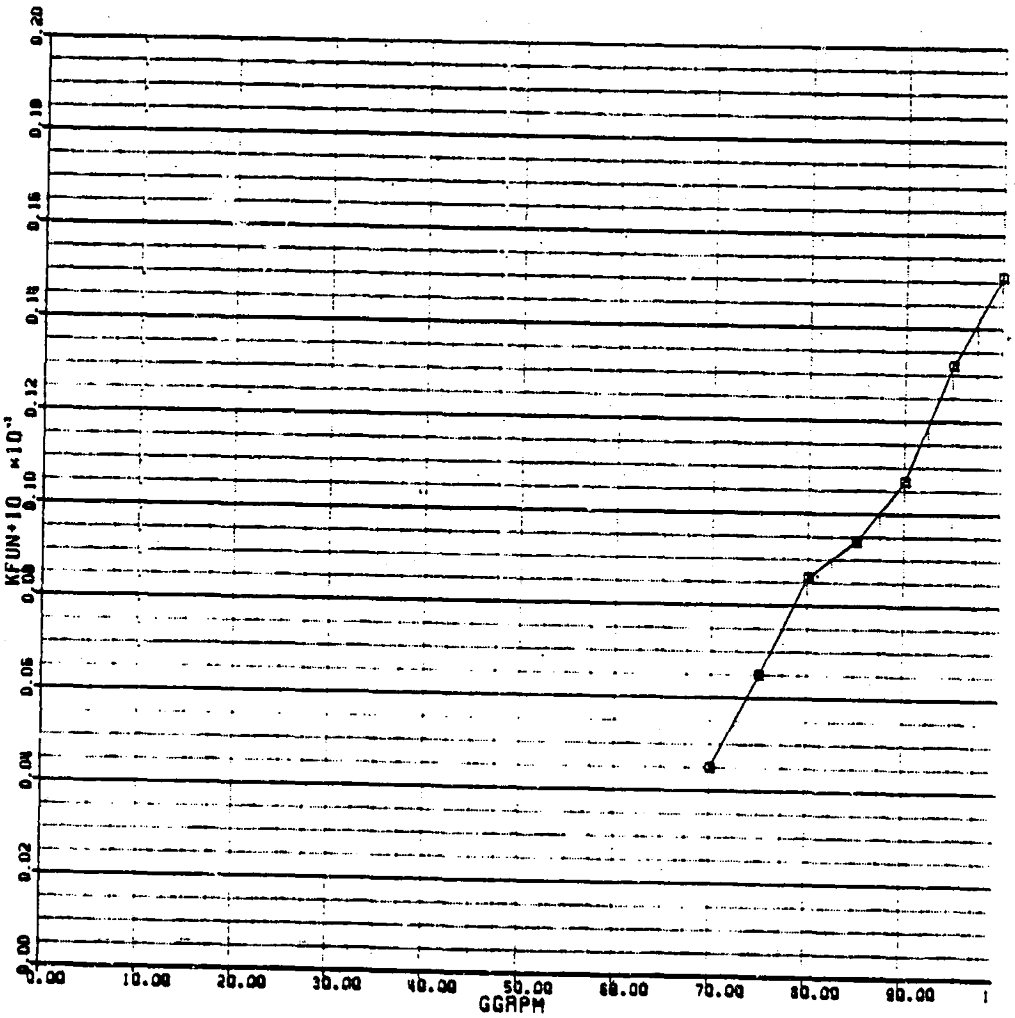

FIGURE 6.5.12

BLACK HAWK - ENGINE TIME VARYING COEFFICIENT

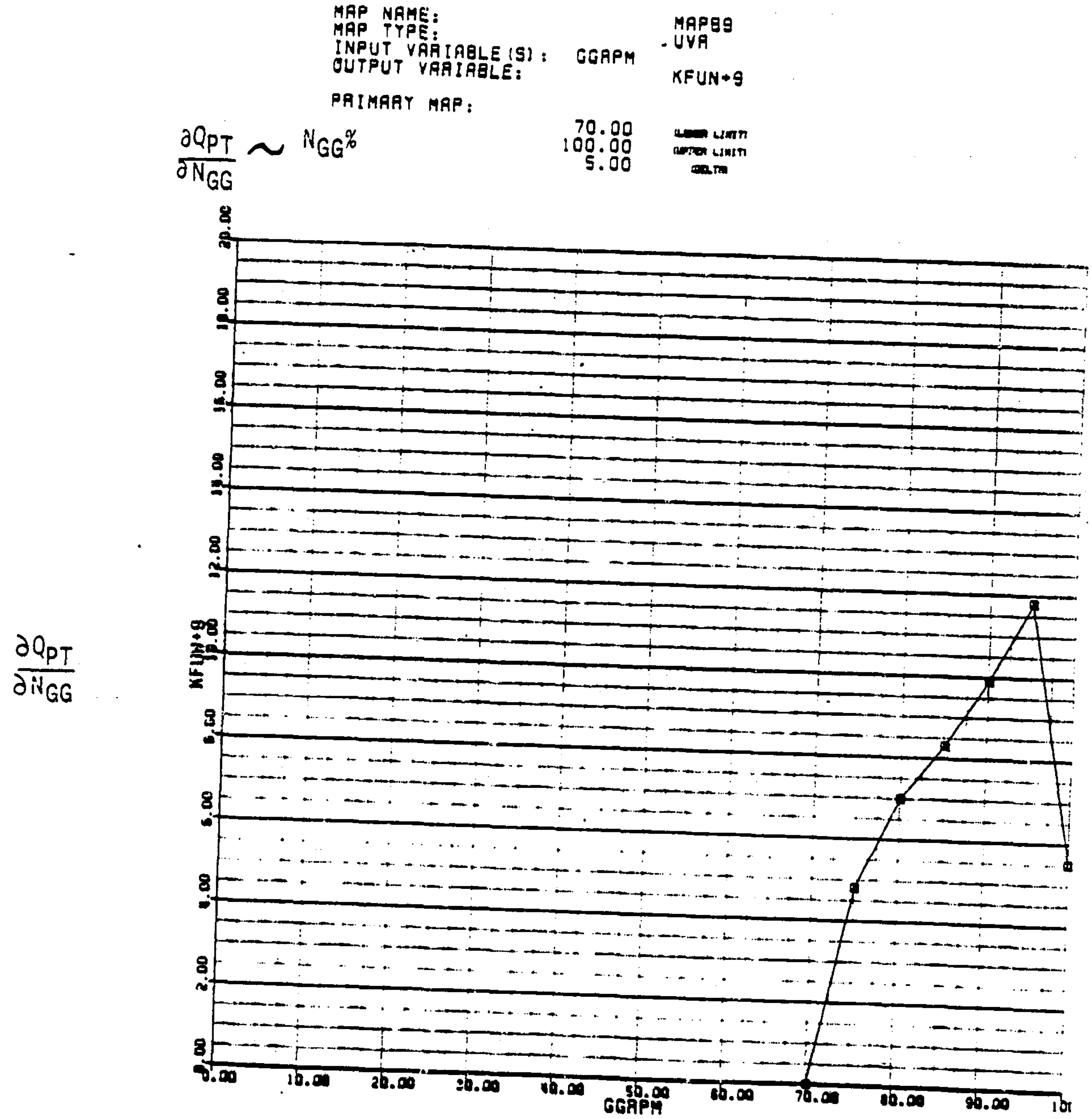

FIGURE 6.5.13

5.6.6 References

1. T700 Fuel and Control System, J. J. Curran, AHS National Forum Paper, May 1973

2. General Electric, T700 Operations Manual

ORIGINAL PAGE IS
OF POOR QUALITY

SIKORSKY AIRCRAFT UNITED TECHNOLOGIES

DOCUMENT NO. SER-70452

5.7 LANDING INTERFACE MODULE

CONTENTS

SA 28 REV. 6

5.7 LANDING INTERFACE MODULE

5.7.1 Module Description

This generalized representation consists of a landing gear force reaction model complete with all necessary space/body geometry calculations to track a free helicopter landing onto a level ground plane. The landing gear is represented by separate non-linear tire and strut dynamic characteristics as shown in Figure 7.1.1. Tire in-ground-plane loads are developed as a non-linear function of the tire deflection and normal load. These forces are adjusted depending on the friction criteria which determines tire skid characteristics at the deck surface. Finally, strut loads are summed with other external forces and moments at the helicopter CG.

Axes Systems. Two axes systems are used in this landing interface module as shown in Figure 7.1.2. All landing gear forces and moments are formulated in axes parallel to the primary body axes system passing through the CG. The space axes system of which the ground plane is set at WLFD is used to determine the landing gear proximity to the ground. Inplane friction forces are cnecked in the space axes system.

Landing gear geometry. In the equations defining the geometry of the landing gear, Figure 7.1.3: It is assumed that the strut moves along the line parallel to the helicopter Z axis. No account is taken of drag linkage constraints which cause the axle to move in an arc in the X-Z plane. This geometry together with the Gen Hel calculated position of the helicopter C.G. position in space,is used to establish the location of the tire, axle reference and gear reference points for each gear in space axes. These coordinates are used later to determine the proximity of tire contact and subsequent tire and strut deflections.

Determination of tire contact. The determination of tire contact, for an arbitrary orientation of the helicopter relies on establishing the length of a normal line from the ground plane to the axle reference position. When the distance along the gear line becomes less than the tire radius, contact has occurred. Subsequently, this difference is defined as radial tire deflection. In practice tire contact can occur at any point on the width of the tire. In the model the contact point is assumed to be at the center of the tire tread, irrespective of the distortion resulting from radial or axial loading.

Determination of tire inplane deflections and loads. In order to establish the degree of inplane deflection and corresponding loading on the tire, it is necessary to track the intersection of the landing gear line relative to the ground plane. Essentially two equations of the gear line, (each projected into a two dimensional plane) are solved for the intersection coordinates with the ground plane. When contact for an individual tire is established, the point of intersection is retained and on subsequent iterations through the program, tire deflection is determined by comparing the new and old gear line intersections. The coordinates of the initial contact are retained until the tire leaves the ground or is modified by the tire slipping. The latter aspect is discussed later. Following the transformation of the deflections into helicopter body axes, the three components of deflection at each tire are used to enter the "tire characteristics data file," to obtain the three components of tire force.

Determination of tire contact conditions. Following the determination of tire forces from the helicopter/ground plane relative motion, a test of the ability of the inplane friction forces to resist the applied forces, without slipping, must be established. The tire forces obtained in helicopter axes must be transferred to the ground plane for the friction check. Classical friction considerations provide for a coefficient of static friction and a coefficient for sliding friction. In the former case (when brakes are set), the maximum amount of inplane load which can be resisted without slipping, is proportional to the coefficient of friction and the normal loading. When this level is exceeded, motion will result. Then the force resisting the motion will depend on a reduced (sliding) coefficient of friction and the normal force. In practice, there is a smooth transistion between the two conditions. However, the model assumes a discrete change. A further assumption is that the test for frictional loads in the model assumes that X and Y inplane components can be tested separately. In practice, the resultant force determines slip conditions. This latter assumption was made to simplify the model and facilitate the introduction of brakes. When the brakes are activated, it is assumed that the wheels are locked. For brakes off, a very low coefficient of friction is introduced into the tire X direction. The wheel degree of freedom is not currently represented and therefore spin up (say on landing) inertia loads are not calculated. If slip is not occurring, calculated tire forces are passed unchanged. If slippage is occurring, the inplane forces are set to the value for sliding friction.

Reinitialization of the original tire contact point as a result of slippage. Under conditions of no-slip the tire inplane deflection is developed from consecutive calculations of the gear line intersection with the ground plane. During slip conditions, the contact point for the tire moves and the initialization of the gear-line intersection must be revised to reflect the tire movement and establish a new value for the contact point to be used on the next pass through the program.

Acceleration of the landing gear strut. Under steady conditions, the loads transferred to the airframe by the strut will be equal to the tire reactions. However, under transient conditions, the acceleration of the unsprung mass can modify the loading. Under light loading condition (where a significant portion of helicopter weight is reacted by the rotor), the strut operates in a preload range. Under these conditions, where tire reaction load is less than the strut preload setting, tire loads are transferred to the airframe with zero strut deflection. Once the preload setting is exceeded, the strut (unsprung mass) is accelerated depending on its own dynamic characteristics, the tire applied loads and the unsprung mass. Note that logic precludes the equation flow reverting back to the preload mode until the natural transient provides a zero strut deflection condition. The strut is assumed to have velocity squared damping and an isothermal air spring. A software switch is provided which allows bypassing the strut calculation. Finally, the strut loads are transferred to the helicopter CG for summation with other external forces.

LANDING GEAR
TIRE AND STRUT REPRESENTATION

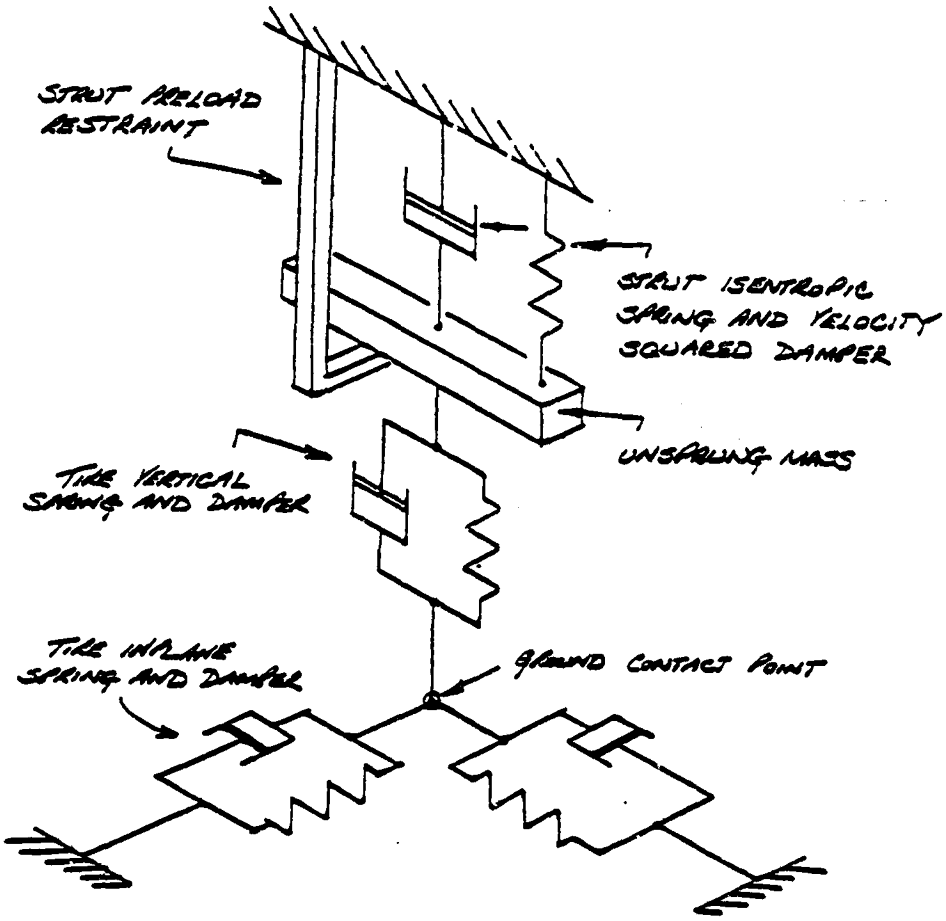

FIGURE 7.1.1

LANDING MODULE AXES SYSTEM

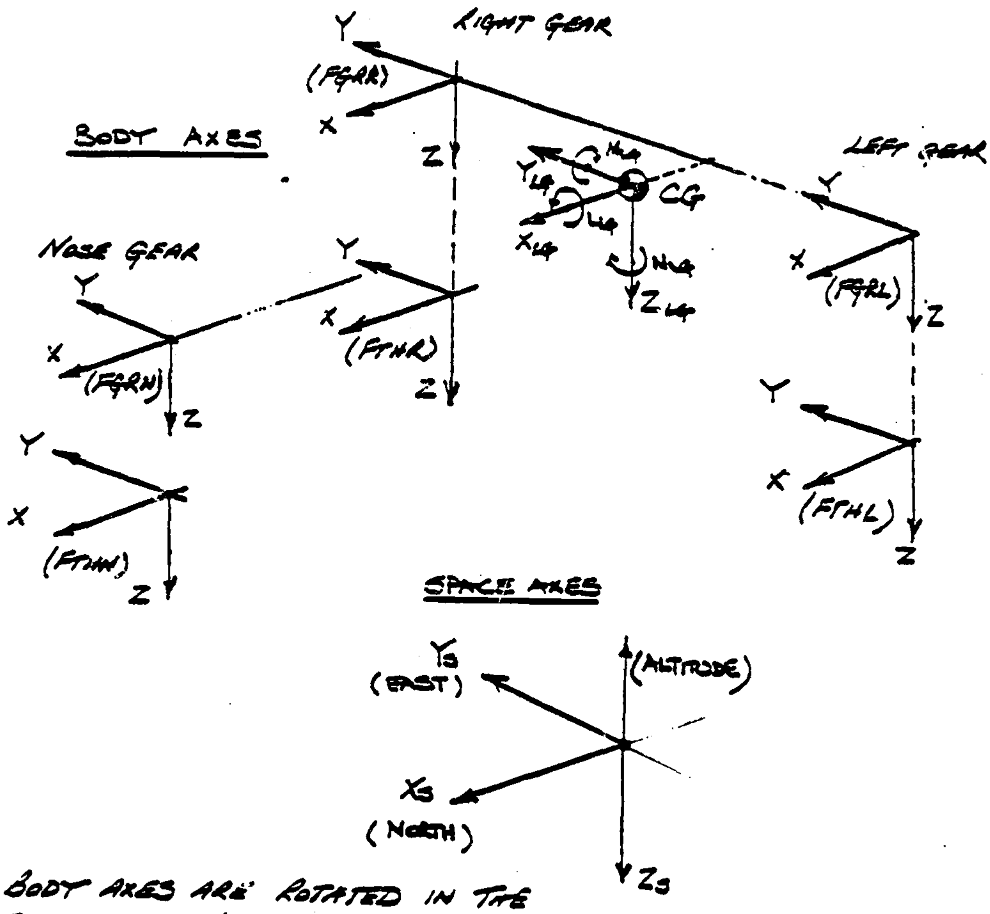

BODY AXES ARE ROTATED IN THE SEQUENCE: ψ_o ABOUT Z_o, θ_o ABOUT Y_o, ϕ_o ABOUT X_o TO REACH THE SPACE AXES SYSTEM

FIGURE 7.1.2

ORIGINAL PAGE IS OF POOR QUALITY

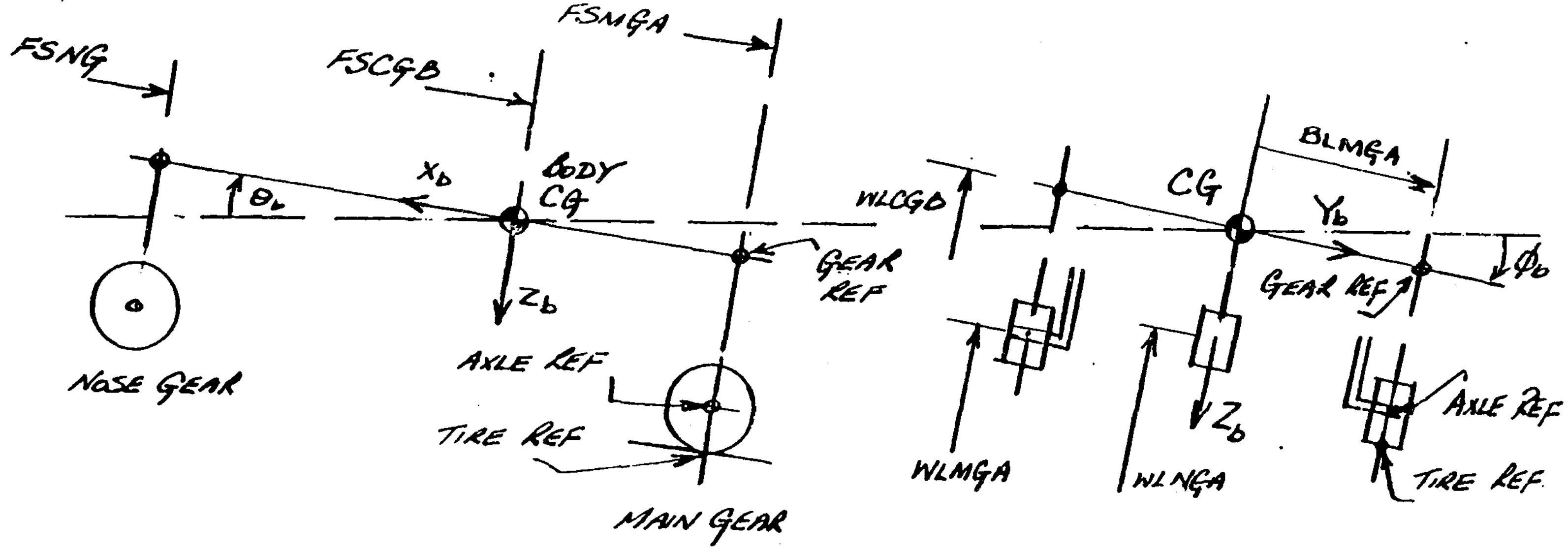

LANDING GEAR GEOMETRY
Figure 7.1.3

LANDING INTERFACE EQUATION FLOW

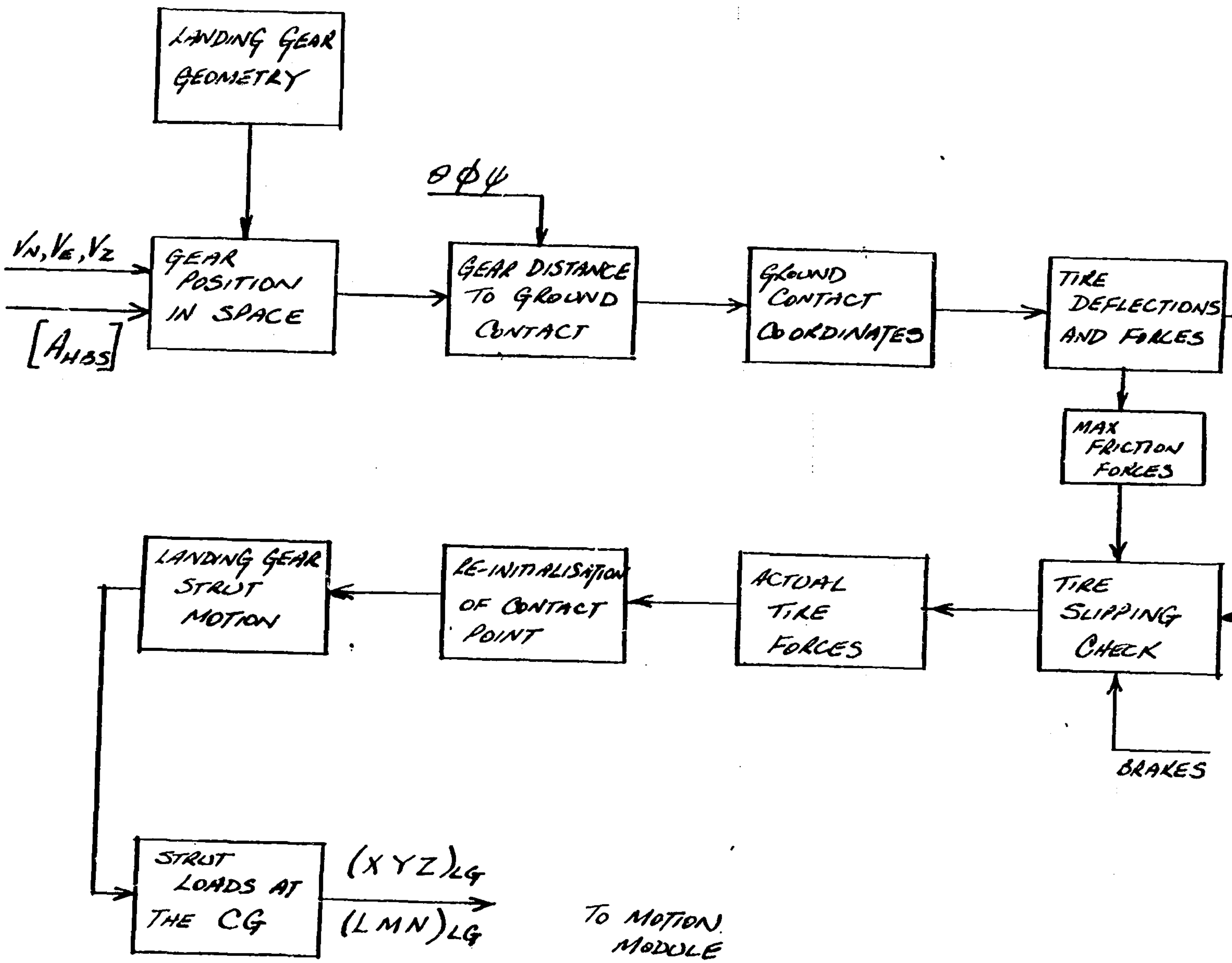

FIGURE 7.1.4

5.7.2 LANDING INTERFACE MODULE EQUATIONS

HELICOPTER CENTER OF GRAVITY POSITION IN SPACE AXES

V_N, V_E, V_Z ARE CALCULATED IN MAIN HELICOPTER PROGRAM

$$X_{SH} = X_{SHO} + \int V_N \, dt \qquad SH$$

$$Y_{SH} = Y_{SHO} + \int V_E \, dt \qquad SH+1$$

$$Z_{SH} = Z_{SHO} - \int V_Z \, dt \qquad SH+2$$

V_Z +VE UP IN MAIN PROGRAM

LANDING GEAR GEOMETRY

FSCGB, WLCGB ARE CALCULATED IN THE MAIN HELICOPTER PROGRAM

NOSE GEAR:

$$X_{NGA} = \frac{(FSCGB - FSNGA)}{12} \qquad NGA$$

$$Y_{NGA} = 0 \qquad NGA+1$$

$$Z_{NGA} = \frac{(WLCGB - WLNGAO)}{12} \qquad NGA+2$$

RIGHT MAIN GEAR:

$$X_{RMGA} = \frac{(FSCGB - FSMGA)}{12} \qquad RMGA$$

$$Y_{RMGA} = \frac{BLMGA}{12} \qquad RMGA+1$$

$$Z_{RMGA} = \frac{(WLCGB - WLMGAO)}{12} \qquad RMGA+2$$

SA 103 REV.

LEFT MAIN GEAR :

$X_{LMGA} = X_{RMGA}$, LMGA

$Y_{LMGA} = Y_{RMGA}$, LMGA +1

$Z_{LMGA} = Z_{RMGA}$, LMGA +2

THESE COORDINATES ARE FOR THE FULLY EXTENDED STRUTS AT THE AXLE LOCATION

FREE EXTENSION POSITIONS OF GEAR IN SPACE AXES

TIRE REFERENCE POSITIONS

NOSE GEAR :

$$\begin{bmatrix} X \\ Y \\ Z \end{bmatrix}_{NTSO} = \begin{bmatrix} A_{HBS} \end{bmatrix} \begin{bmatrix} X_{NGA} \\ Y_{NGA} \\ Z_{NGA} + R_{TN}/12 \end{bmatrix} + \begin{bmatrix} X \\ Y \\ Z \end{bmatrix}_{SH} \quad \begin{matrix} ,\ NTSO \\ ,\ NTSO+1 \\ ,\ NTSO+2 \end{matrix}$$

RIGHT GEAR :

$$\begin{bmatrix} X \\ Y \\ Z \end{bmatrix}_{RMTSO} = \begin{bmatrix} A_{HBS} \end{bmatrix} \begin{bmatrix} X_{RMGA} \\ Y_{RMGA} \\ Z_{RMGA} + R_{TM}/12 \end{bmatrix} \begin{bmatrix} X \\ Y \\ Z \end{bmatrix}_{SH} \quad \begin{matrix} ,\ RMTSO \\ ,\ RMTSO+1 \\ ,\ RMTSO+2 \end{matrix}$$

LEFT GEAR :

$$\begin{bmatrix} X \\ Y \\ Z \end{bmatrix}_{LMTSO} = \begin{bmatrix} A_{HBS} \end{bmatrix} \begin{bmatrix} X_{LMGA} \\ Y_{LMGA} \\ Z_{LMGA} + R_{TM}/12 \end{bmatrix} \begin{bmatrix} X \\ Y \\ Z \end{bmatrix}_{SH} \quad \begin{matrix} LMTSO \\ LMTSO+1 \\ LMTSO+2 \end{matrix}$$

ORIGINAL PAGE IS
OF POOR QUALITY

SER 70452

Prepared	NAME	DATE	SIKORSKY AIRCRAFT	Page 3
Checked			TITLE	Model
Drawing				Report No.

AXLE REFERENCE POSITION IN SPACE

NOTE SIMULARITY TO THE REF. POSITIONS

NOSE GEAR

$$\begin{bmatrix} X \\ Y \\ Z \end{bmatrix}_{NAS} = A_{HAS} \begin{bmatrix} X_{NGA} \\ Y_{NGA} \\ Z_{NGA} - S_{NG} \end{bmatrix} + \begin{bmatrix} X \\ Y \\ Z \end{bmatrix}_{SH} \quad \begin{matrix} ,NAS \\ ,NAS+1 \\ ,NAS+2 \end{matrix}$$

RIGHT GEAR.

$$\begin{bmatrix} X \\ Y \\ Z \end{bmatrix}_{RAS} = A_{HAS} \begin{bmatrix} X_{RMGA} \\ Y_{RMGA} \\ Z_{RMGA} - S_{RG} \end{bmatrix} + \begin{bmatrix} X \\ Y \\ Z \end{bmatrix}_{SH} \quad \begin{matrix} ,RAS \\ ,RAS+1 \\ ,RAS+2 \end{matrix}$$

LEFT GEAR

$$\begin{bmatrix} X \\ Y \\ Z \end{bmatrix}_{LAS} = A_{HBS} \begin{bmatrix} X_{LMGA} \\ Y_{LMGA} \\ Z_{LMGA} - S_{LG} \end{bmatrix} + \begin{bmatrix} X \\ Y \\ Z \end{bmatrix}_{SH} \quad \begin{matrix} ,LAS \\ ,LAS+1 \\ ,LAS+2 \end{matrix}$$

SIKORSKY AIRCRAFT		
Prepared (Name, Date)		
Checked	Title	Model
Drawing		Report No.

GEAR REFERENCE POSITION IN SPACE

NOTE SIMILARITY TO TIRE REF. EQ

NOSE GEAR

$$\begin{bmatrix} X \\ Y \\ Z \end{bmatrix}_{NGSR} = A_{HBS} \begin{bmatrix} X \\ Y \\ Z \end{bmatrix}_{NGAO} + \begin{bmatrix} X \\ Y \\ Z \end{bmatrix}_{SH} \qquad M7$$

RIGHT GEAR

$$\begin{bmatrix} X \\ Y \\ Z \end{bmatrix}_{MGRSR} = A_{HBS} \begin{bmatrix} X \\ Y \\ Z \end{bmatrix}_{RMGAO} + \begin{bmatrix} X \\ Y \\ Z \end{bmatrix}_{SH} \qquad M8$$

LEFT GEAR

$$\begin{bmatrix} X \\ Y \\ Z \end{bmatrix}_{MGLSR} = A_{HBS} \begin{bmatrix} X \\ Y \\ Z \end{bmatrix}_{LMGAO} + \begin{bmatrix} X \\ Y \\ Z \end{bmatrix}_{SH} \qquad M9$$

SA 109 REV

DISTANCE OF NORMAL FROM GROUND PLANE TO AXLE REFERENCE POINT

$$D_{NNA} = Z_{NAS} + WLFD \qquad , DNNA$$

$$D_{NRA} = Z_{RAS} + WLFD \qquad , DNRA$$

$$D_{NLA} = Z_{LAS} + WLFD \qquad , DNLA$$

DIRECTION COSINES OF GEAR LINE

THE GEAR LINE OF DEFLECTION IS ASSUMED TO BE PARALLEL TO AIRCRAFT BODY AXES. THUS THE DIRECTION COSINES ARE EQUIVALENT TO THE 3RD COLUMN OF A_{HBS} FOR A UNITY VECTOR

$$\cos \alpha_{NG} = \sin\theta_B \cos\phi_B \cos\psi_B + \sin\phi_B \sin\psi_B \qquad , CSANG$$

$$\cos \beta_{NG} = \sin\theta_B \cos\phi_B \sin\psi_B - \sin\phi_B \cos\psi_B \qquad , CSBNG$$

$$\cos \gamma_{NG} = \cos\theta_B \cos\phi_B \qquad , CSGNG$$

$$\cos \alpha_{RMR} = \cos \alpha_{LMR} = \cos \alpha_{NG}$$

$$\cos \beta_{RMR} = \cos \beta_{LMR} = \cos \beta_{NG}$$

$$\cos \gamma_{RMR} = \cos \gamma_{LMR} = \cos \gamma_{NG}$$

CHECK FOR TIRE CONTACT WITH GROUND PLANE

IF

$$\delta_{TNG} = \left(\frac{R_{TN}}{12} + \frac{DNNA}{\cos \gamma_{NG}} \right) \geq 0 \quad , DLTNG$$

$$\delta_{TRG} = \left(\frac{R_{TM}}{12} + \frac{DNRA}{\cos \gamma_{RMG}} \right) \geq 0 \quad , DLTRMG$$

$$\delta_{TLG} = \left(\frac{R_{TM}}{12} + \frac{DNLA}{\cos \gamma_{LMG}} \right) \geq 0 \quad , DLTLMG$$

SET CONTACT FLAG FOR CORRESPONDING GEAR

IF δ_{TNG}, δ_{TRG}, $\delta_{TLG} < 0$

RETURN TO MAIN HELICOPTER PROGRAM

DRAWN FOR LEFT GEAR

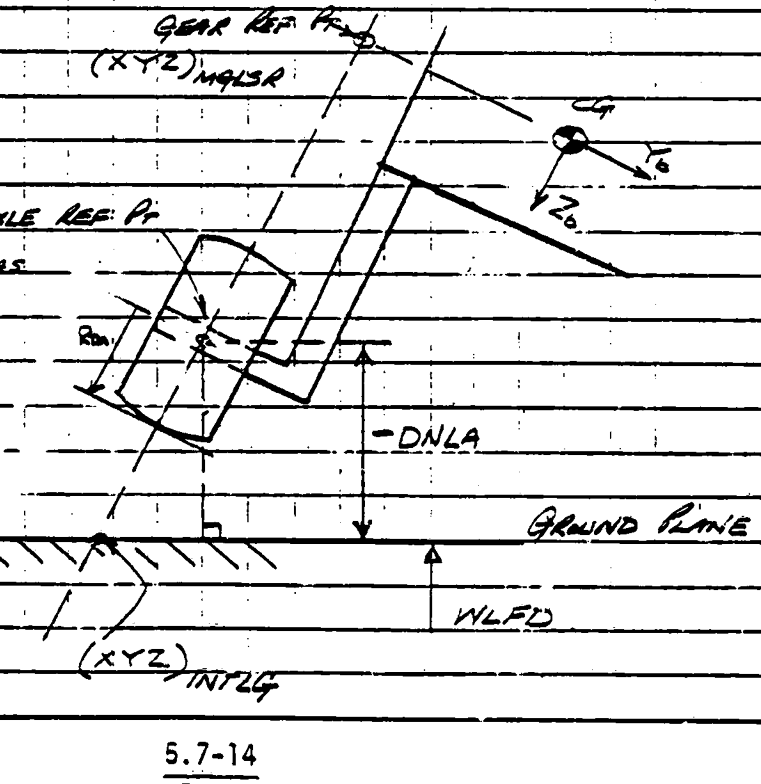

INTERSECTION OF GEAR LINE WITH GROUND PLANE

$$(X_{INT})_{NG,RG,LG} = (a.Z_{INT} + b)_{NG,RG,LG}$$; INTNG ; INTRMG ; INTLMG

$$(a)_{NG} = \left(\frac{X_{NGSR} - X_{NAS}}{Z_{NGSR} - Z_{NAS}}\right) \qquad b_{NG} = (X_{NAS} - a_{NG} Z_{NAS})$$

$$(a)_{RG} = \left(\frac{X_{MGRSR} - X_{RAS}}{Z_{MGRSR} - Z_{RAS}}\right) \qquad b_{RG} = (X_{RAS} - a_{RG} Z_{RAS})$$

$$(a)_{LG} = \left(\frac{X_{MGLSR} - X_{LAS}}{Z_{MGLSR} - Z_{LAS}}\right) \qquad b_{LG} = (X_{LAS} - a_{LG} Z_{LAS})$$

$$(Y_{INT})_{NG,RG,LG} = (C.Z_{INT} + d)_{NG,RG,LG}$$; INTNG+1 ; INTRMG+1 ; INTLMG+1

$$(C)_{NG} = \left(\frac{Y_{NGSR} - Y_{NAS}}{Z_{NGSR} - Z_{NAS}}\right) \qquad d_{NG} = (Y_{NAS} - C_{NG} Z_{NAS})$$

$$(C)_{RG} = \left(\frac{Y_{MGRSR} - Y_{RAS}}{Z_{MGRSR} - Z_{RAS}}\right) \qquad d_{RG} = (Y_{RAS} - C_{RG} Z_{RAS})$$

$$(C)_{LG} = \left(\frac{Y_{MGLSR} - Y_{LAS}}{Z_{MGLSR} - Z_{LAS}}\right) \qquad d_{LG} = (Y_{LAS} - C_{LG} Z_{LAS})$$

$$(Z_{INT})_{NG,RG,LG} = -WLFD$$ FOR FIXED, LEVEL GROUND PLANE

INITIALISATION OF GROUND CONTACT POINT

IF 'CONTACT FLAG' HAS BEEN SET ON THE CURRENT PASS THROUGH THE PROGRAM THEN SET

$$\left[(XYZ)_{ID}\right]_{NG0,\,RG0,\,LG0} = \left[(XYZ)_{INT}\right]_{NG,\,RG,\,LG} \quad , IDNG, +1, +2 \quad , IDRG, +1, +2 \quad , IDLG, +1, +2$$

∴ TO INITIALISE POINT OF CONTACT ON THE GROUND PLANE

IF 'CONTACT FLAG' IS NOT SET

$$\left[(XYZ)_{ID}\right]_{NG0,\,RG0,\,LG0} = 0$$

TIRE DEFLECTIONS IN GROUND PLANE AXES (SPACE AXES)

$$(\Delta X)_{NG,\,RG,\,LG} = (X_{INT})_{NG,\,RG,\,LG} - (X_{ID})_{NG0,\,RG0,\,LG0} \quad , DELNG, DELRMG, DELLMG$$

$$(\Delta Y)_{NG,\,RG,\,LG} = (Y_{INT})_{NG,\,RG,\,LG} - (Y_{ID})_{NG0,\,RG0,\,LG0} \quad , DELNG+1, DELRMG+1, DELLMG+1$$

$$(\Delta Z)_{NG,\,RG,\,LG} = (Z_{INT})_{NG,\,RG,\,LG} - (Z_{ID})_{NG0,\,RG0,\,LG0} \quad , DELNG+2, DELRMG+2, DELLMG+2$$

NOTE: 1. $(\Delta Z) = 0$ CODE AS A CHECK.

2. THE CONTACT FLAG MAY BE SET SEVERAL TIMES DURING THE COURSE OF A LANDING AS THE GEAR BOUNCES IN AND OUT OF CONTACT.

TIRE DEFLECTIONS IN HELICOPTER BODY AXES

$$\begin{bmatrix} \Delta X \\ \Delta Y \\ \Delta Z \end{bmatrix}_{\substack{HNG \\ HRG \\ HLG}} = \begin{bmatrix} A_{HSB} \end{bmatrix} \begin{bmatrix} \Delta X \\ \Delta Y \\ \Delta Z \end{bmatrix}_{\substack{NG \\ RG \\ LG}} + \begin{bmatrix} 0 \\ 0 \\ \delta_T \end{bmatrix}_{\substack{NG \\ RG \\ LG}}$$

, DEL HNG
, DEL HRG.
, DEL HLG.

TIRE FORCES IN HELICOPTER BODY AXES

$$X_{FTHN} = -N_{TN}\left[K_{TXN}\cdot \Delta X_{HNG} + G_{DN}\cdot K_{TXN}\cdot \Delta \dot{X}_{HNG}\right]$$, FTHN

$$Y_{FTHN} = -N_{TN}\left[KTYN\cdot \Delta Y_{HNG} + G_{DN}\cdot K'_{TYN}\cdot \Delta \dot{Y}_{HNG}\right]$$, FTHN+1

$$Z_{FTHN} = -N_{TN}\left[KTZN\cdot \Delta Z_{HNG} + G_{DN}\cdot K'_{TZN}\cdot \Delta \dot{Z}_{HNG}\right]$$, FTHN+2

$$(X)_{\substack{FTHR \\ FTHL}} = -N_{TM}\left[K_{TX\substack{R \\ L}}\cdot \Delta X_{\substack{HRG \\ HLG}} + G_{DM}\cdot K_{TX\substack{R \\ L}}\cdot \Delta \dot{X}_{\substack{HRG \\ HLG}}\right]$$, FTHR / FTHL

$$(Y)_{\substack{FTHR \\ FTHL}} = -N_{TM}\left[KTY\substack{R \\ L}\cdot \Delta Y_{\substack{HRG \\ HLG}} + G_{DM}\cdot KTY\substack{R \\ L}\cdot \Delta \dot{Y}_{\substack{HRG \\ HLG}}\right]$$, FTHR+1 / FTHL+1

$$(Z)_{\substack{FTHR \\ FTHL}} = -N_{TM}\left[KTZ\substack{R \\ L}\cdot \Delta Z_{\substack{HRG \\ HLG}} + \underbrace{G_{DM}\cdot K'_{TZ\substack{R \\ L}}\cdot \Delta \dot{Z}_{\substack{HRG \\ HLG}}}\right]$$, FTHR+2 / FTHL+2

WHERE $\Delta \dot{X} = \left(\Delta X_t - \Delta X_{(t-1)}\right)\frac{1}{\Delta T}$

$\Delta \dot{Y} = \left(\Delta Y_t - \Delta Y_{(t-1)}\right)\frac{1}{\Delta T}$

$\Delta \dot{Z} = \left(\Delta Z_t - \Delta Z_{(t-1)}\right)\frac{1}{\Delta T}$

THIS TIRE DAMPING COMPONENT IS FILTERED THROUGH A FIRST ORDER LAG. $\tau = .01$

NOTE VERTICAL TIRE LOADS ARE PROVIDED AS LOAD ~ DEFLECTION NON LINEAR MAPS. IN ORDER TO PRESERVE CALCULATION LOOP INTEGRATY AN ARTIFICIAL KTZR IS DERIVED (= MAP OUTPUT / ΔZ). THIS STIFFNESS SHOULD NOT BE CONFUSED WITH K'_{TZR} WHICH IS A LOCAL SLOPE

TIRE INPLANE STIFFNESS MAYBE EQUATIONS OR MAPS.

TIRE FORCES IN THE GROUND PLANE (ALIGNED ALONG HELICOPTER BODY AXES)

TEMPORARILY SET $\psi_b = 0$

$$\begin{bmatrix} X \\ Y \\ Z \end{bmatrix}_{\substack{FTDN \\ FTDR \\ FTDL}} = \begin{bmatrix} A_{HBS} \\ \psi_b = 0 \end{bmatrix} \begin{bmatrix} X \\ Y \\ Z \end{bmatrix}_{\substack{FTHN \\ FTHR \\ FTHL}}$$

, FTDN , +1 , +2
, FTDR , +1 , +2
, FTDL , +1 , +2

LOGIC FOR MAIN GEAR BRAKES

IF BRAKES ARE SET $K_{\mu B} = B_{BK}$

IF BRAKES ARE OFF $K_{\mu B} = N_{BRK}$

MAXIMUM REACTION THAT CAN BE SUSTAINED IN THE X DIRECTION

$$(X)_{\substack{FTDNM \\ FTDRM \\ FTDLM}} = K_{\mu B} \cdot \mu \, (|Z|)_{\substack{FTDN \\ FTDR \\ FTDL}}$$

, FTDNM
, FTDRM
, FTDLM

NOTE $K_{\mu B} = N_{BRK}$ ALWAYS FOR NOSE WHEEL

CHECK FOR LONGITUDINAL TIRE SLIP

• IF $(|X|)_{FTDN, FTDR, FTDL} > (X)_{FTDNM, FTDRM, FTDLM}$

THEN TIRE IS SLIPPING, SET SLIP FLAG AND

SET $(X)_{FTDN, FTDR, FTDL} = \left[\dfrac{X_F}{|X_F|}\right]_{TDN, TDR, TDL} K_{SLIP} (X)_{FTDNM, FTDRM, FTDLM}$

• IF $(|X|)_{FTDN, FTDR, FTDL} \leq (X)_{FTDNM, FTDRM, FTDLM}$

THEN TIRE IS NOT SLIPPING

SET $(X)_{FTDN, FTDR, FTDL} = (X)_{FTDN, FTDR, FTDL}$

MAXIMUM REACTION THAT CAN BE SUSTAINED IN THE LATERAL DIRECTION

$(Y)_{FTDNM, FTDRM, FTDLM} = \mu \, (|Z|)_{FTDN, FTDR, FTDL}$

CHECK FOR LATERAL TIRE SLIP

• IF $(|Y|)_{FTDN, FTDR, FTDL} > (Y)_{FTDNM, FTDRM, FTDLM}$

THEN TIRE IS SLIPPING, SET SLIP FLAG AND

SET $(Y)_{FTDN, FTDR, FTDL} = \left[\dfrac{Y_F}{|Y_F|}\right]_{TDN, TDR, TDL} K_{SLIP} (Y)_{FTDNM, FTDRM, FTDLM}$

• IF $(|Y|)_{FTDN, FTDR, FTDL} \leq (Y)_{FTDNM, FTDRM, FTDLM}$

THEN TIRE IS NOT SLIPPING

SET $(Y)_{FTDN, FTDR, FTDL} = (Y)_{FTDN, FTDR, FTDL}$

CORRECTED TIRE LOADS IN HELICOPTER BODY AXES

TEMPORARILY SET $\psi_G = 0$

$$\begin{bmatrix} X \\ Y \\ Z \end{bmatrix}_{\substack{FTHN \\ FTHR \\ FTHL}} = \begin{bmatrix} A_{HSB} \\ \psi_G = 0 \end{bmatrix} \begin{bmatrix} X \\ Y \\ Z \end{bmatrix}_{\substack{FTDN \\ FTDR \\ FTDL}}$$

, FTHN , +1 , +2
, FTHR , +1 , +2
, FTHL , +1 , +2

TIRE LOADS IN HELICOPTER AXES AT THE AXLE REFERENCE POINT

$$\begin{bmatrix} X \\ Y \\ Z \end{bmatrix}_{\substack{FTAN \\ FTAR \\ FTAL}} = \begin{bmatrix} X \\ Y \\ Z \end{bmatrix}_{\substack{FTHN \\ FTHR \\ FTHL}}$$

$$\begin{bmatrix} L \\ M \\ N \end{bmatrix}_{\substack{FTAN \\ FTAR \\ FTAL}} = \begin{bmatrix} Z_{\substack{FTAN \\ FTAR \\ FTAL}} (-\Delta Y)_{\substack{HNG \\ HRG \\ HLG}} - Y_{\substack{FTAN \\ FTAR \\ FTAL}} \left(\frac{R_{TN,M}}{12} - \Delta Z_{\substack{HNG \\ HRG \\ HLG}} \right) \\ Z_{\substack{FTAN \\ FTAR \\ FTAL}} (\Delta X)_{\substack{HNG \\ HRG \\ HLG}} + X_{\substack{FTAN \\ FTAR \\ FTAL}} \left(\frac{R_{TN,M}}{12} - \Delta Z_{\substack{HNG \\ HRG \\ HLG}} \right) \\ Y_{\substack{FTAN \\ FTAR \\ FTAL}} (-\Delta X)_{\substack{HNG \\ HRG \\ HLG}} - X_{\substack{FTAN \\ FTAR \\ FTAL}} (-\Delta Y)_{\substack{HNG \\ HRG \\ ALG}} \end{bmatrix}$$

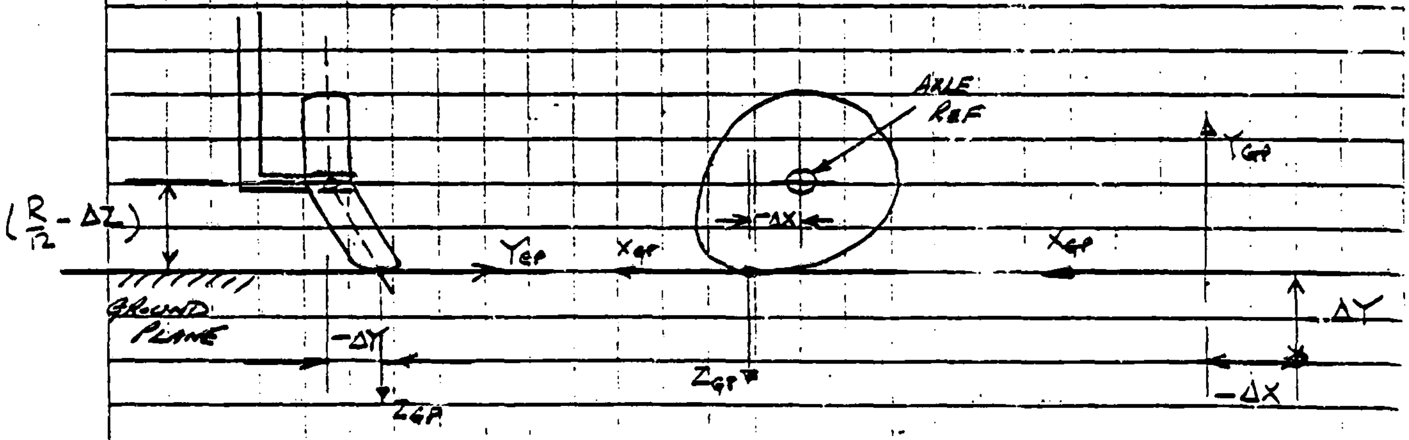

ORIGINAL PAGE IS
OF POOR QUALITY

SER 70452

Name	Date	SIKORSKY AIRCRAFT	Page 7	Temp.	Perm
Prepared					
Checked J.J. HAWLETT		Title	Model		
Drawing			Report No.		

REINITIALISATION OF GEAR LINE / DECK INITIAL INTERSECTION POINT FOR NEXT PROGRAM PASS

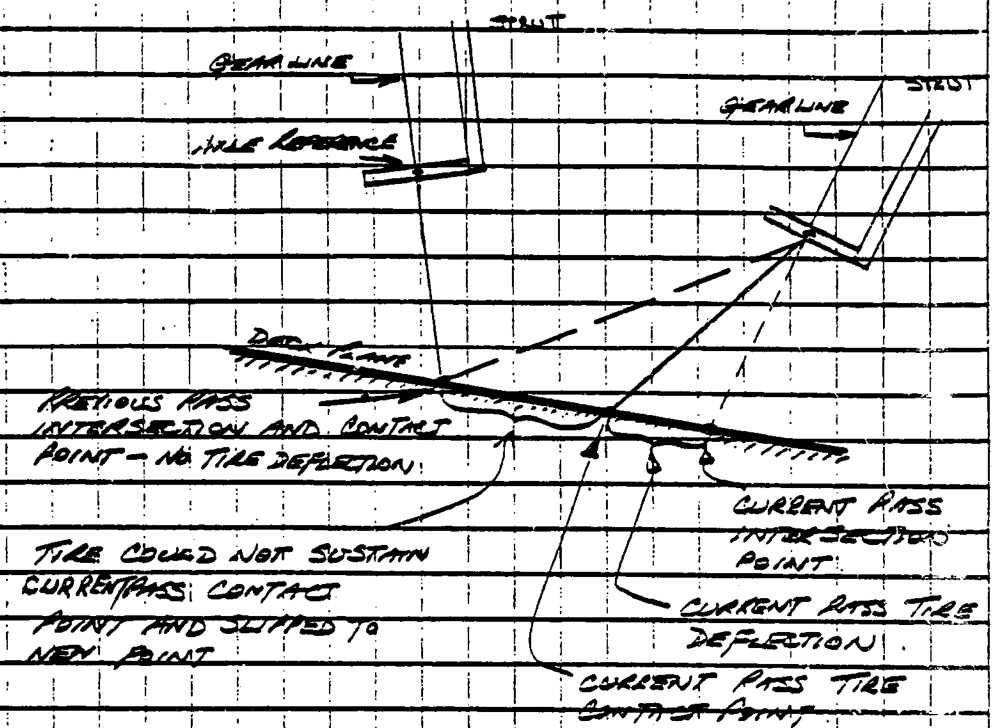

- IF TIRE IS NOT SLIPPING, JUMP OVER THE FOLLOWING EQUATIONS

$$\text{SET } (\Delta X, \Delta Y)_{SLPN,\ SLPR,\ SLPL} = 0$$

- IF TIRE IS SLIPPING IN THE X DIRECTION THE TIRE DEFLECTION IS GIVEN BY

$$(\Delta X_{SLP})_{N,R,L} = -\frac{(X)_{FTHN,\ FTHR,\ FTHL}}{K_{TXN,\ TXR,\ TXL}} \qquad \begin{matrix} DELSDN \\ DELSDR \\ DELSDL \end{matrix}$$

- IF TIRE IS SLIPPING IN THE Y DIRECTION THE TIRE DEFLECTION IS GIVEN BY

$$(\Delta Y_{SLP})_{N,R,L} = -\frac{(Y)_{FTHN,\ FTHR,\ FTHL}}{K_{TYN,\ TYR,\ TYL}} \qquad \begin{matrix} DELSDN+1 \\ DELSDR+1 \\ DELSDL+1 \end{matrix}$$

ORIGINAL PAGE IS
OF POOR QUALITY

SER 70452

SIKORSKY AIRCRAFT

Prepared | Name | Date | Page | Temp | Rev
Checked | Title | Model
Drawing | Report No.

AMOUNT OF WHEEL SLIP IN THE GROUND PLANE

$$\begin{bmatrix}\Delta X\\ \Delta Y\\ \Delta Z\end{bmatrix}_{\substack{SLPSN\\SLPSR\\SLPSL}} = \begin{bmatrix} A_{HBS}\end{bmatrix}\begin{bmatrix}\Delta X\\ \Delta Y\\ \Delta Z\end{bmatrix}_{\substack{SLPN\\SLPR\\SLPL}}$$

→ DELSSN, DELSSR, DELSSL
→ +1, +1, +1
→ +2, +2, +2

INITIAL INTERSECTION POINT AS MODIFIED BY TIRE SLIP FOR NEXT PROGRAM PASS

$$\left(X_{ID}\right)_{\substack{NGO\\RGO\\LGO}} = \left(X_{INT}\right)_{\substack{NG\\RG\\LG}} - \left(\Delta X_{SLPS}\right)_{\substack{N\\R\\L}}$$

→ IDNG, IDRG, IDLG

$$\left(Y_{ID}\right)_{\substack{NGO\\RGO\\LGO}} = \left(Y_{INT}\right)_{\substack{NG\\RG\\LG}} - \left(\Delta Y_{SLPS}\right)_{\substack{N\\R\\L}}$$

→ IDNG+1, IDRG+1, IDLG+1

SA 163 REV

ACCELERATION OF THE UNSPRUNG WHEEL MASS

NOSE GEAR

- IF $Z_{FTAN} > -F_{PREN}$

  SET $\ddot{\delta}_{NG} = \dot{\delta}_{NG} = \delta_{NG} = 0$, DL..NG, DL.NG, DLNG

  $F_{STRN} = -Z_{FTAN}$, FSTRN

- IF $Z_{FTAN} \leq -F_{PREN}$ THIS LOGIC SHOULD BE RETAINED IF $\delta_{NG} > 0$

$$\ddot{\delta}_{NG} = -\frac{1}{M_{NG}}\left\{Z_{FTAN} + F_{STRN}\right\}$$

$$\dot{\delta}_{NG} = \int \ddot{\delta}_{NG}\, dt$$

$$\delta_{NG} = \int \dot{\delta}\, dt$$

FOR NEXT PROGRAM PASS

$$F_{STRN} = \frac{\dot{\delta}_{NG}}{|\dot{\delta}_{NG}|} \cdot \left\{C_{NG}\left(\dot{\delta}_{NG}\right)^2 + F_{DNGO}\right\} + F_{STFN}$$

, FSTRN

, FSTFN

WHERE

$$F_{STFN} = \left\{\frac{C_{PVN}}{\left(\frac{C_{PVN}}{F_{PREN}}\right) - \delta_{NG}}\right\}$$

DENOMINATOR LIMITED TO $\geq .01$

SA 29 REV. 6

RIGHT MAIN GEAR (LEFT GEAR SIMILAR)

- IF $Z_{FTAR} > -F_{PREM}$

  SET $\ddot{\delta}_{RG} = \dot{\delta}_{RG} = \delta_{RG} = 0$, DL..RG, DL.RG, DLRG

  $F_{STRR} = -Z_{FTAR}$, FSTRR

- IF $Z_{FTAR} \leq -F_{PREM}$ THIS LOGIC SHOULD BE RETAINED IF $\delta_{RG} > 0$

$$\ddot{\delta}_{RG} = -\frac{1}{M_{MG}} \left\{ Z_{FTAR} + F_{STRR} \right\}$$

$$\dot{\delta}_{RG} = \int \ddot{\delta}_{RG} \, dt$$

$$\delta_{RG} = \int \dot{\delta}_{RG} \, dt$$

FOR NEXT PROGRAM PASS

$$F_{STRR} = \frac{\dot{\delta}_{RG}}{|\dot{\delta}_{RG}|} \left\{ C_{RG} (\dot{\delta}_{RG})^2 + F_{DRGO} \right\} + F_{STFR}$$

WHERE

$$F_{STFR} = \left\{ \frac{C_{PVM}}{\left(\frac{C_{PVM}}{F_{PREM}}\right) - \delta_{RG}} \right\}$$

DENOMINATOR LIMITED TO $> .01$

GEAR LOADS AT THE GEAR REFERENCE POINT

- IF STRUT LOADS ARE TO BE BYPASSED $(STLDSW \neq 0)$

$$(Z)_{\substack{FGRN\\FGRR\\FGRL}} = (Z)_{\substack{FTAN\\FTAR\\FTAL}} \qquad \substack{,\ FGRN+2\\,\ FGRR+2\\,\ FGRL+2}$$

- IF STRUT LOADS ARE TO BE USED $(STLDSW = 0)$

$$(Z)_{\substack{FGRN\\FGRR\\FGRL}} = -(F)_{\substack{STRN\\STRR\\STRL}}$$

VERTICAL GEAR LOAD FILTERS

$$(Z)_{\substack{FGRN\\FGRR\\FGRL}} = (Z)_{\substack{FGRN\\FGRR\\FGRL}} * \frac{1}{(1+T_{FGR}S)}$$

MOMENTS AT REFERENCE POINT

$$(L)_{\substack{FGRN\\FGRR\\FGRL}} = -Y_{\substack{FTAN\\FTAR\\FTAL}}\left(Z_{\substack{NGA\\RMGA\\LMGA}} - \delta_{\substack{NG\\RG\\LG}}\right) + L_{\substack{FTAN\\FTAR\\FTAL}} \qquad \substack{,\ FGRN+3\\,\ FGRR+3\\,\ FGRL+3}$$

$$(M)_{\substack{FGRN\\FGRR\\FGRL}} = X_{\substack{FTAN\\FTAR\\FTAL}}\left(Z_{\substack{NGA\\RMGA\\LMGA}} - \delta_{\substack{NG\\RG\\LG}}\right) + M_{\substack{FTAN\\FTAR\\FTAL}} \qquad \substack{,\ FGRN+4\\,\ FGRR+4\\,\ FGRL+4}$$

$$(N)_{\substack{FGRN\\FGRR\\FGRL}} = N_{\substack{FTAN\\FTAR\\FTAL}} \qquad \substack{,\ FGRN+5\\,\ FGRR+5\\,\ FGRL+5}$$

GEAR LOADS AT THE HELICOPTER CG

$$X_{LG} = X_{FTAN} + X_{FTAR} + X_{FTAL} \qquad , XLG$$

$$Y_{LG} = Y_{FTAN} + Y_{FTAR} + Y_{FTAL} \qquad , YLG$$

$$Z_{LG} = Z_{FGRN} + Z_{FGRR} + Z_{FGRL} \qquad , ZLG$$

$$L_{LG} = Y_{RMGA}(Z_{FGRR} - Z_{FGRL}) + L_{FGRN} + L_{FGRR} + L_{FRRL} \qquad , LLG$$

$$M_{LG} = -Z_{FGRN} X_{NGA} - (Z_{FGRR} + Z_{FGRL}) X_{RMGA} + M_{FGRN} + M_{FGRR} + M_{FGRL} \qquad , MLG$$

$$N_{LG} = Y_{FTAN} X_{NGA} + (Y_{FTAR} + Y_{FTAL}) X_{RMGA} + (X_{FTAL} - X_{FTAR}) Y_{RMGA} + N_{FGRN} + N_{FGRR} + N_{FGRL} \qquad , NLG$$

5.7.3 LANDING INTERFACE MODULE INPUT/OUTPUT DATA TRANSFER

INPUT TRANSFER	
PARAMETER	ORIGIN MODULE
FSCGB	MAIN ROTOR
WLCGB	MAIN ROTOR
VN	MOTION
VE	MOTION
VZ	MOTION
THETAB	MOTION
PHIB	MOTION
PSIB	MOTION
$[A_{HBS}]$	MOTION

OUTPUT TRANSFER	
PARAMETER	DESTINATION MODULE
XLG	MOTION
YLG	MOTION
ZLG	MOTION
LLG	MOTION
MLG	MOTION
NLG	MOTION

5.7.4 NOTATION FOR GEN. HEL. LANDING SIMULATION

SYMBOL USED IN EQUATIONS	PROGRAM MNEMONIC	UNITS	DESCRIPTION
X_{SH}	SH	FT	Helicopter center of gravity position in space axes.
Y_{SH}	SH+1	FT	
Z_{SH}	SH+2	FT	
X_{SHO}	SHO	FT	Initial position of helicopter in space axes.
Y_{SHO}	SHO+1	FT	
Z_{SHO}	SHO+2	FT	
V_N	V_N	FT/SEC	Helicopter space axes velocities.
V_E	V_E	FT/SEC	
V_Z	V_Z	FT/SEC	
FSCGB	FSCGB	INS.	Helicopter c.g. less rotor.
WLCGB	WLCGB	INS.	
FSNGA	FSNGA	INS.	Fuse. stat. of nose gear strut.
FSMGA	FSMGA	INS.	Fuse. stat. of main gear strut.
BLMGA	BLMGA	INS.	Butt. stat. of main gear strut

NOTATION FOR GEN. HEL. LANDING SIMULATION

SYMBOL USED IN EQUATIONS	PROGRAM MNEMONIC	UNITS	DESCRIPTION
WLNGAO	WLNGAO	INS	WL. position of free extension
WLMGAO	WLRMGA	INS	of the axle.
X_{NGA}	NGA	FT	Position of freely extended
X_{MGA}	RMGA, LMGA.	FT	axles in body axes.
Y_{NGA}	NGA+1	FT	
Y_{RMGA}	RMGA+1	FT	
Y_{LMGA}	LMGA+1	FT	
Z_{NGA}	NGA+2	FT	
Z_{MGRA}	RMGA+2	FT	
Z_{MGLA}	LMGA+2	FT	
R_{TN}	RTNF	INS	Nominal nose tire radius.
R_{TM}	RTMF	INS	Nominal main tire radius.
$[A_{HBS}]$	Defined in the Motion Module		Helicopter body to space axes transformation matrix.
X_{NTSO}	NTSO	FT	Nose tire reference position
Y_{NTSO}	NTSO+1	FT	in space axes under free
Z_{NTSO}	NTSO+2	FT	extension.
X_{RMTSO}	RMTSO	FT	Right tire reference position
Y_{RMTSO}	RMTSO+1	FT	in space axes under free
Z_{RMTSO}	RMTSO+2	FT	extension.

NOTATION FOR GEN. HEL. LANDING SIMULATION

SYMBOL USED IN EQUATIONS	PROGRAM MNEMONIC	UNITS	DESCRIPTION
X_{LMTSO}	LMTSO	FT	Left tire reference position in space axes under free extension.
Y_{LMTSO}	LMTSO+1	FT	
Z_{LMTSO}	LMTSO+2	FT	
δ_{NG}	DLNG	FT	Nose strut deflection
δ_{RG}	DLRG	FT	Right
δ_{LG}	DLLG	FT	Left
X_{NAS}	NAS	FT	Nose axle referen. position in space axes.
Y_{NAS}	NAS+1	FT	
Z_{NAS}	NAS+2	FT	
X_{RAS}	RAS	FT	Right axle reference position in space axes.
Y_{RAS}	RAS+1	FT	
Z_{RAS}	RAS+2	FT	
X_{LAS}	LAS	FT	Left axle reference position in space axes.
Y_{LAS}	LAS+1	FT	
Z_{LAS}	LAS+2	FT	
X_{NGSR}	NGSR	FT	Nose gear reference position in space axes
Y_{NGSR}	NGSR+1	FT	
Z_{NGSR}	NGSR+2	FT	

NOTATION FOR GEN. HEL. LANDING SIMULATION

SYMBOL USED IN EQUATIONS	PROGRAM MNEMONIC	UNITS	DESCRIPTION
X_{MGRSR}	RMGSR	FT	Right gear reference position in space axes
Y_{MGRSR}	RMGSR+1	FT	
Z_{MGRSR}	RMGSR+2	FT	
X_{MGLSR}	LMGSR	FT	Left gear reference position in space axes
Y_{MGLSR}	LMGSR+1	FT	
Z_{MGLSR}	LMGSR+2	FT	
WLFD	WLFD	FT	Height of ground plane.
d_{NNA}	DNNA	FT	Normal distance from the ground plane to axle reference point for nose, right and left gear.
d_{NRA}	DNRA	FT	
d_{NLA}	DNLA	FT	
$\cos\alpha_{NG}$	CSANG		Direction cosines of gear line.
$\cos\beta_{NG}$	CSBNG		
$\cos\gamma_{NG}$	CSGNG		
δ_{TNG}	DLTNG	FT	Nose tire radial deflection.
δ_{TRG}	DLTRG	FT	Right tire radial deflection.
δ_{TLG}	DLTLG	FT	Left tire radial deflection.
$(a)_{NG,\ RG,\ LG}$			Coefficients of gear line equation projections in 2D for the nose, right and left landing gear.
$(b)_{NG,\ RG,\ LG}$			
$(c)_{NG,\ RG,\ LG}$			
$(d)_{NG,\ RG,\ LG}$			

NOTATION FOR GEN. HEL. LANDING SIMULATION

SYMBOL USED IN EQUATIONS	PROGRAM MNEMONIC	UNITS	DESCRIPTION
$(X_{ID})_{NGO}$	IDNG	FT	Initial deck contact positions before distortion of tires.
$(Y_{ID})_{NGO}$	IDNG+1	FT	
$(Z_{ID})_{NGO}$	IDNG+2	FT	
$(X_{ID})_{RGO}$	IDRG	FT	
$(Y_{ID})_{RGO}$	IDRG+1	FT	
$(Z_{ID})_{RGO}$	IDRG+2	FT	
$(X_{ID})_{LGO}$	IDLG	FT	
$(Y_{ID})_{LGO}$	IDLG+1	FT	
$(Z_{ID})_{LGO}$	IDLG+2	FT	
$(X_{INT})_{NG}$	INTNG	FT	Intersection of gear line with deck plane in space axes for the nose gear.
$(Y_{INT})_{NG}$	INTNG+1	FT	
$(Z_{INT})_{NG}$	INTNG+2	FT	
$(X_{INT})_{RG}$	INTRMG	FT	Intersection of gear line with deck plane in space axes for the right gear.
$(Y_{INT})_{RG}$	INTRMG+1	FT	
$(Z_{INT})_{RG}$	INTRMG+2	FT	
$(X_{INT})_{LG}$	INTLMG	FT	Intersection of gear line with deck plane in space axes for for left gear.
$(Y_{INT})_{LG}$	INTLMG+1	FT	
$(Z_{INT})_{LG}$	INTLMG+2	FT	
$(\Delta X)_{NG}$	DELNG	FT	Tire deflections in the deck plane for the nose gear.
$(\Delta Y)_{NG}$	DELNG+1	FT	
$(\Delta Z)_{NG}$	DELNG+2	FT	
$(\Delta X)_{RG}$	DELRNG	FT	Tire deflections in the deck plane for the right gear.
$(\Delta Y)_{RG}$	DELRNG+1	FT	
$(\Delta Z)_{RG}$	DELRNG+2	FT	

NOTATION FOR GEN. HEL. LANDING SIMULATION

SYMBOL USED IN EQUATIONS	PROGRAM MNEMONIC	UNITS	DESCRIPTION
$(\Delta X)_{LG}$	DELLMG	FT	Tire deflections in the deck plane for the left gear.
$(\Delta Y)_{LG}$	DELLMG+1	FT	
$(\Delta Z)_{LG}$	DELLMG+2	FT	
$(\Delta X)_{HNG}$	DELHNG	FT	Tire deflections in helicopter body axes for nose gear.
$(\Delta Y)_{HNG}$	DELHNG+1	FT	
$(\Delta Z)_{HNG}$	DELHNG+2	FT	
$(\Delta X)_{HRG}$	DELHRG	FT	Tire deflections in helicopter body axes for right gear.
$(\Delta Y)_{HRG}$	DELHRG+1	FT	
$(\Delta Z)_{HRG}$	DELHRG+2	FT	
$(\Delta X)_{HLG}$	DELHLG	FT	Tire deflection in helicopter body axes for left gear.
$(\Delta Y)_{HLG}$	DELHLG+1	FT	
$(\Delta Z)_{HLG}$	DELHLG+2	FT	
$[A_{HSB}]$	$(= [A_{HBS}]^T)$		Helicopter space to body axes transformation matrix.
$(KTX)_{N,R,L}$	KTXN,R,L	lb/FT	Tire 3 component stiffness coefficients - Note that these can be replaced by loading maps.
$(KTY)_{N,R,L}$	KTYN,R,L	lb/FT	
$(KTZ)_{N,R,L}$	KYZN,R,L	lb/FT	
$(X)_{FTHN}$	FTHN	LB	Tire forces in helicopter body axes for the nose gear.
$(Y)_{FTHN}$	FTHN+1	LB	
$(Z)_{FTHN}$	FTHN+2	LB	

SA 29 REV. G

NOTATION FOR GEN. HEL. LANDING SIMULATION

SYMBOL USED IN EQUATIONS	PROGRAM MNEMONIC	UNITS	DESCRIPTION
$(X)_{FTHR}$	FTHR	LB	Tire forces in helicopter body axes for the right gear.
$(Y)_{FTHR}$	FTHR+1	LB	
$(Z)_{FTHR}$	FTHR+2	LB	
$(X)_{FTHL}$	FTHL	LB	Tire forces in helicopter body axes for the left gear.
$(Y)_{FTHL}$	FTHL+1	LB	
$(Z)_{FTHL}$	FTHL+2	LB	
d_M	DMDM	INCHES	Main gear tire diameter
d_N	DNDN	INCHES	Nose gear tire diameter
P_M	PMRPMR	lb/in^2	Main gear tire pressure
P_{RM}	RAT PRM	lb/in^2	Main gear rated tire pressure
N_{TN}	NTN	-	No. of tail gear wheels
N_{TM}	NTM	-	No. of main gear wheels
P_N	PNPN	lb/in^2	Nose gear tire pressure
P_{RN}	RAT PRN	in/in^2	Nose gear rated tire pressure
$(X)_{FTDN}$	FTDN	LB	Tire forces in the space axes but aligned along helicopter X axis for the nose gear.
$(Y)_{FTDN}$	FTDN+1	LB	
$(Z)_{FTDN}$	FTDN+2	LB	
$(X)_{FTDR}$	FTDR	LB	Tire forces in the space axes but aligned along helicopter X axis for the right gear.
$(Y)_{FTDR}$	FTDR+1	LB	
$(Z)_{FTDR}$	FTDR+2	LB	
$(X)_{FTDL}$	FTDL	LB	Tire forces in the space axes but aligned along helicopter X axis for the left gear.
$(Y)_{FTDL}$	FTDL+1	LB	
$(Z)_{FTDL}$	FTDL+2	LB	

NOTATION FOR GEN. HEL. LANDING SIMULATION

SYMBOL USED IN EQUATIONS	PROGRAM MNEMONIC	UNITS	DESCRIPTION
$K_{\mu B}$	KMUXX		Factor for brakes
BRK	KMUXBK		Value of $K_{\mu B}$ brakes on.
NBRK	KMUXO		Value of $K_{\mu B}$ brakes off.
μ	KMU		Longitudinal tire coef. of friction.
X_{FTDNM}	FTDNM	LB	Max. friction load that can
X_{FTDRM}	FTDRM	LB	be sustained in the X direction.
X_{FTDLM}	FTDLM	LB	
K_{SLIP}	KSLIP		Factor for sliding friction.
Y_{FTDNM}	FTDNM+1	LB	Max. friction load that can be
Y_{FTDRM}	FTDRM+1	LB	sustained in the Y direction.
Y_{FTDLM}	FTDLM+1	LB	
$((\Delta X)_{SLP})_N$	DELSPN	FT	Amount of tire deflection
$((\Delta X)_{SLP})_R$	DELSPR	FT	sustained during slip conditions
$((\Delta X)_{SLP})_L$	DELSPL	FT	in the X direction.
$(\Delta Y_{SLP})_N$	DELSPN+1	FT	Amount of tire deflection
$(\Delta Y_{SLP})_R$	DELSPR+1	FT	sustained during slip conditions
$(\Delta Y_{SLP})_L$	DELSPL+1	FT	in the Y direction.

NOTATION FOR GEN. HEL. LANDING SIMULATION

SYMBOL USED IN EQUATIONS	PROGRAM MNEMONIC	UNITS	DESCRIPTION
$(X)_{FTAN}$	FTAN	LB	Tire forces and moments at the axle reference position, nose gear.
$(Y)_{FTAN}$	FTAN+1	LB	
$(Z)_{FTAN}$	FTAN+2	LB	
$(L)_{FTAN}$	FTAN+3	FT	
$(M)_{FTAN}$	FTAN+4	FT	
$(N)_{FTAN}$	FTAN+5	FT	
$(X)_{FTAR}$	FTAR	LB	Tire forces and moments at the axle reference position, right gear.
$(Y)_{FTAR}$	FTAR+1	LB	
$(Z)_{FTAR}$	FTAR+2	LB	
$(L)_{FTAR}$	FTAR+3	FT	
$(M)_{FTAR}$	FTAR+4	FT	
$(N)_{FTAR}$	FTAR+5	FT	
$(X)_{FTAL}$	FTAL	LB	Tire forces and moments at the axle reference position, left gear.
$(Y)_{FTAL}$	FTAL+1	LB	
$(Z)_{FTAL}$	FTAL+2	LB	
$(L)_{FTAL}$	FTAL+3	FT	
$(M)_{FTAL}$	FTAL+4	FT	
$(N)_{FTAL}$	FTAL+5	FT	
$(\Delta X)_{SLPSN}$	DELSSN	FT	Amount of slippage of gear intersection point is space axes, nose gear.
$(\Delta Y)_{SLPSN}$	DELSSN+1	FT	
$(\Delta Z)_{SLPSN}$	DELSSN+2	FT	

NOTATION FOR GEN. HEL. LANDING SIMULATION

SYMBOL USED IN EQUATIONS	PROGRAM MNEMONIC	UNITS	DESCRIPTION
$(\Delta X)_{SLPSR}$	DELSSR	FT	Amount of slippage of gear
$(\Delta Y)_{SLPSR}$	DELSSR+1	FT	intersection point is space
$(\Delta Z)_{SLPSR}$	DELSSR+2	FT	axes, right gear.
$(\Delta X)_{SLPSL}$	DELSSL	FT	Amount of slippage of gear
$(\Delta Y)_{SLPSL}$	DELSSL+1	FT	intersection point is space
$(\Delta Z)_{SLPSL}$	DELSSL+2	FT	axes, left gear.
$(\ddot{\delta})_{NG}$	DL..NG	FT	Wheel axle motion along strut
$(\ddot{\delta})_{RG}$	DL..RG	FT	line
$(\ddot{\delta})_{LG}$	DL..LG	FT	
$(\dot{\delta})_{NG}$	DL.NG	FT	
$(\dot{\delta})_{RG}$	DL.RG	FT	
$(\dot{\delta})_{LG}$	DL.LG	FT	
$(\delta)_{NG}$	DLNG	FT	
$(\delta)_{RG}$	DLRG	FT	
$(\delta)_{LG}$	DLLG	FT	
F_{PREN}	FPREN	LB	Nose gear strut preload.
F_{PREM}	FPREM	LB	Main gear strut preload.
F_{STRN}	FSTRN	LB	Strut force transferred to
F_{STRR}	FSTRR	LB	airframe for the nose, right
F_{STRL}	FSTRL	LB	and left gear.
M_{NG}	MASNG	SLUGS	Unsprung mass of nose gear.
M_{MG}	MASMG	SLUGS	Unsprung mass of main gear.

NOTATION FOR GEN. HEL. LANDING SIMULATION

SYMBOL USED IN EQUATIONS	PROGRAM MNEMONIC	UNITS	DESCRIPTION
C_{NG}	CNG	$LB/(FT/SEC)^2$	Velocity squared damping for
C_{MG}	CMG	$LB/(FT/SEC)^2$	nose and main gear struts
RTRTT	RTRTT	FT/SEC	Velocity break points on
LFRTT	LFRTT	FT/SEC	strut damping
CRGH	CRGH	$LB/(FT/SEC)^2$	Corresponding damping coef.
CLGH	CLGH	$LB/(FT/SEC)^2$	of velocity squared damping
CRGL	CRGL	$LB/(FT/SEC)^2$	for the main gear.
CLGL	CLGL	$LB/(FT/SEC)^2$	
KOLEOM	KOLEOM	LB-FT	Isothermal air spring coef. main gear.
	KSP+7	FT	Free extension of main gear.
	KSP+10	FT	
KOLEON	KOLEON	LB-FT	Isothermal air spring coef. nose gear
	KSP+6	FT	Free extension of nose gear.
$(X)_{FGRN}$	FGRN	LB	Gear forces and moment at
$(Y)_{FGRN}$	FGRN+1	LB	the gear reference positions —
$(Z)_{FGRN}$	FGRN+2	LB	nose gear.
$(L)_{FGRN}$	FGRN+3	FT	
$(M)_{FGRN}$	FGRN+4	FT	
$(N)_{FGRN}$	FGRN+5	FT	
$(X)_{FGRR}$	FGRR	LB	Gear forces and moment at
$(Y)_{FGRR}$	FGRR+1	LB	the gear reference positions —
$(Z)_{FGRR}$	FGRR+2	LB	right gear.
$(L)_{FGRR}$	FGRR+3	FT	
$(M)_{FGRR}$	FGRR+4	FT	
$(N)_{FGRR}$	FGRR+5	FT	

NOTATION FOR GEN. HEL. LANDING SIMULATION

SYMBOL USED IN EQUATIONS	PROGRAM MNEMONIC	UNITS	DESCRIPTION
$(X)_{FGRL}$	FGRL	LB	Gear forces and moment at the gear reference positions — left gear.
$(Y)_{FGRL}$	FGRL+1	LB	
$(Z)_{FGRL}$	FGRL+2	LB	
$(L)_{FGRL}$	FGRL+3	FT	
$(M)_{FGRL}$	FGRL+4	FT	
$(N)_{FGRL}$	FGRL+5	FT	
X_{LG}	XLG	LB	Total gear loads at the helicopter CG in body axes.
Y_{LG}	YLG	LB	
Z_{LG}	ZLG	LB	
L_{LG}	LLG	FT	
M_{LG}	MLG	FT	
N_{LG}	NLG	FT	

5.7.5 BLACKHAWK LANDING MODULE INPUT DATA

MAIN GEAR

TIRE INPUT CONSTANTS:

$R_{TM} = 12.65''$ $D_{TM} = 25.3''$

$P_M = 140$ PSI

$P_{RM} = 110$ PSI

$N_{TM} = 1$

$FSMGA = 297.43$

$WLMGA = 184.8$

$BLMGA = 53.2$

$M_{MG} = 2.6708$ SLUGS.

$G_{DR} = .003$ $(= G_{DL})$

STRUT INPUT CONSTANTS:

$C_{PYM} = 3465.$ Ft lbs

$F_{PREM} = 3000$ lb

$\gamma = 1.34$

IF $|\dot{S}|_{RG,LG} \leq 1.4167$ ft/sec $C_{RG,LG} = 1382.4$ lb $\frac{sec^2}{ft^2}$

$F_{DRGO}, F_{DLGO} = 0$

IF $|\dot{S}|_{RG,LG} > 1.4167$ ft/sec $C_{RG,LG} = 216.0$ lb $\frac{sec^2}{ft^2}$

$F_{DRGO}, F_{DLGO} = 2340.98$

SA 29 REV. G

TABLE 7.5.1

SOLUTION FOR CUBE ROOT IN TIRE INPLANE STIFFNESS EQUATIONS

LET $$P = \left(\frac{12 \cdot \Delta Z_{HNG,\ HRG,\ HLG}}{D_{TN,\ TM}} \right)$$

RANGE $0 \leq P \leq .02$

P	$P^{1/3}$
0	·0
·002	·12599
·004	·15874
·006	·18171
·008	·20000
·010	·21544
·012	·22894
·014	·24101
·016	·25198
·018	·26207
·020	·27144

RANGE $.02 < P \leq .3$

P	$P^{1/3}$
·020	·27144
·04	·34200
·06	·39149
·08	·43089
·10	·46416
·12	·49324
·14	·51925
·16	·54288
·18	·56462
·20	·58480
·22	·60368
·24	·62145
·26	·63825
·28	·65421
·30	·66943

(MAIN GEAR CONT)

TIRE LONGITUDINAL STIFFNESS :

$$K_{TXR} = .53\, D_{TM}(P_M + 4 P_{RM})\left(\frac{12\ \Delta Z_{HRG}}{D_{TM}}\right)^{1/3} .\ 12 \quad lb/ft$$

$$K_{TXL} = .53\, D_{TM}(P_M + 4 P_{RM})\left(\frac{12\ \Delta Z_{HLG}}{D_{TM}}\right)^{1/3} .\ 12 \quad lb/ft$$

TABLE 7.5.2 TIRE LATERAL STIFFNESS $0 \le \Delta Z_{HRG,HLG} \le .11667$

	P_M PSI		
	90	120	150
$12*\lvert\Delta Z_{HRG}\rvert$ / $12*\lvert\Delta Z_{HLG}\rvert$	K_{TYR} / K_{TYL} lb/INCH		
0	0	0	0
.1	950	1030	1090
.2	1260	1340	1430
.3	1430	1560	1700
.4	1560	1740	1920
.5	1630	1840	2080
.6	1680	1940	2210
.7	1710	2000	2310
.8	1730	2060	2410
.9	1740	2080	2530
1.0	1740	2100	2560
1.1	1735	2155	2530
1.2	1730	2210	2500
1.3	1720	2155	2460
1.4	1710	2120	2420

NOTE : OUTPUT OF THIS MAP TO BE MULTIPLIED BY 12 TO OBTAIN lb/ft

SA 29 REV. G

(MAIN GEAR CONT)

LATERAL STIFFNESS (CONT)

$$.11667 \le \Delta Z_{HRG,HLG} \le .25$$

	90	120	150
1.4	1710	2120	2420
3.0	1360	1800	2140

NOTE: OUTPUT OF THIS MAP TO BE MULTIPLIED BY 12 TO OBTAIN lb/ft

TABLE 7.5.3 TIRE VERTICAL LOAD DEFLECTION DATA

	P_M PSI		
	90	120	150
$12 * \lvert \Delta Z_{HRG} \rvert$ $12 * \lvert \Delta Z_{HLG} \rvert$	Z_{FTHR} , Z_{FTHL}		
0	0	0	0
.1	3100	3800	4600
2	6900	8800	10600
3	11500	14200	17000
4	16300	19900	23900
5	21000	26300	31600
6	32100	42000	51900
7	48150	63000	77850
8	72220	94490	116760

CALCULATE $K_{TZR,TZL} = \dfrac{Z_{FTHR,FTHL}}{\Delta Z_{HRG,HLG}}$

FOR ENTRY INTO GENERAL EQUATIONS

SA 29 REV. 6

(MAIN GEAR CONT)

TABLE 7.5.4 VERTICAL TIRE STIFFNESS (USED IN DAMPING CALCULATIONS)

	PM PSI		
	90	120	150
$-Z_{FTHR}$; lb $-Z_{FTHL}$; lb	K_{TZR}', K_{TZL}, lb/INCH		
0	2970	3600	4170
4000	3710	4630	5390
8000	4320	5240	6030
12000	4600	5510	6300
16000	4780	5710	6500

NOTE OUTPUT OF THIS MAP TO BE MULTIPLIED BY 12 TO OBTAIN lb/ft.

TAIL GEAR

TIRE INPUT CONSTANTS :

$R_{TN} = 7.5''$ $D_{TN} = 15''$
$P_N = 90$ PSI
$P_{RN} = 110$ PSI
$N_{TN} = 1$
$FSNGA = 644.62$
$WLNGA = 180.4$
$BLNGA = 0$
$M_{NG} = 1.0$ SLUGS.
$G_{DN} = .003$

STRUT INPUT CONSTANTS :

$C_{PVN} = 2208.0$ FT 6
$F_{AREN} = 1251.0$
$\gamma = 1.34$

$C_{NG} = 66.72$
$F_{DNGO} = 0.0$

(TAIL GEAR CONT)

TIRE LONGITUDINAL STIFFNESS

$$K_{TXN} = .53\, D_{TN}(P_N + 4P_{RN})\left(\frac{12\,\Delta Z_{HNG}}{D_{TN}}\right)^{1/3} \cdot 12 \quad lb/ft$$

TIRE LATERAL STIFFNESS

$$K_{TYN} = 19.7\,(Z_{FTHN})^{1/2} \cdot 12 \quad lb/ft$$

TABLE 7.5.5 VERTICAL LOAD ~ DEFLECTION DATA

	P_N PSI		
	90	120	150
$12 * \Delta Z_{HNG}$	Z_{FTHN}, lb		
0	0	0	0
.5	950	1150	1380
1.0	2100	2500	2900
1.5	3350	4000	4690
2.0	4700	5600	6500
2.5	6300	7450	8600
3.0	10000	11800	13700
3.5	18300	21900	25800
4.0	26600	32000	38000
4.5	34900	42100	50100
5.0	43200	52200	62300

(TAIL GEAR CONT)

VERTICAL STIFFNESS FOR USE IN THE TIRE DAMPING EQUATIONS
TABLE 7.5.6

$-Z_{FTHN}$	K'_{TZN}
0	2040
4000	2630
8000	4050
12000	6000
16000	6000

NOTE OUTPUT OF THIS MAP TO BE MULTIPLIED BY 12 TO OBTAIN lb/ft

GENERAL LANDING MODULE INPUT DATA

$W_{LFD} = 0$
$\mu = 0.6$
$B_{RK} = 1.0$
$N_{BRK} = .01$
$K_{SLIP} = .85$

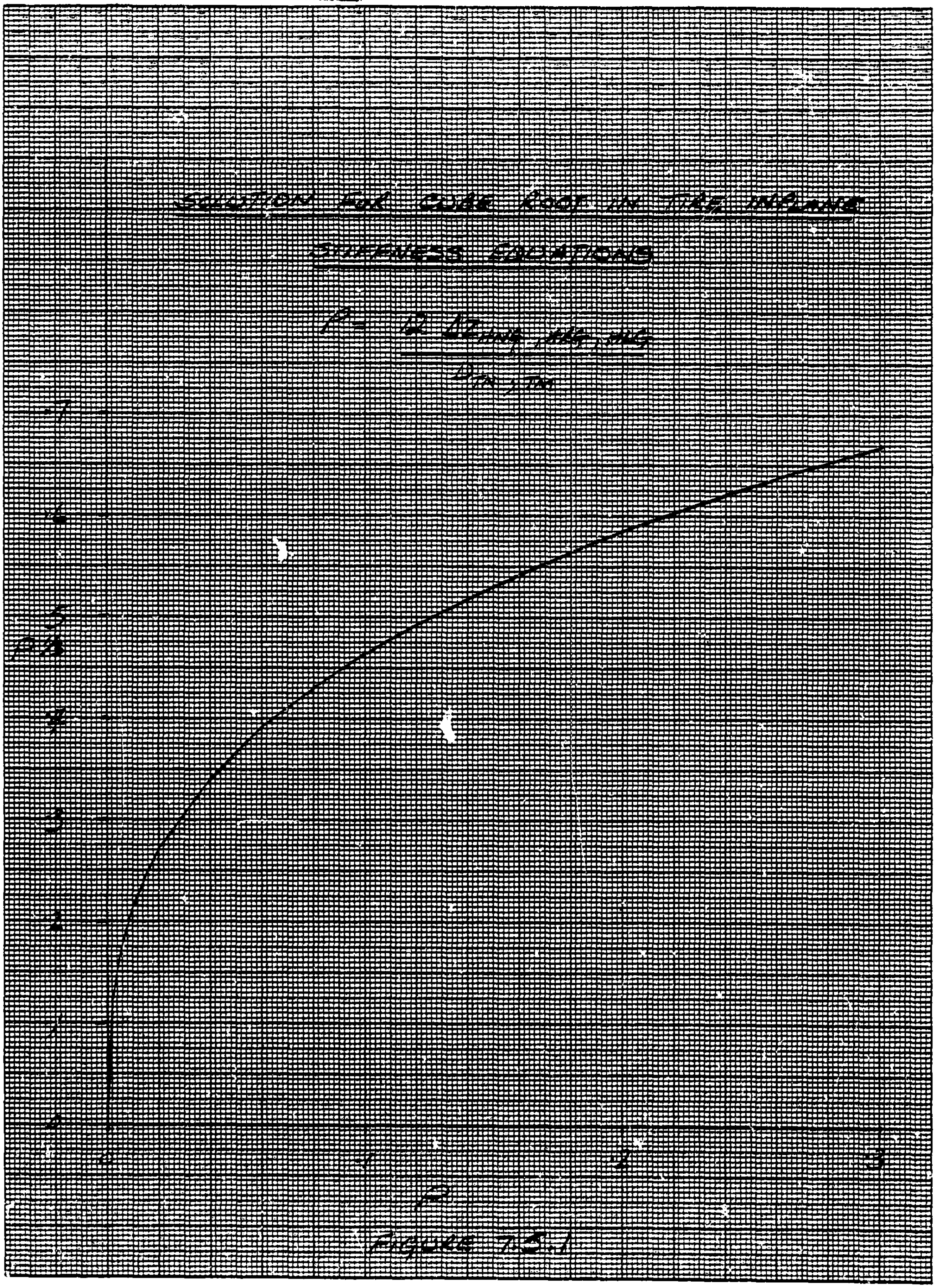
SOLUTION FOR CUBE ROOT IN THE INPLANE
STIFFNESS EQUATIONS
.7
.6
.5
.4
.3
.2
.1
0
0
.1
.2
.3
ρ

FIGURE 7.5.1

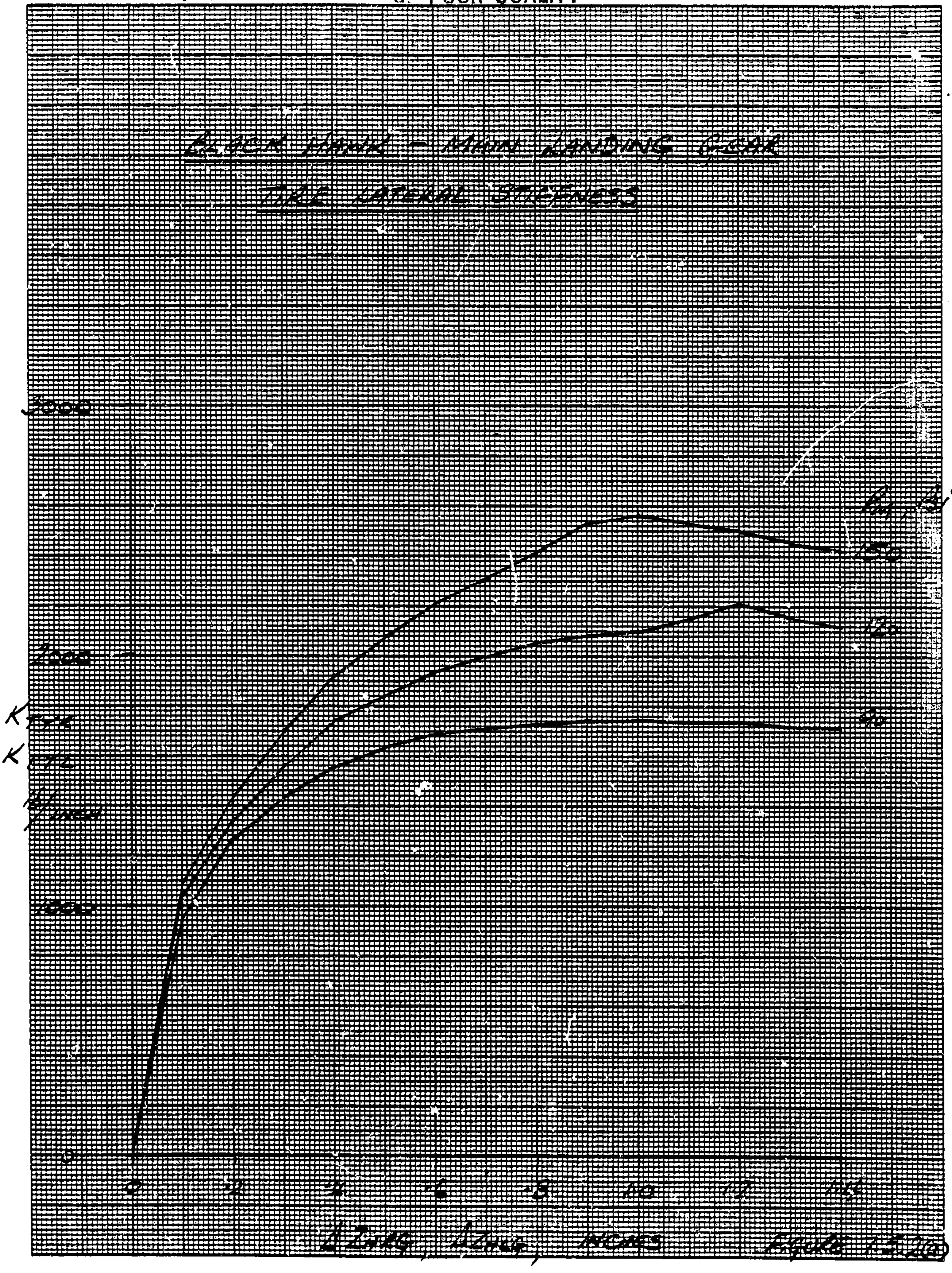
BLACK HAWK - MAIN LANDING GEAR
TIRE LATERAL STIFFNESS
3000
2000
1000
0
K TYR
K TYL
LB/INCH
150
120
90
0
.2
.4
.6
.8
1.0
1.2
1.4
ΔZNRG, ΔZNLG, INCHES

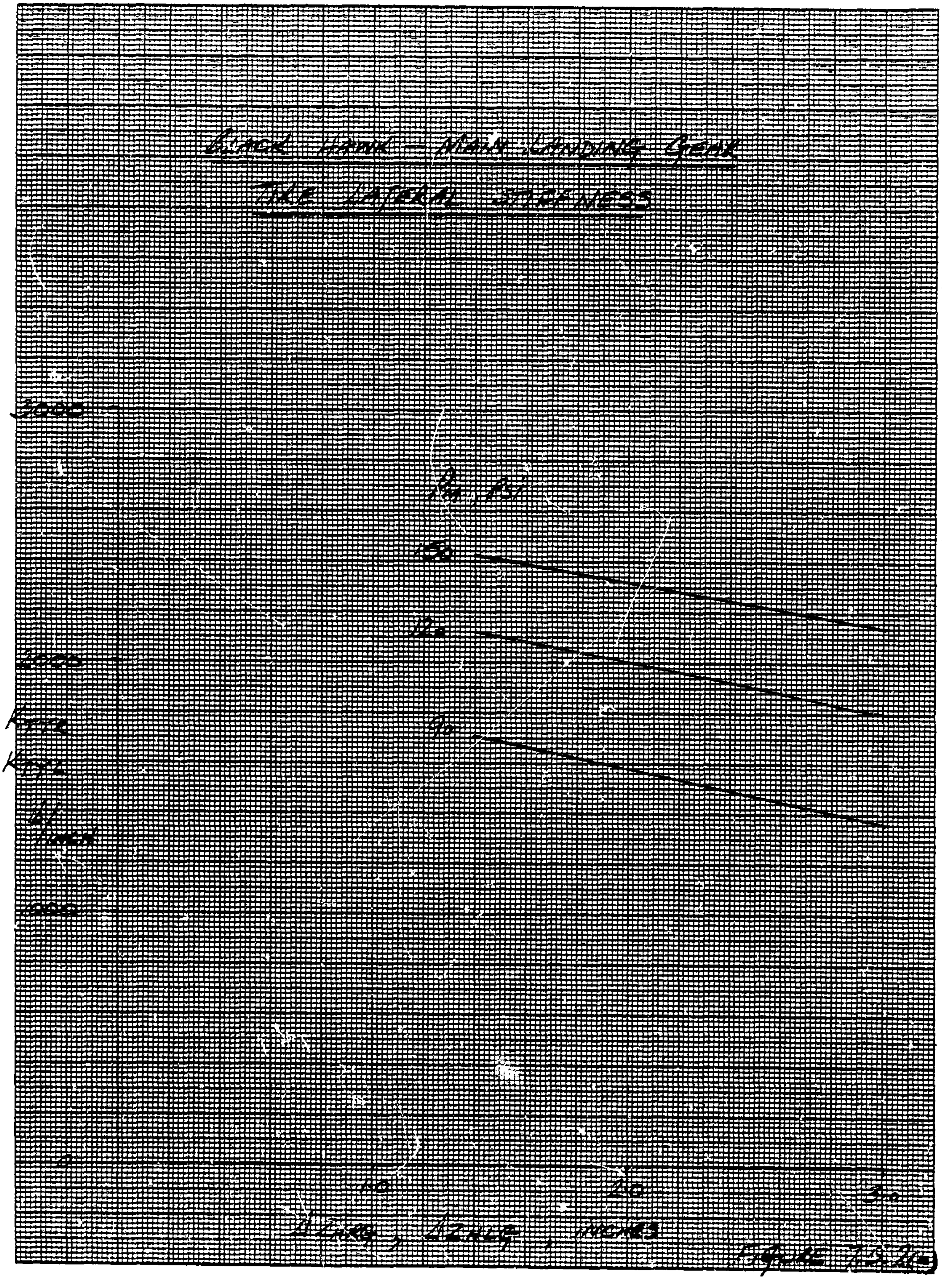
BLACK HAWK — MAIN LANDING GEAR
TIRE LATERAL STIFFNESS
3000
2000
1000
0
PSI
150
120
90
LB/INCH
10
20
30
INCHES

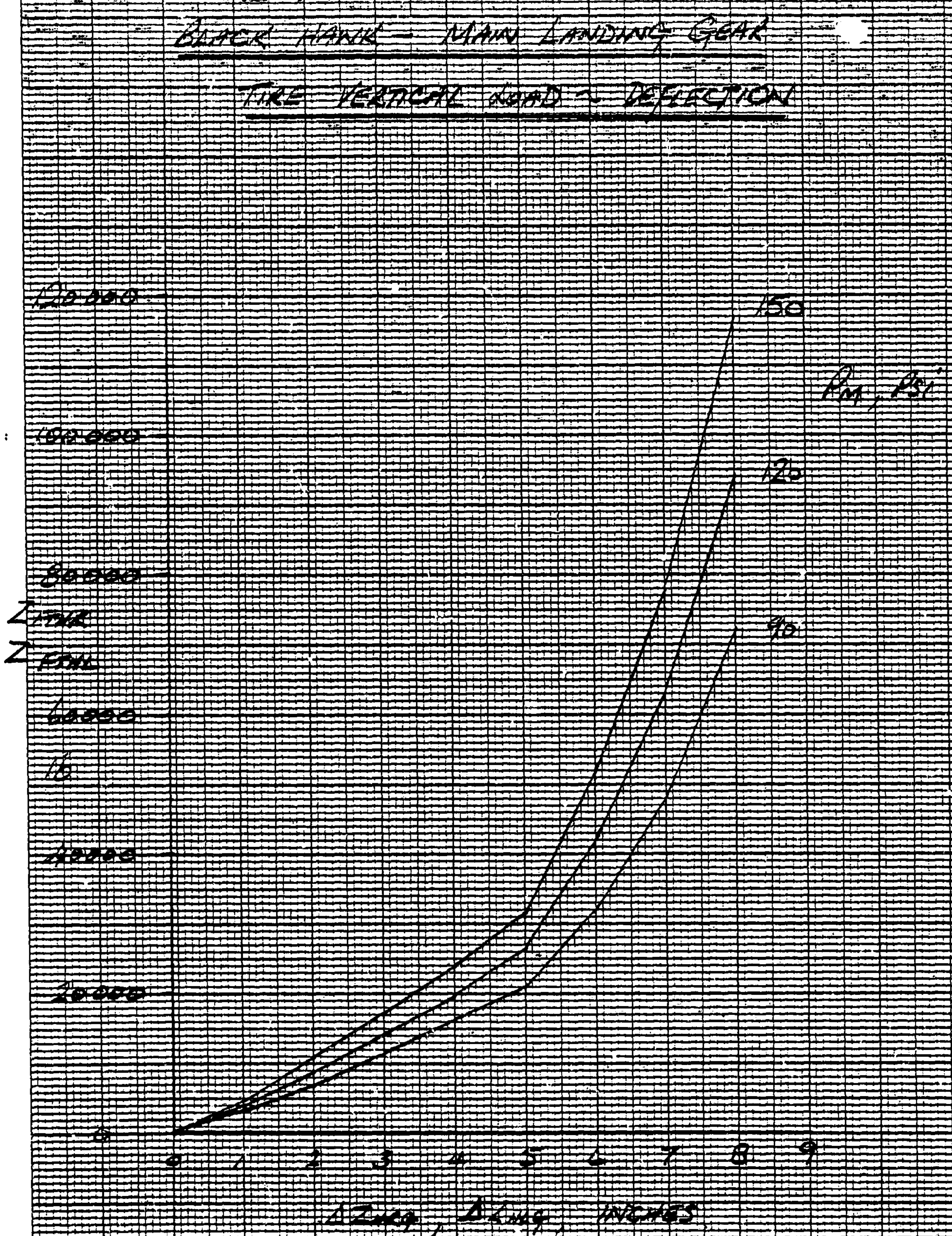
BLACK HAWK - MAIN LANDING GEAR
TIRE VERTICAL LOAD ~ DEFLECTION
120000
100000
80000
60000
40000
20000
0
0 1 2 3 4 5 6 7 8 9
150
120
90
PM, PSI
ΔZMG, ΔZMG, INCHES

FIGURE 15.3

BLACK HAWK – MAIN LANDING GEAR

TIRE VERTICAL STIFFNESS
(USED ONLY FOR TIRE DAMPING)

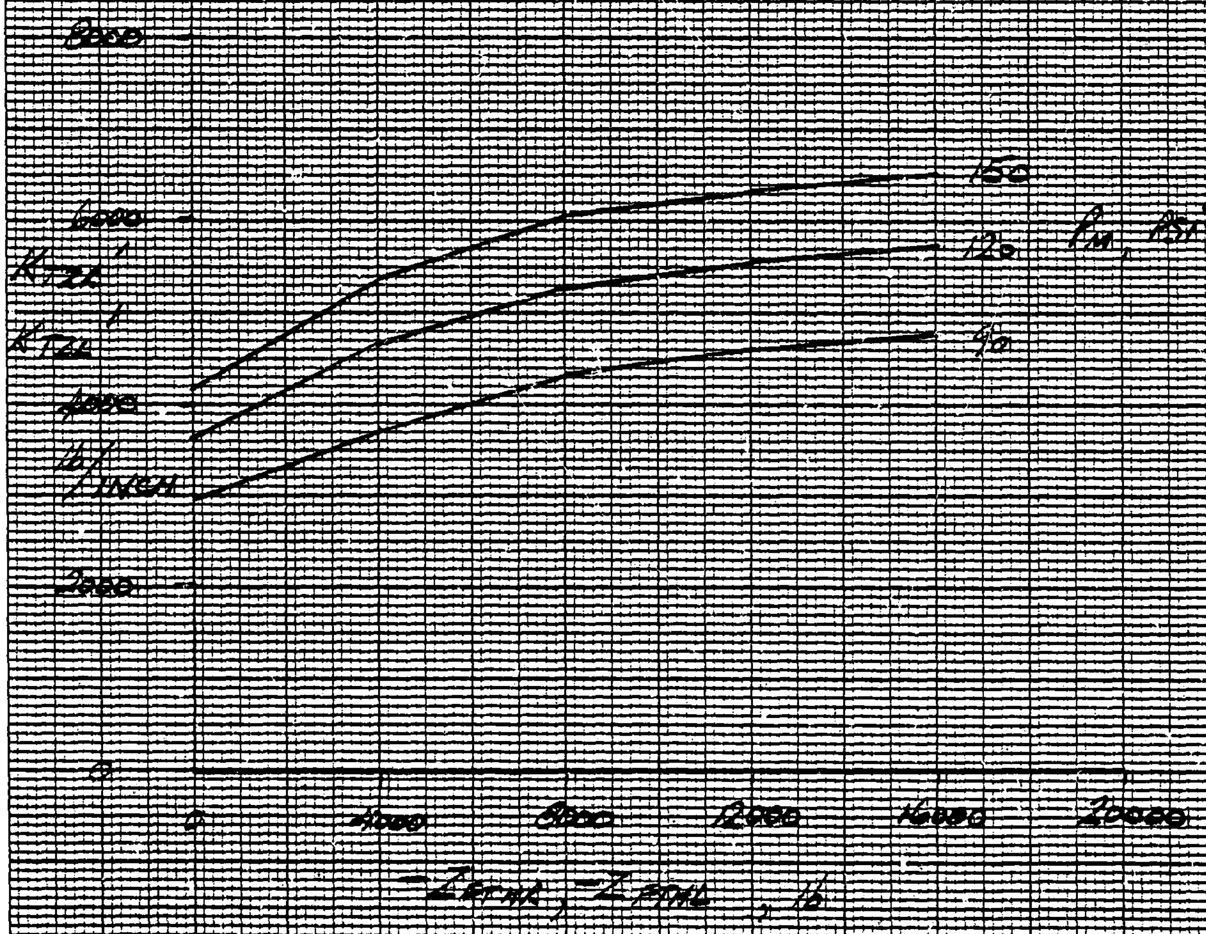

FIGURE 7.5.4

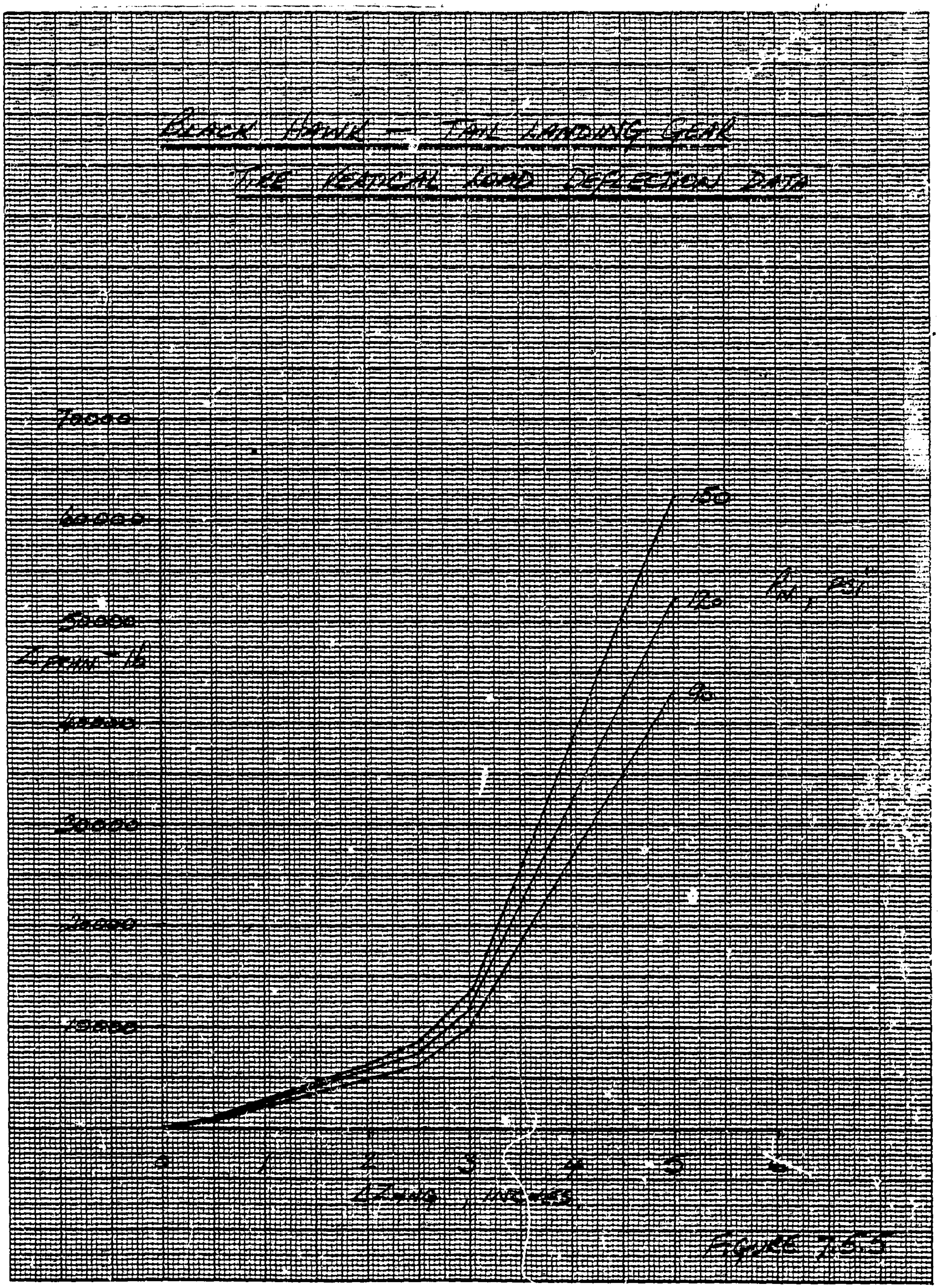
BLACK HAWK — TAIL LANDING GEAR
TIRE VERTICAL LOAD DEFLECTION DATA
150
120
90
P, PSI
70000
60000
50000
40000
30000
20000
10000
lb
0
1
2
3
4
5
6
INCHES
FIGURE 7.5.5

BLACK HAWK - TAIL LANDING GEAR

TIRE VERTICAL STIFFNESS
(USED ONLY IN DAMPING CALCULATION)

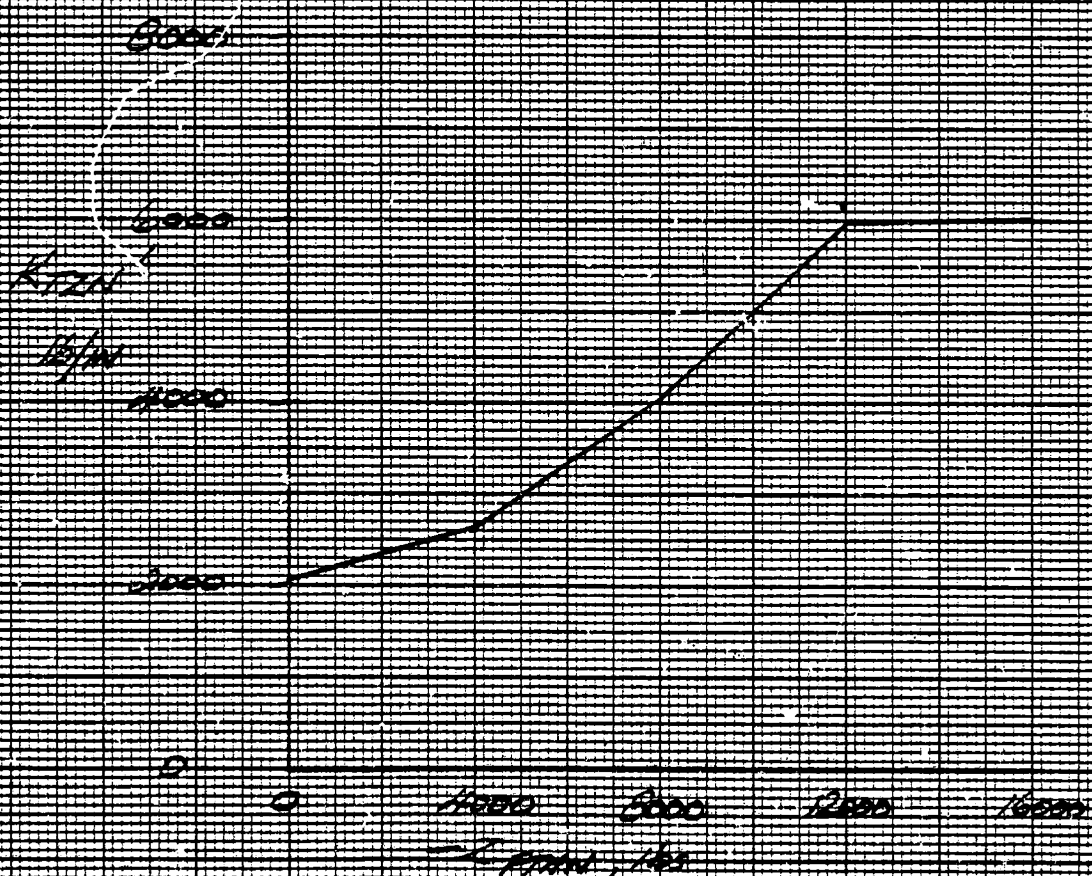

FIGURE 7.5.6

5.8 GROUND EFFECT MODULE

5.8.1 Module Description

This module simulates the effect of ground proximity on a helicopter by modifying the main rotor downwash equation.

The modification factor was derived from Black Hawk hover-power flight test results (Reference 5.8.6-1).

The modification factor is reduced as flight speed is increased at constant height by a wake angle correction .

It is likely that recent and on-going research on this subject (Reference 5.8.6-2) will lead eventually to an empirical model describing the local rotor inflow velocity due to the hyperbolically shaped ground vortex and its image that has been shown to exist at low speeds. Unfortunately, sufficient data for correlation of such a model has not yet been published.

5.8.2 GROUND EFFECT MODULE EQUATIONS

$$DWSHMR = \frac{K_{CT} \cdot C_{TA}}{2\mu_{TOT}} \left\{ \frac{1}{1 + \frac{T_{DWD} \cdot S}{\mu_{TOT}}} \right\} \cdot K_{GE}$$

$$K_{GE} = \left[1 + .115 \left(\frac{R}{Z}\right)^2 \left(\frac{\lambda}{\mu_{TOT}}\right) \right]^{-2/3}$$

$$Z = \frac{(WLMR - WLGND)}{12} - \int \dot{Z} \, dt$$

The part is square brackets [ ] is the ground proximity effect (usually switched to 1 when $Z > 5 \times R$), the rest of the equation is as quoted in the main rotor downwash section.

5.8.3 GROUND EFFECTS MODULE INPUT/OUTPUT DATA TRANSFER

INPUT TRANSFER	
PARAMETER	ORIGIN MODULE
DWSHMR	MAIN ROTOR
LAMMR	
UTOTMR	
VZ	MOTION

OUTPUT TRANSFER	
PARAMETER	DESTINATION MODULE
DWSHMR	MAIN ROTOR

5.8.4 NOTATION FOR THE GROUND EFFECT MODULE

SYMBOL USED IN EQUATIONS	PROGRAM MNEMONIC	UNITS	DESCRIPTION
C_T	CTHAMR	-	Main rotor thrust coefficent
DW_O	DWSHMR		Main rotor uniform self induced velocity
KCT	KCTMR	-	Thrust gain for uniform downwash
R	RMR	FT	Main rotor radius
S		-	Laplace operator
T_{DWO}	TDWOMR	SEC	Time constant for uniform downwash calculation
Z		FT	Height of rotor hub above ground
λ	LAMBMR		Main rotor inflow $(=\mu_{Z_s} - D_{W_o})$
μ_{TOT}	UTOTMR	-	Total main rotor inflow $(=[\mu_{X_s}{}^2 = \mu_{Y_s}{}^2 + \lambda_{tot}^2]^{1/2})$
μ_{X_s}	MUXSMR	-	Velocity in X direction, shaft axes
μ_{Y_s}	MUYSMR	-	Velocity in Y direction, shaft axes
μ_{Z_s}	MUZSMR	-	Velocity in Z direction, shaft axes
WLMR	WLMR	IN	Waterline Station of Rotor Hub
WLGND	WLGND	IN	Waterline Station of the Ground (Nominal)
V_Z	V_Z	FT/SEC	Vertical Velocity

5.8.5 Input Data

No separate input data is required. The parameters .115 and 2/3 in equation 5.8.2-1, were empirically derived from data in Reference 5.8.6-1 which is pertinent to Black Hawk aircraft.

5.8.6 References

1. LTC Alan R. Todd to Mr. R. Merritt, Sikorsky Aircraft Letter "Free hover performance" 22 October 1976

2. Sheridan & Wiesman "Aerodynamics of Helicopter Flight Near the Ground" AHS Paper 77.33-04 May, 1977

5.9 GUST MODULE

CONTENTS

5.9 Gust Module

5.9.1 Description

This module produces local air velocities at all rotor-blade segment positions and at the fuselage and empennage aerodynamic centers, caused by various types of gusts. The input gusts may be discrete or continuous.

The output velocities are calculated in the local axis-system in which they are to be used. Thus the fuselage and tail terms are in body axes while those at the blade segments are in blade flapped and lagged axes.

The discrete gusts are characterized by having a front line designating the beginning of a disturbance, travelling through the atmosphere at velocity V_{HW} on a compass bearing ψ_W (Figure 5.9.1.1). Behind this front line, the change in air velocity can assume a step or rounded ramp or pulse shape, characterized by a magnitude V_{HGAMP} and rise-time G_{HDIS} (Figure 5.9.1.2). Since the aircraft is defined to be flying initially at V_{KTS} on compass bearing ψ_{BO}, the gust front can sweep across the aircraft (or be penetrated by the aircraft) from any direction and at any speed, by manipulating the relative speeds and compass bearings.

The continuous gusts are represented by the Dryden Model. The gust is assumed to be aligned with the aircraft heading such that only longitudinal and vertical vectors are defined. This is a necessary restriction, which avoids frequency shifts that would invalidate the gust spectrum model. At aircraft trim speeds greater than 50 ft/sec, a stationary gust field is traversed by the aircraft; at trim speeds less than 50 ft/sec, the gust field traverses the aircraft at 50 ft/sec. While the latter process is not a very appealing artifice mathematically, it is necessary in order to avoid unrealistic time lags in the gust definition equations and flying the aircraft in a constant up or down-draught at hover.

A penetration distance G (ft.) is defined which represents the distance that the aircraft reference hub centroid has penetrated into the gust. Initially the gust front is assumed to be close to the edge of the rotor disk in the upwind direction.
A rearward approaching gust is not possible without further manipulation of the model. The propagation rate of the gust field across the rotor is defined by V_{FLD} which then allows the penetration of any blade-segment, to be calculated (GPR_{jk}, see figure 5.9.1.3).

5.9.1 Description (Continued)

For the discrete gusts GPR_{ijk} is introduced expl- -ly into the profile equations and the gust increment can b ed directly. However, for the continuous gust c. a table of gust values, determined at fixed time (dista) intervals, (TABINK) are available. These data are obtained by passing independent, Gaussian, unit R.M.S.noise signals, produced by passing uniformly distributed white noise through the inverse Gaussian distribution function (Reference 5.9.6-2), through the Dryden filters. The assumption is made that perturbations in speed and heading are small enough such that the time constants in the gust functions can be considered constant, and that data can be loaded into the tables at fixed displacement intervals. These assumptions are consistent with the frequency/airspeed contraints of the Dryden Model application.

The gust velocities generated by either discrete or continuous functions, are in an axis set defined by the horizontal gust front. Three transformation matrices are required to orient into the blade axes and one for the body axes. These velocities are added to the other local velocities at the various stations.

The vertical gust component contributes to the total inflow of the main rotor. Because a basically uniform inflow is assumed in the Gen Hel rotor simulation, the change in inflow can be simulated by adding a representative velocity over the whole disc. The division of the blade into segments in Gen Hel is such as to give equal areas of swept annuli, making it possible to take a simple mean as the representative velocity of the additional inflow. Following the transformation of the z-direction component from space to (through body) shaft axes, the mean incremental velocity (VGAVMR) can be added to the downwash equation to compensate the total inflow.

The gust velocity at the fuselage is assumed to be the same value experienced at the rotor hub. The empennage velocities are based on the hub velocity with an approximate time delay to account for the penetration of the specific component.

This model of gust penetration may be criticized on the grounds that the point fuselage airload used is not consistant with the detailed penetration of the rotor blades. Fixed wing simulations commonly overcome the distribution problem by introducing correlated non-inertial rotational rates due to gust (Reference 5.9.6-1).

5.9.1 Description (Continued)

It is felt that the separation of the tail used here, accounts for a sufficiently large portion of the non-rotor component gust distribution effects and that further terms (for which there are little if any data) are unnecessary. In the same vein it is sufficiently accurate (and convenient in the implementation) to assume the aerodynamic center of the fuselage to be at the c.g.

Discrete lateral gusts may be handled by orientation of ψ_w. However, the continuous gust case is invalidated by using any value other than zero for ψ_w, due to apparent frequency shifts in the gust spectrum.

ORIGINAL PAGE IS
OF POOR QUALITY

SIKORSKY AIRCRAFT UNITED TECHNOLOGIES

DOCUMENT NO. SER 70452

GUST FRONT GEOMETRY

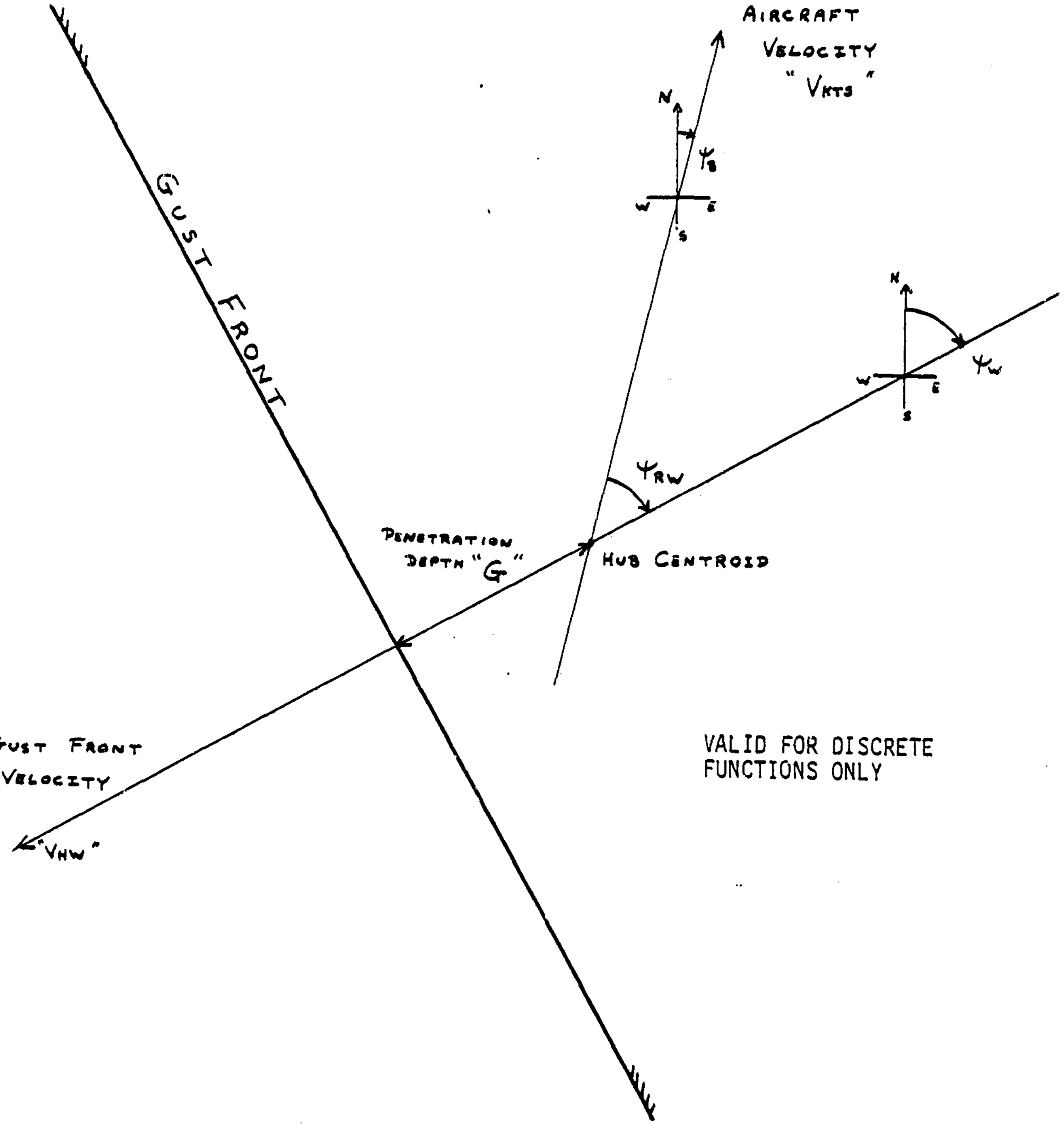

VALID FOR DISCRETE
FUNCTIONS ONLY

Figure 5.9.1.1

SA 29 REV. G

GUST SELECTION (f_{0-4})

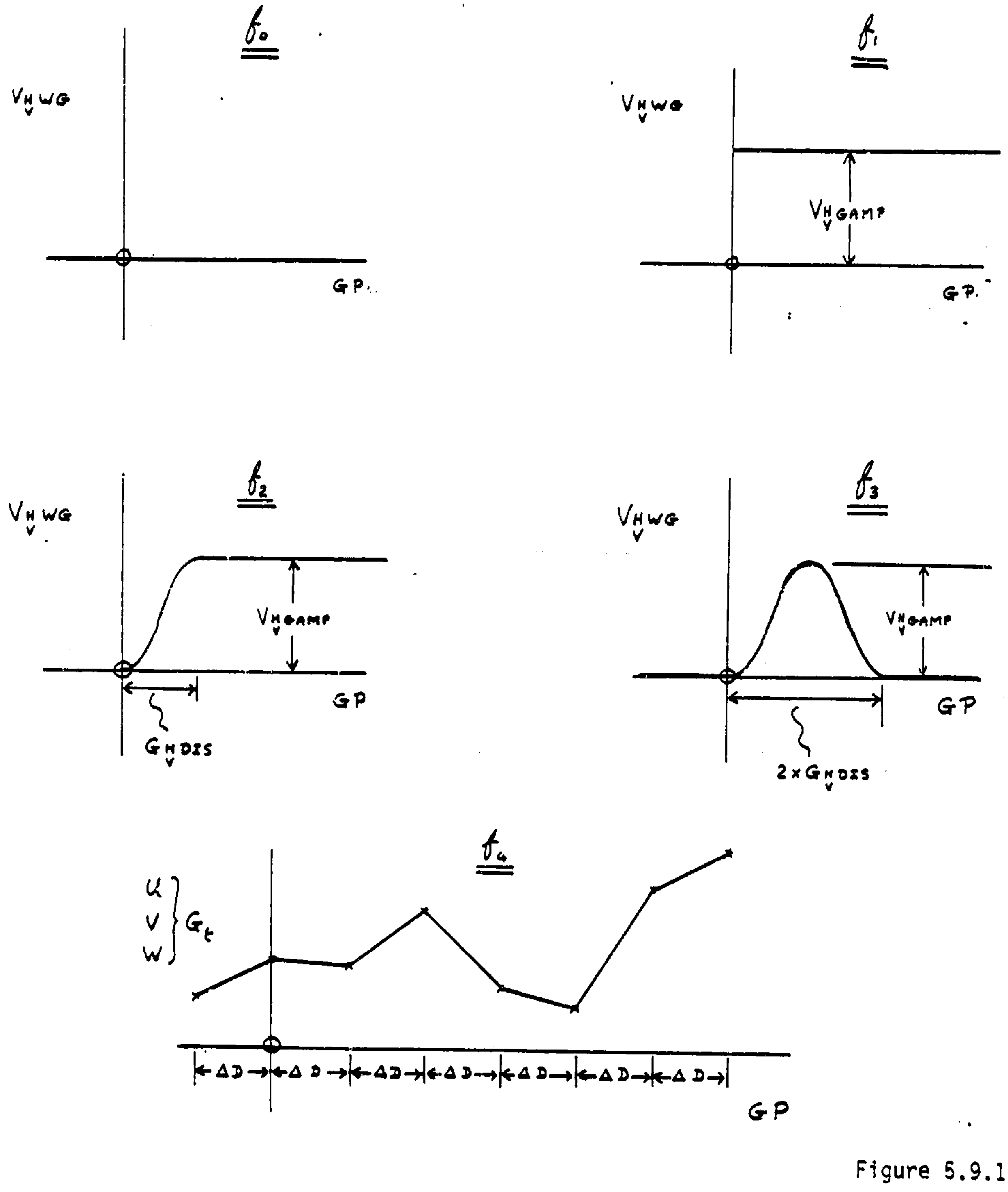

Figure 5.9.1.2

GUST PENETRATION GEOMETRY

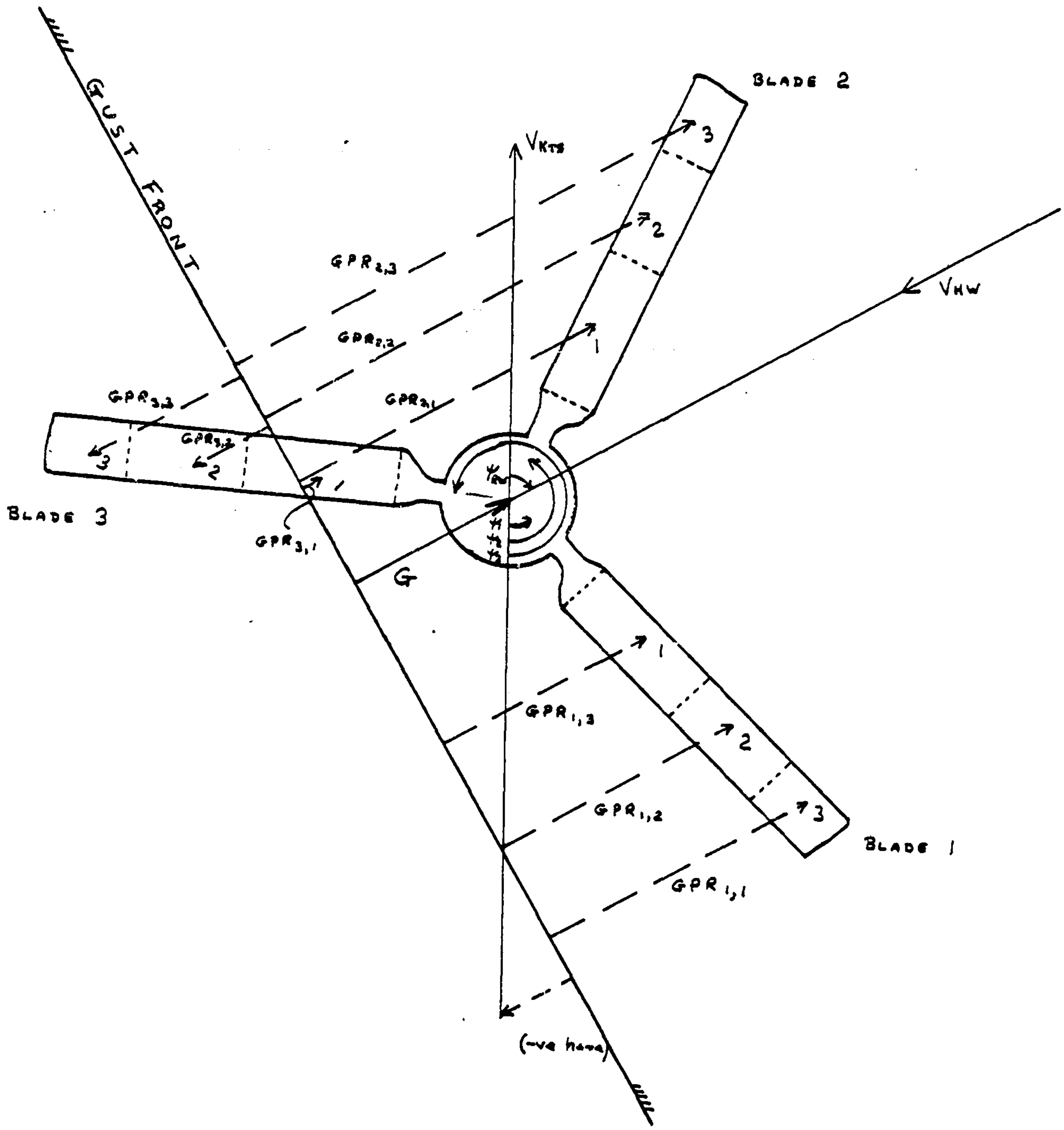

Figure 5.9.1.3

5.9.2 GUST MODULE EQUATIONS

AIRCRAFT HEADING

$$\underset{(PSIB)}{\psi_b} = \psi_{b0} + 57.3 \int \dot{\psi}_b \, dt$$

RELATIVE GUST DIRECTION

$$\underset{(PSIRW)}{\psi_{RW}} = \psi_W - \psi_b$$

AIRCRAFT VELOCITY

$$V_{KT} = \left[(V_{Xb} + V_{Xg})^2 + (V_{Zb} + V_{Zg})^2 \right]^{1/2} * .591715 \quad (\text{KNOTS})$$

(CALCULATED IN MOTION MODULE)

GUST PROPOGATION VELOCITY

$$V_{FLD} = V_{KT}(1.689) \cos \psi_{RW} + V_{HW}$$

V_{HW} = INPUT FOR DISCRETE GUST FUNCTIONS $(f_{0,1,2,3})$

$V_{HW} = 50 - 1.689 V_{KT} \cos \psi_{RW}$, $0 \leq V_{HW}$

FOR THE CONTINUOUS GUST FUNCTIONS (f_4)

GUST TABLE SET UP PARAMETERS

$$\underset{(TABINK)}{\Delta D} = V_{FLD} * TIME \quad \text{---- I.C. MODE ONLY}$$

$$\Delta FT = \left(\frac{FSTR}{12} + RTR\right) - \left(\frac{FSMR}{12} + RMR\right) \quad \text{--- I.C MODE ONLY}$$

$$INPPNT = \left(\frac{MAXPNT}{2} - 1\right) + \left[\frac{G_0}{TABINK}\right]_{FIX.PT} \quad \text{---- I.C. MODE ONLY}$$

WHERE $G_0 = -R_{MR}$

INITIALISATION OF TABLE PARAMETERS

$$\underset{(TABRUN)}{G\rho} = 0$$

$$ICUPD = \left[\frac{G_\phi + R_{MR} + \Delta FT}{TABINK}\right]_{FIX.\,PT}$$

CLEAR TABLES TABLEH $0 \rightarrow MAXPNT-1$

TABLEV $0 \rightarrow MAXPNT-1$

HUB CENTROID PENETRATION DISTANCE

$$\underset{(GGGPRM)}{G'} = G_0 + \int_0^t V_{FLD}\, dt$$

ROTOR BLADE-SEGMENT TABLE LOOK-UP POINTER

$$\underset{(GPRSP)}{GPR_I'} = G' - R_{MR}(\xi + y_2)_{IS} \cos(\psi_{MR} + \delta + \psi_{RW})_{IB}$$

WHERE $G' = G - G_0'$

$G_0' = 0$ IN IC.

$G_0' = G$ WHEN $G' \geq G_{MAX}$

$\underset{(GGGMAX)}{G_{MAX}} = (TABMAX)(TABINK)$

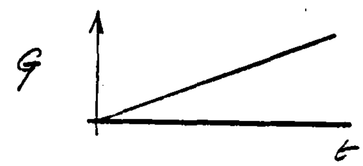

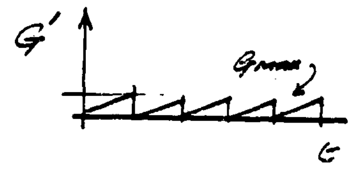

(MAP LOOK-UP PARAMETER)

$$GPR_I = GPR_I' \quad , \quad 0 \le GPR_I' \le G_{MAX}.$$
$$= GPR_I' + G_{MAX} \qquad GPR_I' < 0$$
$$= GPR_I' - G_{MAX} \qquad GPR_I' > G_{MAX}$$

DISCRETE GUST FUNCTIONS.

DEFINE $\underset{(TABROW)}{GP} = GP + \Delta D \qquad GP_{IC} = 0$

HORIZONTAL GUST $VHWG = f_{\ell_1}(GP)$ SET INTO TABLE TABLEH

VERTICAL GUST $VVWG = f_{\ell_2}(GP)$ SET INTO TABLE TABLEV

$$\ell_{1,2} = 0, 1, 2, 3, 4.$$

f_0 NO GUST VELOCITY

$$V^H_V WG = 0$$

SA 29 REV. G

f_1 STEP GUST

$$V^H_V WG = 0 \quad , \quad GP \leq 0$$

$$V^H_V WG = V^H_V GAMP \quad , \quad GP > 0$$

f_2 SHAPED RAMP

$$V^H_V WG = 0 \quad , \quad GP \leq 0$$

$$V^H_V WG = \frac{1}{2} V^H_V GAMP \left[1 + \cos\left\{ \pi \left(\frac{GP}{G^H_V DIS} - 1 \right) \right\} \right]$$

$$, \quad 0 < GP < G^H_V DIS$$

$$V^H_V WG = V^H_V GAMP \quad , \quad GP \geq G^H_V DIS$$

f_3 SHAPED PULSE

$$V^H_V WG = 0 \quad , \quad GP \leq 0$$

$$V^H_V WG = \frac{1}{2} V^H_V GAMP \left[1 + \cos\left\{ \pi \left(\frac{GP}{G^H_V DIS} - 1 \right) \right\} \right]$$

$$, \quad 0 < GP < 2 * G^H_V DIS$$

$$V^H_V WG = 0 \quad , \quad GP \geq 2 * G^H_V DIS$$

CONTINUOUS GUST FUNCTION

f_4 BASED ON THE DRYDEN MODEL.

VFLD REFERS TO THE IC VALUE

$$VHWG = \frac{\sigma_u \left(\frac{2}{\pi}\ \frac{VFLD}{L_u}\right)^{1/2}}{\left(S + \frac{VFLD}{L_u}\right)} * \left(\frac{\pi}{TIME}\right)^{1/2} * \eta_{1t}$$

$$VVWG = \sigma_v \frac{\left(\frac{3}{\pi}\ \frac{VFLD}{L_v}\right)^{1/2}\left(S + \left(\frac{1}{3}\right)^{1/2} \frac{VFLD}{L_v}\right)}{\left(S + \frac{VFLD}{L_v}\right)^2} * \left(\frac{\pi}{TIME}\right)^{1/2} * \eta_{2t}$$

THE η_t ARE INDEPENDENT, GAUSSIAN, UNIT R.M.S NOISE SIGNALS, PRODUCED BY PASSING UNIFORMLY DISTRIBUTED WHITE NOISE THROUGH THE INVERSE OF THE GAUSSIAN DISTRIBUTION FUNCTION (REF 5.9.6-2)

THIS APPROACH COULD BE EXPANDED TO INCLUDE A LATERAL GUST COMPONENT (VLWG). HOWEVER, ITS USE BELOW 50KTS MAY BE QUESTIONABLE.

FUSELAGE PENETRATION OF GUST

$$L'_{AC} = \frac{(FSCGB - FSMR)}{12}$$
(LPRAC)

$$GPAC' = G' - L'_{AC} \cos \psi_{RW}$$
(GPACP)

TRANSFORMATION MATRICES

ELEMENTS OF THESE MATRICES ARE USED IN OTHER MODULES, THEY ARE REPEATED HERE FOR COMPLETENESS SAKE

SPACE → BODY (VLNG SET = 0, 2ND COLUMN = 0)

$$[T_1] = \begin{bmatrix} \cos\theta_b \cos\psi_{RW} , & 0 , & -\sin\theta_b \\ \sin\theta_b \sin\phi_b \cos\psi_{RW} + \cos\phi_b \sin\psi_{RW} , & 0 , & \cos\theta_b \sin\phi_b \\ \sin\theta_b \cos\phi_b \cos\psi_{RW} - \sin\phi_b \sin\psi_{RW} , & 0 , & \cos\theta_b \cos\phi_b \end{bmatrix}$$
(T1MAXT)

BODY → SHAFT

$$[T_2] \begin{bmatrix} \cos i_\theta , & 0 , & -\sin i_\theta \\ \sin i_\theta \sin i_\phi , & \cos i_\phi , & \cos i_\theta \sin i_\phi \\ \sin i_\theta \cos i_\phi , & -\sin i_\phi , & \cos i_\theta \cos i_\phi \end{bmatrix}$$
(T2MAXT)

SA 29 REV. G

SHAFT → BLADE

$$[T_3] = \begin{bmatrix} -\sin\beta\cos(\psi+\delta), & \sin\beta\sin(\psi+\delta), & \cos\beta \\ \sin(\psi+\delta), & \cos(\psi+\delta), & 0 \\ \cos\beta\cos(\psi+\delta), & -\cos\beta\sin(\psi+\delta), & \sin\beta \end{bmatrix}$$

(T3MAXT)

GUST VELOCITIES AT THE BLADE SEGMENT

(VHWGR, VVWGR FROM TABLES FOR EACH SEGMENT)

$$\begin{bmatrix} UPGMRD \\ UTGMRD \\ URGMRD \end{bmatrix}_I = [T_3]_I * [T_2] * [T_1] * \begin{bmatrix} VHWGR \\ 0 \\ VVWGR \end{bmatrix}_I$$

$$UPGMR = \frac{UPGMRD}{R_{MR}\,\Omega_{MR}}$$

$$UTGMR = \frac{UTGMRD}{R_{MR}\,\Omega_{MR}}$$

$$URGMR = \frac{URGMRD}{R_{MR}\,\Omega_{MR}}$$

ROTOR DOWNWASH COMPENSATION

$$\lambda_t = \mu_{zs} - DW_{0_t} + VGAVMR$$

WHERE $VGAVMR = \dfrac{\sum_{I=0}^{I=I} VZSGUS}{(b_{MR} + NSS)} \cdot \dfrac{1}{R_{MR}\,\Omega_{MR}}$

AND VZSGUS IS OBTAINED FROM THE THIRD ROW OF

$$\begin{bmatrix} VXSGUS \\ VYSGUS \\ VZSGUS \end{bmatrix}_I = \begin{bmatrix} T_2 \end{bmatrix} * \begin{bmatrix} T_1 \end{bmatrix} * \begin{bmatrix} VHWGR \\ 0 \\ VVWGR \end{bmatrix}_I$$

GUST VELOCITIES AT THE FUSELAGE
(VHWGAC, VVWGAC FROM TABLES)

$$\begin{bmatrix} VXGWF \\ VYGWF \\ VZGWF \end{bmatrix} = \begin{bmatrix} T_1 \end{bmatrix} * \begin{bmatrix} VHWGAC \\ 0 \\ VVWGAC \end{bmatrix}$$

GUST VELOCITIES AT THE EMPENNAGE

$$VXG_{\substack{HT\\VT\\TR}} = VXGWF \text{ DELAYED BY } \frac{FS_{\substack{HT\\VT\\TR}} - FSCGB}{12 * VXB}$$

$$VYG_{\substack{HT\\VT\\TR}} = VYGWF \quad '' \quad ''$$

$$VZG_{\substack{HT\\VT\\TR}} = VZGWF \quad '' \quad ''$$

5.9.3 GUST MODULE INPUT/OUTPUT DATA TRANSFER

INPUT TRANSFER

PARAMETER	ORIGIN MODULE
LGMR PSIMR OFSTMR KMRBX1	MAIN ROTOR
THETAB PHIB PSIB VKT VXB	MOTION

OUTPUT TRANSFER.

PARAMETER	DESTINATION MODULE
VGAVMR UPGMR UTGMR URGMR	MAIN ROTOR
VXGWF VYGWF VZGWF	FUSELAGE
VXGHT VYGHT VZGHT	HORIZONTAL TAIL
VXGVT VYGVT VZGVT	VERTICAL TAIL
VXGTR VYGTR VZGTR	TAIL ROTOR.

5.9.4 Notation for Gust Module

SYMBOL USED IN EQUATIONS	PROGRAM MNEMONIC	UNITS	DESCRIPTION
$\dot{\psi}_b$	PSIDOT	RAD/SEC	Rate of Change of A/C Heading
ψ_b	PSIB	DEG	A/C Heading
ψ_{bo}	PSIBO	DEG	Initial Heading
ψ_{RW}	PSIRW	DEG	Relative Wind Heading
ψ_W	PSIWD	DEG	Wind Heading
VKT	VKT	KNOTS	Airspeed
VHW	VHW	FT/SEC	Wind Speed
VFLD	VFLD	FT/SEC	Gust Propagation Rate
ΔD	TABINK	FT	Gust Table Space
TIME	TIME	SEC	Integration Time Interval
ΔFT	DELFT	FT	Table Initial Dead Space
FSMR	FSMR	INS	Fuse. Station for T.R. Hub
FSTR	FSTR	INS	Fuse. Station for T.R. Hub
R_{MR}	RMR	FT	Radius of Main Rotor
INPPNT	INPPNT	-	Table Loading in I.C. Mode
MAXPNT	MAXPNT	-	Maximum Table Points
GO	GOO	FT	$(= -R_{MR})$
GP	TABRUN	FT	Table Run Distance
ICUPD	ICUPD	FT	Start of Data in Table

ORIGINAL PAGE IS
OF POOR QUALITY

5.9.4 Notation for Gust Module (Continued)

SYMBOL USED IN EQUATIONS	PROGRAM MNEMONIC	UNITS	DESCRIPTION
TABLEH	TABLEH	-	Table of Horizontal Velocities
TABLEV	TABLEH	-	Table of Vertical Velocities
G'	GGGPRM	FT	Hub Centroid Penetration Distance
ξ	KSGMR	ND	Normalized Offset
y_2	KMRBK1	ND	Distance from Hinge to Segment Midpoint
ψ_{MR}	PSIMR	DEG	Rotor Azimuth Position
δ	LGMR	RADS	Lagging Angle
GPR'	GPRSP	FT	Penetration of Any Blade Segment
TABMAX	TABMAX	-	Max Number of Table Locations
GMAX	GGGMAX	FT	Max Distance in the Tables
VHWG	VHWG	FT/SEC	Horizontal Gust Velocity
VVWG	VVWG	FT/SEC	Vertical Gust Velocity
VHGAMP	VHGAMP	FT/SEC)	Discrete Gust Profile Amplitude Functions
VVGAMP	VVGAMP	FT/SEC)	
GHDIS	GHDIS	FT)	Discrete Gust Profile Distance Functions
GVDIS	GVDIS	FT)	
σu		)	Dryden Filter Inputs
σv		)	
L_u		)	

SA 29 REV. G

ORIGINAL PAGE IS
OF POOR QUALITY

5.9.4 Notation for Gust Module (Continued)

SYMBOL USED IN EQUATIONS	PROGRAM MNEMONIC	UNITS	DESCRIPTION
L_v			
η_u	GAUSSH	-	Horizontal and Vertical Gaussian Random Number
η_v	GAUSSV	-	
L_{AC}	LPRAC	FT	Rotor to CG Offset
FSCGB	FSCGB	INS	Fuselage Station for C.G.
FSMR	FSMR	INS	Fuselage Stations for Main Rotor
GPAC'	GPACP	FT	Gust Penetration of C.G.
θ_b	THETAB	DEG	Airframe Pitch Attitude
ϕ_b	PHIB	DEG	Airframe Roll Attitude
i_θ		DEG	Long. Rotor Shaft Incidence
i_ϕ		DEG	Lat. Rotor Shaft Incidence
T_1	T1MAXT	-	Space→Body Transf. Matrix
T_2	T2MAXT	-	Body→Shaft Transf. Matrix
T_3	T3MAXT	-	Shaft→Blade Transf. Matrix
VHWGR	VHWGR	FT/SEC	Horizontal Gust Vel. from Table
VVWGR	VVWGR	FT/SEC	Vertical Gust Vel. from Table
UPGMRD	UPGMR	FT/SEC	Three Component Gust Velocities at the Blade Segment
UTGMRD	UTGMR	FT/SEC	

ORIGINAL PAGE IS
OF POOR QUALITY

5.9.4 Notation for Gust Module

SYMBOL USED IN EQUATIONS	PROGRAM MNEMCNIC	UNITS	DESCRIPTION
URGMR	URGMR	FT/SEC	)
UPGMR	-	ND	)Three Component Interfer-)ence. Components at the)Rotor. Summed to Memory
UTGMR	-	ND	)UPIMRI, UTIMRI, URMRI.)
URGMR	-	ND	)
λ_T	LAMBMR	ND	Total Normal Rotor Inflow Velocity
μ_{zs}	MUZSMR	ND	Vertical Shaft Velocity, Normalized
DWo	DWSHMR	ND	Uniform Component of Down-Wash
VGAVMR	VGAVMR	ND	Average Gust Velocity at the Rotor Disk
VZSGUS		FT/SEC	Vertical Shaft Component, Av. Gust Velocity
Ω_T	OMGTMR	RADS/SEC	Rotor Speed
b_{MR}	BMR	-	Number of Rotor Blades
N_{SS}	N_{SS}	-	Number of Segments/Blade
VHWGAC	VHWGAC	FT/SEC)	Horizontal and Veritcal Com-
VVWGAC	VVWGAC	FT/SEC)	ponents of Gust Velocity at the Fuse C.G.
VXGWF	VXGWF	FT/SEC)	Components of Gust Velocity in Body Axes at the C.G.
VYGWF	VYGWF	FT/SEC)	
VZGWF	VZGWF	FT/SEC)	

5.9.4 Notation for Gust Module (Continued)

SYMBOL USED IN EQUATIONS	PROGRAM MNEMONIC	UNITS	DESCRIPTION
V_{xb}	VXB	FT/SEC	Body Axes Longitudinal Velocity
$\begin{bmatrix} V_{XG} \\ V_{YG} \\ V_{ZG} \end{bmatrix}_{\substack{HT \\ VT \\ TR}}$	$\begin{bmatrix} VXG \\ VYG \\ VZG \end{bmatrix}_{\substack{HT \\ VT \\ TR}}$	FT/SEC	Components of Gust Velocity at the Horizontal Tail, Vertical Tail and Tail Rotor.

5.9.5 Data

The only data of concern here are the continous gust power spectrum parameters. All other data is defined elsewhere in Gen Hel or is arbitrary (e.g. V_{HGAMP} and G_{HDIS} describing a discrete gust).

The following values are taken from Reference 5.9.6-1:

	Altitude (h) ≤ 1750 ft	Altitude (h) > 1750 ft
L_u	1750	$145\ h^{1/3}$
L_w	1750	h
σ_u	$\sqrt{L_u/L_w}\ \sigma_w$	

(For lateral gusts, $\sigma_v = \sigma_u$ and $L_v = L_u$.)

5.9.6 References

1. "Background Information and User Guide for MIL-F-8785B(ASG)," "Military Specification - Flying Qualities of Piloted Airplanes", AFFDL-TR-69-72, C. R. Chalk, et. al., August 1969.

2. "Modeling Turbulence for Flight Simulation at NASA-Ames", CSCR No. 4, Benton L. Parris, January, 1975.

5.10 HELICOPTER MOTION MODULE

CONTENTS

5.10 Helicopter Motion Module

5.10.1 Module Description

The forces and moments derived from the various simulated components of the aircraft are summed to develop the total external forces and moments at the airframe center of gravity in body axes, Figure 10.1.1. Introduced at this point, for convenience, are the gyroscopic moments resulting from rotating components. These equations are set up to cover any number of items of rotating mass aligned with the three body axes. The total external forces and moments are introduced into the general equations of motion from which the 6 components of acceleration are solved. It will be seen by comparing with those on page 116 of Reference 10.6.1, that certain small terms have been eliminated. It should be noted that these are the equations of the aircraft less rotor blades, (which have their own degrees of freedom) and the appropriate mass is used. In order to obtain stable solutions under all operational conditions it is recommended that some velocity prediction technique be used in the determination of the body axes velocities, as presented. It should also be noted that since the p and r equation are coupled, they should be solved simultaneously as written. The Euler angular rate equations are given, followed by the body to space velocity axes transformation. Large angles are assumed.

The three component equations of motion for any specified point on the helicopter are presented in general form basically for output. However, lateral acceleration is fed back to the control system. It is recommend that at least two entries to these equations be provided to cover subsequent analyst requirements. The remaining equations in this section are provided for analyst output.

BODY AXES SYSTEM

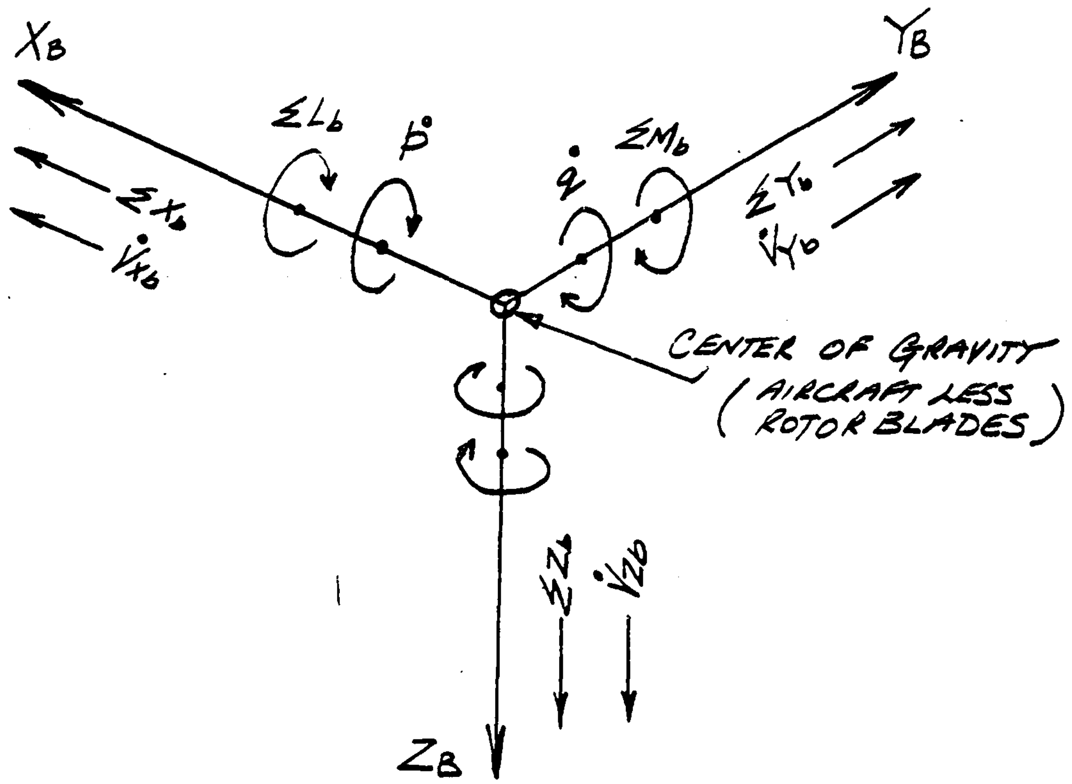

X_b, Y_b, Z_b Body Axes System. Origin at the Center of Gravity. X Axis Parallel to Aircraft Center Line.

FIGURE 10.1.1

5.10.2 HELICOPTER MOTION MODULE EQUATIONS

SUMMATION OF EXTERNALLY APPLIED FORCES AND MOMENTS AT THE CENTER OF GRAVITY

$$SUMXB = X_{MR} + X_{TR} + X_T + X_{WF} + X_{LG} + X_{ADD}$$

$$SUMYB = Y_{MR} + Y_{TR} + Y_T + Y_{WF} + Y_{LG} + Y_{ADD}$$

$$SUMZB = Z_{MR} + Z_{TR} + Z_T + Z_{WF} + Z_{LG} + Z_{ADD}$$

$$SUMLB = L_{MR} + L_{TR} + L_T + L_{WF} + L_{LG} + L_{ADD} + L_{GY}$$

$$SUMMB = M_{MR} + M_{TR} + M_T + M_{WF} + M_{LG} + M_{ADD} + M_{GY}$$

$$SUMNB = N_{MR} + N_{TR} + N_T + N_{WF} + N_{LG} + N_{ADD} + N_{GY}$$

WHERE

$$HXGY = \sum_{i=1}^{N} (J_{xgy_i} * \omega_{xgy_i})$$

$$HYGY = \sum_{i=1}^{N} (J_{ygy_i} * \omega_{ygy_i})$$

$$HZGY = \sum_{i=1}^{N} (J_{zgy_i} * \omega_{zgy_i})$$

$$L_{GY} = H_{YGY}(r) - H_{ZGY}(q)$$

$$M_{GY} = -H_{XGY}(r) + H_{ZGY}(p)$$

$$N_{GY} = H_{XGY}(q) - H_{YGY}(p)$$

$(XYZLMN)_{ADD}$ ARE PROVIDED FOR ADDITIONAL ARBITRARY INPUT

TRANSLATIONAL VELOCITY PREDICTORS

$$V'_{xb(t)} = V_{xb(t-1)} + \dot{V}_{xb(t-1)} (\Delta t/2)$$

$$V'_{yb(t)} = V_{yb(t-1)} + \dot{V}_{yb(t-1)} (\Delta t/2)$$

$$V'_{zb(t)} = V_{zb(t-1)} + \dot{V}_{zb(t-1)} (\Delta t/2)$$

ORIGINAL PAGE IS
OF POOR QUALITY

BODY AXES ACCELERATIONS

$$VXBDOT = g/W_{BD}\left(SUMXB - W_{BD}\sin\theta_b\right) + r V'_{Yb} - q V'_{Zb}$$

$$VYBDOT = g/W_{BD}\left(SUMYB + W_{BD}\cos\theta_b \sin\phi_b\right) + p V'_{Zb} - r V'_{Xb}$$

$$VZBDOT = g/W_{BD}\left(SUMZB + W_{BD}\cos\theta_b \cos\phi_b\right) + q V'_{Xb} - p V'_{Yb}$$

$$P_{DOT} = \frac{I_Z}{(I_X I_Z - I_{XZ}^2)}\left\{SUMLB - (I_Z - I_Y) q r + I_{XZ}(pq)\right\}$$

$$+ \frac{I_{XZ}}{(I_X I_Z - I_{XZ}^2)}\left\{SUMNB - (I_Y - I_X) pq - I_{XZ}(rq)\right\}$$

$$Q_{DOT} = \frac{1}{I_Y}\left\{SUMMB - (I_X - I_Z) pr + I_{XZ}(r^2 - p^2)\right\}$$

$$R_{DOT} = \frac{I_X}{(I_X I_Z - I_{XZ}^2)}\left\{SUMNB - (I_Y - I_X) pq - I_{XZ}(rq)\right\}$$

$$+ \frac{I_{XZ}}{(I_X I_Z - I_{XZ}^2)}\left\{SUMLB - (I_Z - I_Y) q r + I_{XZ}(pq)\right\}$$

NOTE THESE ANGULAR ACCELERATION EQUATIONS DO NOT INCLUDE DYNAMIC COMPONENTS REFLECTING LATERAL CG OFFSET

SA 29 REV. G

AIRCRAFT VELOCITY AND DISPLACEMENT

BODY AXES VELOCITIES

$$VXB = \int \dot{V}_{Xb}\, dt$$
$$VYB = \int \dot{V}_{Yb}\, dt$$
$$VZB = \int \dot{V}_{Zb}\, dt$$
$$p = \int \dot{p}\, dt + p_0$$
$$q = \int \dot{q}\, dt + q_0$$
$$r = \int \dot{r}\, dt + r_0$$

ONLY EXECUTED IN THE COMPUTE MODE

EULER RATES

$$THEDOT = 57.3 \{ q \cos\phi_b - r \sin\phi_b \}$$
$$PSIDOT = 57.3 \left\{ \frac{r \cos\phi_b + q \sin\phi_b}{\cos\theta_b} \right\}$$
$$PHIDOT = 57.3\, p + \dot{\psi}_b \sin\theta_b$$

ONLY EXECUTED IN THE COMPUTE MODE

ORIGINAL PAGE IS
OF POOR QUALITY

SIKORSKY AIRCRAFT UNITED TECHNOLOGIES

DOCUMENT NO. SER 70452

EULER ANGLES

$$PHIB = \int \dot{\phi}_b \, dt$$
$$THETAB = \int \dot{\theta}_b \, dt$$
$$PSIB = \int \dot{\psi}_b \, dt$$

ONLY EXECUTED IN THE COMPUTE MODE

BODY AXES RATES

$$PDEG = 57.3\,(p)$$
$$QDEG = 57.3\,(q)$$
$$RDEG = 57.3\,(r)$$

BODY ATTITUDE FUNCTIONS

SNTHEB, CSTHEB — DERIVED FROM SINCOS (θ_b) ROUTINE

SNPHIB, CSPHIB — DERIVED FROM SINCOS (ϕ_b) ROUTINE

SNPSIB, CSPSIB — DERIVED FROM SINCOS (ψ_b) ROUTINE

SA 29 REV. 6

BODY TO SPACE AXES TRANSFORMATION MATRIX

$$
\left[A_{HBS}\right] = \begin{bmatrix} (\cos\theta_b \cos\psi_b), & (\sin\theta_b \sin\phi_b \cos\psi_b - \cos\phi_b \sin\psi_b), & (\sin\theta_b \cos\phi_b \cos\psi_b + \sin\phi_b \sin\psi_b) \\ (\cos\theta_b \sin\psi_b), & (\sin\theta_b \sin\phi_b \sin\psi_b + \cos\phi_b \cos\psi_b), & (\sin\theta_b \cos\phi_b \sin\psi_b - \sin\phi_b \cos\psi_b) \\ (-\sin\theta_b), & (\cos\theta_b \sin\phi_b), & (\cos\theta_b \cos\phi_b) \end{bmatrix}
$$

THIS BODY AXES TO SPACE AXES TRANSFORMATION IS PERFORMED IN THE SEQUENCE $\phi \rightarrow \theta \rightarrow \psi$.

BODY AXES TO SPACE AXES VELOCITY TRANSFORMATION

$$
\begin{bmatrix} V_N \\ V_E \\ V_Z \end{bmatrix} = \left[A_{HBS}\right] \begin{bmatrix} V_{Xb} \\ V_{Yb} \\ V_{Zb} \end{bmatrix}
$$

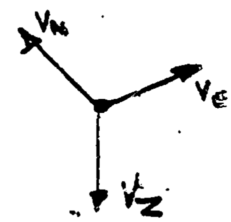

BODY POSITION IN SPACE

$$NORTH = \int (V_N)\,dt$$

$$EAST = \int (V_E)\,dt$$

$$ALT = ALT_0 - \int (V_Z)\,dt$$

EQUATIONS FOR MOTION AT ANY POINT ON THE AIRFRAME

GEOMETRY

$$l_{ps} = \frac{(FSCGB - FSPS)}{12}$$

$$h_{ps} = \frac{(WLCGB - WLPS)}{12}$$

$$b_{ps} = \frac{(BLCGB - BLPS)}{12}$$

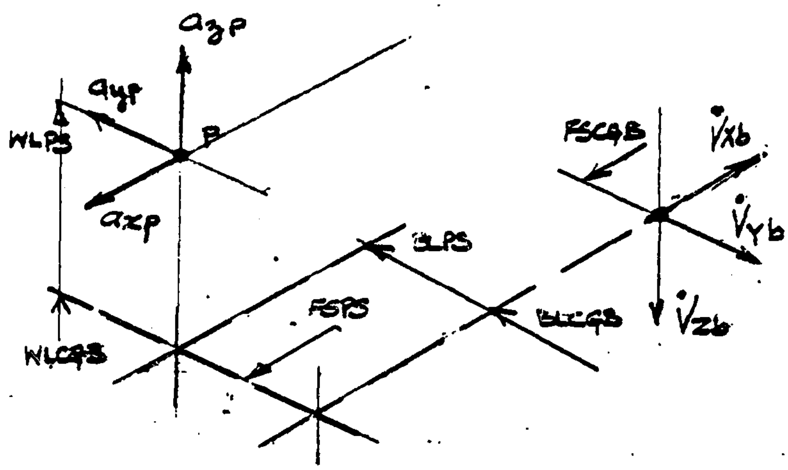

ACCELERATIONS AT A POINT

<u>NOTE</u>: a_{xp}, a_{yp}, a_{zp} ARE ACCELERATIONS THAT A BOB WEIGHT WOULD EXPERIENCE WHICH ARE IN THE OPPOSITE DIRECTION TO $\dot{V}_{xb}$ $\dot{V}_{yb}$ $\dot{V}_{zb}$

$$AXPS = +\left(SUMXB \cdot \frac{g}{W_{bd}} - l_{ps}(q^2+r^2) + b_{ps}(pq-\dot{r}) + h_{ps}(pr+\dot{q})\right)$$

$$AYPS = +\left(SUMYB \cdot \frac{g}{W_{bd}} + l_{ps}(pq+\dot{r}) - b_{ps}(p^2+r^2) + h_{ps}(qr-\dot{p})\right)$$

$$AZPS = +\left(SUMZB \cdot \frac{g}{W_{bd}} + l_{ps}(pr-\dot{q}) + b_{ps}(qr+\dot{p}) - h_{ps}(p^2+q^2)\right)$$

VELOCITIES AT A POINT

$$VXPS = V_{xb} + h_{ps}\,q - b_{ps}\,r$$

$$VYPS = V_{yb} + \ell_{ps}\,r - h_{ps}\,p$$

$$VZPS = V_{zb} - \ell_{ps}\,q + b_{ps}\,p$$

GRAVITY VECTOR ANGLES

LATERAL $\underset{(\phi_{gr})}{LATBL} = \tan^{-1}\left(\dfrac{a_{yp}}{a_{zp}}\right)$

LONGITUDINAL $\underset{(\theta_{gr})}{LNGBL} = \tan^{-1}\left(\dfrac{a_{xp}}{a_{zp}}\right)$

RATE OF CLIMB PARAMETERS

$$VC = -60\,V_Z$$

$$GAMTRU = -\tan^{-1}\frac{V_Z}{(V_N^2 + V_E^2)^{1/2}}$$

THIS IS THE TRUE ANGLE OF CLIMB

LOAD FACTORS AT THE AIRFRAME CG

$$N_X = SUMXB/W_{bd}$$

$$N_Y = SUMYB/W_{bd}$$

$$N_Z = SUMZB/W_{bd}$$

AIRSPEED

$$VKT = \left[(V_{xb}+V_{xg})^2 + (V_{zb}+V_{zg})^2\right]^{1/2} * .591715 \quad \text{KNOTS}$$

$$VXBIKT = (V_{xb}+V_{xg})\left\{\frac{\rho}{.002378}\right\}^{1/2} * .591715 \quad \text{KNOTS INDICATED}$$

FREE STREAM VARIABLES

$$\underset{(\alpha_F)}{ALFRE} = \tan^{-1}\frac{(V_{zb}+V_{zg})}{(V_{xb}+V_{xg})}$$

$$\underset{(\beta_F)}{BETFRE} = \tan^{-1}\frac{(V_{yb}+V_{yg})}{\left[(V_{xb}+V_{xg})^2 + (V_{zb}+V_{zg})^2\right]^{1/2}}$$

$$\underset{(q_F)}{QFRE} = \frac{1}{2}\rho\left[(V_{xb}+V_{xg})^2 + (V_{yb}+V_{yg})^2 + (V_{zb}+V_{zg})^2\right]$$

5.10.3 MOTION MODULE INPUT/OUTPUT DATA TRANSFER

INPUT TRANSFER

PARAMETER	ORIGIN MODULE
$(\cdots)_{MR}$	MAIN ROTOR
WBD	
FSCGB	
WLCGB	
BLCGB	
$(\cdots)_{WF}$	FUSELAGE
$(\cdots)_{T}$	EMPENNAGE
$(\cdots)_{TR}$	TAIL ROTOR
$(\cdots)_{LG}$	LANDING
$(\ \ )_{ADD}$	ADDITION
β_{WF}	FUSELAGE

OUTPUT TRANSFER

PARAMETER	DESTINATION MODULE
VXBDOT	MAIN ROTOR
VYBDOT	
VZBDOT	
PDOT	
QDOT	
RDOT	
VXB	FUSELAGE EMPENNAGE TAIL ROTOR
VYB	
VZB	
P	
Q	
R	
THETAB	
PHIB	
PSIB	LANDING
VN	
VE	
VZ	
QDEG	
PDEG	
RDEG	
VXBIKT	FLIGHT CONTROL
AYPSI	
THETAB	
PHIB	
PSIB	
VZ	GROUND EFFECT
[AHBS]	LANDING

5.10.4 NOTATION FOR THE HELICOPTER MOTION MODULE

SYMBOL USED IN EQUATIONS	PROGRAM MNEMONIC	UNITS	DESCRIPTION
SUMXB	SUMXB	LB	Total external force acting at
SUMYB	SUMYB	LB	the fuselage c.g. along the X Y
SUMZB	SUMZB	LB	and Z axes respectively
SUMLB	SUMLB	FT LB	Total external moments acting about
SUMMB	SUMMB	FT LB	the X, Y and Z axes respectively
SUMNB	SUMNB	FT LB	
$(\ldots)_{MR}$			Main rotor components
$(\ldots)_{TR}$			Tail rotor components
$(\ldots)_{WF}$			Fuselage components
$(\ldots)_{T}$			Empennage components
$(\ldots)_{LG}$			Landing Gear components
$(\ldots)_{ADD}$			Additional Arbitrary Inputs
H_{XGY}	HXGY		Gyroscopic effects, angular
H_{YGY}	HYGY		Momentum
H_{ZGY}	HZGY		
J_{XGY}	JXGY	SLUG FT^2	Rotation inertia about the X, Y and
J_{YGY}	JYGY	SLUG FT^2	Z axes respectively.
J_{ZGY}	JZGY	SLUG FT^2	
W_{XGY}	WXGY	RADS/SEC	Rotational speed of components.
W_{YGY}	WYGY	RADS/SEC	
W_{ZGY}	WZGY	RADS/SEC	
LGY	LGY	FT LB	Gyroscopic effects. Total
MGY	MGY	FT LB	moments in body axes.
NGY	NGY	FT LB	

5.10.4 NOTATION FOR THE HELICOPTER MOTION MODULE

SYMBOL USED IN EQUATIONS	PROGRAM MNEMONIC	UNITS	DESCRIPTION
V_{Xb}'		FT/SEC	Half pass predicted body axes velocities.
V_{Yb}'		FT/SEC	
V_{Zb}'		FT/SEC	
W	WEIGHT	LB	Aircraft gross weight
I_X	IX	SLUGS FT^2	Inertia about body X-axis
I_Y	IY	SLUGS FT^2	Inertia about body Y-axis
I_Z	IZ	SLUGS FT^2	Inertia about body Z-axis
I_{XZ}	IXZ	SLUGS FT^2	Cross coupling inertia
W_{bd}	WTBOD	LB	Weight of the body
F_{SCGB}	FSCGB	INS	Fuselage station of the body c.g.
W_{LCGB}	WLCGB	INS	Waterline station of the body c.g.
B_{LCGB}	BLCGB	INS	Buttline station of the body c.g.
$\dot{V}_{Xb}$	VXBDOT	FT/SEC^2	Accel. along X-axis
$\dot{V}_{Yb}$	VYBDOT	FT/SEC^2	Accel. along Y-axis
$\dot{V}_{Zb}$	VZBDOT	FT/SEC^2	Accel. along Z-axis
$\dot{p}$	PDOT	$RADS/SEC^2$	Angular accel. about X-axis
$\dot{q}$	QDOT	$RADS/SEC^2$	Angular accel. about Y-axis
$\dot{r}$	RDOT	$RADS/SEC^2$	Angular accel. about Z-axis
V_{xb}	VXB	FT/SEC	Vel. along Y-axis
V_{yb}	YXB	FT/SEC	Vel. along Y-axis
V_{zb}	YZB	FT/SEC	Vel. along Z-axis

5.10.4 NOTATION FOR THE HELICOPTER MOTION MODULE

SYMBOL USED IN EQUATIONS	PROGRAM MNEMONIC	UNITS	DESCRIPTION
p	P	RADS/SEC	Angular rate about X-axis
q	Q	RADS/SEC	Angular rate about Y-axis
r	R	RADS/SEC	Angular rate about Z-axis
$\dot{\theta}_b$	THEDOT	DEG/SEC	Pitch rate
$\dot{\phi}_b$	PHIDOT	DEG/SEC	Roll rate
$\dot{\psi}_b$	PSIDOT	DEG/SEC	Heading rate
θ_b	THETAB	DEG	Pitch
ϕ_b	PHIB	DEG	Roll
ψ_b	PSIB	DEG	Yaw
p_D	PDEG	DEG/SEC	Angular rate about X-axis
q_D	QDEG	DEG/SEC	Angular rate about Y-axis
r_D	RDEG	DEG/SEC	Angular rate about Z-axis
	SNTHEB	-	SIN(THETAB)
	CSTHEB	-	COS(THETAB)
	SNPHIB	-	SIN(PHIB)
	CSPHIB	-	COS(PHIB)
	SNPSIB	-	SIN(PSIB)
	CSPSIB	-	COS(PSIB)
$[A_{HBS}]$	-	-	Body to space axes transformation matrix.
V_N	VN	FT/SEC	Velocity to the north
V_E	VE	FT/SEC	Velocity to the east
V_Z	VZ	FT/SEC	Velocity down

5.10.4 NOTATION FOR THE HELICOPTER MOTION MODULE

SYMBOL USED IN EQUATIONS	PROGRAM MNEMONIC	UNITS	DESCRIPTION
NORTH	NORTH	FT	Position north
EAST	EAST	FT	Position east
ALT	ALT	FT	Altitude
V_C	VC	FT/MIN	Climb velocity
γ_T	GAMTRU	DEG	True climb angle
N_X	NX	G's	Body Axes load factors
N_Y	NY	G's	
N_Z	NZ	G's	
V_{KT}	VKT	KNOTS	Velocity in X-Z plane
α_F	ALFRE	DEG	Free stream air flow variables
β_F	BETFRE	DEG	
q_F	QFRE	LB/FT^2	
FSPS	$FSPS_i$	INS	Fuselage station of point of interest
WLPS	$WLPS_i$	INS	Waterline station of point of interest
BLPS	$BLPS_i$	INS	Buttline station of point of interest
lps		FT	Longitudinal arm
hps		FT	Vertical arm
bps		FT	Lateral arm
A_{xps}	AXPS1	FT/SEC^2	Point #1 accel. along X-axis
A_{yps}	AYPS1	FT/SEC^2	Point #1 accel. along Y-axis
A_{zps}	AZPS1	FT/SEC^2	Point #1 accel. along Z-axis

5.10.4 NOTATION FOR THE HELICOPTER MOTION MODULE

SYMBOL USED IN EQUATIONS	PROGRAM MNEMONIC	UNITS	DESCRIPTION
V_{xps}	VXPS1	FT/SEC	Point #1 vel. along X-axis.
V_{yps}	VYPS1	FT/SEC	Point #1 vel. along Y-axis.
V_{zps}	VZPS1	FT/SEC	Point #1 vel. along Z-axis.
LNGBL	LNGBL1	DEG	Longitudinal ball.
LATBL	LATBL1	DEG	Lateral ball.

5.10.5 BLACK HAWK MOTION MODULE INPUT DATA

1. GYROSCOPIC COMPONENTS

$JXGY_1 = 0.116$ $\quad$ $WXGY_1 = 4188.0$

$JXGY_2 = 0.124$ $\quad$ $WXGY_2 = 2094.0$

$JXGY_3 = 0.082$ $\quad$ $WXGY_3 = 609.0$

$JYGY_1 = 0.715$ $\quad$ $WYGY_1 = 127.1$

$JZGZ_1 = 18.0$ $\quad$ $WZGY_1 = -27.0$

2. DOWNWASH CORRECTION TERMS

$$Y_{ADD} = -19.45\, Q_{FRE}$$

IF $-30° \leq \beta_{WF}° \leq 0°$, $L_{ADD} = -(70 + 1.17\beta_{WF}°)\, Q_{FRE}$

IF $30 \geq \beta_{WF}° \geq 0°$, $L_{ADD} = -(70 + 5.54\beta_{WF}°)\, Q_{FRE}$

IF $\beta_{WF} > 0$ $\quad M_{AD} = 51.9\,\beta_{WF}$ LIMIT $M_{AD} < 390.$

$$M_{ADD} = M_{AD}\, Q_{FRE}$$

IF $\beta_{WF} < 0$ $\quad M_{AD} = 38.9\,\beta_{WF}$ LIMIT $M_{AD} > -292.$

$$M_{ADD} = M_{AD}\, Q_{FRE}$$

FOR $\beta_{WF} \leq -30, \geq 30$ HOLD VALUES FOR $\beta = -30, 30$ RESPECTIVELY

3 INERTIA DATA

$I_X = 4659.0$

$I_Y = 38512.0$

$I_Z = 36796.0$

$I_{XZ} = 1882.0$

LATERAL ACCELERATION TRANSDUCER

$FSPS = 307.0$ INS

$WLPS = 263.0$ INS

$BLPS = 0$ INS

4 GENERAL INPUT

ALTØ = 0
RHO = .002378
VSOUND = 1117.0

PICON = 3.1415927
RADCON = 57.29578
RADSCL = .01745
GRAVTY = 32.174

5.10.6 References

1. Dynamics of Flight, Etkin, B., John Wiley & Sons Inc., 1959.

SIKORSKY AIRCRAFT UNITED TECHNOLOGIES

DOCUMENT NO. SER 70452

6.0 DEFINITION OF THE BLACK HAWK COCKPIT

6.0 DEFINITION OF THE BLACK HAWK COCKPIT

6.1 Overall Cockpit Arrangement

The overall layout of the cockpit environment is shown on the photograph, Figure 1.1. This general view is supported by identification of cockpit components on Figures 1.2a and 1.2b. The cockpit geometric definition,relating to the pilot's seat, controls and instrumentation, is presented on Figures 1.3a, 1.3b and 1.3c as 3-view general arrangement drawings. Diagrams defining the upper and lower consoles are shown on Figures 1.4 and 1.5 respectively. The most significant items are the switching functions on the upper console and the Stabilator/Auto Flight Control Panel on the lower console. The flight instrument panel arrangement is shown on Figure 1.6.

6.2 Pilot's Primary Controls

A diagram of the pilot's cyclic stick grip is presented on Figure 2.1. The grip incorporates the following functions of significance:

Stick trim - provides for lateral and longitudinal stick trim at 1/2"/sec.

Trim release - while depressed the force system is deactivated leaving a limp stick.

A diagram of the pilot's collective stick grip is presented on Figure 2.2. A friction device on the pilot's lever can be turned to adjust the amount of friction and prevent the collective stick from creeping.

6.3 Control Range Characteristics

The control motion, both in terms of control displacement in inches of travel and angular sweep are presented on Figure 3.1. Also provided are the corresponding angular outputs at the rotor head.

6.4 Control Force Feel Characteristics

The control forces, gradients and breakouts for the primary controls are given on Figure 4.1. The values presented were derived from measurements at the 50% control position.

More detailed information concerning all aspects of the cockpit may be obtained from References 6.5.1 through 6.5.4.

6.5 REFERENCES

1. Black Hawk Pilot Manual TM55-1520-237-10

2. Black Hawk MOS 35K Avionics Mechanics Manual

3. Black Hawk Fault Isolation Manual TM55-1520-237-MTF

4. Black Hawk Simulation Flight Training System Device 2038.
NAVTRAEQIPCEN 76-C-0086-4001 Volume I ADDENDUM 1.

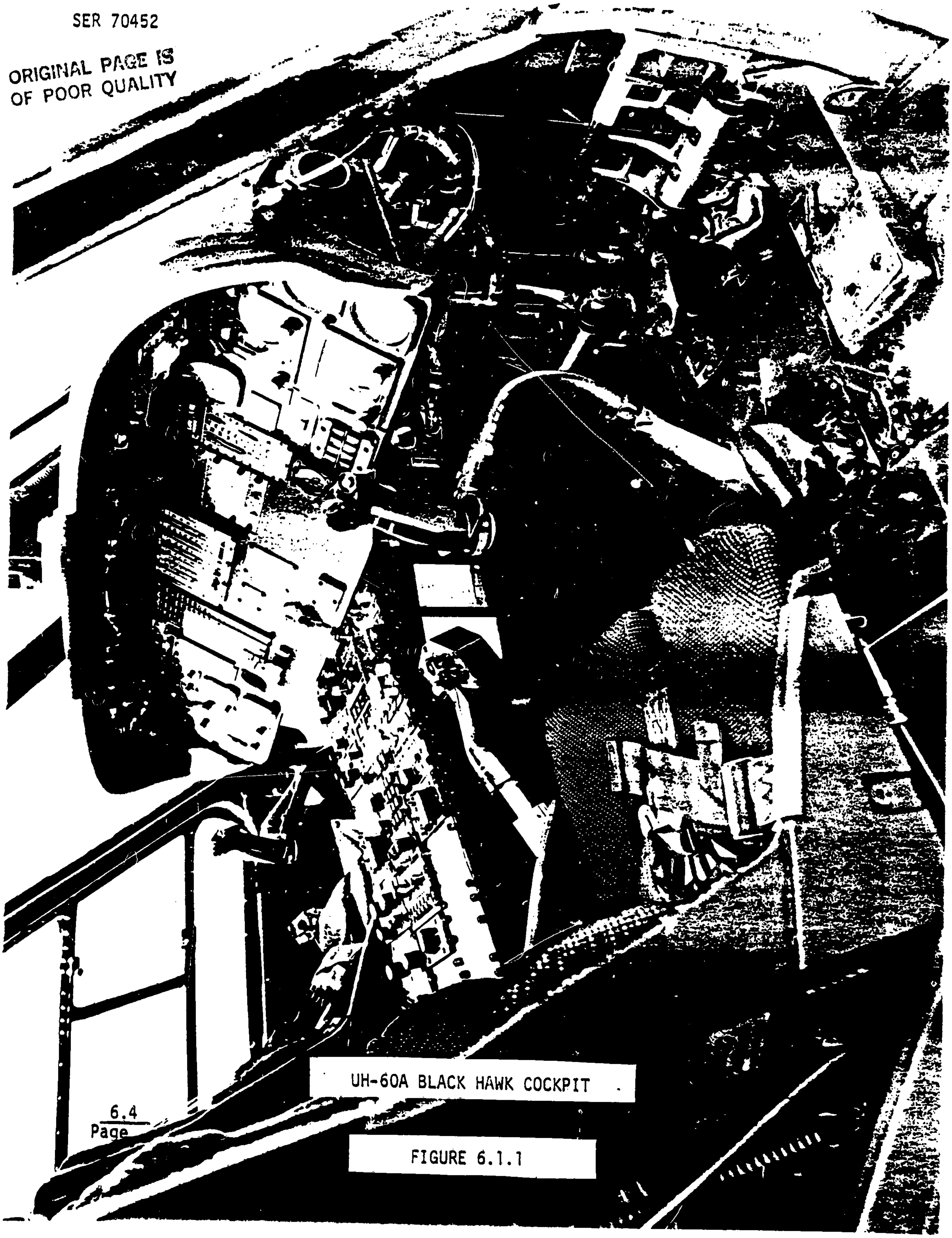

UH-60A BLACK HAWK COCKPIT

FIGURE 6.1.1

COCKPIT COMPONENT IDENTIFICATION

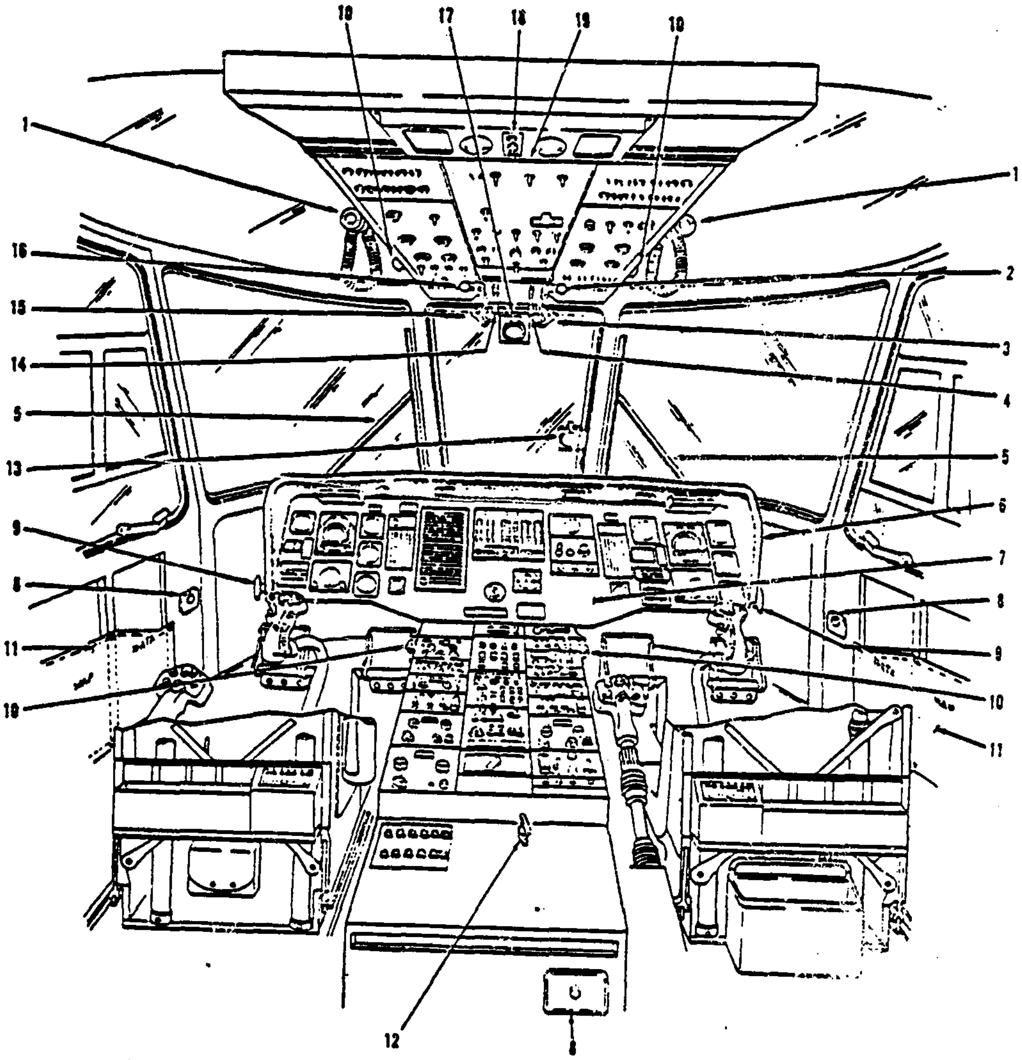

1 UTILITY LIGHT
2 NO. 2 ENGINE FUEL SELECTOR LEVER
3 NO. 2 ENGINE OFF/FIRE T-HANDLE
4 NO. 2 ENGINE POWER CONTROL LEVER
5 WINDSHIELD WIPER
6 INSTRUMENT PANEL GLARE SHIELD
7 INSTRUMENT PANEL
8 ASH TRAY
9 PEDAL ADJUST LEVER
10 VENT
11 MAP/DATA CASE
12 PARKING BRAKE LEVER
13 STANDBY (MAGNETIC) COMPASS
14 NO. 1 ENGINE POWER CONTROL LEVER
15 NO. 1 ENGINE OFF/FIRE T-HANDLE
16 NO. 1 ENGINE FUEL SELECTOR LEVER
17 FREE-AIR TEMPERATURE GAGE
18 COCKPIT FLOODLIGHT CONTROL
19 UPPER CONSOLE

FIGURE 6.1.2(a)

COCKPIT COMPONENT IDENTIFICATION

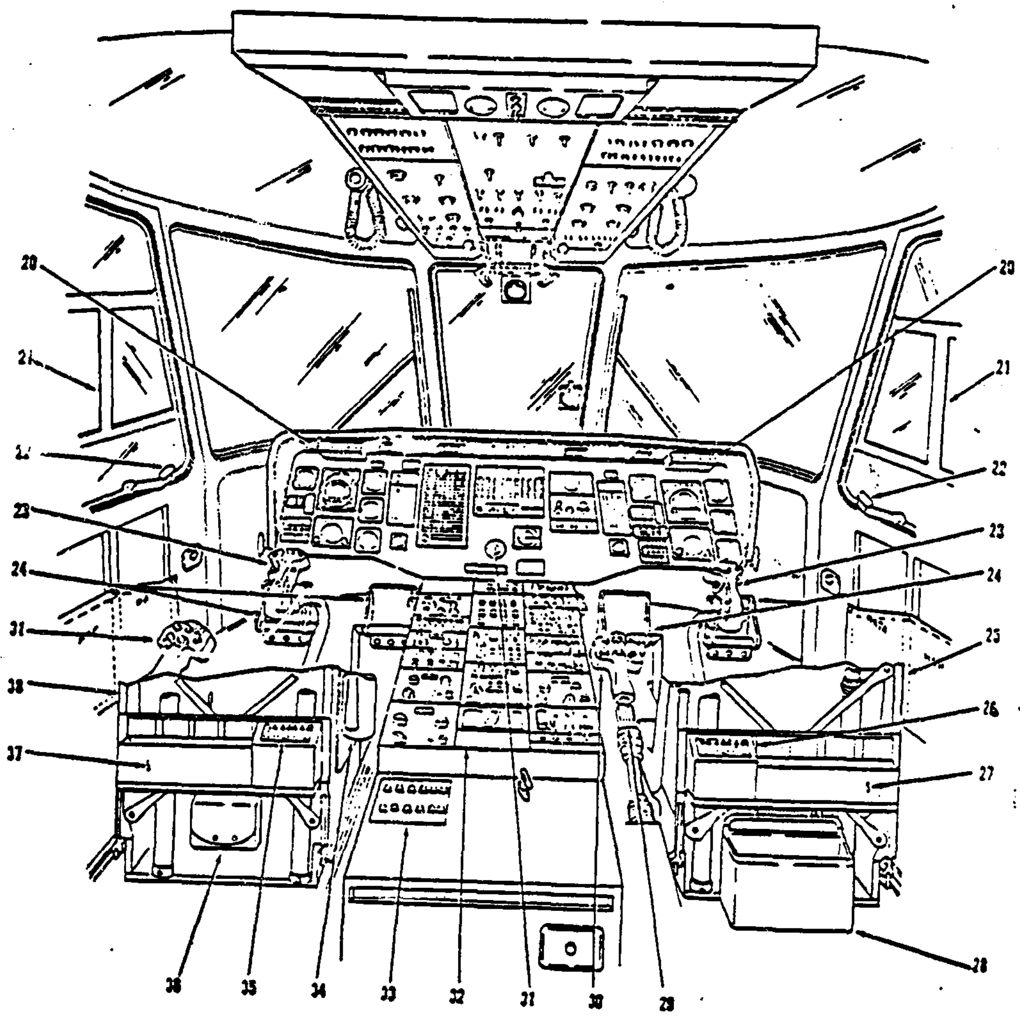

20 MASTER WARNING PANEL
21 SLIDING WINDOW
22 COCKPIT DOOR EMERGENCY RELEASE
23 CYCLIC STICK
24 DIRECTIONAL CONTROL PEDALS
25 PILOT'S SEAT
26 CREW CHIEF/GUNNER ICS CONTROL PANEL
27 CREW CHIEF AMMUNITION/GRENADE STOWAGE COMPARTMENT
28 STOWAGE BAG
29 COLLECTIVE STICK FRICTION CONTROL
30 COLLECTIVE STICK GRIP
31 ENGINE IGNITION KEY LOCK
32 LOWER CONSOLE
33 BATTERY/BATTERY UTILITY BUS CIRCUIT BREAKER PANEL
34 FIRE EXTINGUISHER
35 GUNNER'S ICS CONTROL PANEL
36 FIRST AID KIT
37 GUNNER'S AMMUNITION/GRENADE STOWAGE COMPARTMENT
38 COPILOT'S SEAT

FIGURE 6.1.2(b)

COCKPIT GEOMETRIC DEFINITION

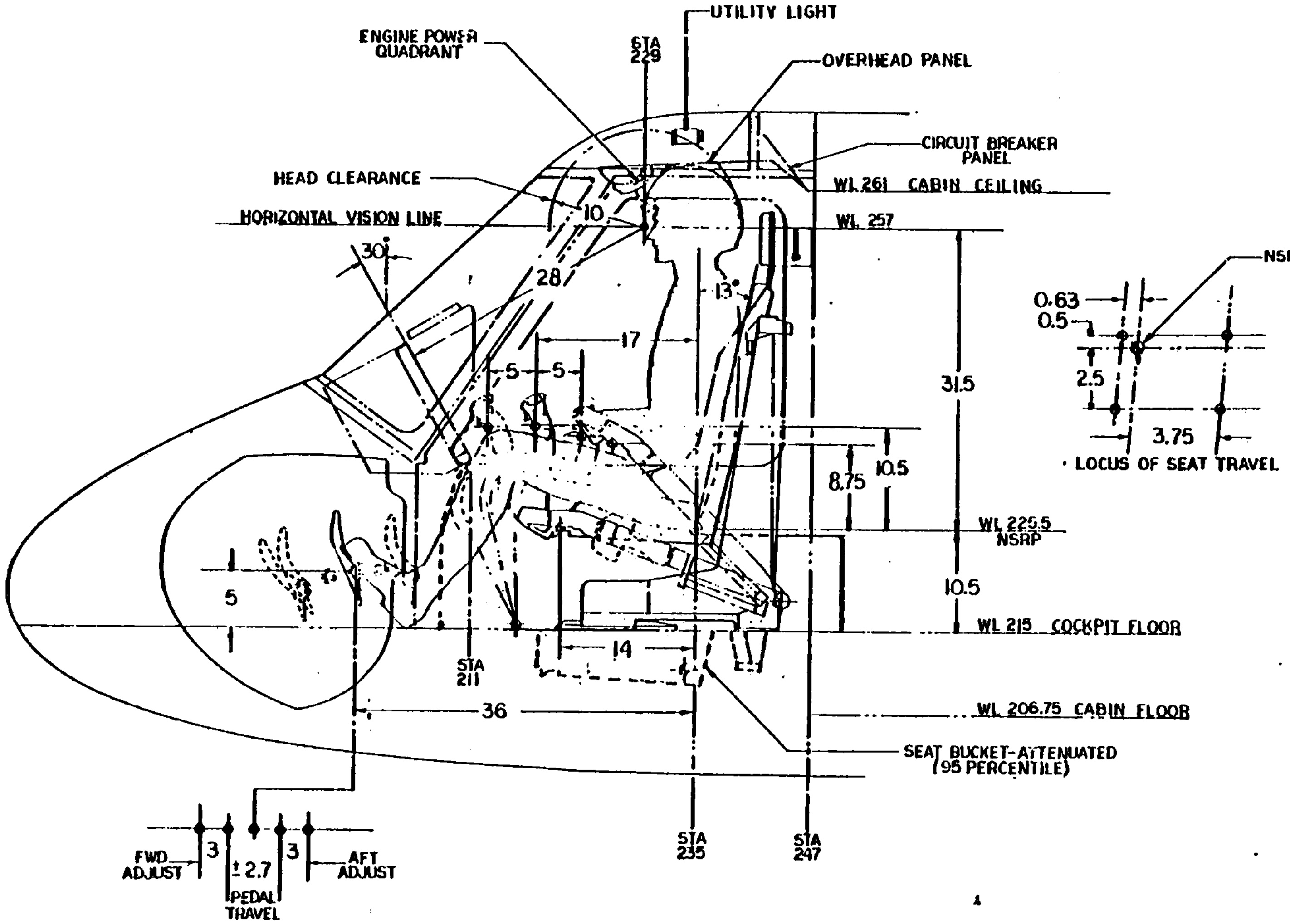

FIGURE 6.1.3(a)

ORIGINAL PAGE IS OF POOR QUALITY

ORIGINAL PAGE IS
OF POOR QUALITY

COCKPIT GEOMETRIC DEFINITION

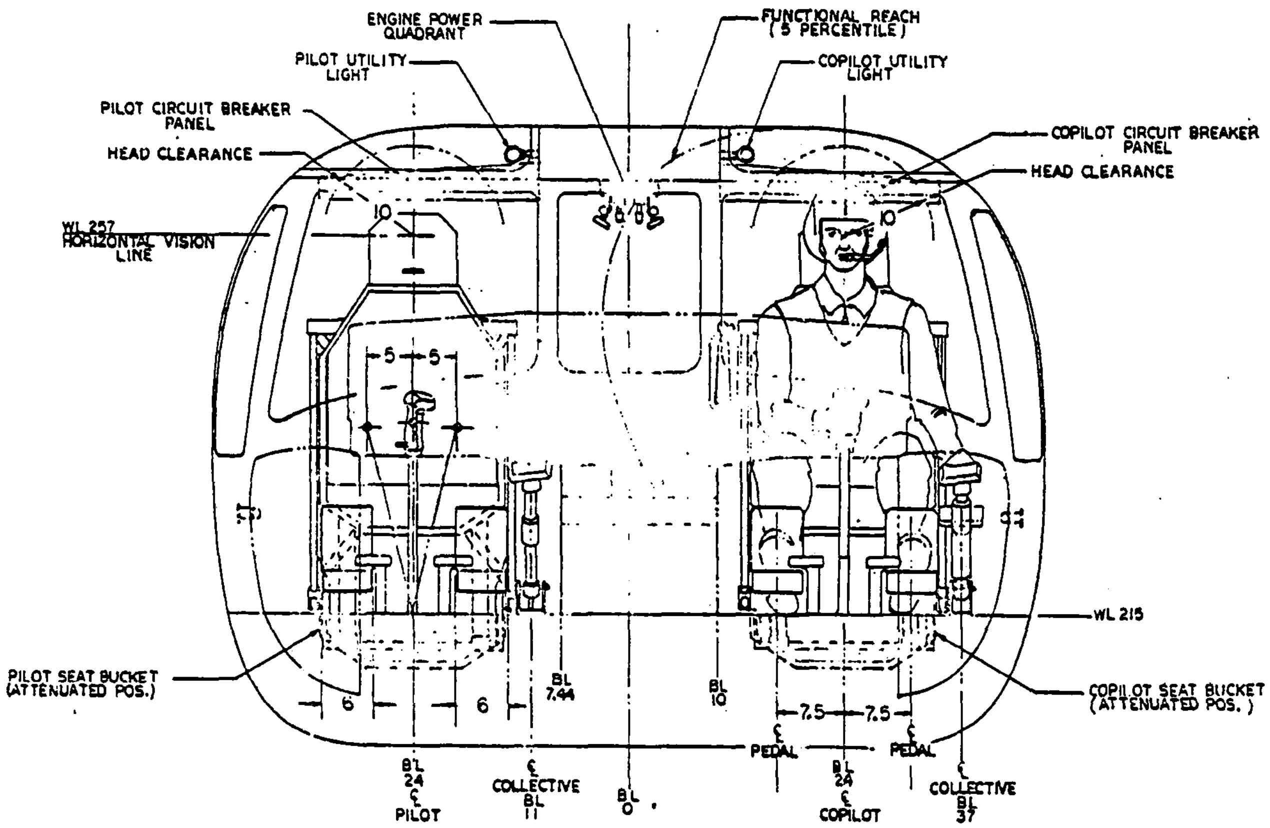

FIGURE 6.1.3(b)

ORIGINAL PAGE IS
OF POOR QUALITY

COCKPIT GEOMETRIC DEFINITION

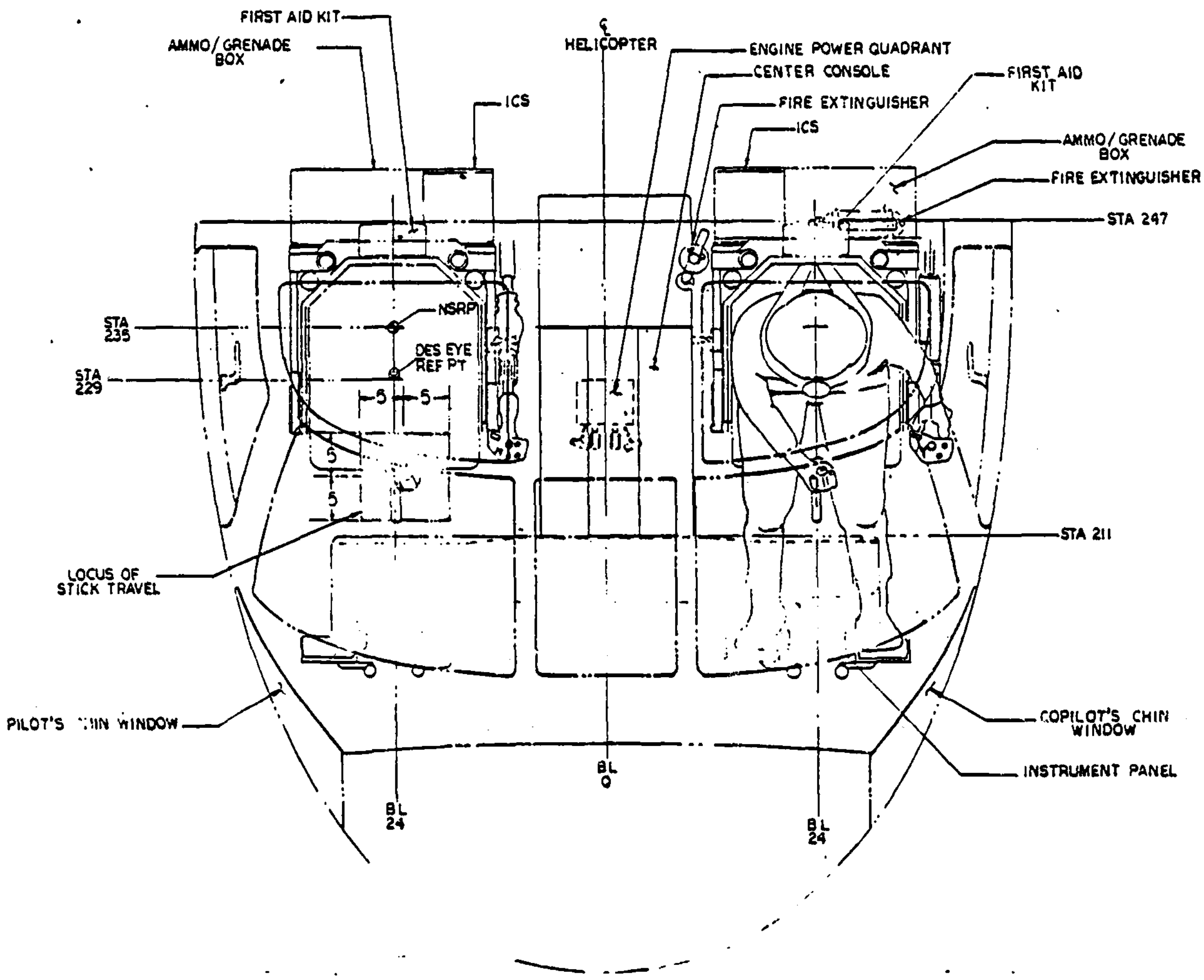

FIGURE 6.1.3(c)

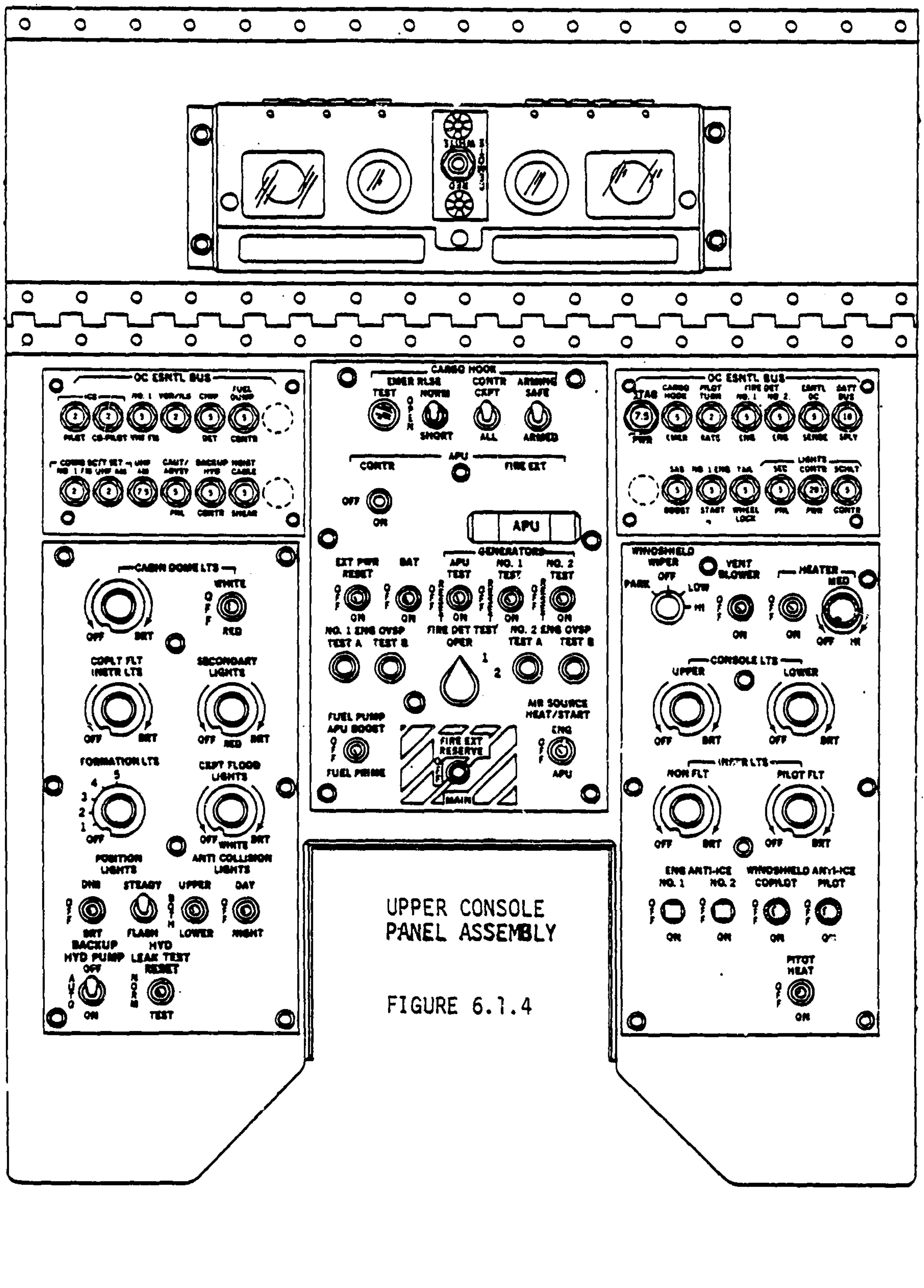

UPPER CONSOLE
PANEL ASSEMBLY

FIGURE 6.1.4

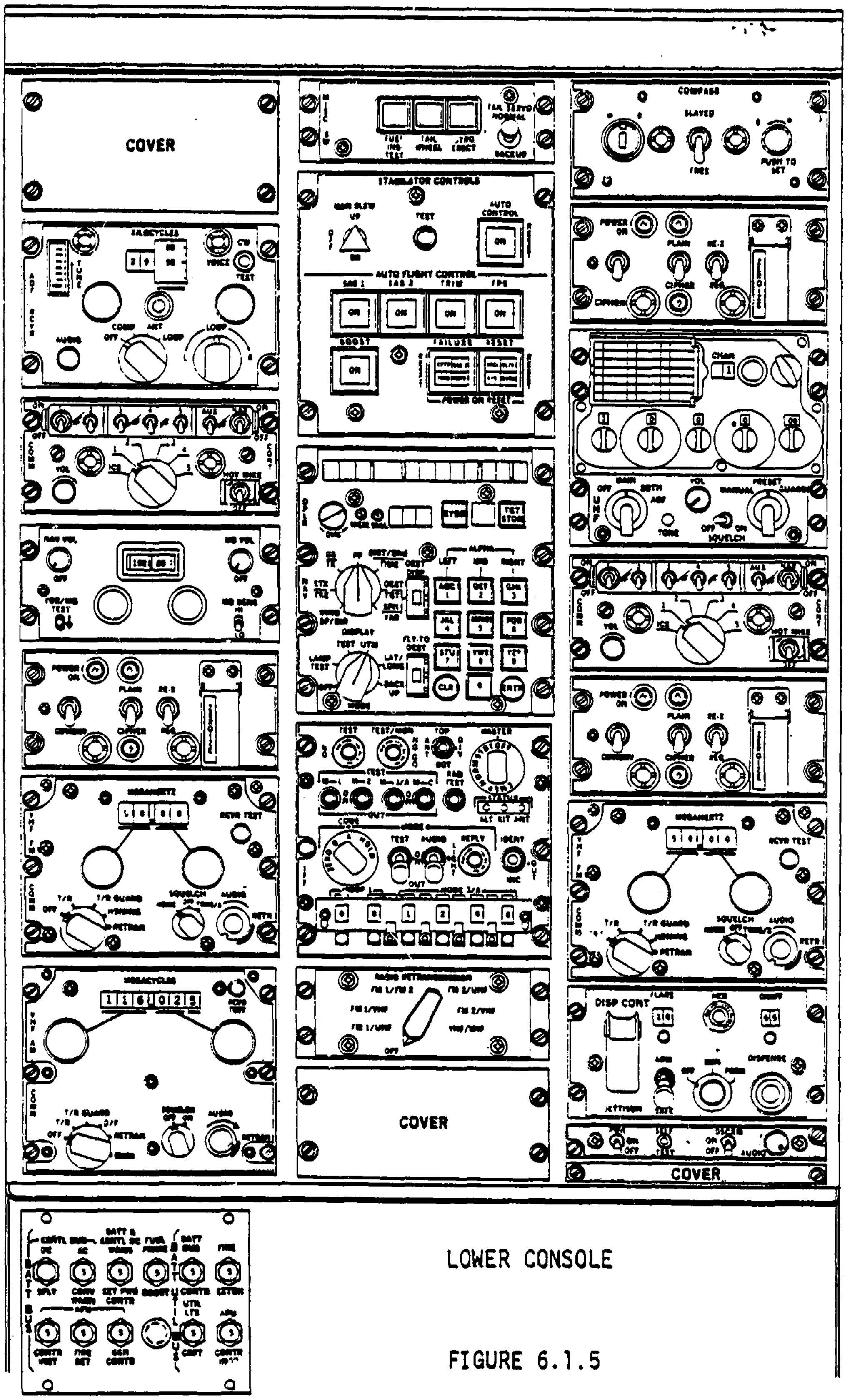

LOWER CONSOLE

FIGURE 6.1.5

ORIGINAL PAGE IS
OF POOR QUALITY

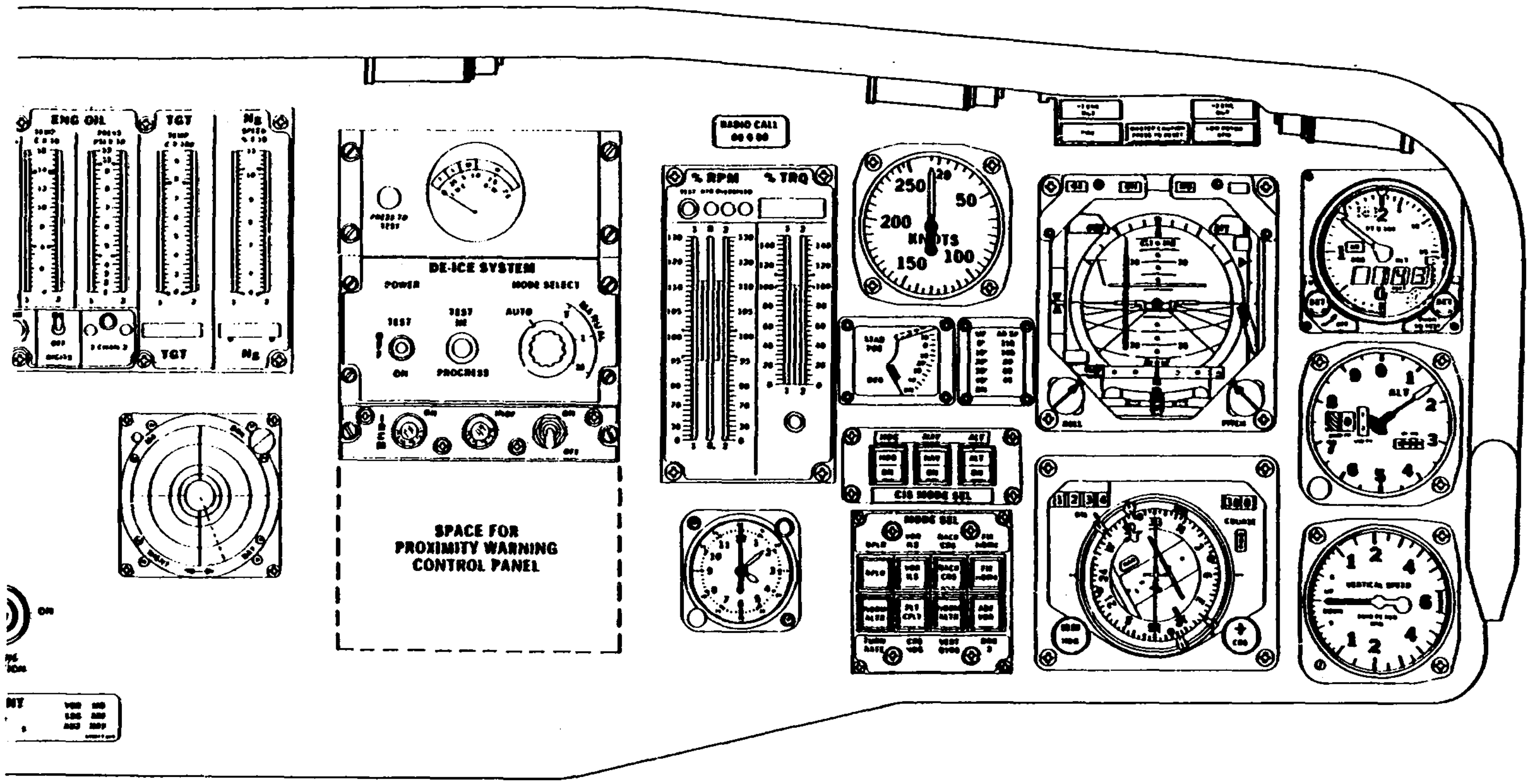

INSTRUMENT PANEL — RIGHT HAND SIDE

FIGURE 6.1.6

ORIGINAL PAGE IS
OF POOR QUALITY

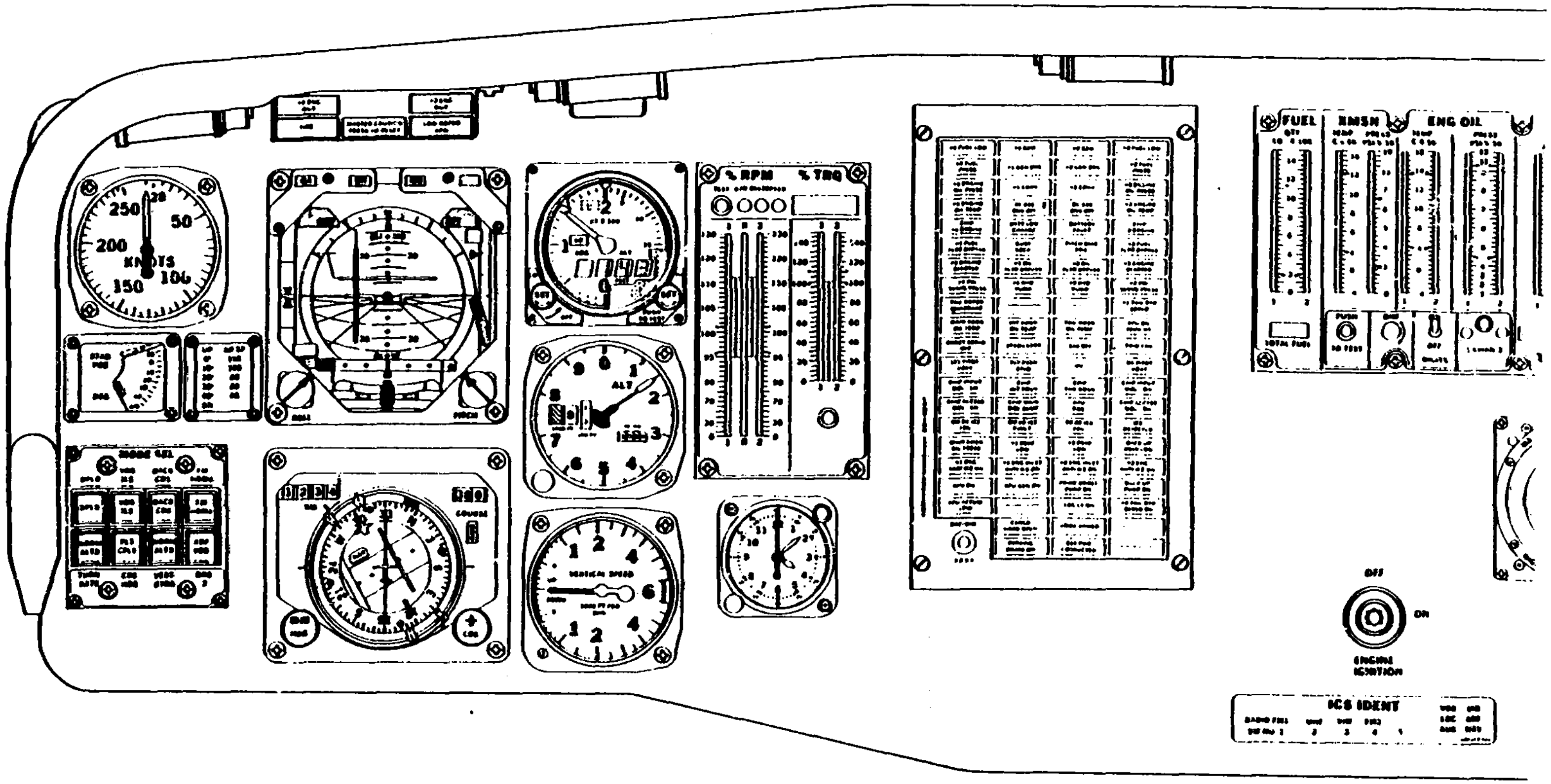

INSTRUMENT PANEL — LEFT HAND SIDE

FIGURE 6.1.6 (Cont'd.)

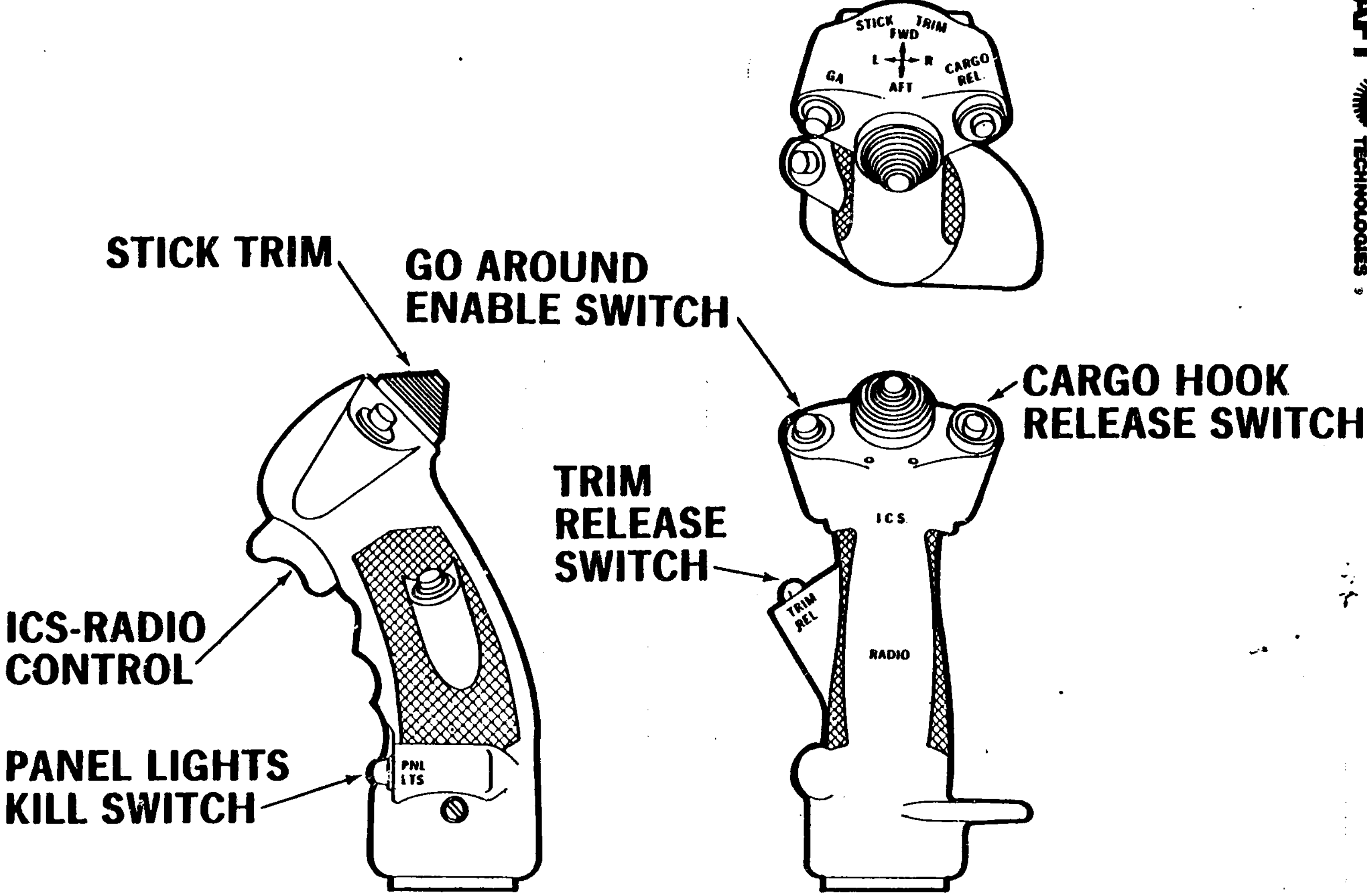

CYCLIC STICK GRIP

ORIGINAL PAGE IS OF POOR QUALITY

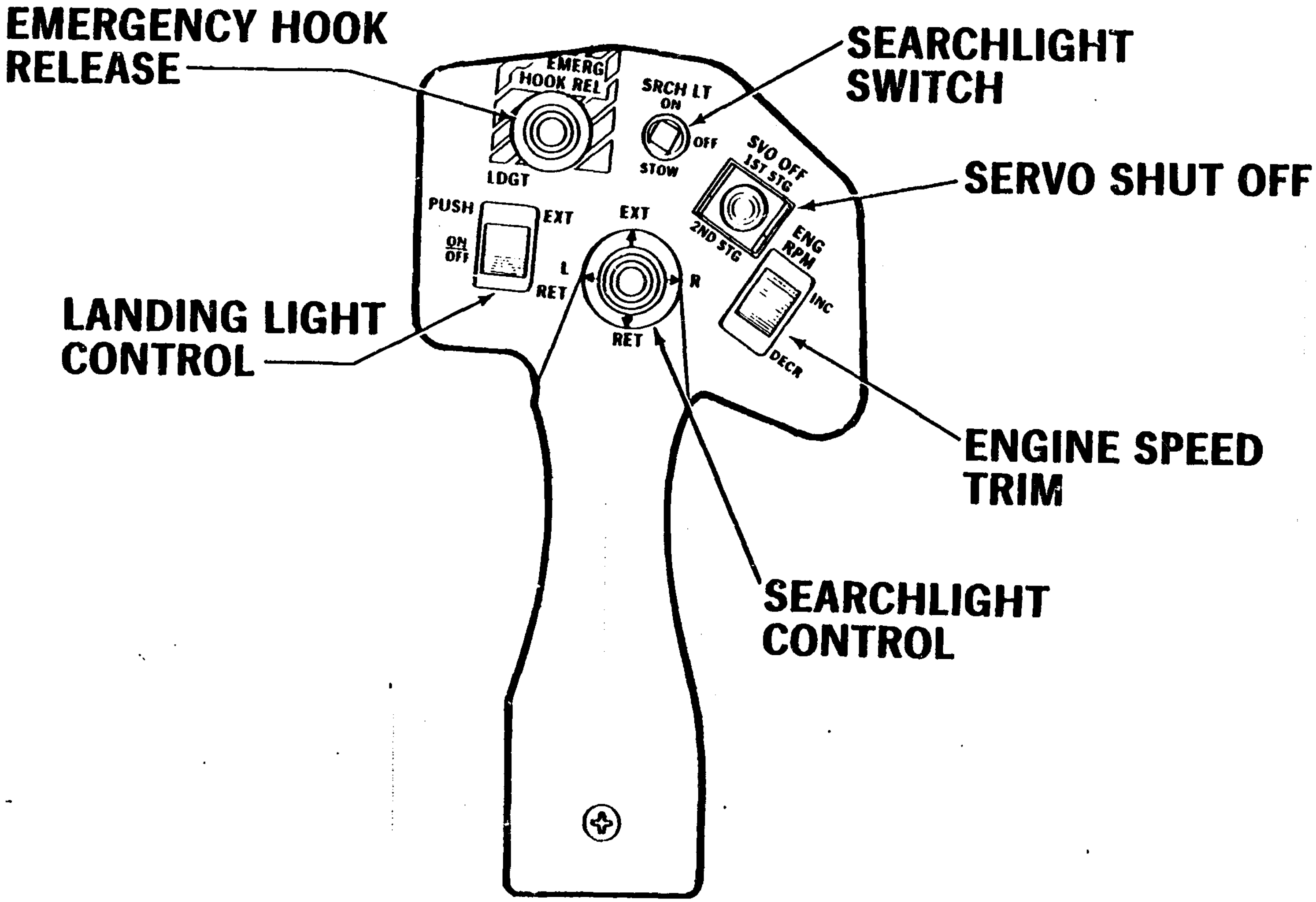

COLLECTIVE STICK GRIP

BLACK HAWK ANGULAR CONTROL MOTIONS AND DISPLACEMENTS

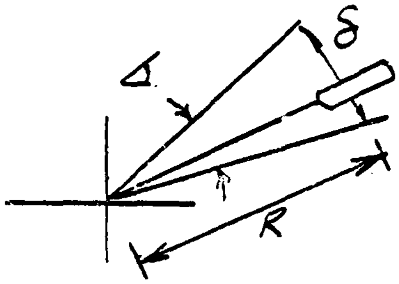

* High Collective
** Low Collective
*** Mid Collective
**** With Overtravel
***** Considers Control Reduction due to redundant quadrant

CONTROL-POSITION	R(IN.)	δ (IN.)	∠ (DEG)	REFERENCE	OUTPUT @ ROTOR (DEG)
COLLECTIVE	24.0	–	–	Horizontal	θ_{CUFF}
Low	-	0	22.5	Above	9.9
High	-	10.0	46.55	Above	25.9
Δ	-	10.0	24.05	-	16.0
LONGITUDINAL CYCLIC	20.75	-	-	Neutral Cyclic	B_{IS}
Forward *	-	5.0	13.95	Forward	16.5
Pinned**	-	3.89	10.84	Aft	-11.0
Aft ***	-	5.0	13.95	Aft	-12.3
Δ	-	10.0	27.9	-	28.8
LATERAL CYCLIC	24.80	-	-	Vertical	A_{IS}
Left **	-	5.0	11.63	Left	-8.0
Pinned **	-	.96	2.24	Left	-1.54
Right	-	5.0	11.63	Right	8.0
Δ	-	10.0	23.26	-	16.0
PEDAL	15.0	-	-	Vertical	θ_{TRCUFF} *****
Left****	-	2.69	10.33	Left	29.9
Pinned ***	-	0	0	On	15.0
Right ****	-	2.69	10.33	Right	0.1
Δ ****	-	5.38	20.66	-	29.8

FIGURE 6.3.1

BLACK HAWK CONTROL FORCES AND GRADIENTS

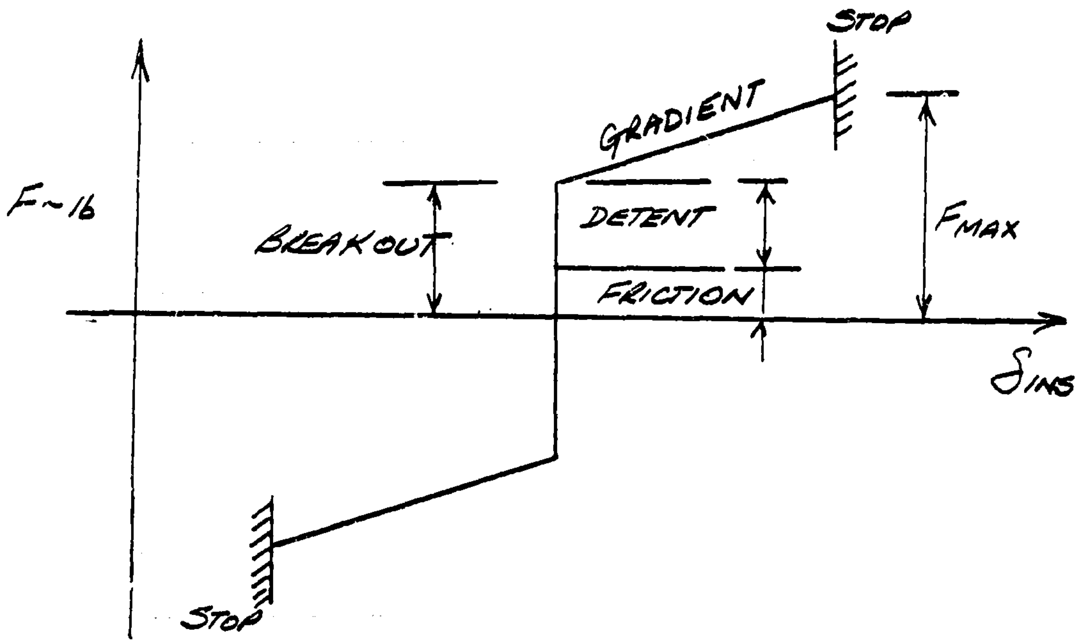

DATA DERIVED FROM ATP 27000

CONTROL	STROKE	MAXIMUM TRIM OFF FRICTION	NOMINAL TRIM ON BREAKOUT*	NOMINAL TRIM ON GRADIENT	NOMINAL TRIM ON F_{MAX}
Lateral Cyclic	10.0 in.	.625 lb.	.95 lb.	.54 lb/in	3.65 lb.
Longitudinal Cyclic	10.0 in.	.625 lb.	1.35 lb.	.73 lb/in	5.0 lb.
Pedal (+ Overtravel)	4.92 in. (5.38 in)	4.0 lb.	7.2 lb.	6.5 lb/in	23.2 lb. (24.7 lb)
Collective	10.0 in.	.625 lb	-	-	-

* Breakout (Trim On) = Detent + Friction (Trim Off)
All Values Measured From 50% Control Position

FIGURE 6.4.1